FORMATION AND CHARACTERIZATION OF ZEIN-BASED OLEOGELS

BY

KO-LAN TSUNG

DISSERTATION

Submitted in partial fulfillment of the requirements
for the degree of Doctor of Philosophy in Food Science and Human Nutrition
with a concentration in Food Science
in the Graduate College of the
University of Illinois at Urbana-Champaign, 2020

Urbana, Illinois

Doctoral Committee:

    Professor Nicki Engeseth, Chair
    Research Professor Graciela Padua
    Associate Professor Youngsoo Lee
    Professor Keith R. Cadwallader

ABSTRACT

Oil structuring techniques in food science field have been focused on finding alternative oil-thickening methods for substitution of partial hydrogenation and interesterification. Oleogelation without chemically modification of liquid oils becomes the solution to exclude *trans* fat in the final products. One of the common oleogelation approaches to fabricate solid-like oil is using oleogelators to form stable network which can immobilize the oil phase and further construct into an oleogel system. Among various type of gelators, it is important and challenging to find an oleogelator that meet the needs of safe, biocompatible, biodegradable and cost-effective before and after digestion. Which natural proteins originated from animals or plants are suitable candidates for their ability to self-assembly into supramolecular structures and eventually lead to continuous networks that involve in the gel formation with non-covalent interactions. In this research, oleogelation mechanism of zein in 70% ethanol and oleic acid mixture was investigated.

Zein, a corn prolamin contains around 50% hydrophobic amino acid residues was used as an oleogelator in a 70% ethanol/zien/oleic acid emulsion system stored for 7, 14 and 21 days. Ternary phase diagrams were constructed and mapped out the numbers and extents of the phases. Within 21 days of storage time, up to five phases were identified, and self-assembled oleogels with different transparency were observed. The flow behavior of emulsions and viscoelastic properties of zein-based oleogels were determined by rheological measurements. The emulsions showed shear thinning behaviors with viscosity positively correlated with oleic acid content. It was assumed to be the high volume fraction of the dispersed oil phase that affected the interfacial tension of the emulsion. Both viscosity and storage modulus increased with increasing of protein concentration, which indicated the rigidity of the network was contributed mainly by the zein structures. After storage, all of the gel elasticity increased with time. And accordingly, the highest gel strength was found at the solvent composition where 70% ethanol and oleic acid ratio closed to 1. Although higher amount of oleic acid could act as fillers in the emulsion system, but excess amount might affect the solvent polarity and cause the zein molecules to aggregate instead of forming into elongated entangled network structures. Which at 15% zein concentration, the optimum composition for most rigid gel was 45-15-40 and 40-15-45 (70% ethanol/zein/oleic acid, (%, w/w/w) for 14 and 21 storage days, respectively.

The microstructural changes during zein molecules self-assembly process were monitored by ultra-small x-ray scattering (USAXS). The results showed one to two levels of structures were formed inside zein-based oleogels. The primary level of zein building blocks with radius of gyration R_{g1} and shape factor P_1 revealed between high q and intermediate q region ($0.01 < q < 0.5$ Å^{-1}) would self-assemble from 1D rod-like structure to 2D plate of sheet-like structures. At this level, the size and shape were mainly affected by solvent composition, which R_{g1} enlarged with the increasing of 70% ethanol, but not by storage time. The secondary level structures located at low q ($q < 10^{-3}$ Å^{-1}) showed the network were composed of similar 3D fractal structures with R_{g2} ranged from 251 to more than 1200 nm. The R_{g2} values increased with higher 70% ethanol content and longer storage time indicated the dynamic gelation process of zein-based oleogel was resulted from the rearrangement of zein molecules in different solvent environment. It was suspected that with less oleic acid and lower protein concentration, zein molecules had higher mobility to attach onto the surface of oleic acid oil droplets and further developed into larger scale of structures.

Lutein was successfully encapsulated in the zein-based oleogel with modified preparation method which sonication was applied. Based on tube inversion method and the rheological measurements, the gelation process was significantly facilitated by high shear which the formation of up-side-down gel with G' > G" was observed at 3rd day instead of 21st day of storage (30-15-55). And with the determination of conductivity and microscopy, the oleogel system was confirmed as an oil-in-water emulsion with micro-sized oil droplets distributed within the hydrophilic continuous phase. And the ribbon-like strands observed by AFM could be the network structures that formed by zein with the interactions between oleic acid.

The results of this study provided insights about the self-assembly gelation mechanism of the zein-based oleogel. As a model system, it demonstrated similar behavior to spontaneous protein aggregation inside the cell. By understanding the effects of protein concentration, solvent composition, storage time, shear force applied and addition of antioxidant on the gelation process of the oil-in-water emulsion gel system, this research not only help to design the desirable texture and structural properties of the controlled-release system for chemically or heat sensitive compounds, but also a different perspective to approach the aging phenomenon.

ACKNOWLEDGEMENTS

Frist and foremost, I would like to express my profound gratitude to my advisor, Dr. Graciela Wild Padua. Without her guidance, support, and inspiration, I cannot image I will be the author of a dissertation one day, which is today. Throughout my study, she granted me with infinite understanding, patience, kindness, and freedom, so that I can survive and not giving up. She generously shared and taught me the knowledge, insight and vision in food science, material science, food engineering and technology, which constantly reminds me how lucky I am to have the opportunity to be her student and work with her.

I greatly appreciate all my committee members, Dr. Engeseth, Dr. Cadwallader and Dr. Lee, not only for all your help, suggestions and recommendations regarding to the research, but also playing important roles at different stages of my PhD life.

Thank you Dr. Engeseth, for being there for me ever since I received the offer letter from the department. You provided me with the warmest care, encouraged me to make the right decision even if I was so desperate. Without your support, I don't think I can complete the degree.

Thank you Dr. Cadwallader, for accepting me as your TA and leading me to be a better one. I enjoyed your lab, your teaching style and every chances chatting with you. Your devotion and enthusiasm in research, and the humor you possess, all showed me what a scientist is like when he/she is in love with the career. You let me find my value and know what I want to become.

Thank you Dr. Lee for your generosity and trust, so that I can learn and use the instrument thoroughly and freely. I am so grateful to have you as one of my committees, without you, without rheology. Besides teaching me the scientific background, you let me take steps out of my comfort zone to contact with the technician and the machine directly. These experiences are so valuable than anything.

In addition, I would like to thank Dr. Ilavsky, Dr. De Mejia, Dr. Feng, Dr. Wang, Dr. Takhar and other faculties for their assistances during our collaborating experiences. My gratitude also goes to staffs and members of the Department of Food Science and Human Nutrition for their administrative support.

I sincerely thank to my friends in AESB, ABL, Bevier Hall and at Purdue University, your

company is the fuel to push me move forward. Especially thankful to Xueqian, Luis Real, Luis Ibarra, Eric, Fengjia, Ying and Mengyi, for your selfless help and time on me.

Beyond I can express, there is never enough gratitude to my family, my parents and brother, for their unconditional love and support. With them, I can be who I am and who I want to be.

To my parents: Ying-Hsien Han – Shing-Been Tsorng

and my bother: Hao-Lan Tsung

TABLE OF CONTENTS

CHAPTER 1 INTRODUCTION

Oleogels are fascinating for their ability to immobilize a hydrophobic liquid phase by a three-dimension network composed of crystallite, cross-linked or self-assembled gelators and exhibit a semi soft solid-like gel texture. The various applications have been utilized in chemistry for paint and coating, pharmaceuticals for drug and vaccine delivery platforms, and cosmetics as sunscreen or makeups. In the past decades, the needs for biocompatible oleogels served as oral drug delivery vehicles and tissue bioengineering matrices in biotechnology make the oleogelation technology progress rapidly for researchers from wide range of backgrounds to discover and investigate novel ingredients and innovative processing ways to create non-toxic organic solvent oleogel products. Moreover, in the food industry, the US Food and Drug Administration (FDA) banned the use of trans-fats, and lead to replacing saturated fat with poly-unsaturated fat and essential fatty acids, which promote the development of new oil-structuring methods for fat-replacer and the use of Generally Recognized as Safe (GRAS) oleogelators.

Conventionally, oleogels could be prepared by directly dispersing lipidic additives such as saturated fatty acids, waxes, fatty alcohols to develop crystal aggregates or even agglomerates in the unsaturated liquid oil phase by heat-induced sol-gel process. Recently, new oleogelation techniques have introduced which incorporating not only lipid-based gelators but also polysaccharides, proteins or polymeric strands. Among these, natural derived proteins with amphiphilic characteristics are gaining attention. For instance, whey proteins can partially unfold and absorb at the o/w interface, under suitable condition, they become denatured and form aggregates as building blocks to form 3D network structures. The entanglements of these structures can develop into framework that entrap the liquid oil and form oleogels. While the driving forces of the gelation processes only consist of H-bonding, π-π stacking, hydrophobic, van der Waals and donor–acceptor interactions, it is possible to fabricate thermo-reversible controlled release carriers for heat-sensitive compounds only by protein self-assembly properties.

Zein, a corn storage protein, which has self-assembly characteristics include its amphiphilicity. Being reported to self-assemble into various distinct structures by solvent evaporation such as lamellar sheets, elongated fiber and micro or nanospheres, zein has been used in various applications for making films, foams, microencapsulation, and also can be used to stabilize the oil-in-water Pickering emulsion. Although the spontaneous gelling ability of zein in water/ethanol

binary solutions has long been reported, and the gelation of zein could be controlled by changing pH, salt addition and temperature, not until recently, zein used in preparation of oil-in-glycerol oleogels have been discussed.

Here, this work propose the self-assembly and amphiphilic properties of zein in ethanol binary solutions to act as a GRAS oleogelator. While incorporating the oleic acid as the unsaturated hydrophobic phase in to the system, zein building blocks rearrangements are facilitated to organize into ordered 2D and 3D structures. The aim of this research is to understand the self-assembly mechanism of zein in ethanol and oleic acid mixtures. By investigating the spontaneous gelation process of this emulsion oleogel system, hoping to get insights relate to protein aggregations that leads to aging.

Objectives:

1. To explore and determine the number and extent of the 70% ethanol/zein/oleic acid emulsion system phases with the construction of ternary phase diagrams. Time effects were continuously monitored for 21 days.

2. To evaluate the effects of solvent composition, zein concentration and storage time on the viscoelastic properties of 70% ethanol/zein/oleic acid system. The flow behaviors of liquid samples will be examined by flow sweep tests before gelling. For oleogel samples, strain and frequency sweep tests will be conducted.

3. To investigate the self-assembly process of zein in 70% ethanol added with oleic acid, ultra-small angle x-ray scattering (USAXS) will be used. The effects of solvent composition, protein concentration, storage time and high shear (sonication) applied on the microstructural changes will be analyzed by USAXS.

4. Zein-based oleogels has been proposed as fat replacer and also an encapsulation carrier for hydrophobic nutrient; however, oleogel prepared at room temperature simply by self-assembly properties of zein remains unclear unexplored. Thus, to understand the potential and feasibility for encapsulating lipid soluble bioactive compound, lutein will be encapsulated by the oleogels. The rheological behaviors, microstructures will be evaluated by rheometry, USAXS, conductivity, optical microscopy, confocal laser scanning microscopy (CLSM) and atomic force microscopy (AFM).

CHAPTER 2   LITERATURE REVIEW

2.1 Gels general considerations

Gel, as defined in the Polymer Science Dictionary (Alger, 2017), is "a substance composed of two or more components, which one acts as a liquid solvent interacts with the others that are insoluble and forming cross-linked solid part of the network." The solid-like fibrous structures would provide the framework to prevent the liquid-like phase to flow (Cornwell & Smith, 2015). According to Flory, a more commonly accepted definition of gels states that "a gel has a continuous structure that is permanent on the analytical time scale and is solid-like in its rheological behavior"(Flory, 1974). This type of soft matter consists of three dimensional gel network chemically or physically cross-linked (Thakur & Thakur, 2018).

Chemically cross-linked gels are constructed by covalent bonds between different polymers, where polymerization is usually involved. Despite the fact that they are stable and having high gel strength in solvents without dissociation, chemical gels are not favored in food of pharmaceutical applications due to the possible toxicity of the used crosslinking agents (Ebara et al. 2014). Apart from that, gelation through non-covalent interactions including hydrogen bonding, π-π stacking, van der Waals interactions, solvophobic forces (hydrophobic forces for gels in water), donor-acceptor interactions, metal coordination are categorized as physical gels (Sangeetha & Maitra, 2005; Chakraborty, Das, & Nandi, 2018). Although those exhibit weaker bonding forces between molecules, the high sensibility to the environment factors such as pH, water activity, pressure/ shear, ionic strength, solvent types and temperature makes it excellent candidate for preparation of reversible (ex: thermoreversible) gels with unique gel structure in biomedical engineering, dermocosmetics nutraceutical and food processing (Chakraborty et al., 2018; Buruiana & Ioan, 2018; Nazir, Asghar, & Aslam Maan, 2017).

Within the category of physical cross-linked gels, we could further characterize by the solvent type it largely immobilized as hydrogels (trapping water phase) and/or oleogels (organic liquid phase). As for hydrogels, the water is the main dispersion medium in the polymer chain networks (Gupta, Vermani, & Garg, 2002; Raeburn, Cardoso, & Adams, 2013; Choudhary, Paul, Nayak, Qureshi, & Pal, 2018). The hydrophilic system serves as a water absorber of high capacity (Ahmed, 2015). On the other hand, the three-dimensional cross-linked network forming inside nonpolar

organic liquid phase is classified as an oleogel.

2.2 Oleogels

Oleogel is an emerging trend in various fields including pharmaceuticals, cosmetics, art conservation and food science (O'Sullivan, Barbut, & Marangoni, 2016). The utilization of biopolymers as gelators or stabilizers has expanded the functional properties of oleogels to include biodegradable, biocompatible, edible and environmental (Esposito, Kirilov, & Roullin, 2018). Substitution of the organic solvents used in the chemical industry by food grade oils, has increased the interest in oleogels in the food industry (Dassanayake, Kodali, & Ueno, 2011).

The consumption of *trans* and saturated fats (Chavan, Khedkar, & Bhatt, 2015) has been linked to cardiovascular disease. However, the physical state and functionalities that solid fat can provide are distinctive and hard to replace. Many manufactured food products depend on the high-melting characteristic of fats to create texture, snap, spreadability and palatability (Martins, Vicente, Cunha, & Cerqueira, 2018). Hence, new oil structuring technologies are being developed and oleogel is one of the alternatives to reduce or replace the high levels of *trans* and saturated fats (Hughes, Marangoni, Wright, Rogers, & Rush, 2009).

The common approaches for oil structuring can be identified in four groups as shown in Figure 2.1 Approaches for structuring oils (Patel & Dewettinck, 2016). Patel & Dewettinck, 2016). As for direct dispersion, various types of oleogelators can be added into low melting point liquid oil and gelled the system at concentration as low as 0.5% wt. Lipid-based oleogelators including waxes, fatty acids, fatty alcohols, and monoglycerids (Maria B. Pérez-Gago & Krochta, 2001; Nikiforidis, Gilbert, & Scholten, 2015; M. Zhang & Weiss, 2015; Cerqueira et al., 2017) will entrap liquid oil following steps of nucleation, crystal growth, aggregation and network formation.

Both polymeric and molecular gelators, are excellent candidates to create oleogels as an alternate to partial hydrogenated oils and *trans* fat although they may differ in their performance and biological value. In general, polymeric oleogelation involves either natural or synthetic polymers as the gelators to immobilize vegetable oils. Most polymers are used in hydrogels as thickeners and textural modifiers in foods, very little are considered in hydrophobic system. In the past decade, hydrophobically modified cellulose (e.g., ethylcellulose) has been used for structuring vegetable oils (Zetzl et al., 2014, 2012). When a polymer-based oleogel is ingested, the covalently

linked polymers are enzymatically digested to yield metabolic products composed of an array of oligomers of different chain lengths and not exclusively the starting monomers. These formed oligomers could potentially cause an immunological response and may lead to health problems (e.g., polylactide) (Conway et al., 1997; Burger et al., 2006). On the contrary, the low molecular weight gelators (LMWGs) based oleogel is formed by self-assembly of the LMWGs via non-covalent interactions, such as hydrogen bonds, van der Waals forces, and π-π-stacking. This type of oleogels would yield the gelator building blocks that are safe and digestible after ingested.

The key point for indirect methods is to create a concentrated oil-in-water emulsion by utilizing the functionality of polymers which stabilizes the interfacial tension between the water and oil phases. Following by dehydration process, the removal of large portion of water without damaging the framework could indirectly leave the oil droplet embedded in the polymer and become the oleogel (Chaves, Barrera-Arellano, & Ribeiro, 2018).

Recently, with the growing attention and possible application of porous materials, they are employed as oil absorbents due to their high porosity and high surface area. These oil uptake materials can be considered as another type of oleogel which possess rigid solid behavior with almost non-flow properties.

Last but not least, oleogel can be formed by oil-water biphasic system with different type of emulsions. For water continuous phase emulsion, emulsifiers like polysaccharide or protein are used to stabilize the surface tension between oil droplets and water. Or the dispersed oil is entrapped by the bulk structure formed by gelation of the hydrogel matrix. On the other hand, oil continuous phase emulsions could be achieved by dispersing water droplets which have the ability to gel into the hydrophobic phase.
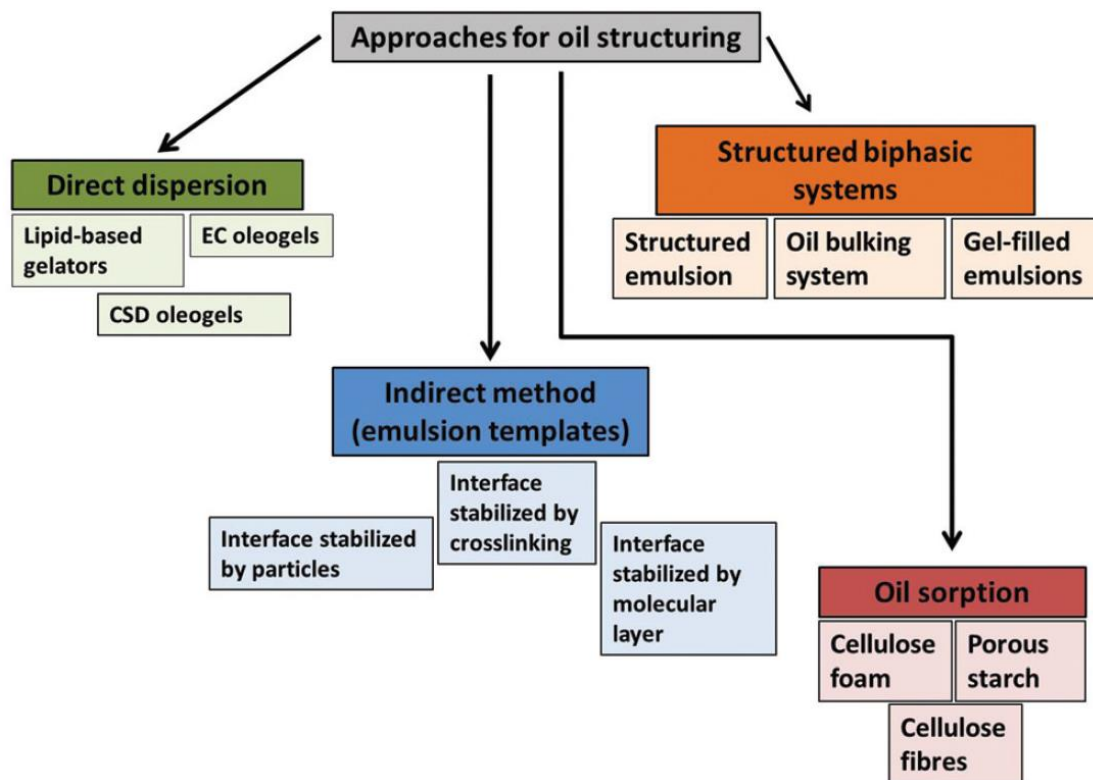
Figure 2.1 Approaches for structuring oils (Patel & Dewettinck, 2016).

2.3 Zein

Zein, the major storage protein of corn (Shukla, Cheryan, & DeVor, 2000), found exclusively in the endosperm, comprises about 50-60% of the total protein in corn. Because of its unique solubility, zein is considered a prolamin which contains high amounts of proline and glutamine. It is insoluble in water unless specifically defined conditions are applied, such as a certain concentration of alcohol, high concentrations of urea, extreme alkali condition (pH > 11), and/or anionic detergents (Dill, 1926). More than 50% of the amino acids of zein are nonpolar such as leucine, proline, alanine, phenylalanine, isoleucine and valine. Besides those, it contains hydrophilic ones includes glutamic acid, glutamine, and asparagine. However, zein lacks the essential amino acids lysine and tryptophan.

Based on the amino acid sequences and solubility in alcohol, zein is classified into four fractions: α-zein (70-85% of total zein), β-zein (1-5%), γ-zein (10-20%) and δ-zein (1-

5%)(Nonthanum, Lee, & Padua, 2013). α-Zein does not dissolve in pure water due to high hydrophobic residues such as phenylalanine (4-6%), alanine (14%), proline (9-11%) and leucine (18-20%).

The structural model of α-zein was proposed by Argos et al. (1982) and Matsushima et al.(1997) (Figure 2.2). The 22 kDa α-zein contains 10 α-helix repeat units and 19 kDa molecular weight fraction has 9 coil-like repeating units where each coil consists of 20 residues. The α-helices are linearly aligned in antiparallel orientation and linked with a glutamine rich turn or loop as the bridge at the connection of two helices (Wang, Crofts & Padua, 2003). Furthermore, it was assumed to form a rectangular block of 13 × 1.2 × 3 nm with a hydrophobic core, accompanied by two parallel hydrophilic surfaces.
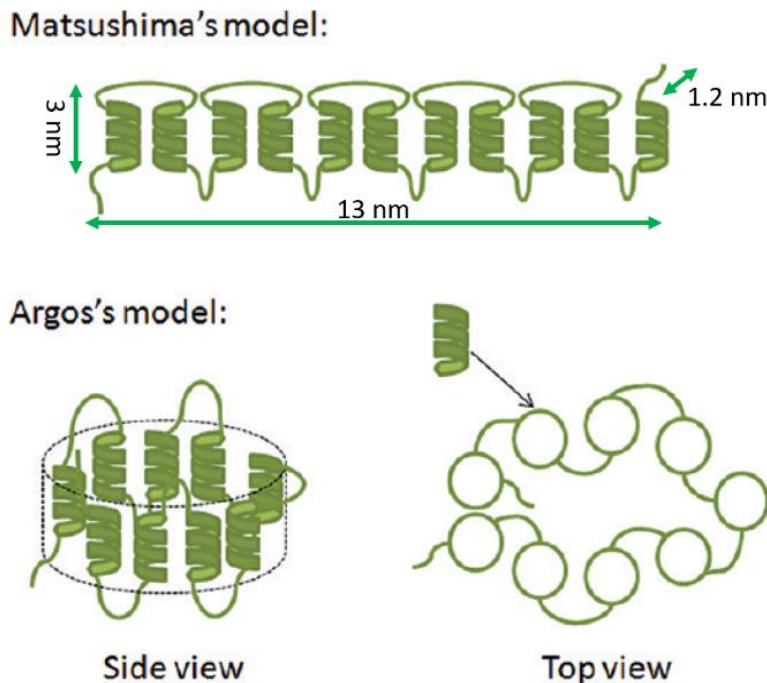
Figure 2.2 The structural model of α-zein was proposed by Argos et al. (1982) and Matsushima et al (1997).

2.3.1 Zein microstructures

Amphiphilic substances are crucial and distictive for their self-assembly ability to transform into variety of structures. For instance, they can form lyotropic microphases such as two-dimensional mono- or bilayer lamellar structures, and more developed three-dimensional

7

structures including micelles, cylindrical rods, hexagonal or cubic phases (Godoy, Valiente, Pons, & Montalvo, 2015). Zein self-assembly properties have been studied by Wang and Padua (2008) and Dong et al.(2010) Zein in ethanol-water solutions was observed to generate lamellar, bicontinuous structures and spheres upon evaporation induced self-assembly (EISA).

According to circular dichroism spectroscopy results, the α-helices experienced conformational transformation into β-sheets during the evaporation process. Followed by side-by-side packing of the anti-parallel β-sheets, a long range hydrophobic ribbon with two hydrophilic surfaces was developed. Accompanied by transmission electron microscopy images, the ribbons would curl into rings and grow into nanospheres as proposed by Wang and Padua (2012) (Figure 2.3).
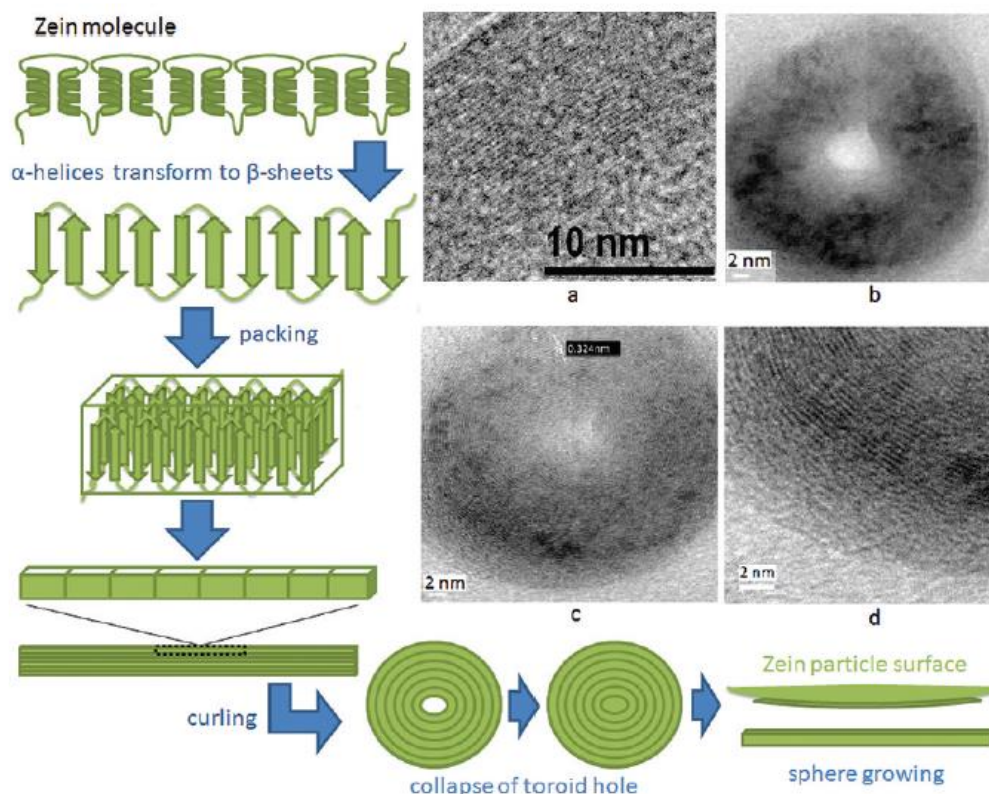

Figure 2.3 Possible mechanism for zein self-assembly form single molecules to nanospheres. Adapted from Wang and Padua (2012).

2.3.2 Zein oleogel

As early as 1946, it was reported that zein solutions would form gel with time and heat, and have the tendency to gel as zein concentration increased. However, the solubility characteristics of

zein hampers its use in most of the applications (Y. Chen, Ye, & Liu, 2013). Often times, zein is used as a pickering agent to design pickering emulsions (De Folter, Van Ruijven, & Velikov, 2012; Rutkevi, Allred, Velev, & Velikov, 2018; Soltani & Madadlou, 2015; L. J. Wang et al., 2013), or in combination of other gelling agent like polysaccharides to form hydrogel (Kasaai, 2018a). Very little of the research focus on using zein as an oleogelator to prepare oleogel. The latest update was mixing zein with glycerol at 150℃ for completely dissolution, then homogenizing with the oil phase at a high temperature (Scholten et al, 2014). During the cooling process, the zein-based oleogel was formed by self-assembly. The product was a thermo-responsive oleogel, which turned into fluid-like material while increases the temperature. On this basis, hydrophobic antioxidant such as β-Carotene was added into the system, showed the ability for zein-based oleogel to be a promising controlled release carrier. On the other side, it could also be utilized in bakery product as a fat replacer(Chen et al., 2016). Similar to other types of oleogels, zein oleogels are characterized by the methods sorted in Table 2.1.

Table 2.1. Summary of methods for oleogel characterization.

Analytical characterization methods	Characterization principles
Method of inverted tube (visual assessment)	Based on the resistance of the gel has to the gravitational flow under the effect of its own weight while the inversion happens.
Rheology	The viscoelastic characteristics can be defined by viscosity (η), storage modulus (G') and loss modulus (G").
Differential scanning calorimetry (DSC) Thermogravimetric analysis (TGA)	Physicochemical properties of gelator, solvent composition and nature of the organic phase via the concentration are thermally analyzed to access the network disruption conditions.
X-ray diffraction (XRD)	The presence of crystalline domains and composition of the internal phase can be observed by X-ray diffraction.
Small angle X-ray scattering (SAXS) and small angle neutron scattering (SANS)	The depiction of structural arrangement, sol-gel transition or the gelation process under wide temperature range are studied by X-ray scattering.
IR spectroscopy	Inter-and intramolecular H-bonding involved in the oleogel system.
Atomic force microscopy (AFM), transmission electron microscopy (TEM)	Visualization of gel network microstructures
^{1}H-NMR	Monitoring the weak chemical bonds such as π-π stacking and H-bonds to understand the gelation phenomena.

2.4 Rheology

Over the past decades, the study of interrelationships between nano to macroscopic features of foods to sensory attributes, physiological performance had expanded rapidly. Not only because people start to aware the importance of food structural properties to nutritional aspects, also the advancing analytical tools has been developed to investigate the relationships sophisticatedly. One of the emerging research topics for understanding the flow or deformation responses to the applied force of a certain substance within certain time frame is knowing as rheology. Rheological properties are determined by measuring force and deformation as a function of time. Which are crucially related to the microstructures of the consisting molecules to their overall viscoelastic behaviors. The obtained parameters are empirical for food acceptability, food processing, food handling and food matrix design for nutrients delivery. Generally, food material can be classified as liquid, semi-solid, gel and hard solid according to its rheological properties (Tabilo-Munizaga & Barbosa-Cánovas, 2005)(Berthaume, 2016).

2.4.1 Flow Behavior

When liquids or gases which have smaller internal binding forces between atoms and molecules, the way they deform to shear stress and keep increasing strain is called flow. The relationship between stress and shear strain is governed by viscosity, which describes the flow behavior by a function of shear rate under simple steady shear. At a given temperature, when liquids showed linear relationship between shear stress and resulting shear rate, the flow behavior is defined as Newtonian or ideal viscous with dynamic viscosity remains constant as,

$$\tau = \eta \cdot \dot{\gamma}$$

$$\eta = \frac{d\tau}{d\dot{\gamma}}$$

where τ is the shear stress, η is the viscosity and $\dot{\gamma}$ is the shear rate.

If the relationship of shear stress and shear rate is not linear, it is categorized as non-Newtonian behavior. The typical flow behaviors are illustrated in Figure 2.4.
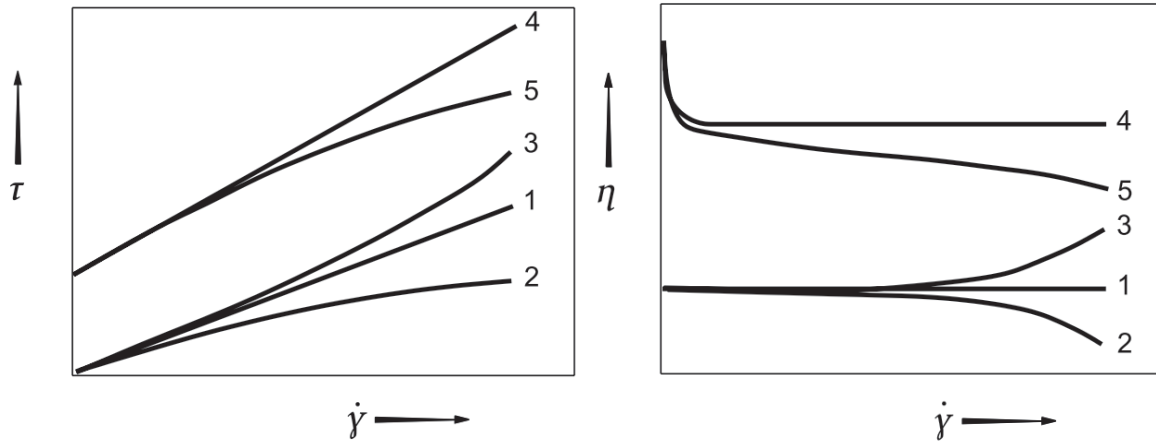
Figure 2.4 Flow behavior curves (left) and viscosity cruves (right). 1: Newtonian, 2: pseudoplastic (shear thinning), 3: dilatant (shear thickeninig), 4: Bingham plastic, 5: Herscel-Buckley (Bingham pseudoplastic).

In order to better explain and distinguish the different behavior, Ostwald-de-Waele model is most commonly used when the stress-shear rate curve passes through origin (no yield stress). The power-law equation expressed as,

$$\tau = K\eta \cdot \dot{\gamma}^n$$

where K is the consistency coefficient (Pa.s^n) and n is the flow behavior index. When $n > 1$, it showed shear thinning behavior (pseudoplastic), other the other hand, $n < 1$ is shear thickening behavior, and for Newtonian liquid $n = 1$.

The flow behaviors of zein in various concentration of ethanol aqueous, temperature, pH and storage time has been discussed (Erickson et al., 2020; Fu & Weller, 1999; Selling, Hamaker, & Sessa, 2007)(Nonthanum, Lee, & Padua, 2012; Nonthanum et al., 2013; Zhong & Ikeda, 2012). In summary, viscosity decreased with the decreasing of protein concentration, increasing of temperature, increasing ethanol concentration from 55% to 80%, and pH departed from neutral value. Recently, Nonthanum et al. (2014) revealed that the consistency index of commercial zein which mostly composed of α-zein is not affected by pH. However, zein contained high content of γ-zein showed increasing of viscosity when pH was raised. Which indicating the viscosity of γ-zein was contributed by the aggregation effect took place at high pH. For heat treated 10% zein dissolved in 65-95% ethanol and isopropanol solutions, samples all exhibited shear-thinning

pseudoplastic behaviors reported by Chen, Ye, & Liu, (2013). Zein micro or nanoparticles have been used as stabilizers in oil-in-water emulsion system. Due to most of the studies discussed the behaviors of zein sphere in Pickering emulsion acting as an amphiphile using its surface charge, or simply as filler, the zein emulsions were shear-thinning viscous liquids with viscosity increased with increasing of zein concentration (De Folter et al., 2012; Gao et al., 2014; Rutkevičius, Allred, Velev, & Velikov, 2018; Soltani & Madadlou, 2015; Zou, Yang, & Scholten, 2018).

2.4.2 Viscoelastic behavior

Viscoelastic materials combine properties of elastic solids with those of viscous fluids, one of best example is gel. According to the definition, a gel is a semi-solid mixture with at least two components that immiscible to each other, and one of them forms solid network structure that immobilizes the other liquid phase (Lopes da Silva & Rao, 1999). Therefore, rheological measurement is crucial to properly evaluate the viscous and elastic natures of the gel system (Tabilo-Munizaga & Barbosa-Cánovas, 2005). With a detailed analysis of viscoelastic properties of gel, it leads to numerous applications by resolving the relationship between structural properties to the macroscale textural properties.

2.4.3 Small amplitude oscillatory tests

Oscillatory testing with small amplitude oscillation is one of the most common dynamic rheological measurement for soft materials. By minimum strain (or stress) applied, weak structures can remain mostly intact before the true viscoelastic information is acquired. In the test, a full oscillation cycle is equivalent to 360° or 2π, and angular frequency represents the number of oscillations per second. While applying a sinusoidal strain (or stress) and measuring the responded sinusoidal stress (or strain) along with the phase differences between the two waves, both elastic and viscous properties of the sample can be analyzed simultaneously. For instance, when there is no phase differences between the stress and strain waves, phase angel $\delta = 0^{\circ}$, indicating the material is elastic. And when $\delta = 90^{\circ}$ ($\pi/2$), the stress and strain waves are out of phase, the sample is completely viscous (Mewis, Wagner, Mewis, & Wagner, 2011a). Besides these two extremes, the viscoelastic materials have a phase angle between $0^{\circ} < \delta < 90^{\circ}$ ($0 < \delta < \pi/2$), where 45° is the transition of sol to gel (Figure 2.5).

$$\tau_{elastic}(t) = \tau_{max}\sin(\delta)$$

for ideal elastic solid, shear stress $\tau_{elastic}$ is completely in phase with deformation ($\delta = 0^0$).

$$\tau_{viscous}(t) = \tau_{max}\cos(\delta)$$

$$\gamma(t) = \gamma_{max}\sin(\delta)$$

in contrast, ideal viscous fluid has shear stress in phase with shear strain ($\gamma(t)$) but not sinusoidal to shear stress.
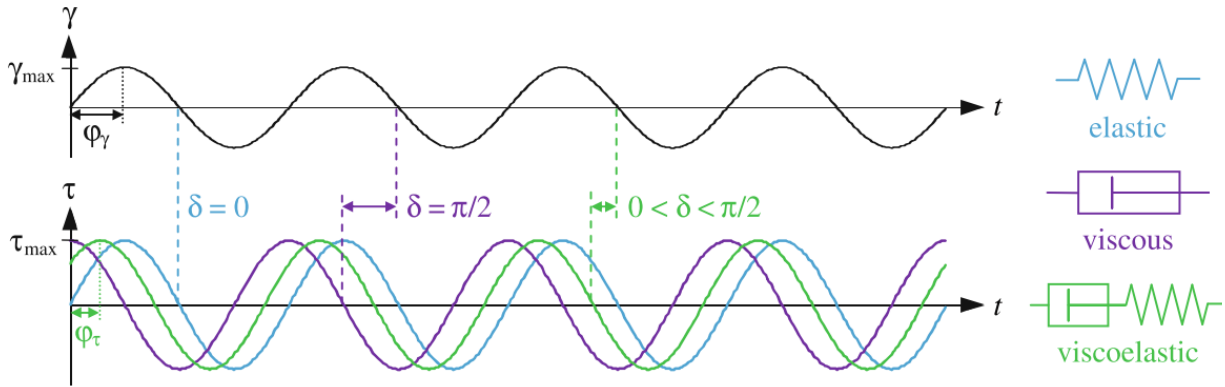

Figure 2.5 Sinusoidal shear strain (top) and stress responses of different materials (bottom) (Laupheimer, 2014).

To characterize the relationship between stress and strain response, complex modulus (G^*) is calculated as below,

$$G^* = \frac{\tau_{max}}{\gamma_{max}}$$

with the trigonometrical laws to extrapolate out two components, one indicating the energy stored by the material and represents the elastic behavior is called storage modulus (G'),

$$G' = G^* \cos(\delta)$$

another imaginary component is loss modulus (G"), which indicates the energy dissipate during the deformation and related to the viscous properties,
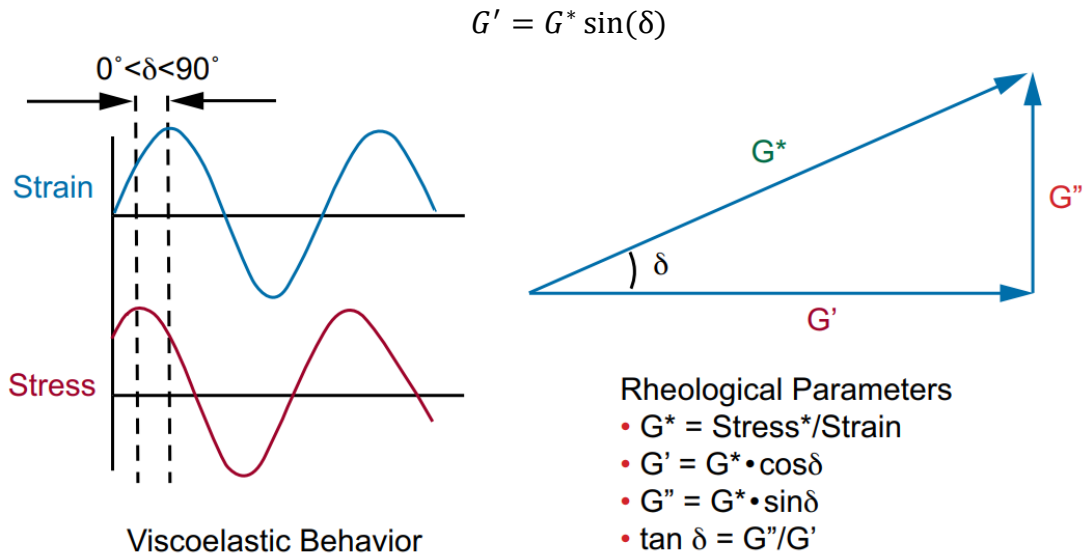
$$G' = G^* \sin(\delta)$$

Figure 2.6 Visualization of G* with the real and imaginary moduli derived from trigonometry.

2.4.4 Oscillation strain sweep test

Viscoelastic properties are monitored at constant angular frequency and temperature in strain sweep test. The stress to strain relationship also the yield point where solid starts to turn into gel are able to determine in this test. Before the yield point, the linear viscoelastic region (LVR) can be identified and proper strain value is chosen to use in the oscillation frequency sweep test. Within the LVR, the molecular level of structures are close to equilibrium and the responses are directly to the dynamic processes which provides reliable data and insights to the true information about the structures.

2.4.5 Oscillation frequency sweep test

In a frequency sweep test, temperature and strain are held constant while the viscoelastic properties are monitored as the frequency is varied. It provides information about the gel rigidity against the frequency which storage modulus (G') and loss modulus (G") are plotted on graphs as a function of frequency. As frequency is the inverse of time, the curve shows the time dependent mechanical response. For instance, in worm-like long chain polymer system, with short times (high frequency) structures tend to entangle and corresponding to solid-like behavior. And at low frequency, liquid–like behavior is observed. However, in the weak-gel system, structures especially with short range aggregate particle network or emulsions, are easily break down into

liquid and flow at high frequency region.

2.5 Ultra-small-angle X-ray scattering

Ultra-small-angle X-ray scattering with advanced techniques developed this decade make it a great tool for non-destructively investigating of the structural information of fragile structures. With the capability of characterizing structure size ranging from 1 nm to 1 μm has expended the application in biomaterial science and food science for understanding the 3D structural while minimizing the damage during the measurements (Kuo, Ilavsky, & Lee, 2016; Yunqi Li et al., 2012; Peyronel, Ilavsky, Mazzanti, Marangoni, & Pink, 2013; Peyronel, Quinn, Marangoni, & Pink, 2014; Yang, Chaisoontornyotin, & Hoepfner, 2018).

According to Bragg's law, $\lambda = 2d \sin\Theta$. When the probed dimension d is measured at very small angle, $\sin\theta \cong \theta$, it proportionally correlates to $\lambda / (2\theta)$. Based on this principle, the scattering vector q is defined and used in small to ultra-small x-ray scattering measurements as,

$$q = \frac{4\pi \sin\theta}{\lambda}$$

where 2θ is the scattering angle and λ is the incident wavelength. The scattering vector of current USAXS instrument can adapt as low as 10^{-4} angstrom (Jan Ilavsky et al., 2009).

2.5.1 Guinier's law

In a dilute system contains randomly distributed particles with similar shape size, the Gaussian function has been derived to approximate the scattering curve at the smallest angle (at low q region), expressed as,

$$I(q) = I(0) \exp\left(-\frac{-q^2 R_g{}^2}{3}\right)$$

where R_g is the radius of gyration, and $I(0)$ is the scattering intensity extrapolated at zero angle.

$I(0)$ correlates with concentration, contrast and average particle volume, which the Guinier's approximation is suitable for particle with narrow size distribution, otherwise, the data is smeared and hard to determine the R_g.

2.5.2 Porod's law

Porod's approach is important because it built on the assumption of non-dilute system, implying it is appropriate for densely packed particle system (A. Balerna & S. Mobilio, 2015). The scattering results at high q region are mostly due to inter-particles distances. Where in most cases, the sample with a sharp interface between two phases shows a fourth power-low decay ($q^4 I(q)$). Power law exponent (P) is described by the equation below,

$$I(q) = Bq^{-P}$$

where B is the Porod prefactor equals to $2\pi N_p \rho_e^2 S_p$, N_p is the number of particles scattered, ρ_e is the electron density differences between two phases, and S_p is the average surface area of the particle. While P deviated from 4 indicating the surface roughness is increasing with more of the fractal structures observed due to the interfacial contrast of the two phases is not sharp anymore.

2.5.3 The unified fit model

Due to the complexity of system composed of multiple size-scale structures, Greg Beaucage (Beaucage, 1995, 1996, 2012) proposed and developed the general equation that capable of describing the scattering functions. The assumption of unified fit model is based on the concept that scattering can be depicted as coming from one or more structural levels. Each structural information is described as a combination of linear Guinier law and an associated Porod power law scattering. While the observed scattering is one level consisted of two components, the unified fit equation is expressed as,

$$I(q) \simeq G \exp\left(-\frac{q^2 R_g^2}{3}\right) + B\left\{[\mathrm{erf}\left(qR_g/6^{\frac{1}{2}}\right)]^3/q\right\}^P$$

where G is the Guinier scale prefactor, related to the volume of the scatters fall in Guinier region. G equals to $N_p \rho_e^2 V_p^2$, N_p is the number of particles in the scattering volume and ρ_e is the electron density difference between the particle and the surrounding. B is the Porod scale prefactor which locates in Porod power law region contains the information of the specific surface area. B equals to $2\pi N_p \rho_e^2 S_p$, which $\rho_e = n/V_p$, which n is the number of electrons in the particle, V_p and S_p are the volume and surface area of the particle, respectively.

The model returns the radius of gyration, R_g, and the Porod exponent, P. P provides information of the internal structure which can sketch out the possible shape of the fractals that formed by aggregates or agglomerate of the scattering particles (Jan Ilavsky & Jemian, 2009). Generally, it can be defined as,

$$P = 1 \text{ (rods)}$$

$$P = 2 \text{ (disk-like, plates or lamellae)}$$

$$P < 3 \text{ (mass fractals)}$$

$$3 \leq P < 4 \text{ (surface fractals)}$$

$$P = 4 \text{ (spheres, smooth sharp surface)}$$

Simply by plotting the $I(q)$ v.s q on double log plot, the slope obtained can be referred to the P value showed in Figure 2.7.
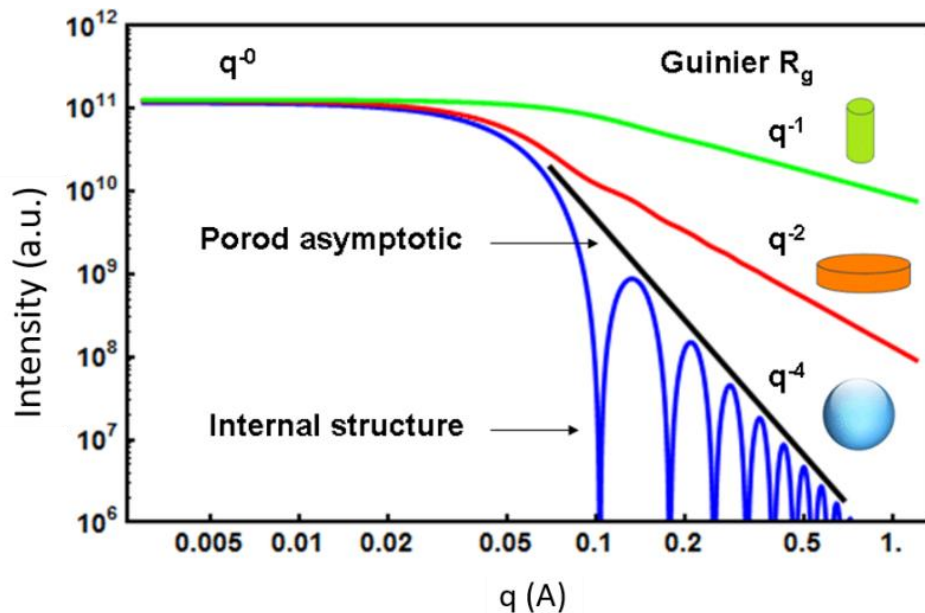

Figure 2.7 The size, shape and the surface roughness information extracted out from the scattering of nano objects can be calculated from the small-angle X-ray scattering (SAXS) curves in a broad q vector range (Angelova et al., 2017).

To better describes different levels of structures in a system, the hierarchical structures of the primary level often defined by the basic unit radius of gyration in the dilute solution. Also, the extended version of the unified function is another useful approach for the analysis of the

17

hierarchical systems (Beaucage, 2012). Which the equation still derived directly from Guinier's law and Porod's law but with multiple levels of Guinier approximation and associated Porod exponent involved,

$$I(q) = \sum_{i=1}^{n} \left(G_i \exp\left(-\frac{-q^2 R_{gi}{}^2}{3}\right) + B_i \exp\left(\frac{-q^2 R_{g,i+1}^2}{3}\right) q_i^{*P_i} \right)$$

where,

$$q^* = \frac{q}{\left\{\text{erf}\left(\frac{kqR_{g,i}}{\sqrt{6}}\right)\right\}^3}$$

This equation indicates each level of structure is generated from the previous smaller structure. The primary unit structure of the particles can aggregate into randomly branched or just aggregate structure in a second level (Hashimoto & Koizumi, 2012). The secondary structure may display as fractals and further built to form larger agglomerates or clusters in the third level. Based on the findings, the k constant value is approximately equal to 1.06 or 1 for a disk-like structure ($P = 2$) and a fractal structure ($P > 3$), respectively.

2.5.4 The Kratky plot

Disordered polymeric chain structure such as proteins, can range arrays of conformation at different conditions. The Kratky plot, $I(q)*q^2$ vs. q plot, is informative to give a first glance by distinguishing the compactness and flexibility of proteins. From the shape of the curve exhibits, we can use for qualitative assessment of protein disorder. For instance, a compact globular protein will have a $I(q)$ decay as q^{-4}, whereas the scattering intensity of a flexible Gaussian chain will decay as q^{-2} or slower. When plotting these data on Kratky plot, at high q region, the compact protein will have $q^2I(q)$ values that approach zero (or baseline), and for unfolded, partial unfolded, or even disordered proteins will gradually plateau at intermediate q range then followed by continuously increasing values of $q^2I(q)$ at higher angle (Kikhney & Svergun, 2015) (Figure 2.8).
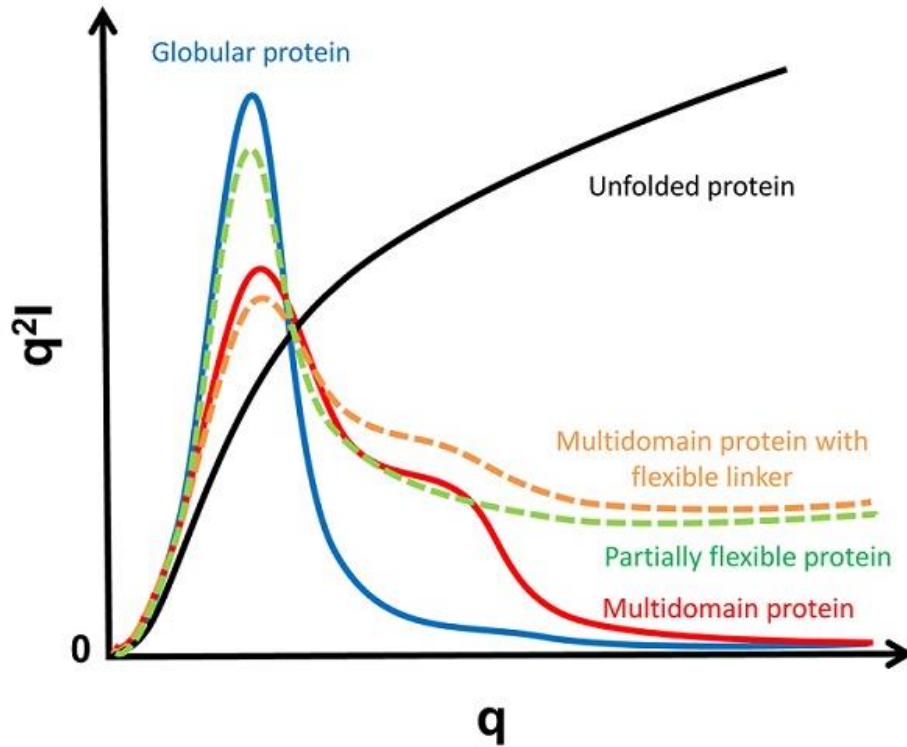
Figure 2.8 The various conformation of proteins illustrated on the Kratky plot with distinct curve shapes (Ochbaum & Bitton, 2018).

Due to the Kratky plot emphasizes the $I(q)$ deviation from the high q region behavior, in polymer science, it is also common to use this plot to understand the behavior of a polymer system. Using three different functions with dimensionless variable $x = q$ to simulate three cases of rigid rod, Gaussian chain and branched system displayed on Kratky plot. First, plotting $I(x) = I_0/(1+x)$ for rigid rod, it linearly increases in high q region. For Gaussian chain, the function of $I(x) = I_0/(1+x^2)$ will gradually come to a plateau. Lastly, the fractal system plotted as $I(x) = I_0/(1+x^3)$ would reach to a maximum then decay to the high x limit (Hammouda, 2010) (Sharma, Verma, Khan, Kumar, & Khan, 2018) (Figure 2.9). The peak position can be also correlated to the radius of gyration where it is inversely proportional to the q value.
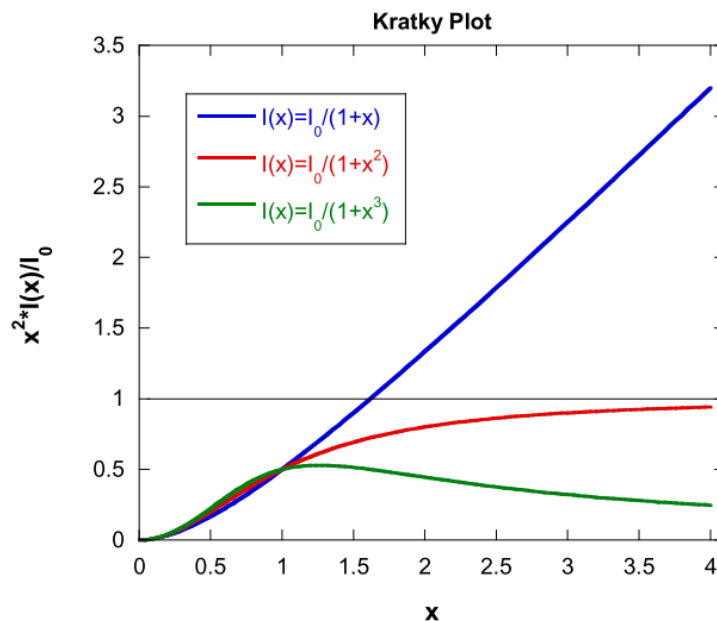
Figure 2.9 Symbolic representation of the Kratky plot for the three cases of a rigid rod (blue), a Gaussian chain (red) and a mass fractal (green) (Ochbaum & Bitton, 2018).

For stiff chains such as Kuhn segments, scattering at high q region is assumed to be rigid thin rods, the low q region is expected to be large dimension of the structure. And in between, there is a transition which can be found on Kratky plot and is used to calculate the Kuhn segment length which consists the worm-like chain. By extrapolating the Gaussian plateau to large q and the rod-like straight line towards smaller q, the kink point q^* showed in Figure 2.10 is defined as the Kuhn segment length (S. B. Ross-Murphy, 1994).
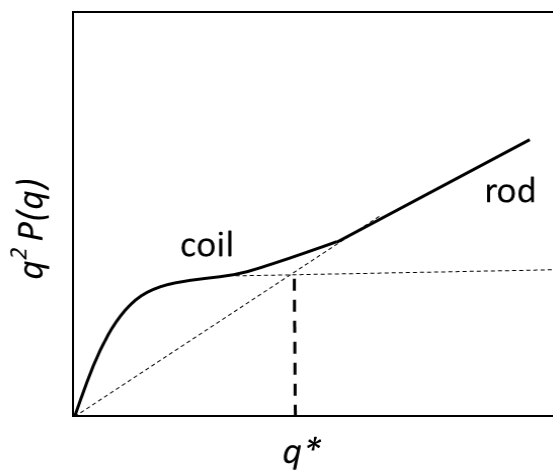

Figure 2.10 Idealized coil and rod behavior of a wormlike chain in the Kratky plot (Burchard, 1993).

2.5.5 The Advanced Photon Source (APS) USAXS instrument at Argonne National Laboratory

At APS, USAXS instrument uses the relativistic electrons produced by radiation source are accelerated passing through magnetic field in a curved path which can provide continuous access to x-rays in the range from 3.2 to 80 keV and even above. Based on the design of Bonse and Hart (1965), a Bonse-Hart camera is installed with even numbers of collimating crystals, Si (111) or (220) of 150 mm (length) × 25 mm (width). Which Si (111) is optimal for x-ray energies below 12 keV, while Si (220) has better performance for energies above 16 keV. The number of reflections between crystals, can effectively improve and optimize the signal-to-noise ratio. With the 1-D collimated USAXS configuration (Figure 2.11), data within a large q rang (1×10^{-4} to 1 Å^{-1}) is able to be collected (J. Ilavsky et al., 2013).
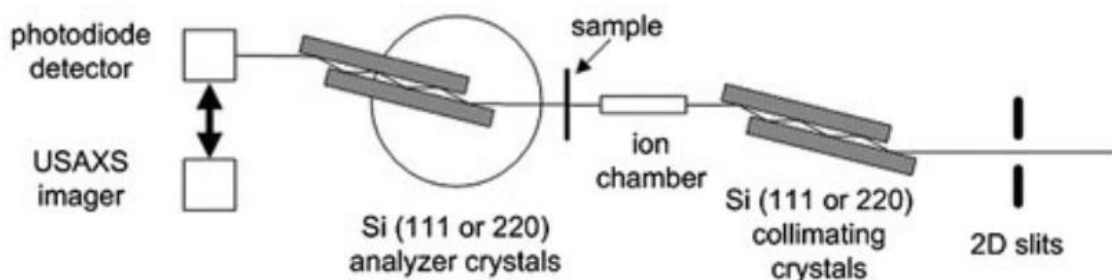

Figure 2.11 Schematic of the APS USAXS instrument in 1D-collimated configuration. (Adapted from Ilavsky et al. (2012)).

2.6 References

Ahmed, E. M. (2015). Hydrogel: Preparation, characterization, and applications: A review. *Journal of Advanced Research*, *6*(2), 105–121. https://doi.org/10.1016/j.jare.2013.07.006

Alavi, F., Momen, S., Emam-Djomeh, Z., Salami, M., & Moosavi-Movahedi, A. A. (2018). Radical cross-linked whey protein aggregates as building blocks of non-heated cold-set gels. *Food Hydrocolloids*, *81*, 429–441. https://doi.org/10.1016/j.foodhyd.2018.03.016

Alger, M. (2017). *Polymer Science Dictionary.* Springer. https://doi.org/10.1007/978-94-024-0893-5

Angelova, A., Garamus, V. M., Angelov, B., Tian, Z., Li, Y., & Zou, A. (2017). Advances in structural design of lipid-based nanoparticle carriers for delivery of macromolecular drugs, phytochemicals and anti-tumor agents. *Advances in Colloid and Interface Science, 249*, 331–345. https://doi.org/10.1016/j.cis.2017.04.006

Argos, P., Pedersen, K., Marksl, M. D., & Larkinsflll, B. A. (1982). Structural model for maize zein proteins. *Journal of Biological Chemistry, 257*(17), 9984–9990.

Balerna, A., & Mobilio, S. (2015). Introduction to synchrotron radiation. In Mobilio, S., Boscherini, F., Meneghini, C. (Eds.) *Synchrotron Radiation: Basics, Methods and Applications*, 3–28. Springer. https://doi.org/10.1007/978-3-642-55315-8

Bajpai, M., Sharma, P. K., & Mittal, A. (2009). A study of oleic acid oily base for the tropical delivery of dexamethasone microemulsion formulations. *Asian Journal of Pharmaceutics*, *3*(3), 208–214. https://doi.org/10.4103/0973-8398.56299

Beaucage, G. (1995). Approximations leading to a unified exponential/power-law approach to small-angle scattering. *Journal of Applied Crystallography*, *28*(6), 717–728. https://doi.org/10.1107/s0021889895005292

Beaucage, G. (1996). Small-angle scattering from polymeric mass fractals of arbitrary mass-fractal dimension. *Journal of Applied Crystallography*, *29*(2), 134–146. https://doi.org/10.1107/S0021889895011605

Beaucage, G. (2012). Combined small-angle scattering for characterization of hierarchically structured polymer systems over nano-to-micron meter: Part II theory. In Matyjaszewski, K. & and Moeller, M. (Eds.). *Polymer Science: A Comprehensive Reference*, *10(*2), 399–409. Elsevier B.V. https://doi.org/10.1016/B978-0-444-53349-4.00032-7

Benson, M. D., Buxbaum, J. N., Eisenberg, D. S., Merlini, G., Saraiva, M. J. M., Sekijima, Y., Westermark, P. (2018). Amyloid nomenclature 2018: recommendations by the International Society of Amyloidosis (ISA) nomenclature committee. *Amyloid*, *25*(4), 215–219. https://doi.org/10.1080/13506129.2018.1549825

Berthaume, M. A. (2016). Food mechanical properties and dietary ecology. *American Journal of Physical Anthropology*, *159*, 79–104. https://doi.org/10.1002/ajpa.22903

Blach, C., Gravelle, A. J., Peyronel, F., Weiss, J., Barbut, S., & Marangoni, A. G. (2016). Revisiting the crystallization behavior of stearyl alcohol : stearic acid (SO : SA) mixtures in edible oil. *RSC Advances*, *6*(84), 81151–81163. https://doi.org/10.1039/c6ra15142f

Brosey, C. A., & Tainer, J. A. (2019). Evolving SAXS versatility: solution X-ray scattering for macromolecular architecture, functional landscapes, and integrative structural biology. *Current Opinion in Structural Biology*, *58*, 197–213. https://doi.org/10.1016/j.sbi.2019.04.004

Burchard, W. (2014). Light scattering techniques. In Ross-Murphy, S. B. (Ed.). *Physical techniques for the Study of Food Biopolymers*, 1, 151–214. Springer-Science+Business Media, B.V.

Buruiana, L. I., & Ioan, S. (2018). Polymer gel composites for bio-applications. In Thakur, V. K., & Thakur, M. K. (Eds.). *Polymer Gels: Perspectives and Applications*, 111–123. Springer. https://doi.org/10.1007/978-981-10-6080-9_5

Buscemi, S., Corleo, D., Di Pace, F., Petroni, M. L., Satriano, A., & Marchesini, G. (2018). The effect of lutein on eye and extra-eye health. *Nutrients*, *10*(9), 1–24.

https://doi.org/10.3390/nu10091321

Cerqueira, M. A., Fasolin, L. H., Picone, C. S. F., Pastrana, L. M., Cunha, R. L., & Vicente, A. A. (2017). Structural and mechanical properties of organogels: Role of oil and gelator molecular structure. *Food Research International*, *96*, 161–170. https://doi.org/10.1016/j.foodres.2017.03.021

Chakraborty, P., Das, S., & Nandi, A. K. (2018). Conducting gels: A chronicle of technological advances. *Progress in Polymer Science*, *88*, 189–219. https://doi.org/10.1016/j.progpolymsci.2018.08.004

Chavan, R. S., Khedkar, C. D., & Bhatt, S. (2015). Fat Replacer. *Encyclopedia of Food and Health*, 589–595. https://doi.org/10.1016/B978-0-12-384947-2.00271-3

Chaves, K. F., Barrera-Arellano, D., & Ribeiro, A. P. B. (2018). Potential application of lipid organogels for food industry. *Food Research International*, *105*, 863–872. https://doi.org/10.1016/j.foodres.2017.12.020

Chen, X., Fu, S., Hou, J., Guo, J., Wang, J., & Yang, X. (2016). Zein based oil-in-glycerol emulgels enriched with b -carotene as margarine alternatives. *Food Chemistry*, *211*, 836–844. https://doi.org/10.1016/j.foodchem.2016.05.133

Chen, Y., Ye, R., & Liu, J. (2013). Understanding of dispersion and aggregation of suspensions of zein nanoparticles in aqueous alcohol solutions after thermal treatment. *Industrial Crops and Products*, *50*, 764–770. https://doi.org/10.1016/j.indcrop.2013.08.023

Cheng, C. J., Ferruzzi, M., & Jones, O. G. (2019). Food hydrocolloids fate of lutein-containing zein nanoparticles following simulated gastric and intestinal digestion. *Food Hydrocolloids*, *87*, 229–236. https://doi.org/10.1016/j.foodhyd.2018.08.013

Choudhary, B., Paul, S. R., Nayak, S. K., Qureshi, D., & Pal, K. (2018). Synthesis and biomedical applications of filled hydrogels. In Pal, K., & Banerjee, I. (Eds.). *Polymeric Gels*, 283–302. Elsevier. https://doi.org/10.1016/B978-0-08-102179-8.00011-9

Cornwell, D. J., & Smith, D. K. (2015). Expanding the scope of gels - Combining polymers with low-molecular-weight gelators to yield modified self-assembling smart materials with high-tech applications. *Materials Horizons*, *2*(3), 279–293. https://doi.org/10.1039/c4mh00245h

Dassanayake, L. S. K., Kodali, D. R., & Ueno, S. (2011). Formation of oleogels based on edible lipid materials. *Current Opinion in Colloid and Interface Science*. https://doi.org/10.1016/j.cocis.2011.05.005

De Almeida, C. B., Corradini, E., Forato, L. A., Fujihara, R., & Filho, J. F. L. (2018). Microstructure and thermal and functional properties of biodegradable films produced using zein. *Polimeros*, *28*(1), 30–37. https://doi.org/10.1590/0104-1428.11516

De Boer, F. Y., Kok, R. N. U., Imhof, A., & Velikov, K. P. (2018). White zein colloidal particles: Synthesis and characterization of their optical properties on the single particle level and in concentrated suspensions. *Soft Matter*, *14*(15), 2870–2878. https://doi.org/10.1039/c7sm02415k

De Folter, J. W. J., Van Ruijven, M. W. M., & Velikov, K. P. (2012). Oil-in-water Pickering

emulsions stabilized by colloidal particles from the water-insoluble protein zein. *Soft Matter*, *8*(25), 6807–6815. https://doi.org/10.1039/c2sm07417f

De Gennes, P. G., & Taupin, C. (1982). Microemulsions and the flexibility of oil/water interfaces. *Journal of Physical Chemistry*, *86*(13), 2294–2304. https://doi.org/10.1021/j100210a011

De Vries, A., Gomez, Y. L., Van der Linden, E., & Scholten, E. (2017). The effect of oil type on network formation by protein aggregates into oleogels. *RSC Advances*, *7*(19), 11803–11812. https://doi.org/10.1039/c7ra00396j

De Vries, A., Jansen, D., van der Linden, E., & Scholten, E. (2018). Tuning the rheological properties of protein-based oleogels by water addition and heat treatment. *Food Hydrocolloids*, *79*, 100–109. https://doi.org/10.1016/j.foodhyd.2017.11.043

De Vries, A., Lopez Gomez, Y., Jansen, B., Van der Linden, E., & Scholten, E. (2017). Controlling agglomeration of protein aggregates for structure formation in liquid oil: A sticky business. *ACS Applied Materials and Interfaces*, *9*(11), 10136–10147. https://doi.org/10.1021/acsami.7b00443

De Vries, A., Nikiforidis, C. V., D., & Scholten, E. (2014). Natural amphiphilic proteins as tri-block Janus particles : Self-sorting into thermo-responsive gels. *Europhysics Letters*, 107,   5, 100–109. https://doi.org/10.1209/0295-5075/107/58003

Derkach, S. R. (2009). Rheology of emulsions. *Advances in Colloid and Interface Science*, *151*(1–2), 1–23. https://doi.org/10.1016/j.cis.2009.07.001

Donsì, F., Voudouris, P., Veen, S. J., & Velikov, K. P. (2017). Zein-based colloidal particles for encapsulation and delivery of epigallocatechin gallate. *Food Hydrocolloids*, *63*, 508–517. https://doi.org/10.1016/j.foodhyd.2016.09.039

Dreher, J., Blach, C., Terjung, N., Gibis, M., & Weiss, J. (2020). Formation and characterization of plant-based emulsified and crosslinked fat crystal networks to mimic animal fat tissue. *Journal of Food Science*, *85*(2), 421–431. https://doi.org/10.1111/1750-3841.14993

Drozdov, A. D., & Christiansen, J. D. (2013). Stress-strain relations for hydrogels under multiaxial deformation. *International Journal of Solids and Structures*, *50*(22–23), 3570–3585. https://doi.org/10.1016/j.ijsolstr.2013.06.023

Erickson, D. P., Ozturk, O. K., Selling, G., Chen, F., Campanella, O. H., & Hamaker, B. R. (2020). Corn zein undergoes conformational changes to higher β-sheet content during its self-assembly in an increasingly hydrophilic solvent. *International Journal of Biological Macromolecules*, *157*, 232–239. https://doi.org/10.1016/j.ijbiomac.2020.04.169

Esposito, C. L., Kirilov, P., & Roullin, V. G. (2018). Organogels, promising drug delivery systems: an update of state-of-the-art and recent applications. *Journal of Controlled Release*, *271*, 1–20. https://doi.org/10.1016/j.jconrel.2017.12.019

Figura, L. O., & A.Teixeira, A. (2007). *Food Physics*. Springer.

Flores-Villaseñor, S. E., Peralta-Rodríguez, R. D., Ramirez-Contreras, J. C., Cortes-Mazatán, G. Y., & Estrada-Ramírez, A. N. (2016). Biocompatible microemulsions for the nanoencapsulation of essential oils and nutraceuticals A2 - Grumezescu, Alexandru Mihai BT

- Encapsulations. *Nanotechnology in the Agri-Food Industry*. Elsevier Inc. https://doi.org/http://dx.doi.org/10.1016/B978-0-12-804307-3.00012-0

Flory, P. J. (1974). Introductory lecture. *Faraday Discussions of the Chemical Society*, *57*, 7–18. https://doi.org/10.1039/DC9745700007

Fu, D., & Weller, C. L. (1999). Rheology of zein solutions in aqueous ethanol. *Journal of Agricultural and Food Chemistry*, *47*(5), 2103–2108. https://doi.org/10.1021/jf9811121

Gao, Z. M., Yang, X. Q., Wu, N. N., Wang, L. J., Wang, J. M., Guo, J., & Yin, S. W. (2014). Protein-based pickering emulsion and oil gel prepared by complexes of zein colloidal particles and stearate. *Journal of Agricultural and Food Chemistry*, *62*(12), 2672–2678. https://doi.org/10.1021/jf500005y

Godoy, C. A., Valiente, M., Pons, R., & Montalvo, G. (2015). Effect of fatty acids on self-assembly of soybean lecithin systems. *Colloids and Surfaces B: Biointerfaces*, *131*, 21–28. https://doi.org/10.1016/j.colsurfb.2015.03.065

Gonzalez-Gutierrez, J., & Scanlon, M. G. (2018). Rheology and mechanical properties of fats. structure-function analysis of edible fats. In Marangoni, A. (Ed.). *Structure-function analysis of edible fats,* 127–172. AOCS Press. https://doi.org/10.1016/B978-0-12-814041-3.00005-8

Gorusupudi, A., & Baskaran, V. (2013). Wheat germ oil: A potential facilitator to improve lutein bioavailability in mice. *Nutrition*, *29*(5), 790–795. https://doi.org/10.1016/j.nut.2012.11.003

Gupta, P., Vermani, K., & Garg, S. (2002). Hydrogels : from controlled release to pH-responsive drug delivery. *Drug Discovery Today, 7*(10), 569–579.

Guzhova, I. V., Lazarev, V. F., Kaznacheeva, A. V., Ippolitova, M. V., Muronetz, V. I., Kinev, A. V., & Margulis, B. A. (2011). Novel mechanism of Hsp70 chaperone-mediated prevention of polyglutamine aggregates in a cellular model of huntington disease. *Human Molecular Genetics*, *20*(20), 3953–3963. https://doi.org/10.1093/hmg/ddr314

Hammouda, B. (2010). *Probing Nanoscale Structures – The Sans Toolbox*. https://www.ncnr.nist.gov/staff/hammouda/the_SANS_toolbox.pdf

Hashimoto, T., & Koizumi, S. (2012). Combined small-angle scattering for characterization of hierarchically structured polymer systems over nano-to-micron meter: Part I experiments. In Matyjaszewski, K. & and Moeller, M. (Eds.). *Polymer Science: A Comprehensive Reference*, *10*(2), 381–398. Elsevier B.V. https://doi.org/10.1016/B978-0-444-53349-4.00297-1

Hughes, N. E., Marangoni, A. G., Wright, A. J., Rogers, M. A., & Rush, J. W. E. (2009). Potential food applications of edible oil organogels. *Trends in Food Science and Technology*, *20*(10), 470–480. https://doi.org/10.1016/j.tifs.2009.06.002

Ikeda, S., & Nishinari, K. (2001). "Weak gel"-type rheological properties of aqueous dispersions of nonaggregated κ-carrageenan helices. *Journal of Agricultural and Food Chemistry*, *49*(9), 4436–4441. https://doi.org/10.1021/jf0103065

Ilavsky, J., Zhang, F., Allen, A. J., Levine, L. E., Jemian, P. R., & Long, G. G. (2013). Ultra-small-angle X-ray scattering instrument at the advanced photon source: History, recent development, and current status. *Metallurgical and Materials Transactions A: Physical Metallurgy and*

Materials Science, *44*(1), 68–76. https://doi.org/10.1007/s11661-012-1431-y

Ilavsky, Jan, & Jemian, P. R. (2009). Irena: Tool suite for modeling and analysis of small-angle scattering. *Journal of Applied Crystallography*, *42*(2), 347–353. https://doi.org/10.1107/S0021889809002222

Ilavsky, Jan, Jemian, P. R., Allen, A. J., Zhang, F., Levine, L. E., & Long, G. G. (2009). Ultra-small-angle X-ray scattering at the Advanced Photon Source. *Journal of Applied Crystallography*, *42*(3), 469–479. https://doi.org/10.1107/S0021889809008802

Iwahashi, M., Yamaguchi, Y., Kato, T., Horiuchi, T., Sakurai, I., & Suzuki, M. (1991). Temperature dependence of molecular conformation and liquid structure of cis-9-octadecenoic acid. *Journal of Physical Chemistry*, *95*(1), 445–451. https://doi.org/10.1021/j100154a078

Kasaai, M. R. (2018a). Trends in food science & technology zein and zein-based nano-materials for food and nutrition applications : A review. *Trends in Food Science & Technology*, *79*, 184–197. https://doi.org/10.1016/j.tifs.2018.07.015

Kasaai, M. R. (2018b). Trends in food science & technology zein and zein -based nano-materials for food and nutrition applications : A review. *Trends in Food Science & Technology*, *79*, 184–197. https://doi.org/10.1016/j.tifs.2018.07.015

Khalil, A. A., Deraz, S. F., Elrahman, S. A., & El-Fawal, G. (2015). Enhancement of mechanical properties, microstructure, and antimicrobial activities of zein films cross-linked using succinic anhydride, eugenol, and citric acid. *Preparative Biochemistry and Biotechnology*, *45*(6), 551–567. https://doi.org/10.1080/10826068.2014.940967

Kharlamova, A., Chassenieux, C., & Nicolai, T. (2018). Acid-induced gelation of whey protein aggregates: Kinetics, gel structure and rheological properties. *Food Hydrocolloids*, *81*, 263–272. https://doi.org/10.1016/j.foodhyd.2018.02.043

Kharlamova, A., Nicolai, T., & Chassenieux, C. (2018). Mixtures of sodium caseinate and whey protein aggregates: Viscosity and acid- or salt-induced gelation. *International Dairy Journal*, *86*, 110–119. https://doi.org/10.1016/j.idairyj.2018.07.002

Kikhney, A. G., & Svergun, D. I. (2015). A practical guide to small angle X-ray scattering (SAXS) of flexible and intrinsically disordered proteins. *FEBS Letters*, *589*(19), 2570–2577. https://doi.org/10.1016/j.febslet.2015.08.027

Kim, S., & Xu, J. (2008). Aggregate formation of zein and its structural inversion in aqueous ethanol. *Journal of Cereal Science*, *47*(1), 1–5. https://doi.org/10.1016/j.jcs.2007.08.004

Komaiko, J. S., & Mcclements, D. J. (2016). Formation of food-grade nanoemulsions using low-energy preparation methods: A review of available methods. *Comprehensive Reviews in Food Science and Food Safety*, *15*(2), 331–352. https://doi.org/10.1111/1541-4337.12189

Kuo, W. Y., Ilavsky, J., & Lee, Y. (2016). Structural characterization of solid lipoproteic colloid gels by ultra-small-angle X-ray scattering and the relation with sodium release. *Food Hydrocolloids*, *56*, 325–333. https://doi.org/10.1016/j.foodhyd.2015.12.032

Lai, H. M., Geil, P. H., & Padua, G. W. (1999). X-ray diffraction characterization of the structure of zein-oleic acid films. *Journal of Applied Polymer Science*, *71*(8), 1267–1281.

https://doi.org/10.1002/(SICI)1097-4628(19990222)71:8<1267::AID-APP7>3.0.CO;2-O

Laupheimer, M. (2014). *Gelled Bicontinuous Microemulsions. A New Type of Orthogonal Self-Assembled Systems.* Springer. http://link.springer.com/10.1007/978-3-319-07719-2

Laurati, M., Petekidis, G., Koumakis, N., Cardinaux, F., Schofield, A. B., Brader, J. M., & Egelhaaf, S. U. (2009). Structure, dynamics, and rheology of colloid-polymer mixtures: From liquids to gels. *Journal of Chemical Physics*, *130*(13). https://doi.org/10.1063/1.3103889

Lee, B. Il, Suh, Y. S., Chung, Y. J., Yu, K., & Park, C. B. (2017). Shedding light on Alzheimer's β-amyloidosis: Photosensitized methylene blue inhibits self-assembly of β-amyloid peptides and disintegrates their aggregates. *Scientific Reports*, *7*(1), 1–10. https://doi.org/10.1038/s41598-017-07581-2

Li, Ying, & Corredig, M. (2020). Acid induced gelation behavior of skim milk concentrated by membrane filtration. *Journal of Texture Studies*, *51*(1), 101–110. https://doi.org/10.1111/jtxs.12492

Li, Yunqi, Li, J., Xia, Q., Zhang, B., Wang, Q., & Huang, Q. (2012). Understanding the dissolution of α-zein in aqueous ethanol and acetic acid solutions. *Journal of Physical Chemistry B*, *116*(39), 12057–12064. https://doi.org/10.1021/jp305709y

Lv, G., Wang, F., Cai, W., Li, H., & Zhang, X. (2014). Influences of addition of hydrophilic surfactants on the W/O emulsions stabilized by lipophilic surfactants. *Colloids and Surfaces A: Physicochemical and Engineering Aspects*, *457*(1), 441–448. https://doi.org/10.1016/j.colsurfa.2014.06.031

Marín, T., Montoya, P., Arnache, O., Pinal, R., & Calderón, J. (2018). Bioactive films of zein/magnetite magnetically stimuli-responsive for controlled drug release. *Journal of Magnetism and Magnetic Materials*, *458*, 355–364. https://doi.org/10.1016/j.jmmm.2018.03.046

Martins, A. J., Vicente, A. A., Cunha, R. L., & Cerqueira, M. A. (2018). Edible oleogels: An opportunity for fat replacement in foods. *Food and Function*, *9*(2), 758–773. https://doi.org/10.1039/c7fo01641g

Marze, S., Guillermic, R. M., & Saint-Jalmes, A. (2009). Oscillatory rheology of aqueous foams: Surfactant, liquid fraction, experimental protocol and aging effects. *Soft Matter*, *5*(9), 1937–1946. https://doi.org/10.1039/b817543h

Masalova, I., Malkin, A. Y., Ferg, E., Kharatiyan, E., Taylor, M., & Haldenwang, R. (2006). Evolution of rheological properties of highly concentrated emulsions with aging —Emulsion-to-suspension transition. *Journal of Rheology*, *50*(4), 435–451. https://doi.org/10.1122/1.2206712

Masamba, K., Li, Y., Hategekimana, J., Liu, F., & Ma, J. (2016). Effect of gallic acid on mechanical and water barrier properties of zein-oleic acid composite films. *Journal of Food Science and Technology*, *53*, 2227–2235. https://doi.org/10.1007/s13197-015-2167-7

Matsushima, N., Danno, G. I., Takezawa, H., & Izumi, Y. (1997). Three-dimensional structure of maize α-zein proteins studied by small-angle X-ray scattering. *Biochimica et Biophysica Acta*

- *Protein Structure and Molecular Enzymology*, *1339*(1), 14–22. https://doi.org/10.1016/S0167-4838(96)00212-9

Mewis, J., & Wagner, N. J. (2011). *Colloidal Suspension Rheology*. Cambridge University Press. https://doi.org/10.1017/CBO9780511977978

Mewis, J., Wagner, N. J., Mewis, J., & Wagner, N. J. (2011a). Introduction to colloid science and rheology. *Colloidal Suspension Rheology*, 1–35. https://doi.org/10.1017/cbo9780511977978.004

Mewis, J., Wagner, N. J., Mewis, J., & Wagner, N. J. (2011b). Suspensions in viscoelastic media. *Colloidal Suspension Rheology*, 2, 325–353. https://doi.org/10.1017/cbo9780511977978.013

Mezzenga, R. (2011). Protein-templated oil gels and powders. In Marangoni, A. G., & Garti, N. (Eds.). *Edible Oleogels: Structure and Health Implications*, 307–329. Elsevier Inc. https://doi.org/10.1016/B978-0-9830791-1-8.50015-2

Milston, R., Madigan, M. C., & Sebag, J. (2016). Vitreous floaters: Etiology, diagnostics, and management. *Survey of Ophthalmology*, *61*(2), 211–227. https://doi.org/10.1016/j.survophthal.2015.11.008

Mobilio, S., Boscherini, F., Meneghini, C. (2015). *Synchrotron Radiation: Basics, Methods and Applications.* Springer. https://doi.org/10.1007/978-3-642-55315-8

Moradkhannejhad, L., Abdouss, M., Nikfarjam, N., Mazinani, S., & Heydari, V. (2018). Morphology investigation electrospinning of zein / propolis nano fibers ; antimicrobial properties and morphology investigation. *Journal of Materials Science: Materials in Medicine*, (November). https://doi.org/10.1007/s10856-018-6174-x

Nabetani, H., Ichikawa, S., Liu, X., Nakajima, M., & Xu, Q. (2007). Factors affecting the properties of ethanol-in-oil emulsions. *Food Science and Technology Research*, *8*(1), 36–41. https://doi.org/10.3136/fstr.8.36

Nephomnyshy, I., Rosen-Kligvasser, J., & Davidovich-Pinhas, M. (2020). The development of a direct approach to formulate high oil content zein-based emulsion gels using moderate temperatures. *Food Hydrocolloids*, *101*, 105528. https://doi.org/10.1016/j.foodhyd.2019.105528

Nikiforidis, C. V., Gilbert, E. P., & Scholten, E. (2015). Organogel formation via supramolecular assembly of oleic acid and sodium oleate. *RSC Advances*, *5*(59), 47466–47475. https://doi.org/10.1039/c5ra05336f

Nonthanum, P., Lee, Y., & Padua, G. W. (2012). Effect of γ-zein on the rheological behavior of concentrated zein solutions. *Journal of Agricultural and Food Chemistry*, *60*(7), 1742–1747. https://doi.org/10.1021/jf2035302

Nonthanum, P., Lee, Y., & Padua, G. W. (2013). Effect of pH and ethanol content of solvent on rheology of zein solutions. *Journal of Cereal Science*, *58*(1), 76–81. https://doi.org/10.1016/j.jcs.2013.04.001

O'Sullivan, C. M., Barbut, S., & Marangoni, A. G. (2016). Edible oleogels for the oral delivery of lipid soluble molecules: Composition and structural design considerations. *Trends in Food Science and Technology*. https://doi.org/10.1016/j.tifs.2016.08.018

Ochbaum, G., & Bitton, R. (2018). Using small-angle X-ray scattering (SAXS) to study the structure of self-assembling biomaterials. In Azevedo, H. S., & De Silva, R. M. P. (Eds.). *Self-Assembling Biomaterials: Molecular Design, Characterization and Application in Biology and Medicine*, 291–304. Elsevier Ltd. https://doi.org/10.1016/B978-0-08-102015-9.00015-0

Ochowiak, M., Broniarz-Press, L., & Rozanski, J. (2012). Rheology and Structure of Emulsions and Suspensions. *Journal of Dispersion Science and Technology*, *33*(2), 177–184. https://doi.org/10.1080/01932691.2010.548694

Pal, R. (2011). Influence of interfacial rheology on the viscosity of concentrated emulsions. *Journal of Colloid and Interface Science*, *356*(1), 118–122. https://doi.org/10.1016/j.jcis.2010.12.068

Patel, A. R. (2017). A colloidal gel perspective for understanding oleogelation. *Current Opinion in Food Science*, *15*, 1–7. https://doi.org/10.1016/j.cofs.2017.02.013

Patel, A. R., Cludts, N., Bin Sintang, M. D., Lewille, B., Lesaffer, A., & Dewettinck, K. (2014). Polysaccharide-based oleogels prepared with an emulsion-templated approach. *ChemPhysChem*, *15*(16), 3435–3439. https://doi.org/10.1002/cphc.201402473

Patel, A. R., & Dewettinck, K. (2016). Edible oil structuring: An overview and recent updates. *Food and Function*, *7*(1), 20–29. https://doi.org/10.1039/c5fo01006c

Patel, A. R., Dumlu, P., Vermeir, L., Lewille, B., Lesaffer, A., & Dewettinck, K. (2015). Rheological characterization of gel-in-oil-in-gel type structured emulsions. *Food Hydrocolloids*, *46*, 84–92. https://doi.org/10.1016/j.foodhyd.2014.12.029

Patel, A. R., & Velikov, K. P. (2014). Zein as a source of functional colloidal nano- and microstructures. *Current Opinion in Colloid and Interface Science*, *19*(5), 450–458. https://doi.org/10.1016/j.cocis.2014.08.001

Pehlivanoğlu, H., Demirci, M., Toker, O. S., Konar, N., Karasu, S., & Sagdic, O. (2018). Oleogels, a promising structured oil for decreasing saturated fatty acid concentrations: Production and food-based applications. *Critical Reviews in Food Science and Nutrition*, *58*(8), 1330–1341. https://doi.org/10.1080/10408398.2016.1256866

Pena-serna, C., & Lopes-filho, J. F. (2013). Influence of ethanol and glycerol concentration over functional and structural properties of zein e oleic acid fi lms. *Materials Chemistry and Physics*, *142*(2–3), 580–585. https://doi.org/10.1016/j.matchemphys.2013.07.056

Pérez-Gago, Maria B., & Krochta, J. M. (2001). Lipid particle size effect on water vapor permeability and mechanical properties of whey protein/beeswax emulsion films. *Journal of Agricultural and Food Chemistry*, *49*(2), 996–1002. https://doi.org/10.1021/jf000615f

Pérez-Gago, Maria Berna, & Rhim, J. W. (2013). Edible coating and film materials: lipid bilayers and lipid emulsions. *Innovations in Food Packaging: Second Edition*, 325–350. https://doi.org/10.1016/B978-0-12-394601-0.00013-8

Peyronel, F., Ilavsky, J., Mazzanti, G., Marangoni, A. G., & Pink, D. A. (2013). Edible oil structures at low and intermediate concentrations. II. Ultra-small angle X-ray scattering of in situ tristearin solids in triolein. *Journal of Applied Physics*, *114*(23). https://doi.org/10.1063/1.4847997

Peyronel, F., Quinn, B., Marangoni, A. G., & Pink, D. A. (2014). Ultra small angle x-ray scattering in complex mixtures of triacylglycerols. *Journal of Physics Condensed Matter*, *26*(46). https://doi.org/10.1088/0953-8984/26/46/464110

Ponton, A., Bose, T. K., & Delbos, G. (1991). Dielectric study of percolation in an oil-continuous microemulsion. *The Journal of Chemical Physics*, *94*(10), 6879–6886. https://doi.org/10.1063/1.460268

Quemada, D., & Berli, C. (2002). Energy of interaction in colloids and its implications in rheological modeling. *Advances in Colloid and Interface Science, 98*(1), 51–85. https://doi.org/10.1016/S0001-8686(01)00093-8

Raeburn, J., Cardoso, A. Z., & Adams, D. J. (2013). The importance of the self-assembly process to control mechanical properties of low molecular weight hydrogels. *Chemical Society Reviews*, *42*(12), 5143–5156. https://doi.org/10.1039/c3cs60030k

Raza, A., Hayat, U., Bilal, M., Iqbal, H. M. N., & Wang, J. Y. (2020). Zein-based micro- and nano-constructs and biologically therapeutic cues with multi-functionalities for oral drug delivery systems. *Journal of Drug Delivery Science and Technology*, *58*. https://doi.org/10.1016/j.jddst.2020.101818

Renner, M., & Melki, R. (2014). Protein aggregation and prionopathies. *Pathologie Biologie*, *62*(3), 162–168. https://doi.org/10.1016/j.patbio.2014.01.003

Roberts, J. E., & Dennison, J. (2015). The photobiology of lutein and zeaxanthin in the eye. *Journal of Ophthalmology*, *2015*. https://doi.org/10.1155/2015/687173

Ross-Murphy, S. B. (1995). Structure–property relationships in food biopolymer gels and solutions. *Journal of Rheology*, *39*(6), 1451–1463. https://doi.org/10.1122/1.550610

Rutkevi, M., Allred, S., Velev, O. D., & Velikov, K. P. (2018). Food Hydrocolloids Stabilization of oil continuous emulsions with colloidal particles from water-insoluble plant proteins, *82*, 89–95. https://doi.org/10.1016/j.foodhyd.2018.04.004

Rutkevičius, M., Allred, S., Velev, O. D., & Velikov, K. P. (2018). Stabilization of oil continuous emulsions with colloidal particles from water-insoluble plant proteins. *Food Hydrocolloids*, *82*, 89–95. https://doi.org/10.1016/j.foodhyd.2018.04.004

Sadeghpour, A., Pirolt, F., & Glatter, O. (2013). Submicrometer-sized pickering emulsions stabilized by silica nanoparticles with adsorbed oleic acid. *Langmuir*, *29*(20), 6004–6012. https://doi.org/10.1021/la4008685

Samateh, M., Sagiri, S. S., & John, G. (2018). *Molecular Oleogels*. *Edible Oleogels*. AOCS Press. https://doi.org/10.1016/b978-0-12-814270-7.00018-6

Sangeetha, N. M., & Maitra, U. (2005). Supramolecular gels: Functions and uses. *Chemical Society Reviews*, *34*(10), 821–836. https://doi.org/10.1039/b417081b

Santos, T. M., Souza Filho, M. de S. M., Muniz, C. R., Morais, J. P. S., Kotzebue, L. R. V., Pereira, A. L. S., & Azeredo, H. M. C. (2017). Zein films with unoxidized or oxidized tannic acid. *Journal of the Science of Food and Agriculture*, *97*(13), 4580–4587. https://doi.org/10.1002/jsfa.8327

Schulz-Schaeffer, W. J. (2010). The synaptic pathology of α-synuclein aggregation in dementia with Lewy bodies, Parkinson's disease and Parkinson's disease dementia. *Acta Neuropathologica*, *120*(2), 131–143. https://doi.org/10.1007/s00401-010-0711-0

Selling, G. W., Hamaker, S. A. H., & Sessa, D. J. (2007). Effect of solvent and temperature on secondary and tertiary structure of zein by circular dichroism. *Cereal Chemistry*, *84*(3), 265–270. https://doi.org/10.1094/CCHEM-84-3-0265

Sengupta, T., & Han, J. H. (2013). Surface Chemistry of Food, Packaging, and Biopolymer Materials. In Han, J. H. (Ed.). *Innovations in Food Packaging: Second Edition*. 51–86. Elsevier Ltd. https://doi.org/10.1016/B978-0-12-394601-0.00004-7

Serrano, J., Goñi, I., & Saura-Calixto, F. (2005). Determination of β-caroten and lutein available from green leafy vegetables by an in vitro digestion and colonic fermentation method. *Journal of Agricultural and Food Chemistry*, *53*(8), 2936–2940. https://doi.org/10.1021/jf0480142

Sharma, S. K. (2018). *Handbook of Materials Characterization. Handbook of Materials Characterization*. Springer. https://doi.org/10.1007/978-3-319-92955-2

Shukla, R., Cheryan, M., & DeVor, R. E. (2000). Solvent extraction of zein from dry-milled corn. *Cereal Chemistry*, *77*(6), 724–730. https://doi.org/10.1094/CCHEM.2000.77.6.724

Siraj, N., Shabbir, M. A., Ahmad, T., Sajjad, A., Khan, M. R., Khan, M. I., & Butt, M. S. (2015). Organogelators as a saturated fat replacer for structuring edible oils. *International Journal of Food Properties*, *18*(9), 1973–1989. https://doi.org/10.1080/10942912.2014.951891

Soltani, S., & Madadlou, A. (2015). Two-step sequential cross-linking of sugar beet pectin for transforming zein nanoparticle-based Pickering emulsions to emulgels. *Carbohydrate Polymers*, *136*, 738–743. https://doi.org/10.1016/j.carbpol.2015.09.100

Tabilo-Munizaga, G., & Barbosa-Cánovas, G. V. (2005). Rheology for the food industry. *Journal of Food Engineering*, *67*(1–2), 147–156. https://doi.org/10.1016/j.jfoodeng.2004.05.062

Terech, P. (1997). Low-molecular weight organogelators. *Specialist Surfactants*, 208–268. https://doi.org/10.1007/978-94-009-1557-2_8

Terech, Pierre, & Weiss, R. G. (1997). Low molecular mass gelators of organic liquids and the properties of their gels. *Chemical Reviews*, *97*(8), 3133–3159. https://doi.org/10.1021/cr9700282

Thakur, V. K., & Thakur, M. K. (2018). *Polymer gels. Science and Fundamentals*. Springer. https://doi.org/10.1007/978-981-10-6086-1

Uzun, S., Ilavsky, J., & Padua, G. W. (2017). Characterization of zein assemblies by ultra-small-angle X-ray scattering. *Soft Matter*, *13*(16), 3053–3060. https://doi.org/10.1039/c6sm02717b

Wang, L. J., Yin, Y. C., Yin, S. W., Yang, X. Q., Shi, W. J., Tang, C. H., & Wang, J. M. (2013).

Development of novel zein-sodium caseinate nanoparticle (ZP)-stabilized emulsion films for improved water barrier properties via emulsion/solvent evaporation. *Journal of Agricultural and Food Chemistry*, *61*(46), 11089–11097. https://doi.org/10.1021/jf4029943

Wang, Q., Crofts, A. R., Padua, G. W. (2003). Protein − lipid interactions in zein films investigated by surface plasmon resonance. *Journal of Agricultural and Food Chemistry 51,* 7439–7444.

Wang, Qin, Yin, L., & Padua, G. W. (2008). Effect of hydrophilic and lipophilic compounds on zein microstructures. *Food Biophysics*, *3*(2), 174–181. https://doi.org/10.1007/s11483-008-9080-9

Wang, Qiuming, Yu, X., Patal, K., Hu, R., Chuang, S., Zhang, G., & Zheng, J. (2013). Tanshinones inhibit amyloid aggregation by amyloid-β peptide, disaggregate amyloid fibrils, and protect cultured cells. *ACS Chemical Neuroscience*, *4*(6), 1004–1015. https://doi.org/10.1021/cn400051e

Wang, Yi, & Padua, G. W. (2010). Formation of zein microphases in ethanol-water. *Langmuir*, *26*(15), 12897–12901. https://doi.org/10.1021/la101688v

Wang, Yi, & Padua, G. W. (2012). Nanoscale characterization of zein self-assembly. *Langmuir*, *28*(5), 2429–2435. https://doi.org/10.1021/la204204j

Wang, Ying, & Padua, G. W. (2006). Water barrier properties of zein-oleic acid films. *Cereal Chemistry, 83*(4), 331–334. https://doi.org/10.1094/CC-83-0331

Watanabe, T., Kawai, T., & Nonomura, Y. (2018). Effects of fatty acid addition to oil-in-water emulsions stabilized with sucrose fatty acid ester. *Journal of Oleo Science*, *67*(3), 307–313. https://doi.org/10.5650/jos.ess17097

Weissmueller, N. T., Lu, H. D., Hurley, A., & Prud'Homme, R. K. (2016). Nanocarriers from GRAS zein proteins to encapsulate hydrophobic actives. *Biomacromolecules*, *17*(11), 3828–3837. https://doi.org/10.1021/acs.biomac.6b01440

Xu, J., Yin, A., Zhao, J., Li, D., & Hou, W. (2013). Surfactant-free microemulsion composed of oleic acid, n-propanol, and H2O. *Journal of Physical Chemistry B*, *117*(1), 450–456. https://doi.org/10.1021/jp310282a

Xu, Q., Nakajima, M., Nabetani, H., Iwamoto, S., & Liu, X. (2001). The effects of ethanol content and emulsifying agent concentration on the stability of vegetable oil-ethanol emulsions. *JAOCS, Journal of the American Oil Chemists' Society*, *78*(12), 1185–1190. https://doi.org/10.1007/s11745-001-0411-z

Yang, Y., Chaisoontornyotin, W., & Hoepfner, M. P. (2018). Structure of asphaltenes during precipitation investigated by ultra-small-angle X-ray scattering. *Langmuir*, *34*(35), 10371–10380. https://doi.org/10.1021/acs.langmuir.8b01873

Yuan, Y., Li, H., Liu, C., Zhang, S., Xu, Y., & Wang, D. (2019). Fabrication and characterization of lutein-loaded nanoparticles based on zein and sophorolipid : Enhancement of water solubility , stability , and bioaccessibility. *Journal of Agricultural and Food Chemistry*, *67*(43), 11977–11985. https://doi.org/10.1021/acs.jafc.9b05175

Zhang, B., Luo, Y., & Wang, Q. (2011). Effect of acid and base treatments on structural, rheological,

and antioxidant properties of α-zein. *Food Chemistry*, *124*(1), 210–220. https://doi.org/10.1016/j.foodchem.2010.06.019

Zhang, M., & Weiss, R. G. (2015). Self-assembled networks and molecular gels derived from long-chain, naturally-occurring fatty acids. *Journal of the Brazilian Chemical Society*, *27*(2), 1–17. https://doi.org/10.5935/0103-5053.20150247

Zhang, Y., Cui, L., Che, X., Zhang, H., Shi, N., Li, C., … Kong, W. (2015). Zein-based films and their usage for controlled delivery: Origin, classes and current landscape. *Journal of Controlled Release*, *206*(2699), 206–219. https://doi.org/10.1016/j.jconrel.2015.03.030

Zhang, Y., Cui, L., Li, F., Shi, N., Li, C., Yu, X., … Kong, W. (2016). Design, fabrication and biomedical applications of zein-based nano/micro-carrier systems. *International Journal of Pharmaceutics*, *513*(1–2), 191–210. https://doi.org/10.1016/j.ijpharm.2016.09.023

Zhong, Q., & Ikeda, S. (2012). Viscoelastic properties of concentrated aqueous ethanol suspensions of α-zein. *Food Hydrocolloids*, *28*(1), 46–52. https://doi.org/10.1016/j.foodhyd.2011.11.014

Zou, Y., Thijssen, P. P., Yang, X., & Scholten, E. (2019). The effect of oil type and solvent quality on the rheological behavior of zein stabilized oil-in-glycerol emulsion gels. *Food Hydrocolloids*, *91*, 57–65. https://doi.org/10.1016/j.foodhyd.2019.01.016

Zou, Y., Yang, X., & Scholten, E. (2018). Rheological behavior of emulsion gels stabilized by zein/tannic acid complex particles. *Food Hydrocolloids*, *77*, 363–371.

CHAPTER 3   TERNARY PHASE DIAGRAM OF ZEIN-BASED EMULSIONS SYSTEM

3.1 Abstract

Oleogels are interesting due to their ability to hold large amounts of oil in a semi-solid gel structure. In the food industry, oleogels are most often investigated as substitutes for saturated and trans-fats. In this work, the lyotropic formation of ethanol-zein-oleic acid gels was observed qualitatively and ternary phase diagrams were constructed to map the observations. The viscoelastic parameters G' and G" were measured to confirm gel formation as observed in phase diagrams. Ultra-small-angle X-ray scattering (USAXS) was used to study the microstructural organization of ethanol/zein/oleic acid gels. Data suggested that the primary unit or building block for gel network structures was the rod-shaped zein molecule. USAXS data suggested that zein-oleic acid gels have a highly organized microstructure, possibly the result of zein self-assembly. Zein was considered an effective oleogelator in ethanol/zein/oleic acid systems.

3.2 Introduction

Food oleogels are soft solids, consisting of vegetable oil[1-3] as the continuous phase and a dispersed gelator network[4-8]. Food oleogelation is intended to enhance physical or organoleptic properties of vegetable oils to increase their use in food products as fat replacers or encapsulation matrices. Oleogels can be structured by polymers that self-assemble via non-covalent interactions, hydrogen bonds and van der Waals forces[9]. Food oleogels based on GRAS polymers is an emerging strategy that holds significant promise in foods and nutrition[10].

Zein ethanol-water solutions are known to form gels upon storage[11, 12]. This behavior is objectionable in various processing operations, for example ultrafiltration. Zein has been used in combination with polysaccharides to form hydrogels[13]. Only limited research has focused on zein as oleogelator. In De Vries et al. (2014) zein was mixed with glycerol at 150 ℃ and homogenized with the oil phase at high temperature[14]. A gel was formed upon cooling. The gel was proposed as fat replacer in baking operations[15]. Oleic acid has been used as plasticizer to overcome the brittleness of zein films. Previous studies using small-angle x-ray scattering suggested that oleic acid facilitated the organization of zein-oleic acid films. A structural model was proposed where

zein and oleic acid stacked, periodically, as two zein layers and a bilayer of oleic acid[16]. It was hypothesized that oleic acid interacted with soluble zein in ethanol-water mixtures and promoted structure organization. Oleic acid was selected in this work for its previously observed affinity with zein.

Phase diagrams are used to depict phase behavior of binary or ternary systems including those containing amphiphiles[17-19]. Phase transformations between structures can occur as functions of composition or temperature. While amphiphiles can dissolve in polar solvents, the non-polar part will shield itself and arrange into micelles or bilayers and allow only their hydrophilic side to be in contact with the solvent. The addition of a non-polar solvent, such as an oil, can prompt a ternary system and trigger structure development at a higher hierarchical level[20]. For micellar systems, lyotropic structures can develop into hexagonal and micellar cubic phases, which are semi-solid gels[20-22]. In this work, the lyotropic formation of ethanol/zein/oleic acid gels was observed qualitatively, by tube inversion, and ternary phase diagrams were constructed to map the observations. Viscosity and the viscoelastic parameters G' and G" were measured to confirm gel formation as observed in phase diagrams.

Ultra-small-angle X-ray scattering (USAXS) has been used to study the microstructural organization of gel samples. USAXS data, consisting of a plot of signal intensity as a function of the scattering vector or the size of scattering particles, can be fitted with the expression for total intensity scattering $I(q)$ [23] using the unified fit model of *Irena* software[23] to obtain the radius of gyration (R_g) and Porod exponent (P), or shape factor, of the scattering particles at different structural levels[24,25].

$$I(q) = F_{\mathrm{B}} + \sum_{i=1}^{n} S_i(Q)\Big(G_i \exp(-Q^2 R_{\mathrm{g}_i}^2/3) + B_i \exp(-Q^2 R_{\mathrm{gcf}_i}^2/3)$$
$$\times \Big\{[\mathrm{erf}(QR_{\mathrm{g}_i}/6^{1/2})]^3/Q\Big\}^{P_i}\Big),$$

where F_B is a flat background and i represents the various structural levels. G_i is the exponential prefactor and B_i is a prefactor specific to the power law, P_i, of each structural level. The unified fit model is based on the unified exponential/power-law approach to small-angle scattering and the code developed by Beaucage and co-workers[24, 25]. The code handles data for which development of an exact scattering model is difficult or impossible. A structural level is

described by Guinier's law and a structurally limited power law, which on a log-log plot shows as a knee (Guinier's knee) and a linear region (Porod region). Porod's law parameters are used as descriptors of local structure. Thin rods are one-dimensional objects, where $P = 1$. Thin lamellar discs are two-dimensional objects, where $P = 2$[24]. For three-dimensional features, $2 < P < 3$ is associated with mass fractals, while $3 < P < 4$ is associated with surface-fractals. $P = 4$ is associated with sharp, smooth interfacial surfaces and $P > 4$ with a diffuse interface[25]. The overall goal of this study was to evaluate zein as an oleogelator for low heat gelation of lipids.

3.3 Materials and Methods

Zein was purchased from Showa Sanyo Co. Ltd. (Tokyo, Japan). Oleic acid was from Fisher Scientific (Hanover Park, IL). Ethanol (200 proof) was supplied by Decon Laboratories Inc. (King of Prussia, PA). Mineral oil was purchased locally.

3.3.1 Phase diagrams

Samples were prepared in 8 mL scintillation vials. Zein was dissolved in 70% (v/v) ethanol and let to stand at 20 ºC for 12 h to promote hydration. Oleic acid was added to the zein solution and mixed by vortex for 3 min to obtain a homogeneous emulsion. Samples contained 5-80% (w/w) of 70% ethanol, 5-30% (w/w) zein and 10-90% (w/w) oleic acid for a total of 46 units. Zein-based oleogels were coded according to their composition and storage time as 70% ethanol (%)-zein (%)-oleic acid (%)-storage days. Samples were stored in air-tight closed vials for 1, 7, 14 or 21 days. Gelation was monitored by tube inversion observations of sample flow behavior. No flow was observed for gels, while viscous liquids were observed to flow under their own weight.

3.3.2 Rheology measurements

Viscosity and viscoelastic parameters, G' and G", of selected ethanol/zein/oleic acid systems were measured to confirm the rheological behavior observed in phase diagrams. An ARES-G2 rheometer (TA Instruments, New Castle, DE) with a DIN concentric cylinder (bob diameter of 27.7 mm and cup diameter of 30 mm) was used. Samples (30 g) were placed in the measuring cup for 12h. The top of the sample was covered with mineral oil to minimize ethanol evaporation during the experiment. Flow sweep tests were carried out at 20 ºC, at constant strain of 0.1%, and shear rate values of 0.1 to 100 1/s, to measure the viscosity parameters consistency index, K Pa·s^n, and flow behavior index, n, applying the *Ostwald-de-Waele* power-law to fit the data. To measure

the viscoelastic parameters, G' and G", the linear viscoelastic region was first determined by amplitude sweep tests at a constant frequency of 1 Hz (strain = 0.01 to 100%). The strain level selected for further experiments was 0.2%. Oscillatory frequency sweep tests were performed over the frequency range of 1 to 100 Hz, at 20 ℃, to measure the storage modulus (G') and loss modulus (G") of zein-based oleogels.

3.3.3 Ultra small-angle X-ray scattering (USAXS)

USAXS data were collected to observe the microstructural organization of sample gels. USAXS experiments, combined with pinhole SAXS, were conducted at beamline 9-ID-C at the Advanced Photon Source in Argonne National Laboratory (Lemont, IL). The instrument is equipped with a Bonse-Hart camera double-crystal configuration and operates at one-dimensional collimation, which enables the collection of slit-smeared data. The specimen was measured at scattering vectors range q = $1 \times 10\text{-}4$ Å^{-1} to 1.2 Å^{-1} with about 200 data points, where q is defined as $q = 4\pi \sin (\theta/2)/\lambda$ and θ, λ are the scattering angle and x-ray beam wavelength, respectively. Emulsion samples were loaded in NMR capillaries with 4 mm internal diameter (Wilmad-LabGlassTM thin-walled high-throughput NMR tubes, Fisher Scientific, MA) and capped with corresponding rubber caps. The monochromatic x-ray energy beam used was of 18 keV. Slit-smeared data were fitted with the unified model by the Modeling II macro of the Irena 2 package in IGOR PRO v8.03 (Wavemetrics, Lake Oswego, OR). The radius of gyration (R_g) and shape factors (P) of aggregates were evaluated. The experimental design consisted of 21 samples with 2 replicates, totaling 42 experimental units, average values were reported.

3.3.4 AFM

Samples of lutein-filled oleogels were prepared by dissolving lutein (0.5% w/w) in oleic acid before mixing with the corresponding amount of zein in 70% ethanol to reach the composition formula 30-15-55. Mixtures were sonicated in an ultrasonic cleaning tank (Crest Ultrasonics, Model no. 4HT-1014-6, Trenton, NJ) for 15 min (40 kHz) at a temperature of 27 ± 2 °C, controlled with running cold water. A 3 g sample was poured into 60 mm × 15 mm polystyrene petri dishes capped and sealed with parafilm. Samples were allowed to stand at room temperature for 24h before testing. AFM images were collected with an Asylum Jupiter XR Atomic Force Microscope (Asylum Research, Oxford Instruments, Santa Barbara, CA) with an ASYELEC.02-R2 cantilever

(Oxford Instruments, Santa Barbara, CA) operating on tapping mode (AC mode) with 3.91 Hz scan rate in a scan size of 1.50 µm under ambient conditions. Images were analyzed using the software provided by the manufacturer.

3.4 Results and Discussion

3.4.1 Ternary phase diagrams

Ternary phase diagrams were constructed to map the lyotropic formation of ethanol-zein-oleic acid gels. Phase diagrams served to identify the different mesophases of ethanol-zein-oleic acid systems in terms of composition. Comparisons between time delayed phase diagrams (1, 7, 14, and 21 days) revealed dynamic changes in mesophase systems. Based on observations of sample flow by tube inversion, five regions (*a*) emulsions, (*b*) colloids, (*c*) phase separated, (*d*) clear gels and (*e*) opaque gels, were identified overall.

On *day 1* samples fell in two groups, (*a*) emulsions and (*b*) colloids (Figure 3.1a). Emulsions were opaque liquids composed of 5-25% zein and 30-85% oleic acid, while colloids were clear liquids prepared with 5-25% zein and 10-30% oleic acid. The zein solubility limit in 70% ethanol (v/v) was also plotted in the figures to mark the zein concentration limits for sample preparation. On *day 7* (data not shown), five regions were observed. Emulsions, originally in region (*a*) split into three types of samples, with two new regions, phase separated (*c*) and opaque gels (*e*). Phase separation was observed when oleic acid content was 40-90% and zein was below 10%. Region *a* was reduced to 12.5-20% zein and 35-65% oleic acid. Opaque gels (*e*) were observed when zein was higher than 20% and oleic acid was 30-40%. Clear gels (*d*) were observed when zein was 20-25% and oleic acid was 15-35%. By *day 14* (Figure 3.1b), the emulsions region (*a*) decreased due to an increase of the phase separated region (*c*) and the opaque gel region (*e*). Emulsions with high amount of oleic acid (> 65%) and zein below 15% were not stable and phase separated out.   Both, opaque and clear gel regions grew larger when zein content increased to 15-25% and oleic acid increased to 31-50% for opaque gels, and 15-35% for clear gels. On *day 21* (data not shown), *d* and *e* regions formed stable gels. It was believed that zein acted as an oleogelator, as gelation was observed sooner when zein content was higher than 15% (data not shown). Gels were not formed below 10% zein.
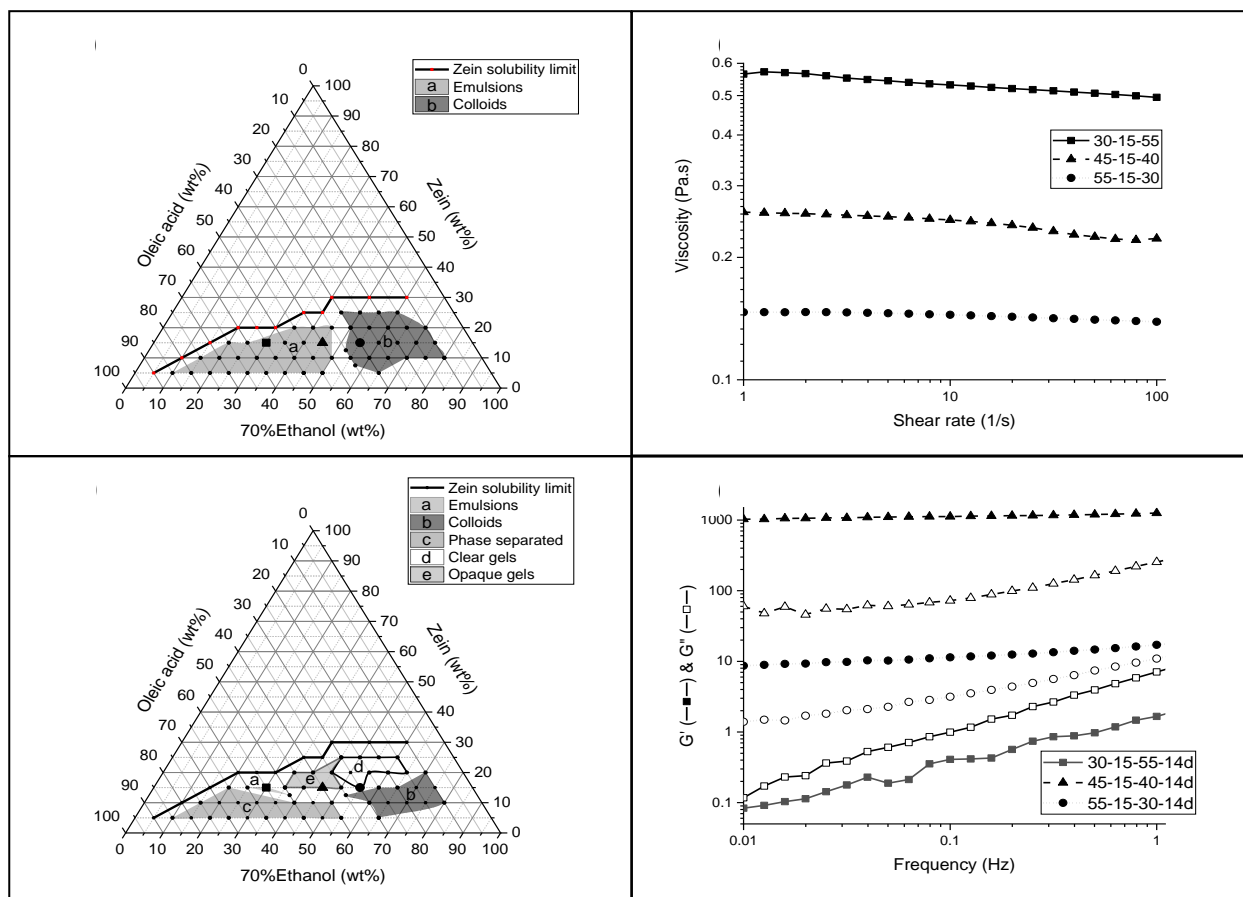
Figure 3.1 Ternary phase diagrams and rheology plots for 70% ethanol/zein/oleic acid (w/w/w %) systems (a) at day 1 and (b) day 14. Three selected points in the phase diagrams, symbols ■, ●, ▲, correspond with viscosity plots (c) and G'- G" plots (d) at day 1 and day 14, respectively.

3.4.2 Rheological parameters

Measurements of rheological parameters were carried out at day 1 and after 14 days of storage to confirm the flow behavior observed by tube inversion. Viscosity measurements for samples 30-15-55, 45-15-40, and 55-15-30, at day 1, are shown in Fig. 1c. The plots indicate the three samples were fluid with viscosity values nearly constant with shear rate. Viscosity consistency coefficient (K) decreased with increasing ethanol content from sample 30-15-55 (0.57 Pa·s) > 45-15-40 (0.27 Pa·s) > 55-15-30 (0.14 Pa·s), suggesting a dominant effect of ethanol in sample rheology. The viscoelastic parameters, storage modulus (G') and loss modulus (G"), measured at day 14 are shown in Fig.1d. The plots indicated that sample 30-15-55 remained fluid after 14 days (G" > G'). On the other hand, samples 45-15-40 and 55-15-30 developed a solid-like behavior (G' > G") with

G' and G" higher for 45-15-40 (1.0×10^3 and 6.0×10^2 Pa, respectively) than for 55-15-30 (8.7 and 1.4 Pa, respectively). Chen et al. (2016) prepared zein-based oleogels mixing zein and β-carotene with glycerol at 150 °C and homogenizing the oil phase at high temperature[15]. A range of gels were formed upon cooling, which contained 3% zein in 60% soybean oil volume fraction incorporated with 0.015-0.045% β-carotene. Based on their stress-sweep measurements carried out at a fixed frequency of 1.0 Hz using parallel plate configuration, G' and G" of oleogels were 2×10^3 Pa - 1.3×10^4 and 8×10^2 - 4×10^3 Pa, respectively[15], in reasonable agreement with present results. Similar results were reported by De Vries et al. (2014)[14]. Rheological measurements did confirm the observations recorded in the phase diagrams.   Results suggested that a critical amount of ethanol-water is needed for gelation, maybe to allow for zein mobility and develop the necessary structure to support gelation. It may be that 45-15-40 is an optimal composition for gelation, 30% ethanol-water may not allow enough mobility, while 55% may dilute zein to the point of preventing the formation of intermolecular bonds. The rheological properties of gels, G" and G", were not measured after 21 days. Previous results obtained with ethanol-30% zein-15 % oleic acid indicated values remained stable for longer than four months (data not published). However, this is a non-equilibrium state and zein strands will tend to associate with each other, eventually expelling oleic acid.

3.4.3 Ultra-small-angle X-ray scattering

USAXS profiles of zein-based oleogels corresponding to the formulas, 30-15-55, 40-15-45, 45-15-40 and 55-15-30, taken at *day14,* are shown in Figure 3.2. Those samples showed "Guinier knees" and "Porod slopes" at the high q region ($q > 10^{-2}$ Å^{-1}). Samples 30-15-55, 40-15-45, 45-15-40 also showed Guinier knees and Porod slopes in the intermediate to low q regions ($q < 10^{-2}$ Å^{-1}), suggesting at least two structural levels are present in oleogels. Based on the Guinier approximation, in the high q region, R_{g1} values for oleogels were 3.5-13.1 nm and P_1 index values were 1.0-1.8 (Table 3.1). R_{g1} values for zein in 70% ethanol averaged 13 nm and P_1 index was 1.0-1.1, close to the P index for rod shape structures, $P_{rod} = 1$. Results were related to the zein molecule, a rod-shape structure 13 nm × 1.2 nm × 3 nm[26] in ethanol-water with an axial ratio of 6:130. USAXS data in the high q region suggested that the zein molecule was the primary unit or basic building block of 2D and 3D structures observed in oleogels[27]. It was thought that R_{g1} values between 3.5 and 13 nm with P_1 index values, 1.2-1.8, represented short range 2D structures formed

by zein or zein-oleic acid [28, 29], as illustrated in Table 1. For the intermediate to low q range, R_{g2} values were smallest (250-300 nm) for sample 30-15-55, increasing to 772 to < 1200 nm for 40-15-45 and to 738-1145 nm for 45-15-40, suggesting that higher amounts of ethanol-water in the system allow for higher zein mobility and permit structure growth. P index remained stable through composition and time changes, most values were 3.4 or 3.5. Data was interpreted as representing 3D structures, but not spheres where $P = 4$. In the intermediate to low q range, R_{g2} values for zein in ethanol-water (no oleic acid) were not observable, neither for sample 55-15-30. It was believed that protein associations or network structure were not developed at this point, thus there was not any detectable signal. Data suggested there is an optimal amount of ethanol-water for a given system, where on the low side, zein molecules do not have enough mobility to develop a supramolecular structure, while on the high side, zein molecules become too far apart for effective structure development. Figure 3.2 (inset) also shows Kratky plots for the corresponding samples at the high q region. A Kratky plot is obtained by plotting the scattering intensity as $I(q)$ x q^2 vs q[30]. In Kratky plots of polymer solutions, the shape of the curve is related to the chain conformation, which at high q, the nearly linear plot indicated a rod-like shape[30].
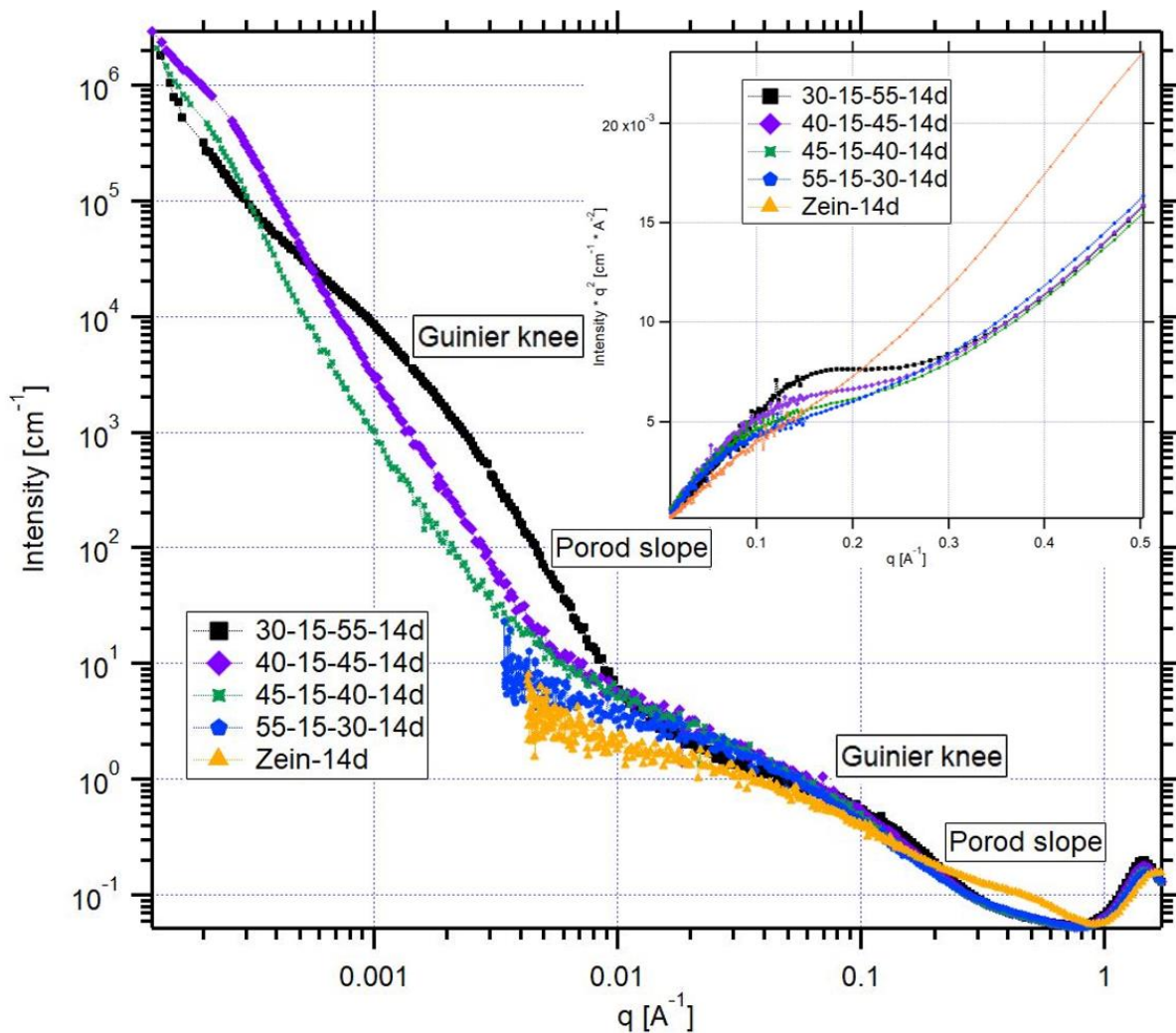
Figure 3.2 Slit desmeared USAXS scattering profile of a 70% ethanol–zein sample at 15% zein and 70% ethanol-zein-oleic acid samples at 15% zein containing 30, 40, 45 and 55% oleic acid with corresponding amount of 70% ethanol. Inset shows the Kratky plots of corresponding samples.

Table 3.1 R_g and P values of zein-based oleogels stored for 7, 14 and 21 days with corresponding proposed structural models.
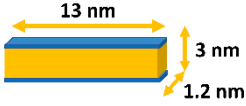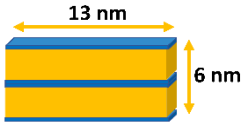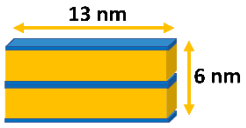
Sample code	R_{g1} (nm)	P_1 index	Schematic model	R_{g2} (nm)	P_2 index
		High q region		Low to intermediate q region	
67-33-0-7d (zein)	12.8	1.1		---	---
67-33-0-14d (zein)	13.1	1.0	13 nm, 3 nm, 1.2 nm	---	---
55-15-30-7d	11.5	1.2		---	---
55-15-30-14d	11.6	1.4		---	---
55-15-30-21d	12.6	1.4		---	---
45-15-40-7d	7.3	1.5		738	3.7
45-15-40-14d	8.5	1.5	13 nm	1145	3.2
40-15-45-7d	5.7	1.6	6 nm	772	3.6
40-15-45-14d	6.2	1.6		745	3.4
40-15-45-21d	10.7	1.5		>1200	3.2
30-15-55-7d	3.8	1.8		251	3.4
30-15-55-14d	3.5	1.8	3 nm	276	3.5
30-15-55-21d	3.9	1.8		300	3.2
45-20-35-7d	6.1	1.6		642	3.4
45-20-35-14d	7.1	1.6	13 nm	665	3.4
45-20-35-21d	10.4	1.6	6 nm	744	3.5
40-20-40-7d	5.9	1.8		571	3.5
40-20-40-14d	6.3	1.8		534	3.5
40-20-40-21d	10.4	1.8		576	3.4

Table 3.1 summarizes R_g and P values calculated with the unified fit model for samples containing 15 and 20% zein and varying content of oleic acid and 70% ethanol. In previous work, Lai and co-workers[16] observed a periodic structure in zein films by wide angle x-ray scattering. Zein was observed to stack into platelets with a 135 Å d-spacing. Oleic acid (14% g/g zein), a good plasticizer for zein[29], was reported to promote the formation of periodic structures in zein films.

In summary, this work investigated the behavior of zein as an oleogelator in the system 70% ethanol-zein-oleic acid. The lyotropic formation of zein based oleogels was mapped on a time delayed set of ternary phase diagrams, where points represented qualitative, tube inversion,

observations. To confirm the observed flow behavior, viscosity was measured for fluid samples and gelation was confirmed when G'/G" > 1. Gel microstructure, as investigated by USAXS, revealed a periodic, highly organized structure supporting a relatively large mass of oleic acid. Gels consisted of three hierarchical structural levels, where the first level corresponding to the structure building blocks was related to the rod-like zein molecules (P = 1). Higher structural levels were interpreted as ribbon-like fractal grown structures (3 < P < 4) that ultimately entrapped oleic acid droplets. Zein was considered to act as an oleogelator in 70% ethanol-zein-oleic acid, further work is needed to explore the incorporation of triglycerides into the system.

3.4.4 AFM

Lutein was selected in this work to explore application possibilities for zein-based oleogels. To that effect, sample 30-15-55 was filled with 0.5% lutein. Figure 3.3 shows an AFM image of the zein-based oleogel 30-15-55 filled with 0.5% lutein, where long ribbons ~ 600 nm are observed. This observation was related to the $R_{g2} \approx 300$ nm (Table 3.1), which is commensurate with the dimensions of the long rods or ribbons observed by AFM[31, 32]. Figure 3.3 Ternary phase diagram of zein-based oleogels with arrow indicating the formula used   for (a) photo of the filled oleogel and (b) AFM image of sample (30-15-55, filled with 0.5% lutein). also shows the corresponding ternary phase diagram and a picture of the zein-based oleogel 30-15-55 filled with 0.5% lutein (w/w oleic acid). The AFM image shows a structure with a large number of droplets embedded in a network of rods or ribbons, which can be related to the lutein filled gel in the picture and to the phase diagram.
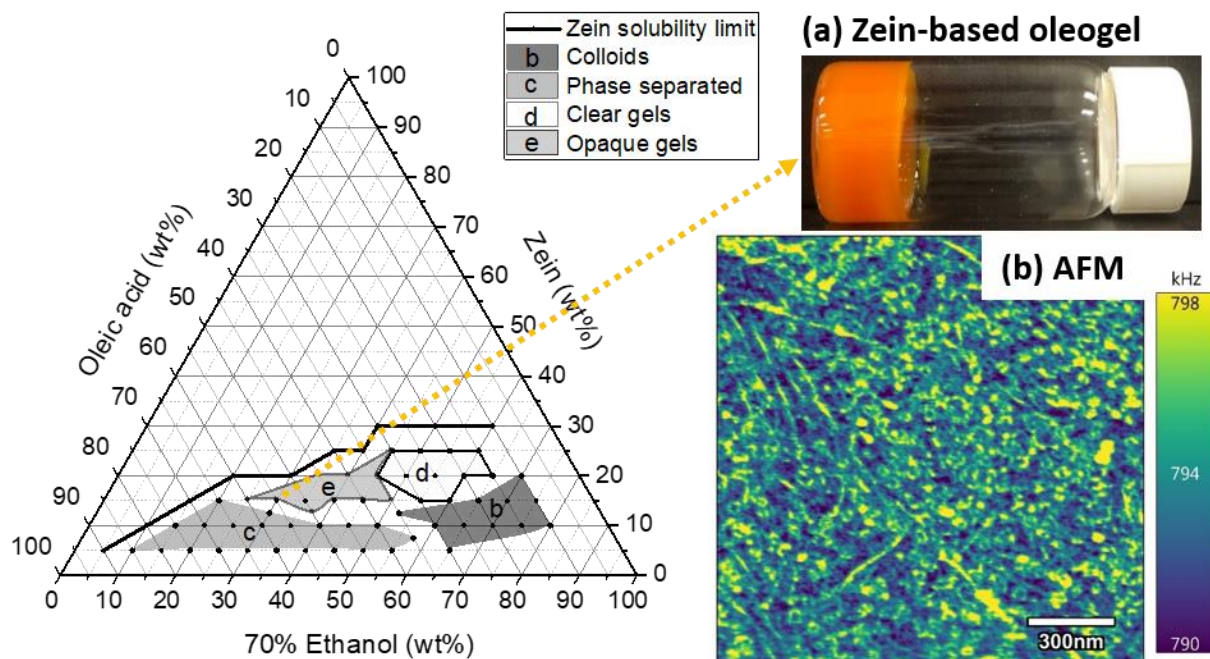
Figure 3.3 Ternary phase diagram of zein-based oleogels with arrow indicating the formula used for (a) photo of the filled oleogel and (b) AFM image of sample (30-15-55, filled with 0.5% lutein).

3.5 References

(1)   Chavan, R. S.; Khedkar, C. D.; Bhatt, S. Fat Replacer. *Encycl. Food Heal.* **2016**, *2*, 589–595.

(2)   Siraj, N.; Shabbir, M. A.; Ahmad, T.; Sajjad, A.; Khan, M. R.; Khan, M. I.; Butt, M. S. Organogelators as a Saturated Fat Replacer for Structuring Edible Oils. *Int. J. Food Prop.* **2015**, *18*, 1973–1989.

(3)   Pehlivanoğlu, H.; Demirci, M.; Toker, O. S.; Konar, N.; Karasu, S.; Sagdic, O. Oleogels, a Promising Structured Oil for Decreasing Saturated Fatty Acid Concentrations: Production and Food-Based Applications. *Crit. Rev. Food Sci. Nutr.* **2018**, *58*, 1330–1341.

(4)   Samateh, M.; Sagiri, S. S.; John, G. Molecular Oleogels: Green Approach in Structuring Vegetable Oils. In *Edible Oleogels: Structure and Health Implications*, 2.; Marangoni, A. G.; Garti, N.; Elsevier Inc., **2018**, 415–438.

(5)   Alger, M. *Polymer Science Dictionary,* 3; Springer: Netherlands, **2017**.

(6)   Sangeetha, N. M.; Maitra, U. Supramolecular Gels: Functions and Uses. *Chem. Soc. Rev.* **2005**, *34*, 821–836.

(7)   Lan, Y.; Corradini, M. G.; Weiss, R. G.; Raghavan, S. R.; Rogers, M. A. To Gel or Not to Gel: Correlating Molecular Gelation with Solvent Parameters. *Chem. Soc. Rev.* **2015**, *44*, 6035–6058.

(8)   DeRossi, D.; Kajiwara, K.; Osada, Y.; Yamauchi, A. *Polymer Gels: Fundamentals and Biomedical Applications*; **1991**, *53*.

(9)   O'Sullivan, C. M.; Barbut, S.; Marangoni, A. G. Edible Oleogels for the Oral Delivery of Lipid Soluble Molecules: Composition and Structural Design Considerations. *Trends Food Sci. Technol.* **2016**, *57*, 59–73.

(10)   Patel, A. R. *Alternative Routes to Oil Structuring.* Springer Internation Publishing: Switzerland, **2015**.

(11)   Evans, C. D. and Manley R. H. Process For Prevention of Gelation of Solutions or Dispersions of Prolamines. *United States Patent No. 2392084*. **1946**.

(12)   Chen, Y.; Ye, R.; Liu, J. Understanding of Dispersion and Aggregation of Suspensions of Zein Nanoparticles in Aqueous Alcohol Solutions after Thermal Treatment. *Ind. Crops Prod.* **2013**, *50*, 764–770.

(13)   Kasaai, M. R. Trends in Food Science & Technology Zein and Zein -Based Nano-Materials for Food and Nutrition Applications : A Review. *Trends Food Sci. Technol.* **2018**, *79*, 184–197.

(14)   De Vries, A.; Nikiforidis, C.V.; Scholten, E. Natural Amphiphilic Proteins as Tri-Block Janus Particles : Self-Sorting into Thermo-Responsive Gels. *EPL.* **2014**, *107*, 1-6.

(15)   Chen, X.; Fu, S.; Hou, J.; Guo, J.; Wang, J.; Yang, X. Zein Based Oil-in-Glycerol Emulgels Enriched with b -Carotene as Margarine Alternatives. *Food Chem.* **2016**, *211*, 836–844.

(16)   Lai, H. M.; Geil, P. H.; Padua, G. W. X-Ray Diffraction Characterization of the Structure of Zein-Oleic Acid Films. *J. Appl. Polym. Sci.* **1999**, *71*, 1267–1281

(17)   Mele, S.; Söderman, O.; Ljusberg-Wahrén, H.; Thuresson, K.; Monduzzi, M.; Nylander, T. Phase Behavior in the Biologically Important Oleic Acid/Sodium Oleate/Water System. *Chem. Phys. Lipids* **2018**, *211,* 30–36.

(18)   Khan, F.; Islam, M. S.; Roni, M. A.; Jalil, R. U. Systematic Development of Self-Emulsifying Drug Delivery Systems of Atorvastatin with Improved Bioavailability Potential. *Sci. Pharm.* **2012**, *80*, 1027–1043.

(19)   Fang, Y.; Chen, L.; Gao, L.; Yan, Z. Effect of 1-Butyl-3-Methylimidazolium Chloride on the Lyotropic Liquid Crystal Structure and Properties of TX-100/Oleic Acid/Water System. *J. Mol. Liq.* **2019**, *294*, 111637.

(20)   Schwarz, U. S. Phase Behavior of Amphiphilic Systems. *Acta Phys. Pol. B* **1998**, *29*, 1815–1825.

(21)   Particle Sciences inc. Cubic Phase Particles in Drug Delivery. *Tech. Br.* **2012**, *4*.

(22)   Kulkarni, C. V. Lipid Crystallization: From Self-Assembly to Hierarchical and Biological Ordering. *Nanoscale* **2012**, *4*, 5779–5791.

(23)   Ilavsky, J.; Jemian, P. R. Irena: Tool Suite for Modeling and Analysis of Small-Angle Scattering. *J. Appl. Crystallogr.* **2009**, 42 (2), 347–353.

(24)   Beaucage, G. Approximations Leading to a Unified Exponential/Power-Law Approach to Small-Angle Scattering. *J. Appl. Crystallogr.* **1995**, *28*, 717–728.

(25)   Beaucage, G. Small-Angle Scattering from Polymeric Mass Fractals of Arbitrary Mass-Fractal Dimension. *J. Appl. Crystallogr.* **1996**, *29*, 134–146.

(26)   Matsushima, N.; Danno, G. I.; Takezawa, H.; Izumi, Y. Three-Dimensional Structure of Maize α-Zein Proteins Studied by Small-Angle X-Ray Scattering. *Biochim. Biophys. Acta - Protein Struct. Mol. Enzymol.* **1997**, *1339*, 14–22.

(27)   Li, Y.; Li, J.; Xia, Q.; Zhang, B.; Wang, Q.; Huang, Q. Understanding the Dissolution of α-Zein in Aqueous Ethanol and Acetic Acid Solutions. *J. Phys. Chem. B.* **2012**, *116*, 12057–12064.

(28)   Uzun, S.; Ilavsky, J.; Padua, G. W. Characterization of Zein Assemblies by Ultra-Small-Angle X-Ray Scattering. *Soft Matter* **2017**, *13*, 3053–3060.

(29)   Kim, S.; Xu, J. Aggregate Formation of Zein and Its Structural Inversion in Aqueous Ethanol. *J. Cereal Sci.* **2008**, *47*, 1–5.

(30)   Burchard, W. Light scattering techniques. In *Physical techniques for the Study of Food Biopolymers*, 1.; Ross-Murphy, S. B. (Ed.); *Springer-Science+Business Media*, B.V: Berlin, Germany, **1994**; 1, 151-214.

(31)   Wang, Y.; Padua, G. W. Nanoscale Characterization of Zein Self-Assembly. *Langmuir.* **2012**, *28*, 2429–2435.

(32)   Wang, Y.; Padua, G. W. Formation of Zein Microphases in Ethanol-Water. *Langmuir.* **2010**, *26*, 12897–12901.

CHAPTER 4   RHEOLOGICAL PROPERTIES OF ZEIN-BASED OLEOGEL SYSTEMS

4.1   Abstract

The fabrication of edible oleogels have attracted attention due to the benefits for human health and broad applications in novel delivery systems for lipophilic compounds. Various oil structuring techniques have been adapted to turn liquid oils into solid lipids without using saturated or *trans* fats. In this study, a self-assembly gelation process of zein-based oleogels were identified and monitored by rheometry. The first aim was to use rheological measurements to validate the tube-inversion observations recorded in the phase diagrams mentioned in Chapter 3. The second aim was to investigate the effects of solvent composition, protein content and storage time on rheological properties of 70% ethanol-zein-oleic acid emulsion systems. The viscous behavior of the liquid-like emulsion samples were evaluated by flow behavior parameters, dynamic viscosity (η), consistency index (K) and flow behavior index (n). Based on Ostwald-de-Waele power law model, 15% and 20% (w/w) zein-ethanol solution behaved as non-Newtonian shear thinning ($n <$ 1) viscous liquid. All three parameters η, K, and n increased with addition of oleic acid due to the increasing volume fraction of the discontinuous phase. For samples stored for 7, 14 and 21 days, storage modulus (G') and loss modulus (G") were obtained from strain and frequency sweep tests. Gels formed at different storage time were confirmed by G' > G" with frequency dependent behavior. With solvent ratio (70% ethanol/oleic acid) equal to 1, zein-based oleogel exhibited the highest gel strength (largest G'). It was assumed that the 70% ethanol provided the mobility for zein molecules to rearrange into entangled network, while oil droplets served as anchor points for zein to attach on the surface and further developed into elongated structures. Only with the suitable balance of the solvent composition could facilitate the gelation process and enhance the rigidity of the oleogel. Time was a crucial factor for gel strength and rigidity, where G' dominantly increased with time in all oleogel samples prepared by self-assembly gelation method.

4.2 Introduction

Ever since 2015, the FDA declared that *trans* fat is banned and removed from the list of "Generally Regarded As Safe (GRAS)", and the higher risks of cardiovascular diseases, obesity and diabetes related to over consumption of saturated fatty acids, oleogels become the alternatives that structuring the oil and transforming liquid into a gel like structure (Pehlivanoğlu et al., 2018; Samateh, Sagiri, & John, 2018) common routes for synthesizing edible oleogels are direct oleogeation method by melting crystalline particles or low-molecular weight gelators into the system and cooling to form liquid crystals, micelles or fibrillar network structures that trap the liquid oil (Blach et al., 2016; Cerqueira et al., 2017; P Terech, 1997; Pierre Terech & Weiss, 1997). And for indirect methods, foams or emulsions are prepared and served as frameworks to absorb considerable amount of oil to form oleogels (Mezzenga, 2011; Patel, 2017; Patel et al., 2014). Upon these wide varieties of oleogel, protein based oleogels with minimum preparation steps is particular important due to their potential of tunable textural sturctures, calorie and fat reduction (Chavan et al., 2015; Martins et al., 2018; Pehlivanoğlu et al., 2018; Siraj et al., 2015). In comparison to hydrophilic carbohydrate derived oleogelators, proteins are often ready to use, no need for further chemical modifications. Not to mention the biocompatibility, wide availability and low price, consumer acceptance is another reason to make protein as a popular oleogelator candidate in food applications, and also for the pharmaceutical or cosmetics industry.

Zein, a corn derived storage protein, has long been used as food coatings, films and tableting (Marín, Montoya, Arnache, Pinal, & Calderón, 2018; Maria Berna Pérez-Gago & Rhim, 2013; Sengupta & Han, 2013; Shukla et al., 2000). With its amphiphilic peptides composition, and contains more than 50% non-polar amino acid residues (Leucine, Alanine and Proline), it is considered as one of the unique hydrophobic water insoluble plant-based protein (Chen et al., 2013; Nonthanum et al., 2012) Being approved for oral use by Food and Drug Administration (Patel & Velikov, 2014), the applications of zein is no longer restrained. Numerous studies has thrived, such as applying zein as stabilizer for colloidal and pickering emulsion systems, fabrication zein based microspheres and nanoparticles for drug delivery and controlled-release system in pharmaceutical and food fields (Chen et al., 2013; De Folter et al., 2012; Gao et al., 2014; Maria B. Pérez-Gago & Krochta, 2001; Soltani & Madadlou, 2015; L. J. Wang et al., 2013). Owing to its gel forming characteristics (Cheryan, & DeVor, 2001), recent research has reported zein as an oleogelator to

form oleogel as a margarine alternatives in baking products (Chen et al., 2016; Scholten, 2014).

Zein-based oleogel (emulgels) has long been studied in Osborne et al. (1897), by dissolving zein in 150 ℃ glycerol and homogenizing with preheated oil, the oleogel with up to 0.4 oil volume fraction would form after cooling. Adapted this preparation method, Scholten et al. (2014) further investigated and proposed the gelation mechanism, which the gel-like structures were formed by the zein tri-blocks. Zein molecules served as building blocks would firstly use oil as nuclei to self-assemble into ribbon-like long strands on the surface of oil droplets, then lead to the formation of the 3D network structure. This oil-in-glycerol zein-based emulsion gel system had been demonstrated the application possibility by encapsulating beta-carotene to retard oil oxidation (Chen et al., 2016). Lately, the effects of different oil types varying in polarity and viscosity on structure formation and rheological properties were evaluated in this system (Zou, Thijssen, Yang, & Scholten, 2019), however, all of them required high processing temperature. Just recently, Nephomnyshy et al. (2020) tried to develop new method by decreasing the dissolving temperature to 90 ℃ with the aid of ethanol, still, they couldn't avoid the chance that heat would abuse the oil. In our research, no extra heat involved, by taking the advantage of the time dependent self-assembly process of zein, oleogels were formed simultaneously at room temperature with ethanol-zein-oleic acid system.

Rheology is not only crucial in process design, but also plays a decisional role in sensory aspect for desirable consumer mouthfeel characteristics (Gonzalez-Gutierrez & Scanlon, 2018). It provides the detailed information of the flow and deformation responds by the substances while force is applied. Especially for semi-solid gel like materials, suitable rheological tests can depict the interactions between the network and the continuous phase. Hence, the viscoelastic behaviors of zein in aqueous ethanol at various pH levels were determined (B. Zhang, Luo, & Wang, 2011). They observed both storage modulus (G') and loss modulus (G") were lower when pH of the solvent was departed from neutral pH. Uzun et al. (2017) also discovered the increasing of viscosity and the gelation of zein-ethanol emulsions after four month storage, which contributed by the self-assembly of the zein molecules. For oil–in–glycerol zein based oleogels prepared by heating homogenization process, gel strength was weakened by the increasing of temperature and revealed as a type of thermal responsive gel (Scholten, 2014). Oil volume fraction leaded to an increase in G' from 0.1 to 0.4 was also discussed in this paper. With the same system, the effect of

oil type, solvent quality and addition of hydrophilic particles, water or active compounds on rheological characteristics were examined (X. Chen et al., 2016; Nephomnyshy et al., 2020; Zou et al., 2019). But nevertheless, zein-based oleogel fabricated under ambient condition has not been reported.

In this study, the effects of solvent composition, protein content and storage time on rheological properties of ethanol-zein-oleic acid emulsion system were investigated. The rheological parameters, viscosity, consistency index (K), flow behavior index (n), storage modulus (G'), and loss modulus (G") were determined with an ARES-G2 rheometer to understand the network formation and interactions between zein and solvents for future applications such as encapsulating heat sensitive compounds.

4.3 Materials and Methods

4.3.1 Materials

Zein was purchased from Showa Sanyo Co. Ltd. (Tokyo, Japan). Oleic acid was from Fisher Scientific (Hanover Park, IL). Ethanol (200 proof) was supplied by Decon Laboratories Inc. (King of Prussia, PA). Mineral oil was purchased in the local market.

4.3.2 Rheology experiments

Total weight of 30 g of emulsion samples was prepared according to 70% ethanol/zein/oleic acid weight fraction (w/w/w %). First, zein (15 or 20%) was dissolved in 70% ethanol solution, and stand for 12 h for complete hydration. Oleic acid was then added into zein/70% ethanol solution and mixed by vortex for 3 min. For 15% zein weight fraction, four levels of 70% ethanol (40, 45, 50, and 55%) and corresponding amount of oleic acid were added. And for 20% zein samples, seven levels of 70% ethanol (25, 30, 35, 40, 45, 50, and 55%) were incorporated. Based on the weight fraction, total of 11 samples were coded as X-Y-Z (70% ethanol/zein/oleic acid).

Rheological behavior of zein-based emulsions was studied by ARES-G2 rheometer (TA Instruments, New Castle, DE) using DIN concentric cylinder (bob diameter of 27.7 mm and cup diameter of 30 mm). The 30 g of sample was placed in the measuring cup and 100% mineral oil (purchased from local market) was used to cover the top of the sample to prevent evaporation during the experiment.

Flow sweep test was carried out at a shear rate ($\delta\gamma/\delta t$) 0.1 to 100 1/s to measure the viscosity parameters K (consistency index, Pa s^n) and n (flow behavior index) with Ostwald-de-Waele power Power Law Model,

$$\eta = K \left(\frac{\delta\gamma}{\delta t}\right)^{n-1}$$

where η is the apparent viscosity (Pa s), and $\frac{\delta\gamma}{\delta t}$ is the shear rate (1/s).

Zein bicontinuous gel structures were generated following the experimental design from the previous objective. Specific zein concentrations were selected from the developed phase diagrams and the required amount of ethanol-zein-oleic acid emulsions were prepared for rheology analysis. Rheology analysis was performed by ARES-G2 rheometer (TA Instruments, New Castle, DE) using DIN concentric cylinder (bob diameter of 27.7 mm and cup diameter of 30 mm). The sample was placed in the measuring cup and measured instantly or incubated in the cup for 12 h, both of the measurement were covered with 100% mineral oil (purchase from local market) on the top of the sample to protect sample from evaporation during the experiment.

The linear viscoelastic region was assessed by amplitude sweep experiments at a constant frequency of 1 Hz (strain = 0.01 to 100%) to obtain the suitable strain which 0.1% of strain was applied to the analysis. Oscillatory frequency sweep tests was performed over the frequency range of 1 to 100 Hz at 20 ºC to measure the storage modulus (G') and loss modulus (G") of zein-based oleogels at 7, 14 and 21 days of standing at room temperature.

4.4 Results and Discussion

4.4.1 Viscous behavior

Based on the observation from previous chapter, freshly prepared samples were liquids which flow sweep tests were conducted. Unlike solids, liquids cannot support their own weight and holding any shape, they flow under the shear stress of their own weight. The flow behavior of liquid can be understand by plotting data on shear stress (τ) - shear rate ($\frac{\delta\gamma}{\delta t}$) diagram (Figure 4.1 Flow behavior curve of 70% ethanol/20% zein/oleic acid (w/w/w, %) emulsions. Figure 4.1 & Figure 4.2). The shear stress of all samples had linear correlations with shear rate showing as straight lines, indicating emulsions were very likely to be ideal viscous. All of the flow behavior

curves closely passed through origin was assumed that there were negligible yield stress owned by each sample (Mewis & Wagner, 2011). Therefore, $\tau / (\frac{\delta\gamma}{\delta t})$ slopes were calculated and listed in Table 4.1. The $\tau / (\frac{\delta\gamma}{\delta t})$ slope data of the emulsions (Table 4.1), also can be interpreted as the dynamic viscosity η were fitted by linear model assumed as Newtonian fluids. In general, the viscosity values were inversely proportional to the ethanol content and positively correlated with oleic acid. Which can be explained by the intermediate to concentrated emulsions systems, where the increasing of droplets volume fraction in the continuous phase would result to the increasing of the viscosity, caused by the limited interfacial mobility and more of the accumulated surface shear (Pal, 2011). Also, the addition of oleic acid could change the polarity of the emulsion and further influence the polymerization of zein, making zein molecules to aggregate instead of single units uniformly distributed in the system (Y. Chen et al., 2013; Fu & Weller, 1999).

While comparing the effect of zein concentration on viscosity, it was identical to the results mentioned by others that higher solid concentration result to higher viscosity (Fu & Weller, 1999). And if we considered zein as filler in this oil-in-water system, this phenomena is also described in other emulsion systems (Komaiko & Mcclements, 2016; Watanabe, Kawai, & Nonomura, 2018).

From the stress-stain diagrams we knew the flow behavior of the samples could be better analyzed by Ostwald-De-Waele model (negligible yield stress) rather than Herschel-Buckley model (if yield stress exists), hence, apparent viscosity versus shear rate were plotted in Figure 4.3, 4.4 and 4.5 with fitted results of consistency index (K) flow behavior index (n) summarized in Table 3.1 (Rao, 1977).

As a control, oleic acid behaved as a Newtonian fluid which the apparent viscosity was independent to shear rate plotted as a horizontal straight line (Figure 4.3). For 15% and 20% (w/w) zein in 70% (v/v) ethanol solution would decrease slightly with high shear rate, indicating shear thinning behavior reported by Nonthanum et al. (2013). On the viscosity-shear rate double log plots, all 70% ethanol-zein-oleic acid fresh samples showed pseudoplastic behavior with viscosity negatively dependent to shear rate (Figure 4.4 & 4.5). The viscosities responded to the addition of 5% oleic acid into the emulsion systems, both viscosities of 15% or 20% zein containing samples would increase with the increasing of oleic acid as well as decreasing of 70% ethanol amount. This behavior is assumed to be caused by decreasing molecular interactions within the molecular

structure of the fluid during flow (Derkach, 2009; Quemada & Berli, 2002).

In Table 4.1, K values fitted by Ostwald-De-Waele model were positively correlated with oleic acid amount and zein concentration. While zein concentration increased from 15% to 20%, the K increased 2.37 times. And looking into the ratios of K between two zein contents with same 70% ethanol amount were 1.88, 2.10, 1.75, 1.87 and 2.44 for samples 55-20-30/55-15-30, 50-20-30/50-15-35, 45-20-35/45-15-40, 40-20-40/40-15-45 and 35-20-45/35-15-50, respectively. The ratios of K fell within 1.75 to 2.44, which seemed to correlate with the zein concentration weight ratio.

The model fitting confirmed oleic acid as a Newtonian liquid with n equals to 1, while the others all had $n < 1$, considered as shear thinning Non-Newtonian liquid. From n values, the differences between oleic acid containing samples were hard to examine, however, when we divided η obtained from τ / γ slope by K, the quotient provided more information about the flow behavior. This ratio (number) can be explained as how different it behaves as an ideal Newtonian liquid, for zein 20% samples, more of the oleic acid and less of the 70% ethanol, the sample exhibited more likely to be shear thinning. Similar to concentrated emulsion system, non-Newtonian behavior decreases with increasing of volume fraction (Mewis, Wagner, Mewis, & Wagner, 2011b). And for zein 15% samples, 40-15-45 had the smallest ratio assuming to be the most shear thinning sample of all, and followed by 25-15-60, 45-15-40, 35-15-50, 30-15-55, 50-15-35 then 55-15-30. This may result from the hydrodynamic diameter changes, here we assumed as zein molecules which created different size of aggregates in different solvent quality (Q. Xu, Nakajima, Nabetani, Iwamoto, & Liu, 2001).
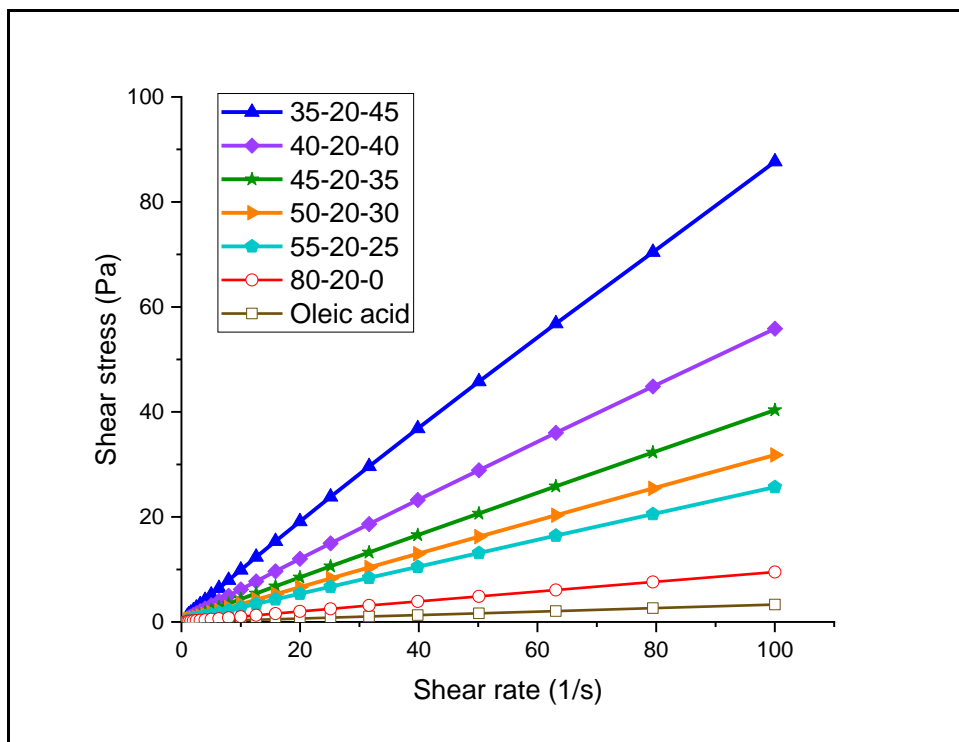
Figure 4.1 Flow behavior curve of 70% ethanol/20% zein/oleic acid (w/w/w, %) emulsions.
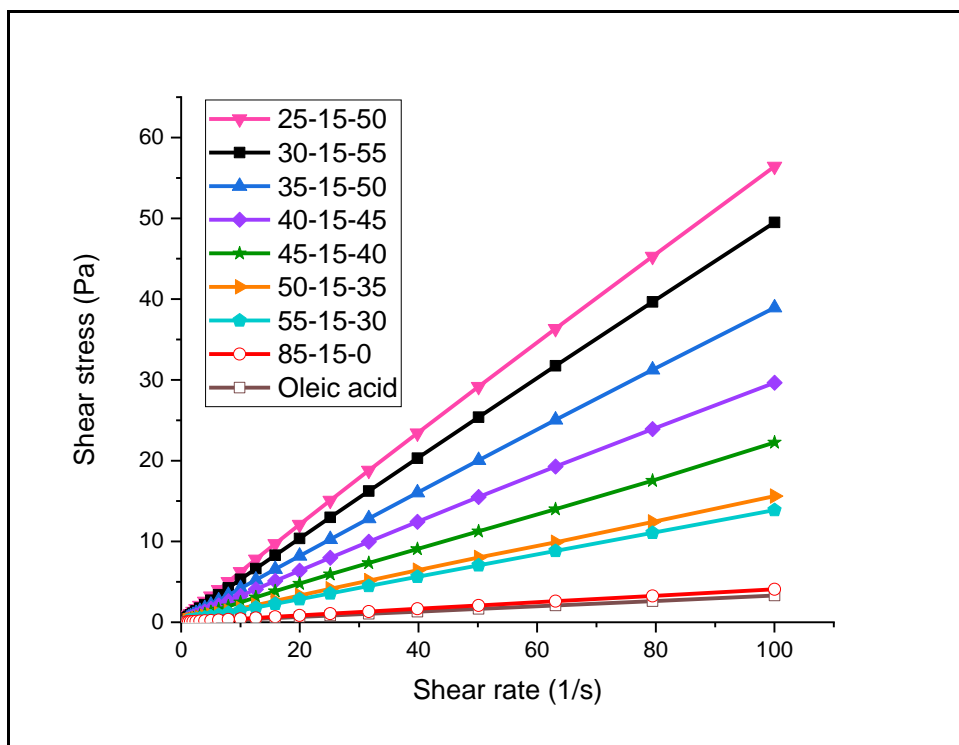

Figure 4.2 Flow behavior curve of 70% ethanol/15% zein/oleic acid (w/w/w, %) emulsions.

Table 4.1 Dynamic viscosity (η), flow behavior index (n), consistency coefficient (K) of 70% ethanol/zein/oleic acid (w/w/w %) emulsions measured after standing for 30 min.

Sample Code	$\tau / (\frac{\delta \gamma}{\delta t})$ slope		Ostwald –De-Waele Model		
	η (Pa.s)	η / K	K (Pa.s^n)	n	R^2
Oleic acid	0.033	1.031	0.032	1.005	0.999
35-20-45	0.881	0.790	1.115	0.944	0.999
40-20-40	0.561	0.812	0.691	0.954	0.999
45-20-35	0.404	0.863	0.468	0.968	1.000
50-20-30	0.319	0.867	0.368	0.967	1.000
55-20-25	0.257	0.977	0.263	0.967	0.999
20% zein	0.096	0.881	0.109	0.972	0.999
25-15-60	0.566	0.816	0.694	0.955	1.000
30-15-55	0.496	0.869	0.571	0.958	1.000
35-15-50	0.391	0.857	0.456	0.966	0.999
40-15-45	0.299	0.810	0.369	0.954	0.999
45-15-40	0.221	0.828	0.267	0.958	0.999
50-15-35	0.156	0.891	0.175	0.961	0.965
55-15-30	0.139	0.993	0.140	0.976	0.999
15% zein	0.041	0.891	0.046	0.974	0.999
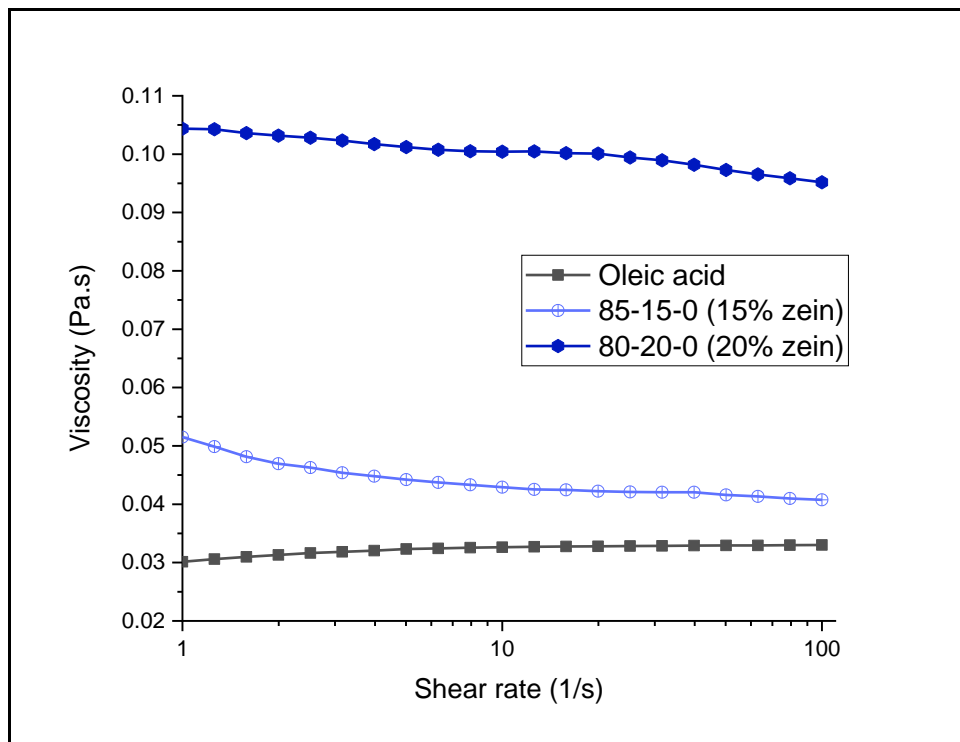
Figure 4.3 Viscosity curve of oleic acid and two zein ethanol solutions (15% and 20% w/w 70% ethanol$_{(aq)}$) at 20 ºC (double log scale).
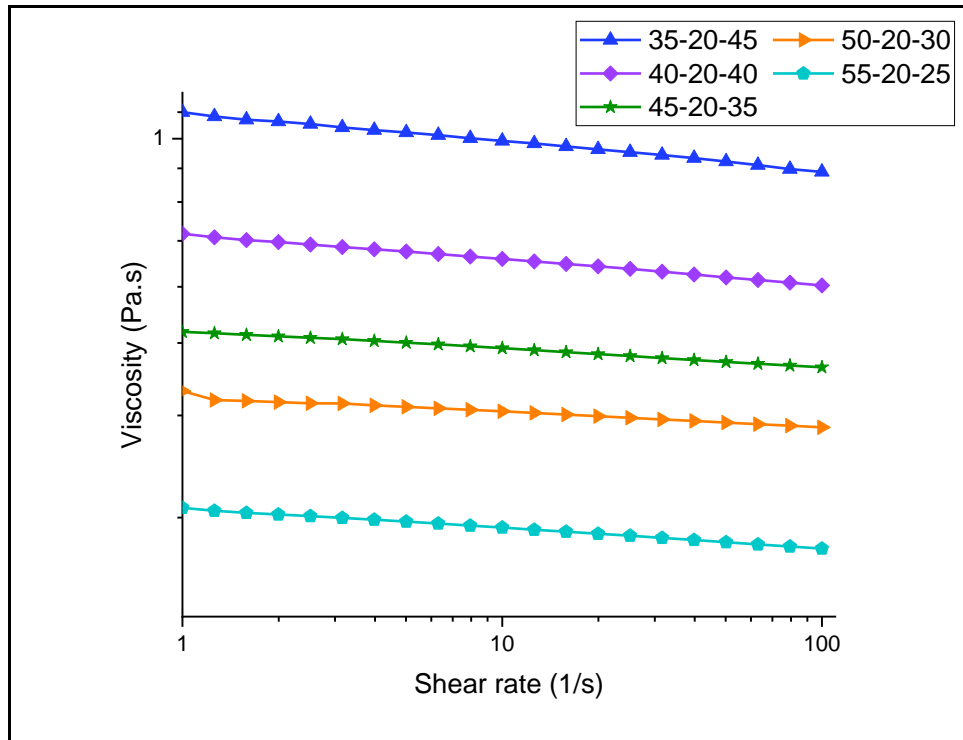
Figure 4.4 Viscosity curve of 70% ethanol/20% zein/oleic acid (w/w/w, %) emulsions.
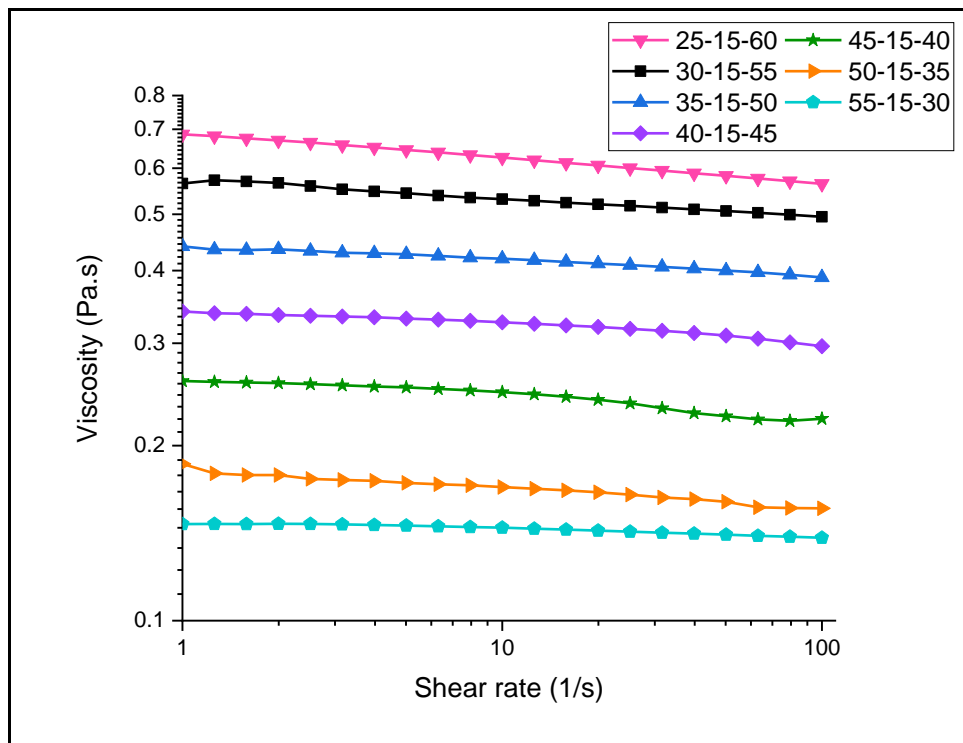

Figure 4.5 Viscosity curve of 70% ethanol/15% zein/oleic acid (w/w/w, %) emulsions.

Stress-strain curves

Based on the findings from the ternary phase diagrams mentioned in chapter 3, samples discovered to form visually homogeneous up-side down stable gels were selected to be measured in rheological experiments. With zein concentration fixed at 20% (w/w), we firstly observed formula samples 35-20-45, 40-20-40, 45-20-35 and 50-20-30 turned into stable gel while inverted the capped vials after storage for 7 days. And for 15% zein concentration, not until stored for 14 days, samples 35-15-50, 40-15-45, 45-15-40, 50-15-35 and 55-15-30 behaved as gels. In order to investigate the effect of time on viscoelastic properties, both 14 and 21 days with 15% zein samples were chosen and examined.

The relationship between applied force and the responding deformation of the material is the core for us to study rheology. By converting the load force into stress, and the deformability into strain, we could mathematically describe the corresponding behaviors of material (Figura & Teixeira, 2007).When stress is plotted along the vertical axis and strain is plotted along the horizontal axis, a stress-strain diagram can be constructed and many of the rheological properties information for viscoelastic materials can be calculated and extracted. Typically, stress-strain curves could be defined as elastic and plastic regions. And for most of the food systems, it is common to start with a plastic region then continue with a plastic region with curved shapes. In elastic region, the stress and stain exhibits a linear relationship which providing information about elasticity of a material (ability for deformation to recover once unloading). While the curve passes the yield point and begins to bend away from linearity, this is characterized as plastic region, meaning the deformation is permanent and the material starts to flow or yield (Drozdov & Christiansen, 2013).

From figure 4.6, all 20% zein-based oleogel stored for 7 days samples displayed as straight lines began from the origin all the way till the end of the measurement, which no distinct yield point can be seen. And the transition from elastic to plastic behavior was also difficult to determine. With the linear fitting of the oscillatory stress and strain, slopes stood for the shear modulus (G) of the samples were listed in Table 4.2, indicating the low elasticity they possessed. And G increased with the increasing of oleic acid amount from 0.035 to 0.095 (Pa), supposing more of the oleic acid in the system would promote a more compact 3D network which was discussed in mayonnaise type of oil-in-water emulsion samples (Ma and Barbosa-Cánovas, 1995).

Yield stress is crucial for determine the transition point where material transform from elastic to plastic behavior. It is defined as the minimum shear stress required to initiate flow (Dzuy and Broger, 1983., and Steffe, 1996). While applying stress beyond this point, the displacement of strain cannot be retrieved. However, for many food and biological materials, especially ductile samples, the stress-strain profile shows as monotone, instead of a point, the yield stress falls in a range. In this type of situations, a technique uses 0 to 0.2% strain as the elastic region and the stress occurs at 0.2% strain is proposed as 0.2% offset strength also the (Callister, 2004., and Laurati et al., 2009). According to the method, 0.2% offset strengths were calculated and summarized in Table 4.2. Similar to G results, the yield stress at 0.2% strain increased with addition of oleic acid into the system. 35-20-45-7d had the largest stress of 3.102 Pa and gradually decreased by 5% of oleic acid to the lowest stress 1.453 Pa owned by 50-20-30-7d. This could result from the increasing particle fraction of the oil droplets which interact inside the colloidal system and consider as a concentrated colloid (Quemada and Berli, 2002).

In Figure 4.7, 15% zein concentration with 70% ethanol ranging from 30% (w/w) to 55% (w/w) (corresponding oleic acid 55-30% (w/w)) stored for 14 days were selected from ternary phase diagrams. The samples could be separated into two groups, 30-15-55-14d, 50-15-35-14d and 55-15-30-14d showed as smooth gradual straight lines passing through origin. For 35-15-50-14d, 40-15-45-14d and 45-15-40-14d, they began with steeper straight lines connected with concaved curves, meaning there were more obvious behavior changing from elastic to plastic. The slope of linear region indicating G increased with increasing amount of 70% ethanol from 35-45% (Table 4.1), possibly due to the zein molecules are fully swollen and have high mobility to attach to the surface of the oil droplets forming a more stable network structure.

For calculated yield stress at 0.2% strain, we can observe sample 45-15-40-14d had the highest stress value then followed by 40-15-45-14d, 35-15-50-14d, next the linear curves with high ethanol or oleic acid content samples 50-15-35-14d, 55-15-30-14 and 30-15-55-14d (Table 3.2). Understandably, large amount of 70% ethanol provides a diluted emulsion which less of the inter-particle interaction in place, in turn, smaller the yield stress it has. It is evidenced by Ochowiak, Broniarz-Press, & Rozanski, 2012, that the increasing the oil volume fraction of the O/W emulsion would create larger droplet size. And the dynamic coalescence of droplets may affect the gelation of the zein-based oleogels, causing 30-15-55-14d had the weakest structure with the lowest yield

stress.

With the storage time extended from 14 days to 21 days, 15% zein concentration oleogels on stress-strain diagram could be distinguished into four categories (Figure 4.8). First, the highest oleic acid containing sample 30-15-55-21d still behaved as a straight linear line without distinct curvature had the lowest G 0.087 Pa. The second group, high ethanol containing samples 50-15-35-21d and 55-15-30-21d displayed as small curvature smooth curves with slightly higher G between 0.272 to 0.321 Pa. While 45-15-40-21d and 35-15-50-21d had large curvatures after linear region which were considered as another group. Lastly, 40-15-45-21d had a point located around 10% strain where the profile started to deviate from the linear region (G = 3.903 Pa) was called the proportional limit. Stresses beyond this point lead to nonlinear deformation. And yield point at strain around 25% was shown on the graph, indicating the stable solid structure was disrupted permanently and began to flow. The deformation continued with the nonlinear curve after that point, no rupture point was reached (Ross-Murphy, 1995).

While investigating the 0.2% offset yield stress of 21 days samples, 40-15-45-21d could be considered as a rigid gel with high yield stress (33.878 Pa). Next, altering the formula either by adding 5% of oleic acid (45-15-40) or 70% ethanol (35-15-50) could induce soft gels with yield stress 1/3 or 1/4 in comparison to 45-15-40-21d, respectively. The yield stress would further declined by incorporating more ethanol into the system. Both oleogels 50-15-35-21d and 55-15-30-21d had relatively high amount of ethanol and similar yield stresses (< 3Pa). For 30-15-55-21d, it held the lowest yield stress which implying its structure was fragile and easy to flow.

In order to understand the time effect, oleogels with 15% zein concentration stored for 14 and 21 days were compared between same compositions. All of the 21 days samples had considerable increment of the elasticity due to the slow self-assembly of the structure, forming a more compact network while retaining the plasticity which the structure would not crack nor break into small pieces during the measurement (Gonzalez-Gutierrez & Scanlon, 2018; Ikeda & Nishinari, 2001). And the yield stress differences were pronounced with long-term gelation period, which we could categorize 14 days samples in two groups but four groups for 21 days.
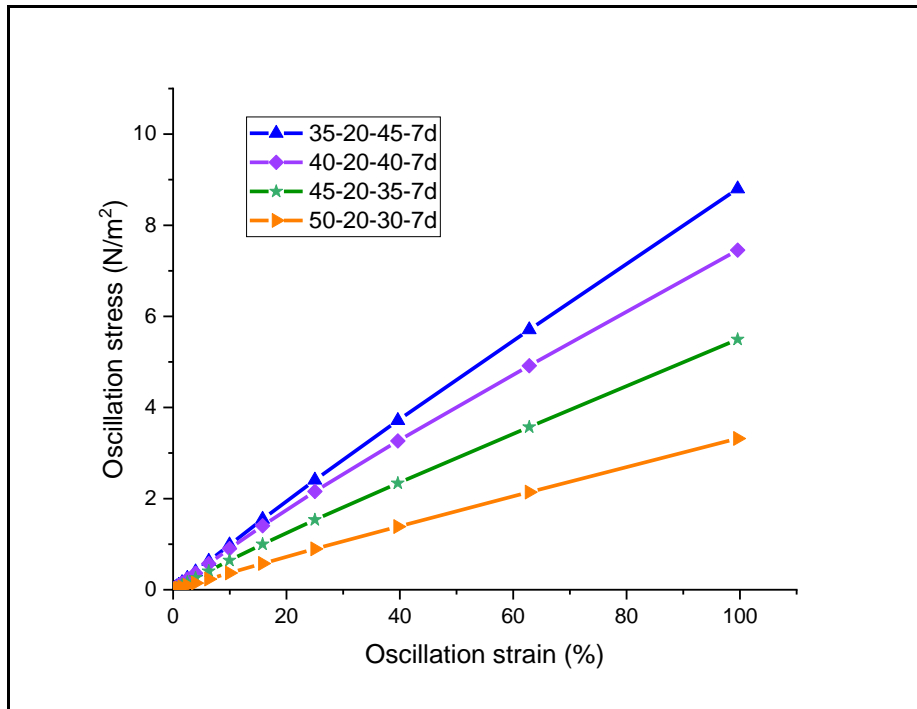
Figure 4.6 Stress-strain diagram of 20% zein-based oleogels stored for 7 days with sample coding as 70% ethanol (wt%)-zein (wt%)-oleic acid (wt%)-7(days).
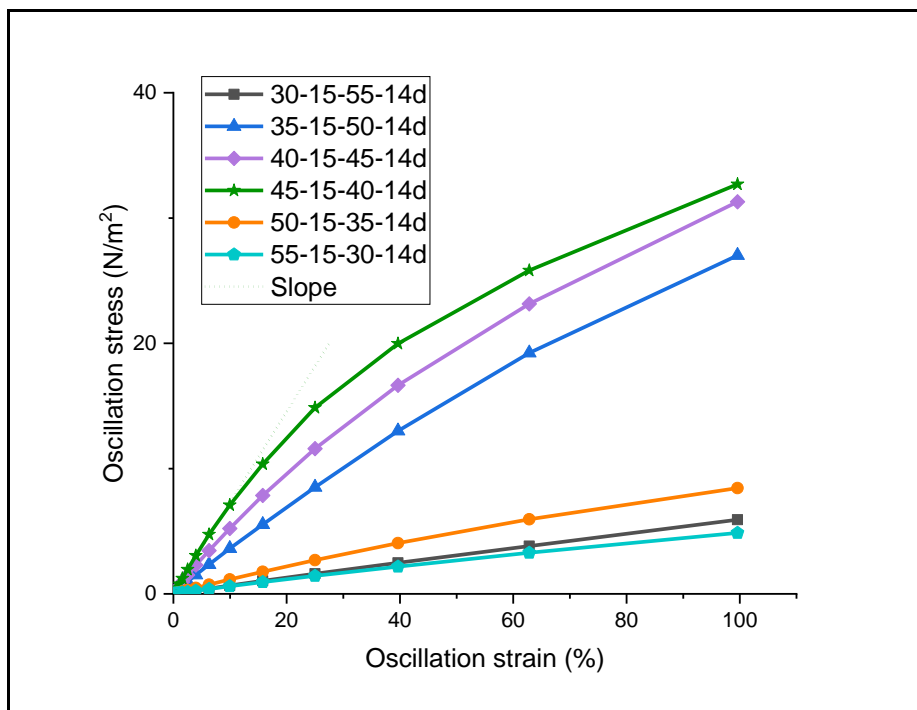

Figure 4.7 Stress-strain diagram of 15% zein-based oleogel stored for 14 days with sample coding as 70% ethanol (wt%)-zein (wt%)-oleic acid (wt%)-14(days).
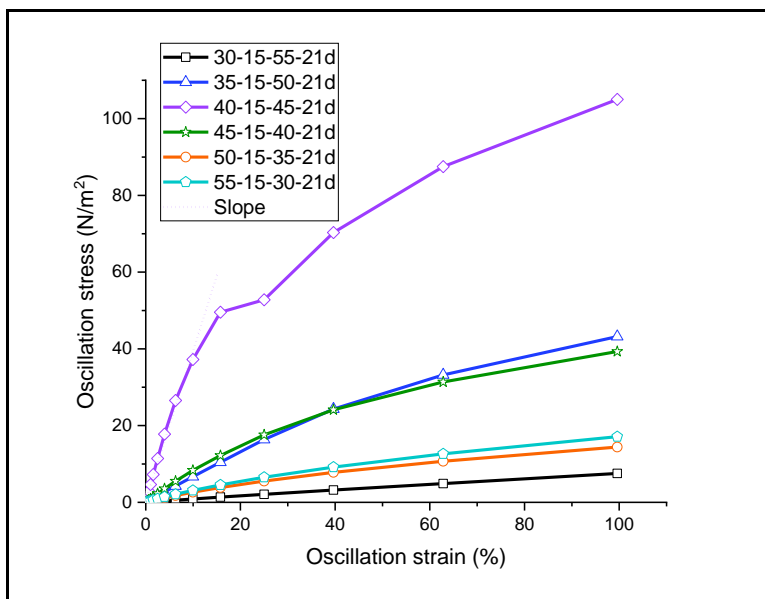
Figure 4.8 Stress-strain diagram of 15% zein-based oleogel stored for 21 days with sample coding as 70% ethanol (wt%)-zein (wt%)-oleic acid (wt%)-21(days).

Table 4.2 Storage modulus (*G*) of stress-strain diagrams linear region and 0.2% offset yield stress obtained from 0.2% strain limit technique.

Code	Stress (σ) /strain (γ) shear modulus, *G* (Pa)	0.2% offset strength (Pa)
35-20-45-7d	0.095	3.102
40-20-40-7d	0.084	2.786
45-20-35-7d	0.060	1.971
50-20-30-7d	0.035	1.453
30-15-55-14d	0.067	0.871
35-15-50-14d	0.366	3.806
40-15-45-14d	0.533	4.973
45-15-40-14d	0.726	6.817
50-15-35-14d	0.116	1.253
55-15-30-14d	0.061	0.780
30-15-55-21d	0.087	1.193
35-15-50-21d	0.673	8.506
40-15-45-21d	3.903	33.878
45-15-40-21d	0.851	12.186
50-15-35-21d	0.272	2.546
55-15-30-21d	0.321	2.947

4.4.2 Viscoelastic behavior

Strain sweep test results

To determine the material viscoelastic properties, conducting oscillating small strain sweep experiment could provide two important dynamic moduli, the storage modulus G', a measure of the elasticity, and the loss modulus G", representing viscous components. The strain sweep results of 20% zein (w/w) oleogels stored for 7 days were summarized in Figure 3.9 and Table 4.3. According to Figure 4.9, all 4 samples showed liquid like behavior (G'< G") in strain sweep tests with constant frequency at 1 Hz, instead of what we observed in tube inversion method as up-side-down gels. This difference could possibly due to the under developed structures are easily disrupted by the perturbation, which in here will be the frequency applied.

Comparing storage modulus (G'), 40-20-40-7d had the highest reading and followed by 35-20-45-7d, 45-20-35-7d then 50-20-30-7d. However, when we looked at tanδ values in plateau region listed in Table 3.3 to understand which sample had less liquid like behavior, the order slightly changed between 35-20-45-7d and 45-20-35-7d. It seems like when the ratios between 70% ethanol and oleic acid is close to 1, the emulsion system has more gel like behavior and less liquid behavior than the samples with ratios depart from 1 (Figure 4.10) (Ikeda & Nishinari, 2001)(Tabilo-Munizaga & Barbosa-Cánovas, 2005).

When we decreased the amount of zein concentration to 15%, none of the compositions could be observed as up-side-down gel at 7th days of storage time, so 14 days and 21 days were chosen to be examined for their viscoelastic properties. Based on Figures 4.11 and Table 3.3, among samples stored for 14 days, 45-15-40-14d was the only sample had G' larger than G", defined as a gel at this measuring condition. And the other 5 samples behaved as liquid with G' < G".

G' and G" were independent of the applied strain in the plateau region, where the structures remained intact and the deformation of the sample was assumed to be reversible (Mezger, 2014). Noticeably, while strain was larger than 10%, the G' curves decayed, indicating the structures were interrupted and causing the weak gel structures to collapse. And this phenomenon was more obvious with formula that had higher G' value. Similar to 20% zein concentration samples, the ratio of 70% ethanol to oleic acid approached to 1 would attribute higher G', in this case, G' value of 45-15-40-14d was the highest followed by 40-15-45-14d and 35-15-50-14d, then with high 70%

ethanol samples 50-15-35-14d and 55-15-30-14d, lastly 30-15-55-14d.

Although 45-15-40-14d was the only sample behaved like solid, when we looked at the tan δ value of 15% zein concentration samples, except 30-15-55-14d with highest amount of oleic acid, the others were getting close to 1 assuming some compact structures formed and the behaviors were gradually transforming to be more rigid than liquid (Figure 4.12). Mentioned in concentrated colloid system (Masalova et al., 2006; Pal, 2011), tan δ value could be used to reflect the strength of the colloidal forces. And decreasing of tan δ to less than 1 suggested that the particles are highly associated and sometimes is described as structured fluids.

After stored for 21 days, except high oleic acid sample 30-15-55-21d, all others were confirmed as gel with cross point (G' = G") showed in Figure 4.13 indicating the flow point where the structures no longer sustained its original structure and ruptured from semi-solid into viscous liquid. After the flow point, both G' and G" smoothly curved downward instead of a sharp decay meaning the breakdown of the network was more likely to be a continuous plastic deformation which is commonly exist in colloidal system (Marze, Guillermic, & Saint-Jalmes, 2009).

For better distinguishing the gel strength, both tan δ value (Figure 4.14 and Table 4.3) and G' value in plateau region were used. When using tan δ as indicator, the order was 40-15-45-21d, 45-15-40-21d, and 55-15-0-21d, then two similar ones 35-15-50-21d and 50-15-35-21d. But the order slightly changed when using G' as indicator. 40-15-45-21d kept as the strongest gel, while 45-15-40-21 was the second and followed by 35-15-50-21d then 55-15-30-21d, and lastly, 50-15-30-21d. When we looked into the originally G' and G" value of samples 35-15-50-21d and 50-15-35-21d, the G' was twice larger for 35-15-50-21d than 50-15-35-21d. And once the G" increased a little in 50-15-35-21d measurement would make the ratio seem to enlarge more. However, the actual storage modulus also the elasticity was relatively different and larger for 35-15-50-21d in comparison to 50-15-35-21d.

Both Figure 4.12 and Figure 4.14 showed the effect of time on gel rigidity by the decreasing of tan δ and also the increasing of G'. It is assumed that the zein molecules are acting as an oleogelator. And by its ability to self-assembly into ordered fibrous like structure, it could not only stabilize the emulsion system but also create network structure to further stationary the oil droplets and forming a gel with time elapsed.
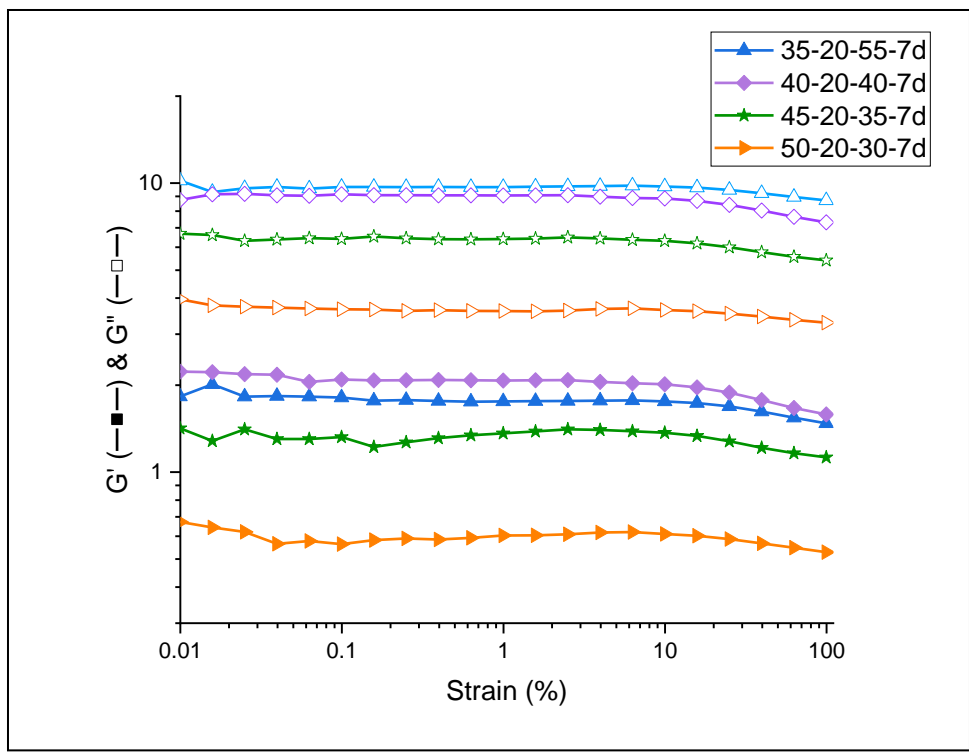
Figure 4.9 Strain sweep results of 20% zein-based oleogel stored for 7 days with sample coding as 70% ethanol (wt%)-zein (wt%)-oleic acid (wt%)-7(days).
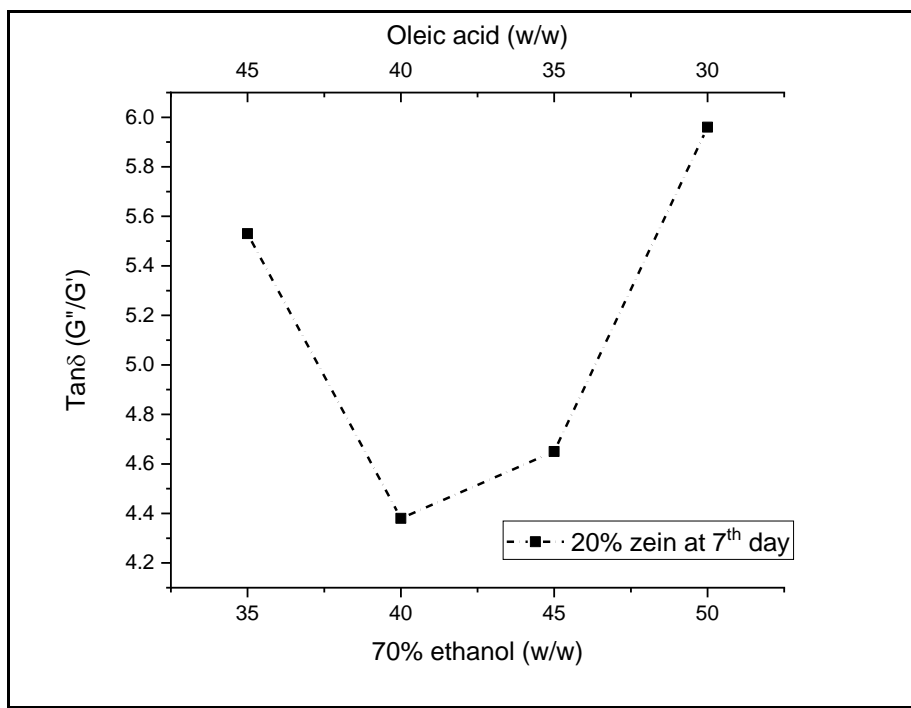

Figure 4.10 Tanδ results of 20% zein-based oleogel stored for 7 days.
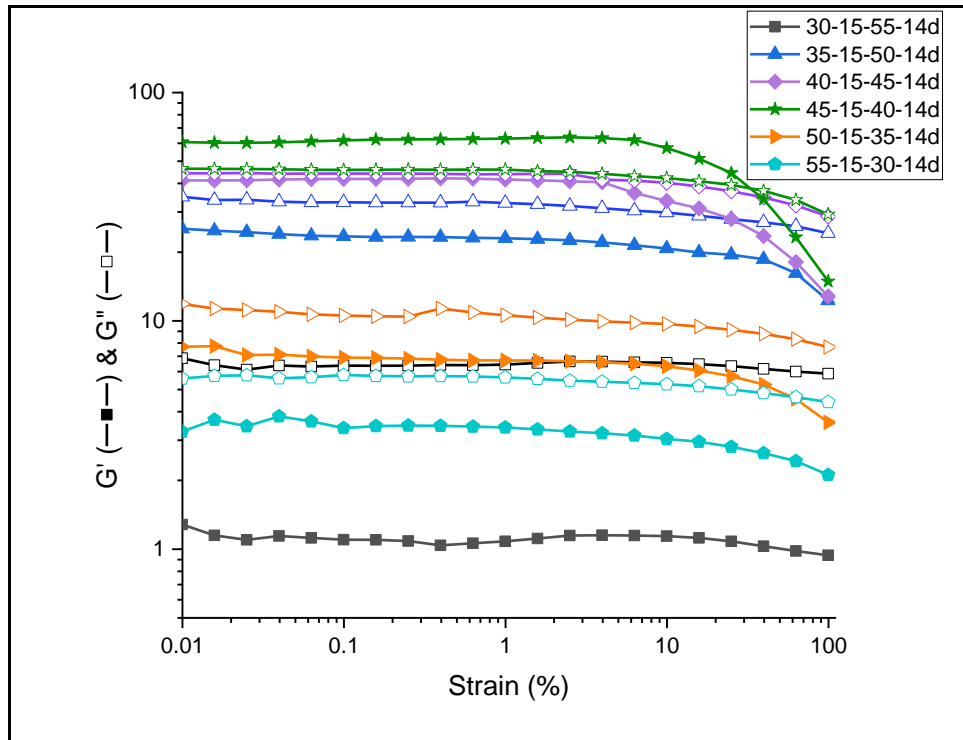
Figure 4.11 Strain sweep results of 15% zein-based oleogel stored for 14 days with sample coding as 70% ethanol (wt%)-zein (wt%)-oleic acid (wt%)-14(days).
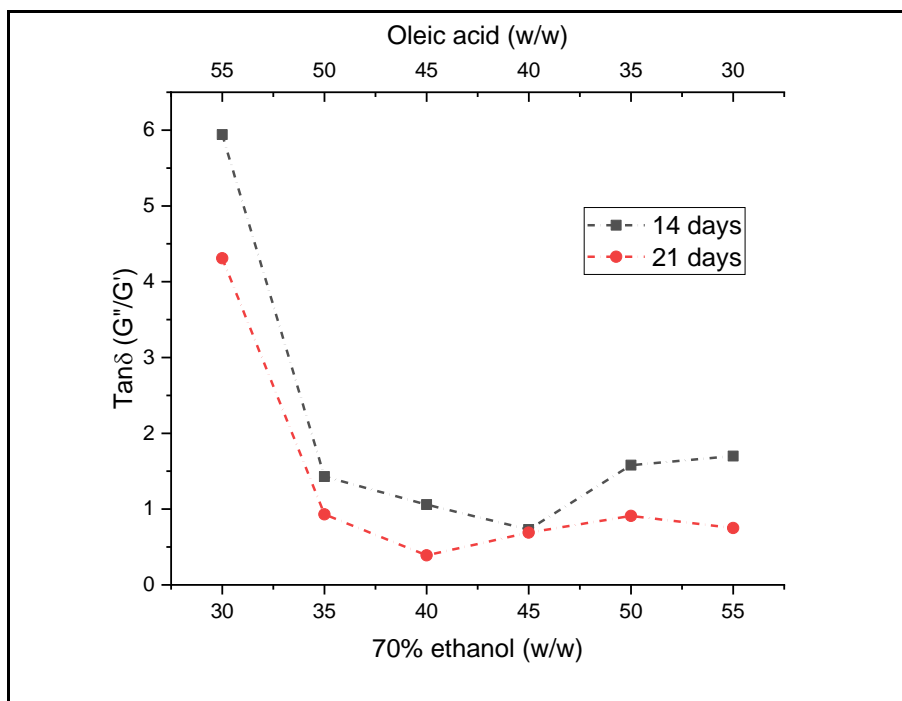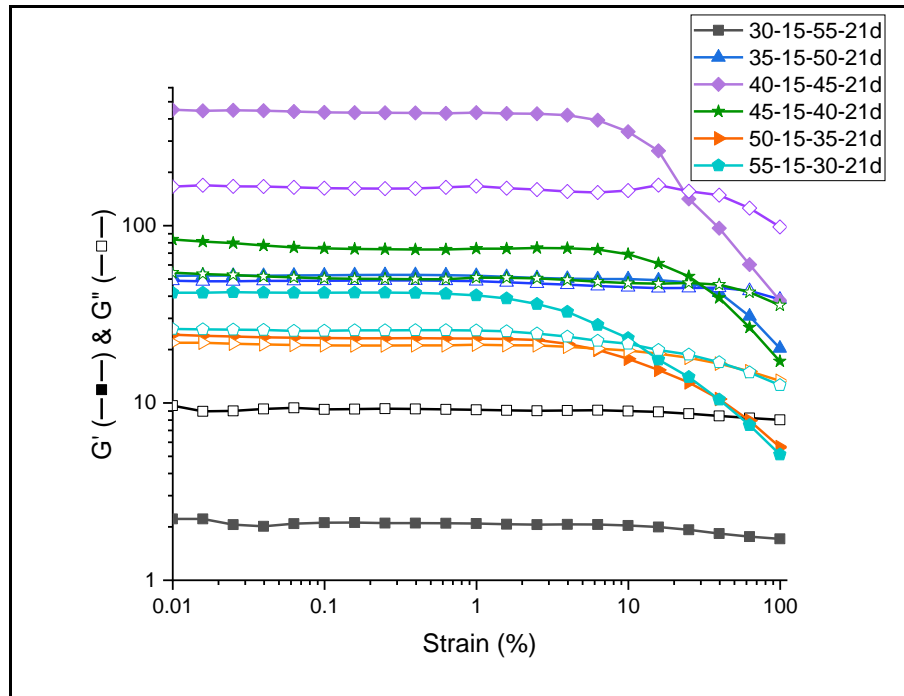

Figure 4.12 Tan δ results of 15% zein-based oleogel stored for 14 and 21 days.

Figure 4.13. Strain sweep results of 15% zein-based oleogel stored for 21 days with sample coding as 70% ethanol (wt%)-zein (wt%)-oleic acid (wt%)-21(days).
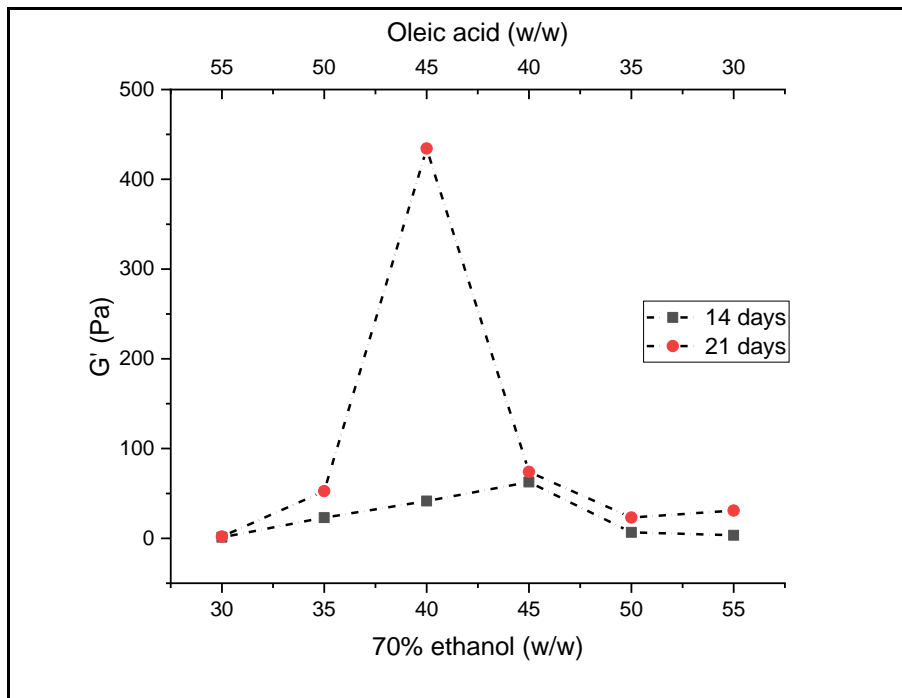

Figure 4.14 Storage modulus values at strain sweep flow points (G'≤G") of 15% zein-based oleogels stored for 21 days.

Table 4.3 Frequency sweep and strain sweep results of zein-based oleogels at 7, 14 and 21 days.

| Sample code | Strain sweep | | | | Frequency sweep | |
| | In plateau region | | At cross point (G'=G") | | At cross point (G'=G") | |
	Tan δ	Frequency (Hz)	Strain (%)	G' (Pa)	Frequency (Hz)	G' (Pa)
35-20-45-7d	5.53	0.03	---	---	0.03	2.32
40-20-40-7d	4.38	0.20	---	---	0.20	10.53
45-20-35-7d	4.65	0.04	---	---	0.04	1.68
50-20-30-7d	5.96	<0.01	---	---	<0.01	---
30-15-55-14d	5.94	<0.01	---	---	<0.01	---
35-15-50-14d	1.43	12.60	---	---	12.60	1276.34
40-15-45-14d	1.06	19.96	---	---	19.96	1868.60
45-15-40-14d	0.73	39.83	39.65	34.07	39.83	2691.56
50-15-35-14d	1.58	6.31	---	---	6.31	112.55
55-15-30-14d	1.70	2.04	---	---	2.04	19.56
30-15-55-21d	4.31	<0.01	---	---	<0.01	---
35-15-50-21d	0.93	25.13	39.65	42.02	25.13	1990.90
40-15-45-21d	0.39	79.61	25.02	141.64	79.61	8591.20
45-15-40-21d	0.69	50.14	39.65	39.18	50.14	3174.10
50-15-35-21d	0.91	12.61	6.29	19.94	12.61	258.65
55-15-30-21d	0.75	7.95	9.96	20.76	7.95	90.93

Frequency sweep test results

For physical-linked gel, it can be categorized as strong or weak gel by small amplitude frequency sweep tests. In our frequency sweep test (Figure 4.15), except composition 50-20-30, other three samples showed gel like behavior (G' > G") at different frequency range and would eventually turning into viscous liquid during the measurements. All samples were frequency dependent for both G' and G", and for the three gel-like samples (excluded 50-20-30), they had cross points of G' = G" at varied frequencies summarized in Table 4.3 and Figure 4.16.

Sample 40-20-40-7d had the highest G' (Figure 4.16) and the cross-point frequency at 0.20 Hz, indicating this sample was most rigid and had the strongest gel structures to resist the agitation applied by the rheometer. Followed by 45-20-35-7d at 0.04 Hz and 35-20-45-7d at 0.03 Hz, and the most fragile oleogel 50-20-30-7d below 0.01 Hz. All four samples' cross points were below 0.1 Hz which was the constant used in strain sweep tests, it explained why the results of strain sweep determined the samples as liquid rather gel. Lopes da Silva and Rao (2007) explained that

in a strong gel G' would predominate over G" throughout the frequency range, showing that parameters were independence of frequency, while weak gels tended to be frequency dependent. In order to better distinct between strong or weak gel, it was proposed in condensed colloidal system that when G' was 10 times larger than G" could be defined as a strong gel, whereas $1 > G''/G' > 0.1$ was considered as a weak gel. So once again confirmed that 20% zein based oleogels stored for 7 days only were weak gels.

With lesser amount of zein (15%) but prolonged storage time, sample 30-15-55-14d was the only exception that still behaved like liquid instead of gel. The other 15% zein oleogels showed thixotropic behavior which at high frequency the gel would turning into viscous liquid (Figure 3.17). Using G'/G" ratio calculated in Table 3.3 we could classified the six samples into three groups. First would be liquid-like 30-15-55 (G' < G"), the second group were 35-15-50, 40-15-45 and 45-15-40 with solvents ratio close to 1, also their 0.1 G' > G", indicating they were strong gel. The third were 50-15-35 and 55-15-30 that the G's were larger than G"s but not yet to reach ten times of the magnitude which were defined as weak gel. The firmness of the strong gel that rose from the network structure was represented by the magnitude of G' and also the resistance of G' to the distribution caused by frequency change.

In Figure 4.18 the independency of the G' to frequency was more obvious than G", evidenced the samples were homogenous colloidal systems. Higher the frequency not only disrupted the aggregated network but also enhanced the chance for particles to flow and collide which explained why both G' and G" kept increasing before and after the flow point. And we could also assume that group 2 we mentioned above had a relatively concentrated emulsion system and the internal structures were similar between three composition after intense agitation confirmed by the coinciding value of G' and G" at high frequency.

Similar rheological results could be obtained from 21 days samples, but with longer storage time, gels gained higher rigidity which represented by higher G', and also more developed network structure which could resist higher frequency during the measurement (Figure 4.19 and Table 4.3). All of the G" values increased with the increasing of the frequency, not only indicating the samples were thixotropic but also meaning the systems were colloidal like emulsions which the molecules flow and encounter more frequently during the test.

Sample 40-15-45-21d was the toughest gel with overall highest G', followed by 5% less oleic acid 45-15-40-14d and 5% more oleic acid 35-15-50-21d samples. While lowering 5-10% more of oleic acid, the G' suddenly dropped 10 times lower. And for sample 30-15-55-21d which contained highest amount of oleic acid still behaved like liquid under this measurement resulted from the insufficient degree of structure to trap or stationary the oil droplets (Dreher, Blach, Terjung, Gibis, & Weiss, 2020). By summarizing the G' values at viscoelastic transition point in frequency sweep test (Table 4.4), it is obvious when the solvent ratio closed to 1 would exhibit the highest gel strength (40-15-45-21d). And the rigidity decreased with increasing either the amount of 70% ethanol or oleic acid. It may because zein was not only absorbed at the interface of the oil droplets, but also formed a three-dimensional continuous, percolating network when the system had suitable HLB for molecules to reorganize (Nephomnyshy et al., 2020).

While comparing cross points G' value at where G" became greater than G" in frequency sweep experiments at different storage time, we found out the maximum gel strength was owned by 45-15-40 at 14 days but 40-15-45 for 21 days. The solvent ratios of these two formula approached to 1, assuming to be the right composition for obtaining higher gel strength, and seems like with higher amount of oleic acid requires more time for the gel network to form, and once the structures formed, it would dramatically increase the elastic properties and possibly having a better self-assembled rigid structure. This phenomenon has been discussed in emulsion systems, and the storage modulus is a useful index to understand the stability of the sample against settling or separation while the internal structures interact and hold the fluid droplets.

All of the storage modulus G' were significantly increased with storage time, as summarized in Table 4.4 and Figure 4.19. Cross point of G' and G" were also delayed to higher frequencies (Table 4.3), which demonstrated the self-assembly process was dominantly affected by time. The slow gelation of zein were also discussed and confirmed in Guardiola & Padua, 2020. Under non alkaline ethanol extraction method, 20% (w/v) zein dissolved in 70% ethanol would gradually formed gels after three weeks of storage.
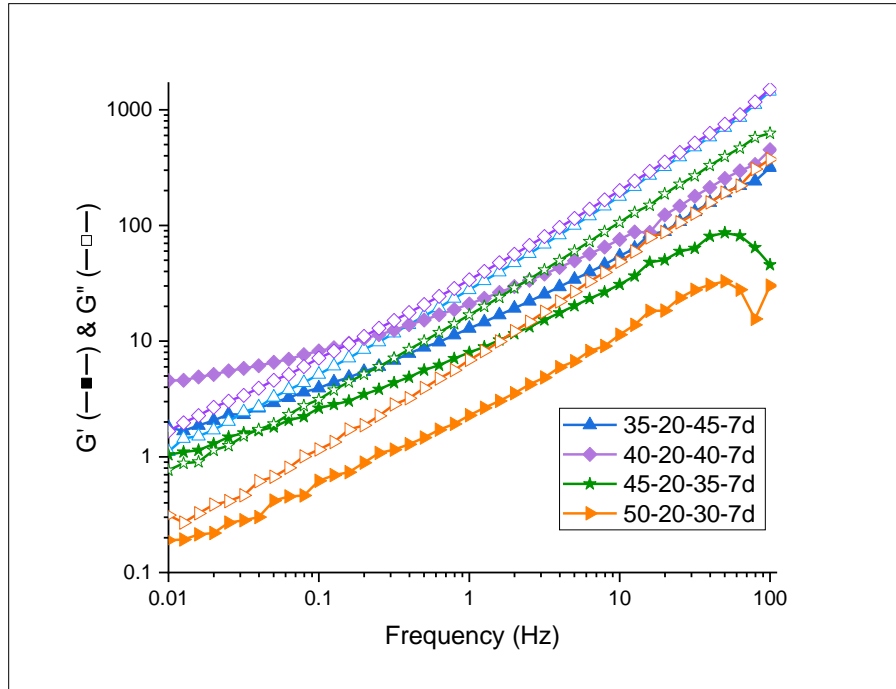
Figure 4.15 Frequency sweep results of 20% zein-based oleogel stored for 7 days with sample coding as 70% ethanol (wt%)-zein (wt%)-oleic acid (wt%)-7(days).
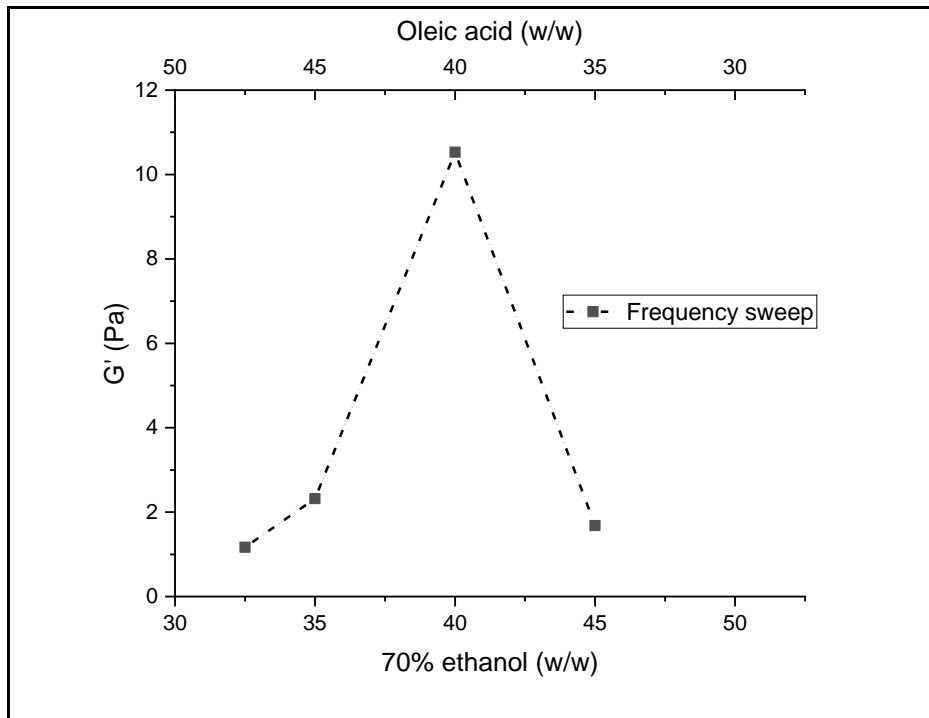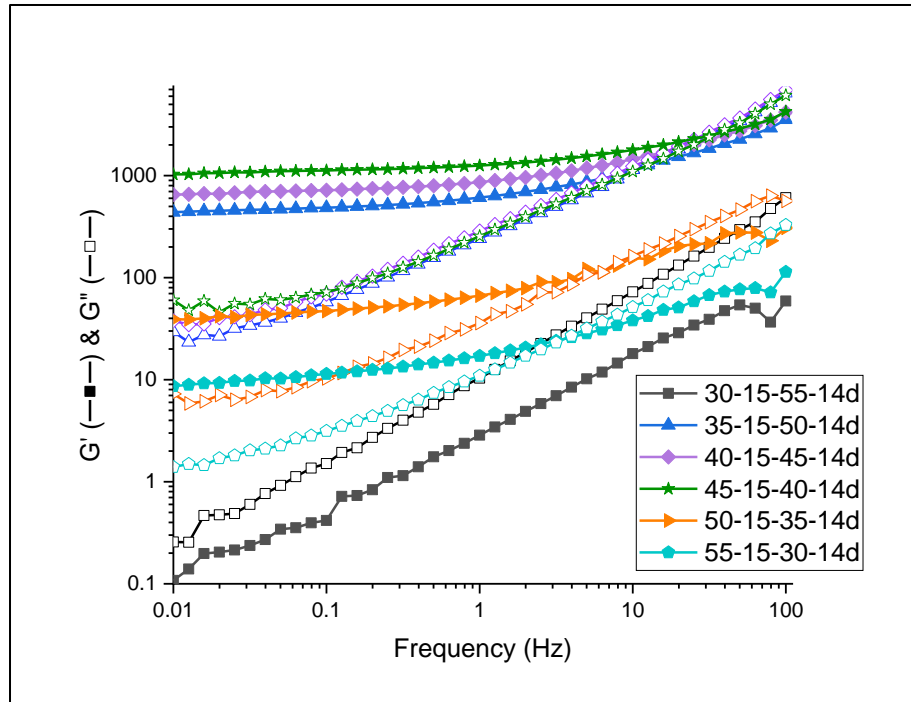

Figure 4.16 Storage modulus values at frequency sweep flow points (G' ≤ G") of 20% zein-based oleogels stored for 7 days.

Figure 4.17 Frequency sweep results of 15% zein-based oleogel stored for 14 days with sample coding as 70% ethanol (wt%)-zein (wt%)-oleic acid (wt%)-14(days).
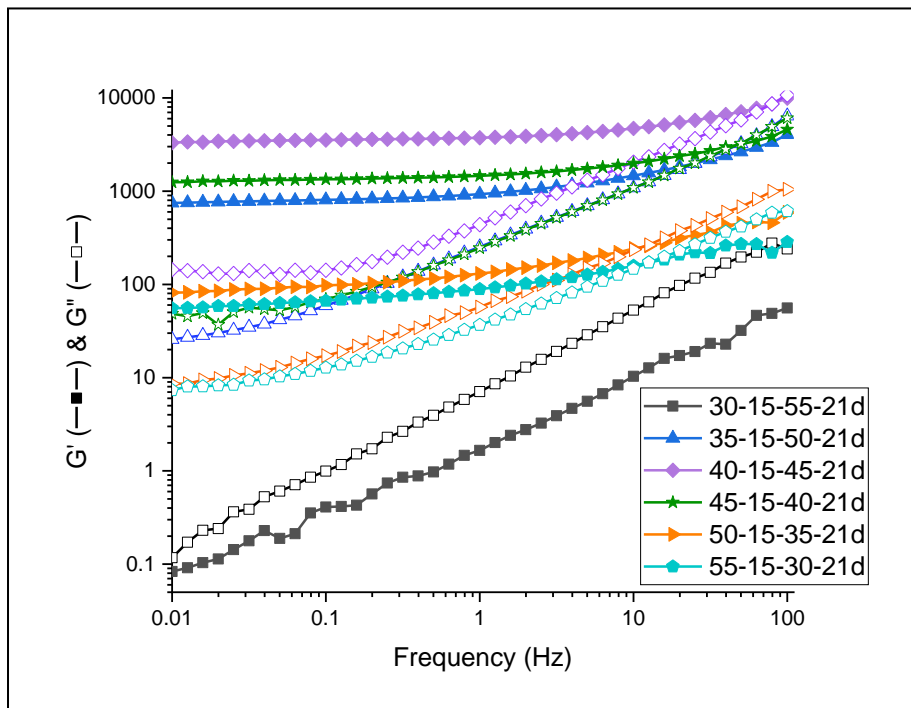

Figure 4.18 Strain sweep results of 15% zein-based oleogel stored for 21 days with sample coding as 70% ethanol (wt%)-zein (wt%)-oleic acid (wt%)-21(days).
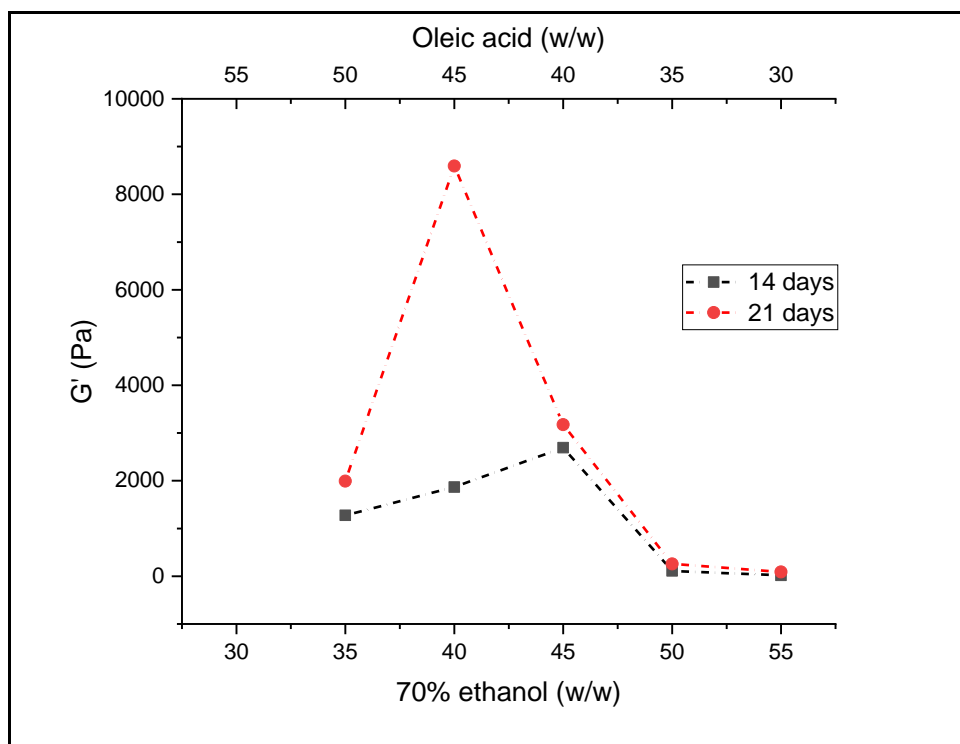
Figure 4.19 Storage modulus values at frequency sweep flow points (G' ≤ G") of 15% zein-based oleogels stored for 14 and 21 days.

Table 4.4 Summary of changes in G' and G" at 0.01 Hz of zein-based oleogels during storage.

Sample code	14 day			21 day		
	G' (Pa)	G" (Pa)	G''/G'	G' (Pa)	G" (Pa)	G"/G'
30-15-55	0.083	0.117	0.71	0.108	0.257	0.42
35-15-50	438.95	29.54	14.86	748.23	25.74	29.07
40-15-45	652.44	37.90	17.21	3298.46	143.71	22.95
45-15-40	1028.72	60.21	17.09	1248.14	48.61	25.65
50-15-35	39.08	7.269	5.38	81.39	8.626	9.44
55-15-30	8.651	1.394	6.21	55.34	7.346	7.53

4.5 Conclusions

The present study demonstrated a non-thermal method for fabrication of zein-based oleogels at room temperature. The effect of solvent composition, zein concentration and time on rheological properties were investigated. The 70% ethanol-zein-oleic acid system started as pseudoplastic viscous behavior emulsions determined by flow sweep test. The apparent viscosity and consistency index (K) increased oleic acid and decreasing of 70% ethanol content, which that the volume

fraction of oil droplets dominantly influenced the emulsion viscosity. Increasing the zein concentration also increased the viscosity resulted from the addition of solid content in the system. The zein molecules acting as oleogelator would self-assembled into 3D network structures and entrapped up to 50% (w/w) weight fraction of oleic acid after 7 days with 20% zein concentration. And it required more time for samples with 15% zein to develop into gel like behavior determined by G' > G" from strain sweep and frequency sweep tests. The oleogels were frequency dependent which was commonly seen in emulsion gels (emulgel) cases that the structures were consisted of non-covalent physical bonds.

By summarizing the G' values at viscoelastic transition point in frequency sweep test, it observed when the solvent ratio closed to 1 would exhibit the highest gel strength (40-15-45-21d). In this case, when an increase in the oil content making the solvent ratio depart from 1, the changing of the solvent hydrophobicity limited the mobility of zein molecules to further rearrange into wider range of network structure. And it caused the gel strength weaker and easily disrupted by shear force. Other way around, when breaking the solvent balance by adding more of the 70% ethanol into the system, the gel strength weakened might owing to loss of anchor points provided by oil droplets for zein to deposit on and organized into extended 3D structures.

Due to the gelation mechanism of this oleogel system was mainly dependent on the self-assembly process of zein, time is a crucial factor for the gel strength and rigidity. All oleogels showed a shear reversible behavior at room temperature, and the gelation rate and strength varied with the rearrangement of the zein self-assembly network. These results show that the rheological behavior of zein-based olegel can be manipulated by changing solvent composition, zein concentration and storage time, which may provide interesting features for different applications in the field of food, drug delivery, and cosmetic.

4.6 References

Ahmed, E. M. (2015). Hydrogel: Preparation, characterization, and applications: A review. *Journal of Advanced Research*, *6*(2), 105–121. https://doi.org/10.1016/j.jare.2013.07.006

Alavi, F., Momen, S., Emam-Djomeh, Z., Salami, M., & Moosavi-Movahedi, A. A. (2018). Radical cross-linked whey protein aggregates as building blocks of non-heated cold-set gels. *Food Hydrocolloids*, *81*, 429–441. https://doi.org/10.1016/j.foodhyd.2018.03.016

Alger, M. (2017). *Polymer Science Dictionary*. Springer. https://doi.org/10.1007/978-94-024-

0893-5

Angelova, A., Garamus, V. M., Angelov, B., Tian, Z., Li, Y., & Zou, A. (2017). Advances in structural design of lipid-based nanoparticle carriers for delivery of macromolecular drugs, phytochemicals and anti-tumor agents. *Advances in Colloid and Interface Science*, *249*, 331–345. https://doi.org/10.1016/j.cis.2017.04.006

Argos, P., Pedersen, K., Marksl, M. D., & Larkinsflll, B. A. (1982). Structural Model for Maize Zein Proteins. *Journal of Biological Chemistry, 257*(17), 9984–9990.

Balerna, A., & Mobilio, S. (2015). Introduction to Synchrotron Radiation. In Mobilio, S., Boscherini, F., Meneghini, C. (Eds.) *Synchrotron Radiation: Basics, Methods and Applications:* 3–28. Springer. https://doi.org/10.1007/978-3-642-55315-8

Bajpai, M., Sharma, P. K., & Mittal, A. (2009). A study of oleic acid oily base for the tropical delivery of dexamethasone microemulsion formulations. *Asian Journal of Pharmaceutics*, *3*(3), 208–214. https://doi.org/10.4103/0973-8398.56299

Beaucage, G. (1995). Approximations leading to a unified exponential/power-law approach to small-angle scattering. *Journal of Applied Crystallography*, *28*(6), 717–728. https://doi.org/10.1107/s0021889895005292

Beaucage, G. (1996). Small-angle scattering from polymeric mass fractals of arbitrary mass-fractal dimension. *Journal of Applied Crystallography*, *29*(2), 134–146. https://doi.org/10.1107/S0021889895011605

Beaucage, G. (2012). Combined small-angle scattering for characterization of hierarchically structured polymer systems over nano-to-micron meter: Part II theory. In Matyjaszewski, K. & and Moeller, M. (Eds.). *Polymer Science: A Comprehensive Reference, 10 (2*), 399–409. Elsevier B.V. https://doi.org/10.1016/B978-0-444-53349-4.00032-7

Benson, M. D., Buxbaum, J. N., Eisenberg, D. S., Merlini, G., Saraiva, M. J. M., Sekijima, Y., Westermark, P. (2018). Amyloid nomenclature 2018: recommendations by the International Society of Amyloidosis (ISA) nomenclature committee. *Amyloid*, *25*(4), 215–219. https://doi.org/10.1080/13506129.2018.1549825

Berthaume, M. A. (2016). Food mechanical properties and dietary ecology. *American Journal of Physical Anthropology*, *159*, 79–104. https://doi.org/10.1002/ajpa.22903

Blach, C., Gravelle, A. J., Peyronel, F., Weiss, J., Barbut, S., & Marangoni, A. G. (2016). Revisiting the crystallization behavior of stearyl alcohol : stearic acid (SO : SA) mixtures in edible oil. *RSC Advances*, *6*(84), 81151–81163. https://doi.org/10.1039/c6ra15142f

Brosey, C. A., & Tainer, J. A. (2019). Evolving SAXS versatility: solution X-ray scattering for macromolecular architecture, functional landscapes, and integrative structural biology. *Current Opinion in Structural Biology*, *58*, 197–213. https://doi.org/10.1016/j.sbi.2019.04.004

Buruiana, L. I., & Ioan, S. (2018). Polymer Gel Composites for Bio-Applications. In Thakur, V. K., & Thakur, M. K. (Eds.). *Polymer Gels: Perspectives and Applications*, 111–123. Springer. https://doi.org/10.1007/978-981-10-6080-9_5

Buscemi, S., Corleo, D., Di Pace, F., Petroni, M. L., Satriano, A., & Marchesini, G. (2018). The effect of lutein on eye and extra-eye health. *Nutrients*, *10*(9), 1–24. https://doi.org/10.3390/nu10091321

Cerqueira, M. A., Fasolin, L. H., Picone, C. S. F., Pastrana, L. M., Cunha, R. L., & Vicente, A. A. (2017). Structural and mechanical properties of organogels: Role of oil and gelator molecular structure. *Food Research International*, *96*, 161–170. https://doi.org/10.1016/j.foodres.2017.03.021

Chakraborty, P., Das, S., & Nandi, A. K. (2018). Conducting gels: A chronicle of technological advances. *Progress in Polymer Science*, *88*, 189–219. https://doi.org/10.1016/j.progpolymsci.2018.08.004

Chavan, R. S., Khedkar, C. D., & Bhatt, S. (2015). Fat Replacer. *Encyclopedia of Food and Health*, (January), 589–595. https://doi.org/10.1016/B978-0-12-384947-2.00271-3

Chaves, K. F., Barrera-Arellano, D., & Ribeiro, A. P. B. (2018). Potential application of lipid organogels for food industry. *Food Research International*, *105*(December 2017), 863–872. https://doi.org/10.1016/j.foodres.2017.12.020

Chen, X., Fu, S., Hou, J., Guo, J., Wang, J., & Yang, X. (2016). Zein based oil-in-glycerol emulgels enriched with beta-carotene as margarine alternatives. *Food Chemistry*, *211*, 836–844. https://doi.org/10.1016/j.foodchem.2016.05.133

Chen, Y., Ye, R., & Liu, J. (2013). Understanding of dispersion and aggregation of suspensions of zein nanoparticles in aqueous alcohol solutions after thermal treatment. *Industrial Crops and Products*, *50*, 764–770. https://doi.org/10.1016/j.indcrop.2013.08.023

Cheng, C. J., Ferruzzi, M., & Jones, O. G. (2019). Food Hydrocolloids Fate of lutein-containing zein nanoparticles following simulated gastric and intestinal digestion. *Food Hydrocolloids*, *87*, 229–236. https://doi.org/10.1016/j.foodhyd.2018.08.013

Choudhary, B., Paul, S. R., Nayak, S. K., Qureshi, D., & Pal, K. (2018). Synthesis and biomedical applications of filled hydrogels. In Pal, K., & Banerjee, I. (Eds.). *Polymeric Gels*, 283–302. Elsevier. https://doi.org/10.1016/B978-0-08-102179-8.00011-9

Cornwell, D. J., & Smith, D. K. (2015). Expanding the scope of gels - Combining polymers with low-molecular-weight gelators to yield modified self-assembling smart materials with high-tech applications. *Materials Horizons*, *2*(3), 279–293. https://doi.org/10.1039/c4mh00245h

Dassanayake, L. S. K., Kodali, D. R., & Ueno, S. (2011). Formation of oleogels based on edible lipid materials. *Current Opinion in Colloid and Interface Science*. https://doi.org/10.1016/j.cocis.2011.05.005

De Almeida, C. B., Corradini, E., Forato, L. A., Fujihara, R., & Filho, J. F. L. (2018). Microstructure and thermal and functional properties of biodegradable films produced using zein. *Polimeros*, *28*(1), 30–37. https://doi.org/10.1590/0104-1428.11516

De Boer, F. Y., Kok, R. N. U., Imhof, A., & Velikov, K. P. (2018). White zein colloidal particles: Synthesis and characterization of their optical properties on the single particle level and in concentrated suspensions. *Soft Matter*, *14*(15), 2870–2878.

https://doi.org/10.1039/c7sm02415k

De Folter, J. W. J., Van Ruijven, M. W. M., & Velikov, K. P. (2012). Oil-in-water Pickering emulsions stabilized by colloidal particles from the water-insoluble protein zein. *Soft Matter*, *8*(25), 6807–6815. https://doi.org/10.1039/c2sm07417f

De Gennes, P. G., & Taupin, C. (1982). Microemulsions and the flexibility of oil/water interfaces. *Journal of Physical Chemistry*, *86*(13), 2294–2304. https://doi.org/10.1021/j100210a011

De Vries, A., Gomez, Y. L., Van der Linden, E., & Scholten, E. (2017). The effect of oil type on network formation by protein aggregates into oleogels. *RSC Advances*, *7*(19), 11803–11812. https://doi.org/10.1039/c7ra00396j

De Vries, A., Jansen, D., van der Linden, E., & Scholten, E. (2018). Tuning the rheological properties of protein-based oleogels by water addition and heat treatment. *Food Hydrocolloids*, *79*, 100–109. https://doi.org/10.1016/j.foodhyd.2017.11.043

De Vries, A., Lopez Gomez, Y., Jansen, B., Van der Linden, E., & Scholten, E. (2017). Controlling Agglomeration of Protein Aggregates for Structure Formation in Liquid Oil: A Sticky Business. *ACS Applied Materials and Interfaces*, *9*(11), 10136–10147. https://doi.org/10.1021/acsami.7b00443

De Vries, A., Nikiforidis, C. V., D., & Scholten, E. (2014). Natural amphiphilic proteins as tri-block Janus particles : Self-sorting into thermo-responsive gels. *Europhysics Letters*, 107, 5, 100–109. https://doi.org/10.1209/0295-5075/107/58003

Derkach, S. R. (2009). Rheology of emulsions. *Advances in Colloid and Interface Science*, *151*(1–2), 1–23. https://doi.org/10.1016/j.cis.2009.07.001

Donsì, F., Voudouris, P., Veen, S. J., & Velikov, K. P. (2017). Zein-based colloidal particles for encapsulation and delivery of epigallocatechin gallate. *Food Hydrocolloids*, *63*, 508–517. https://doi.org/10.1016/j.foodhyd.2016.09.039

Dreher, J., Blach, C., Terjung, N., Gibis, M., & Weiss, J. (2020). Formation and characterization of plant-based emulsified and crosslinked fat crystal networks to mimic animal fat tissue. *Journal of Food Science*, *85*(2), 421–431. https://doi.org/10.1111/1750-3841.14993

Drozdov, A. D., & Christiansen, J. D. (2013). Stress-strain relations for hydrogels under multiaxial deformation. *International Journal of Solids and Structures*, *50*(22–23), 3570–3585. https://doi.org/10.1016/j.ijsolstr.2013.06.023

Erickson, D. P., Ozturk, O. K., Selling, G., Chen, F., Campanella, O. H., & Hamaker, B. R. (2020). Corn zein undergoes conformational changes to higher β-sheet content during its self-assembly in an increasingly hydrophilic solvent. *International Journal of Biological Macromolecules*, *157*, 232–239. https://doi.org/10.1016/j.ijbiomac.2020.04.169

Esposito, C. L., Kirilov, P., & Roullin, V. G. (2018). Organogels, promising drug delivery systems: an update of state-of-the-art and recent applications. *Journal of Controlled Release*, *271*(December 2017), 1–20. https://doi.org/10.1016/j.jconrel.2017.12.019

Figura, L. O., & A.Teixeira, A. (2007). *Food Physics*. Springer.

Flores-Villaseñor, S. E., Peralta-Rodríguez, R. D., Ramirez-Contreras, J. C., Cortes-Mazatán, G. Y., & Estrada-Ramírez, A. N. (2016). Biocompatible microemulsions for the nanoencapsulation of essential oils and nutraceuticals. In Grumezescu, A. M. (Ed.). *Encapsulations*. *Nanotechnology in the Agri-Food Industry*, 503–558 Elsevier Inc. https://doi.org/http://dx.doi.org/10.1016/B978-0-12-804307-3.00012-0

Flory, P. J. (1974). Introductory lecture. *Faraday Discussions of the Chemical Society*, *57*, 7–18. https://doi.org/10.1039/DC9745700007

Fu, D., & Weller, C. L. (1999). Rheology of zein solutions in aqueous ethanol. *Journal of Agricultural and Food Chemistry*, *47*(5), 2103–2108. https://doi.org/10.1021/jf9811121

Gao, Z. M., Yang, X. Q., Wu, N. N., Wang, L. J., Wang, J. M., Guo, J., & Yin, S. W. (2014). Protein-based pickering emulsion and oil gel prepared by complexes of zein colloidal particles and stearate. *Journal of Agricultural and Food Chemistry*, *62*(12), 2672–2678. https://doi.org/10.1021/jf500005y

Godoy, C. A., Valiente, M., Pons, R., & Montalvo, G. (2015). Effect of fatty acids on self-assembly of soybean lecithin systems. *Colloids and Surfaces B: Biointerfaces*, *131*, 21–28. https://doi.org/10.1016/j.colsurfb.2015.03.065

Gonzalez-Gutierrez, J., & Scanlon, M. G. (2018). Rheology and Mechanical Properties of Fats. In Marangoni, A. G. (Ed.). *Structure-Function Analysis of Edible Fats*, (2), 119–168. AOCS Press. https://doi.org/10.1016/B978-0-12-814041-3.00005-8

Gorusupudi, A., & Baskaran, V. (2013). Wheat germ oil: A potential facilitator to improve lutein bioavailability in mice. *Nutrition*, *29*(5), 790–795. https://doi.org/10.1016/j.nut.2012.11.003

Gupta, P., Vermani, K., & Garg, S. (2002). Hydrogels : from controlled release to pH-responsive drug delivery. *Drug Discovery Today, 7*(10), 569–579.

Guzhova, I. V., Lazarev, V. F., Kaznacheeva, A. V., Ippolitova, M. V., Muronetz, V. I., Kinev, A. V., & Margulis, B. A. (2011). Novel mechanism of Hsp70 chaperone-mediated prevention of polyglutamine aggregates in a cellular model of huntington disease. *Human Molecular Genetics*, *20*(20), 3953–3963. https://doi.org/10.1093/hmg/ddr314

Hammouda, B. (2010). *Probing Nanoscale Structures – The Sans Toolbox*. https://www.ncnr.nist.gov/staff/hammouda/the_SANS_toolbox.pdf

Hashimoto, T., & Koizumi, S. (2012). Combined Small-Angle Scattering for Characterization of Hierarchically Structured Polymer Systems over Nano-to-Micron Meter: Part I Experiments. . In Matyjaszewski, K. & and Moeller, M. (Eds.). *Polymer Science: A Comprehensive Reference*, *10*(2), 381–398. Elsevier B.V. https://doi.org/10.1016/B978-0-444-53349-4.00297-1

Hughes, N. E., Marangoni, A. G., Wright, A. J., Rogers, M. A., & Rush, J. W. E. (2009). Potential food applications of edible oil organogels. *Trends in Food Science and Technology*, *20*(10), 470–480. https://doi.org/10.1016/j.tifs.2009.06.002

Ikeda, S., & Nishinari, K. (2001). "Weak gel"-type rheological properties of aqueous dispersions of nonaggregated κ-carrageenan helices. *Journal of Agricultural and Food Chemistry*, *49*(9),

4436–4441. https://doi.org/10.1021/jf0103065

Ilavsky, J., Zhang, F., Allen, A. J., Levine, L. E., Jemian, P. R., & Long, G. G. (2013). Ultra-small-angle X-ray scattering instrument at the advanced photon source: History, recent development, and current status. *Metallurgical and Materials Transactions A: Physical Metallurgy and Materials Science*, *44*(1), 68–76. https://doi.org/10.1007/s11661-012-1431-y

Ilavsky, Jan, & Jemian, P. R. (2009). Irena: Tool suite for modeling and analysis of small-angle scattering. *Journal of Applied Crystallography*, *42*(2), 347–353. https://doi.org/10.1107/S0021889809002222

Ilavsky, Jan, Jemian, P. R., Allen, A. J., Zhang, F., Levine, L. E., & Long, G. G. (2009). Ultra-small-angle X-ray scattering at the Advanced Photon Source. *Journal of Applied Crystallography*, *42*(3), 469–479. https://doi.org/10.1107/S0021889809008802

Iwahashi, M., Yamaguchi, Y., Kato, T., Horiuchi, T., Sakurai, I., & Suzuki, M. (1991). Temperature dependence of molecular conformation and liquid structure of cis-9-octadecenoic acid. *Journal of Physical Chemistry*, *95*(1), 445–451. https://doi.org/10.1021/j100154a078

Kasaai, M. R. (2018a). Trends in Food Science & Technology Zein and zein -based nano-materials for food and nutrition applications : A review. *Trends in Food Science & Technology*, *79*, 184–197. https://doi.org/10.1016/j.tifs.2018.07.015

Kasaai, M. R. (2018b). Trends in Food Science & Technology Zein and zein -based nano-materials for food and nutrition applications : A review. *Trends in Food Science & Technology*, *79*, 184–197. https://doi.org/10.1016/j.tifs.2018.07.015

Khalil, A. A., Deraz, S. F., Elrahman, S. A., & El-Fawal, G. (2015). Enhancement of mechanical properties, microstructure, and antimicrobial activities of zein films cross-linked using succinic anhydride, eugenol, and citric acid. *Preparative Biochemistry and Biotechnology*, *45*(6), 551–567. https://doi.org/10.1080/10826068.2014.940967

Kharlamova, A., Chassenieux, C., & Nicolai, T. (2018). Acid-induced gelation of whey protein aggregates: Kinetics, gel structure and rheological properties. *Food Hydrocolloids*, *81*, 263–272. https://doi.org/10.1016/j.foodhyd.2018.02.043

Kharlamova, A., Nicolai, T., & Chassenieux, C. (2018). Mixtures of sodium caseinate and whey protein aggregates: Viscosity and acid- or salt-induced gelation. *International Dairy Journal*, *86*, 110–119. https://doi.org/10.1016/j.idairyj.2018.07.002

Kikhney, A. G., & Svergun, D. I. (2015). A practical guide to small angle X-ray scattering (SAXS) of flexible and intrinsically disordered proteins. *FEBS Letters*, *589*(19), 2570–2577. https://doi.org/10.1016/j.febslet.2015.08.027

Kim, S., & Xu, J. (2008). Aggregate formation of zein and its structural inversion in aqueous ethanol. *Journal of Cereal Science*, *47*(1), 1–5. https://doi.org/10.1016/j.jcs.2007.08.004

Komaiko, J. S., & Mcclements, D. J. (2016). Formation of food-grade nanoemulsions using low-energy preparation methods: A review of available methods. *Comprehensive Reviews in Food Science and Food Safety*, *15*(2), 331–352. https://doi.org/10.1111/1541-4337.12189

Kuo, W. Y., Ilavsky, J., & Lee, Y. (2016). Structural characterization of solid lipoproteic colloid

gels by ultra-small-angle X-ray scattering and the relation with sodium release. *Food Hydrocolloids*, *56*, 325–333. https://doi.org/10.1016/j.foodhyd.2015.12.032

Lai, H. M., Geil, P. H., & Padua, G. W. (1999). X-ray diffraction characterization of the structure of zein-oleic acid films. *Journal of Applied Polymer Science*, *71*(8), 1267–1281. https://doi.org/10.1002/(SICI)1097-4628(19990222)71:8<1267::AID-APP7>3.0.CO;2-O

Laupheimer, M. (2014). *Gelled Bicontinuous Microemulsions. A New Type of Orthogonal Self-Assembled Systems.* Springer. http://link.springer.com/10.1007/978-3-319-07719-2

Laurati, M., Petekidis, G., Koumakis, N., Cardinaux, F., Schofield, A. B., Brader, J. M., Egelhaaf, S. U. (2009). Structure, dynamics, and rheology of colloid-polymer mixtures: From liquids to gels. *Journal of Chemical Physics*, *130*(13). https://doi.org/10.1063/1.3103889

Lee, B. Il, Suh, Y. S., Chung, Y. J., Yu, K., & Park, C. B. (2017). Shedding light on Alzheimer's β-amyloidosis: Photosensitized methylene blue inhibits self-assembly of β-amyloid peptides and disintegrates their aggregates. *Scientific Reports*, *7*(1), 1–10. https://doi.org/10.1038/s41598-017-07581-2

Li, Ying, & Corredig, M. (2020). Acid induced gelation behavior of skim milk concentrated by membrane filtration. *Journal of Texture Studies*, *51*(1), 101–110. https://doi.org/10.1111/jtxs.12492

Li, Yunqi, Li, J., Xia, Q., Zhang, B., Wang, Q., & Huang, Q. (2012). Understanding the dissolution of α-zein in aqueous ethanol and acetic acid solutions. *Journal of Physical Chemistry B*, *116*(39), 12057–12064. https://doi.org/10.1021/jp305709y

Lv, G., Wang, F., Cai, W., Li, H., & Zhang, X. (2014). Influences of addition of hydrophilic surfactants on the W/O emulsions stabilized by lipophilic surfactants. *Colloids and Surfaces A: Physicochemical and Engineering Aspects*, *457*(1), 441–448. https://doi.org/10.1016/j.colsurfa.2014.06.031

Marín, T., Montoya, P., Arnache, O., Pinal, R., & Calderón, J. (2018). Bioactive films of zein/magnetite magnetically stimuli-responsive for controlled drug release. *Journal of Magnetism and Magnetic Materials*, *458*, 355–364. https://doi.org/10.1016/j.jmmm.2018.03.046

Martins, A. J., Vicente, A. A., Cunha, R. L., & Cerqueira, M. A. (2018). Edible oleogels: An opportunity for fat replacement in foods. *Food and Function*, *9*(2), 758–773. https://doi.org/10.1039/c7fo01641g

Marze, S., Guillermic, R. M., & Saint-Jalmes, A. (2009). Oscillatory rheology of aqueous foams: Surfactant, liquid fraction, experimental protocol and aging effects. *Soft Matter*, *5*(9), 1937–1946. https://doi.org/10.1039/b817543h

Masalova, I., Malkin, A. Y., Ferg, E., Kharatiyan, E., Taylor, M., & Haldenwang, R. (2006). Evolution of rheological properties of highly concentrated emulsions with aging —Emulsion-to-suspension transition. *Journal of Rheology*, *50*(4), 435–451. https://doi.org/10.1122/1.2206712

Masamba, K., Li, Y., Hategekimana, J., Liu, F., & Ma, J. (2016). Effect of gallic acid on mechanical

and water barrier properties of zein-oleic acid composite films. *Journal of Food Science and Technology*, *53*(May), 2227–2235. https://doi.org/10.1007/s13197-015-2167-7

Matsushima, N., Danno, G. I., Takezawa, H., & Izumi, Y. (1997). Three-dimensional structure of maize α-zein proteins studied by small-angle X-ray scattering. *Biochimica et Biophysica Acta - Protein Structure and Molecular Enzymology*. https://doi.org/10.1016/S0167-4838(96)00212-9

Mewis, J., & Wagner, N. J. (2011). *Colloidal Suspension Rheology*. Cambridge University Press. https://doi.org/10.1017/CBO9780511977978

Mezzenga, R. (2011). Protein-templated oil gels and powders. In Marangoni, A. G., & Garti, N. (Eds.). *Edible Oleogels: Structure and Health Implications*, 307–329. Elsevier Inc. https://doi.org/10.1016/B978-0-9830791-1-8.50015-2

Milston, R., Madigan, M. C., & Sebag, J. (2016). Vitreous floaters: Etiology, diagnostics, and management. *Survey of Ophthalmology*, *61*(2), 211–227. https://doi.org/10.1016/j.survophthal.2015.11.008

Moradkhannejhad, L., Abdouss, M., Nikfarjam, N., Mazinani, S., & Heydari, V. (2018). morphology investigation electrospinning of zein / propolis nano fibers; antimicrobial properties and morphology investigation. *Journal of Materials Science: Materials in Medicine*, *29,* 165. https://doi.org/10.1007/s10856-018-6174-x

Nabetani, H., Ichikawa, S., Liu, X., Nakajima, M., & Xu, Q. (2007). Factors affecting the properties of ethanol-in-oil emulsions. *Food Science and Technology Research*, *8*(1), 36–41. https://doi.org/10.3136/fstr.8.36

Nazir, A., Asghar, A., & Aslam Maan, A. (2017). *Chapter 13 - Food Gels: Gelling Process and New Applications A2 - Ahmed, J. Advances in Food Rheology and Its Applications*. Elsevier Ltd. https://doi.org/https://doi.org/10.1016/B978-0-08-100431-9.00013-9

Nephomnyshy, I., Rosen-Kligvasser, J., & Davidovich-Pinhas, M. (2020). The development of a direct approach to formulate high oil content zein-based emulsion gels using moderate temperatures. *Food Hydrocolloids*, *101*, 105528. https://doi.org/10.1016/j.foodhyd.2019.105528

Nikiforidis, C. V., Gilbert, E. P., & Scholten, E. (2015). Organogel formation via supramolecular assembly of oleic acid and sodium oleate. *RSC Advances*, *5*(59), 47466–47475. https://doi.org/10.1039/c5ra05336f

Nonthanum, P., Lee, Y., & Padua, G. W. (2012). Effect of γ-zein on the rheological behavior of concentrated zein solutions. *Journal of Agricultural and Food Chemistry*, *60*(7), 1742–1747. https://doi.org/10.1021/jf2035302

Nonthanum, P., Lee, Y., & Padua, G. W. (2013). Effect of pH and ethanol content of solvent on rheology of zein solutions. *Journal of Cereal Science*, *58*(1), 76–81. https://doi.org/10.1016/j.jcs.2013.04.001

O'Sullivan, C. M., Barbut, S., & Marangoni, A. G. (2016). Edible oleogels for the oral delivery of lipid soluble molecules: Composition and structural design considerations. *Trends in Food*

Science and Technology, *57*, 59–73. https://doi.org/10.1016/j.tifs.2016.08.018

Ochbaum, G., & Bitton, R. (2018). Using small-angle X-ray scattering (SAXS) to study the structure of self-assembling biomaterials. In Azevedo, H. S., & De Silva, R. M. P. (Eds.). *Self-Assembling Biomaterials: Molecular Design, Characterization and Application in Biology and Medicine*, 291–304. Elsevier Ltd. https://doi.org/10.1016/B978-0-08-102015-9.00015-0

Ochowiak, M., Broniarz-Press, L., & Rozanski, J. (2012). Rheology and Structure of Emulsions and Suspensions. *Journal of Dispersion Science and Technology*, *33*(2), 177–184. https://doi.org/10.1080/01932691.2010.548694

Ochowiak, M., & Rozanski, J. (2012). Rheology and structure of emulsions and suspensions. *Journal of Dispersion Science and Technology, 33*(2), 177–184. https://doi.org/10.1080/01932691.2010.548694

Pal, R. (2011). Influence of interfacial rheology on the viscosity of concentrated emulsions. *Journal of Colloid and Interface Science*, *356*(1), 118–122. https://doi.org/10.1016/j.jcis.2010.12.068

Patel, A. R. (2017). A colloidal gel perspective for understanding oleogelation. *Current Opinion in Food Science*, *15*, 1–7. https://doi.org/10.1016/j.cofs.2017.02.013

Patel, A. R., Cludts, N., Bin Sintang, M. D., Lewille, B., Lesaffer, A., & Dewettinck, K. (2014). Polysaccharide-based oleogels prepared with an emulsion-templated approach. *ChemPhysChem*, *15*(16), 3435–3439. https://doi.org/10.1002/cphc.201402473

Patel, A. R., & Dewettinck, K. (2016). Edible oil structuring: An overview and recent updates. *Food and Function*, *7*(1), 20–29. https://doi.org/10.1039/c5fo01006c

Patel, A. R., Dumlu, P., Vermeir, L., Lewille, B., Lesaffer, A., & Dewettinck, K. (2015). Rheological characterization of gel-in-oil-in-gel type structured emulsions. *Food Hydrocolloids*, *46*, 84–92. https://doi.org/10.1016/j.foodhyd.2014.12.029

Patel, A. R., & Velikov, K. P. (2014). Zein as a source of functional colloidal nano- and microstructures. *Current Opinion in Colloid and Interface Science*, *19*(5), 450–458. https://doi.org/10.1016/j.cocis.2014.08.001

Pehlivanoğlu, H., Demirci, M., Toker, O. S., Konar, N., Karasu, S., & Sagdic, O. (2018). Oleogels, a promising structured oil for decreasing saturated fatty acid concentrations: Production and food-based applications. *Critical Reviews in Food Science and Nutrition*, *58*(8), 1330–1341. https://doi.org/10.1080/10408398.2016.1256866

Pena-serna, C., & Lopes-filho, J. F. (2013). Influence of ethanol and glycerol concentration over functional and structural properties of zein-oleic acid films. *Materials Chemistry and Physics*, *142*(2–3), 580–585. https://doi.org/10.1016/j.matchemphys.2013.07.056

Pérez-Gago, Maria B., & Krochta, J. M. (2001). Lipid particle size effect on water vapor permeability and mechanical properties of whey protein/beeswax emulsion films. *Journal of Agricultural and Food Chemistry*, *49*(2), 996–1002. https://doi.org/10.1021/jf000615f

Pérez-Gago, Maria Berna, & Rhim, J. W. (2013). Edible Coating and Film Materials: Lipid Bilayers and Lipid Emulsions. *Innovations in Food Packaging: Second Edition*, 325–350.

https://doi.org/10.1016/B978-0-12-394601-0.00013-8

Peyronel, F., Ilavsky, J., Mazzanti, G., Marangoni, A. G., & Pink, D. A. (2013). Edible oil structures at low and intermediate concentrations. II. Ultra-small angle X-ray scattering of in situ tristearin solids in triolein. *Journal of Applied Physics*, *114*(23). https://doi.org/10.1063/1.4847997

Peyronel, F., Quinn, B., Marangoni, A. G., & Pink, D. A. (2014). Ultra small angle x-ray scattering in complex mixtures of triacylglycerols. *Journal of Physics Condensed Matter*, *26*(46). https://doi.org/10.1088/0953-8984/26/46/464110

Ponton, A., Bose, T. K., & Delbos, G. (1991). Dielectric study of percolation in an oil-continuous microemulsion. *The Journal of Chemical Physics*, *94*(10), 6879–6886. https://doi.org/10.1063/1.460268

Quemada, D., & Berli, C. (2002). Energy of interaction in colloids and its implications in rheological modeling. *Advances in Colloid and Interface Science, 98*(1), 51–85. https://doi.org/10.1016/S0001-8686(01)00093-8

Raeburn, J., Cardoso, A. Z., & Adams, D. J. (2013). The importance of the self-assembly process to control mechanical properties of low molecular weight hydrogels. *Chemical Society Reviews*, *42*(12), 5143–5156. https://doi.org/10.1039/c3cs60030k

Raza, A., Hayat, U., Bilal, M., Iqbal, H. M. N., & Wang, J. Y. (2020). Zein-based micro- and nano-constructs and biologically therapeutic cues with multi-functionalities for oral drug delivery systems. *Journal of Drug Delivery Science and Technology*, *58*. https://doi.org/10.1016/j.jddst.2020.101818

Renner, M., & Melki, R. (2014). Protein aggregation and prionopathies. *Pathologie Biologie*, *62*(3), 162–168. https://doi.org/10.1016/j.patbio.2014.01.003

Roberts, J. E., & Dennison, J. (2015). The Photobiology of Lutein and Zeaxanthin in the Eye. *Journal of Ophthalmology*, *2015*. https://doi.org/10.1155/2015/687173

Ross-Murphy, S. B. (1995). Structure–property relationships in food biopolymer gels and solutions. *Journal of Rheology*, *39*(6), 1451–1463. https://doi.org/10.1122/1.550610

Rutkevi, M., Allred, S., Velev, O. D., & Velikov, K. P. (2018). Food Hydrocolloids Stabilization of oil continuous emulsions with colloidal particles from water-insoluble plant proteins, *82*, 89–95. https://doi.org/10.1016/j.foodhyd.2018.04.004

Rutkevičius, M., Allred, S., Velev, O. D., & Velikov, K. P. (2018). Stabilization of oil continuous emulsions with colloidal particles from water-insoluble plant proteins. *Food Hydrocolloids*, *82*, 89–95. https://doi.org/10.1016/j.foodhyd.2018.04.004

Sadeghpour, A., Pirolt, F., & Glatter, O. (2013). Submicrometer-sized pickering emulsions stabilized by silica nanoparticles with adsorbed oleic acid. *Langmuir*, *29*(20), 6004–6012. https://doi.org/10.1021/la4008685

Samateh, M., Sagiri, S. S., & John, G. (2018). *Molecular Oleogels*. *Edible Oleogels*. AOCS Press. https://doi.org/10.1016/b978-0-12-814270-7.00018-6

Sangeetha, N. M., & Maitra, U. (2005). Supramolecular gels: Functions and uses. *Chemical Society Reviews*, *34*(10), 821–836. https://doi.org/10.1039/b417081b

Santos, T. M., Souza Filho, M. de S. M., Muniz, C. R., Morais, J. P. S., Kotzebue, L. R. V., Pereira, A. L. S., & Azeredo, H. M. C. (2017). Zein films with unoxidized or oxidized tannic acid. *Journal of the Science of Food and Agriculture*, *97*(13), 4580–4587. https://doi.org/10.1002/jsfa.8327

Schulz-Schaeffer, W. J. (2010). The synaptic pathology of α-synuclein aggregation in dementia with Lewy bodies, Parkinson's disease and Parkinson's disease dementia. *Acta Neuropathologica*, *120*(2), 131–143. https://doi.org/10.1007/s00401-010-0711-0

Selling, G. W., Hamaker, S. A. H., & Sessa, D. J. (2007). Effect of solvent and temperature on secondary and tertiary structure of zein by circular dichroism. *Cereal Chemistry*, *84*(3), 265–270. https://doi.org/10.1094/CCHEM-84-3-0265

Sengupta, T., & Han, J. H. (2013). Surface Chemistry of Food, Packaging, and Biopolymer Materials. In Han, J. H. (Ed.). *Innovations in Food Packaging: Second Edition*. 51–86. Elsevier Ltd. https://doi.org/10.1016/B978-0-12-394601-0.00004-7

Serrano, J., Goñi, I., & Saura-Calixto, F. (2005). Determination of β-caroten and lutein available from green leafy vegetables by an in vitro digestion and colonic fermentation method. *Journal of Agricultural and Food Chemistry*, *53*(8), 2936–2940. https://doi.org/10.1021/jf0480142

Sharma, S. K. (2018). *Handbook of Materials Characterization*. Springer. https://doi.org/10.1007/978-3-319-92955-2

Shukla, R., Cheryan, M., & DeVor, R. E. (2000). Solvent extraction of zein from dry-milled corn. *Cereal Chemistry*, *77*(6), 724–730. https://doi.org/10.1094/CCHEM.2000.77.6.724

Siraj, N., Shabbir, M. A., Ahmad, T., Sajjad, A., Khan, M. R., Khan, M. I., & Butt, M. S. (2015). Organogelators as a saturated fat replacer for structuring edible oils. *International Journal of Food Properties*, *18*(9), 1973–1989. https://doi.org/10.1080/10942912.2014.951891

Soltani, S., & Madadlou, A. (2015). Two-step sequential cross-linking of sugar beet pectin for transforming zein nanoparticle-based Pickering emulsions to emulgels. *Carbohydrate Polymers*, *136*, 738–743. https://doi.org/10.1016/j.carbpol.2015.09.100

Tabilo-Munizaga, G., & Barbosa-Cánovas, G. V. (2005). Rheology for the food industry. *Journal of Food Engineering*, *67*(1–2), 147–156. https://doi.org/10.1016/j.jfoodeng.2004.05.062

Terech, P. (1997). Low-molecular weight organogelators. *Specialist Surfactants*, 208–268. https://doi.org/10.1007/978-94-009-1557-2_8

Terech, Pierre, & Weiss, R. G. (1997). Low molecular mass gelators of organic liquids and the properties of their gels. *Chemical Reviews*, *97*(8), 3133–3159. https://doi.org/10.1021/cr9700282

Thakur, V. K., & Thakur, M. K. (2018). *Polymer gels. Science and Fundamentals*. Springer. https://doi.org/10.1007/978-981-10-6086-1

Uzun, S., Ilavsky, J., & Padua, G. W. (2017). Characterization of zein assemblies by ultra-small-

angle X-ray scattering. *Soft Matter*, *13*(16), 3053–3060. https://doi.org/10.1039/c6sm02717b

Wang, L. J., Yin, Y. C., Yin, S. W., Yang, X. Q., Shi, W. J., Tang, C. H., & Wang, J. M. (2013). Development of novel zein-sodium caseinate nanoparticle (ZP)-stabilized emulsion films for improved water barrier properties via emulsion/solvent evaporation. *Journal of Agricultural and Food Chemistry*, *61*(46), 11089–11097. https://doi.org/10.1021/jf4029943

Wang, Qin, Yin, L., & Padua, G. W. (2008). Effect of hydrophilic and lipophilic compounds on zein microstructures. *Food Biophysics*, *3*(2), 174–181. https://doi.org/10.1007/s11483-008-9080-9

Wang, Qiuming, Yu, X., Patal, K., Hu, R., Chuang, S., Zhang, G., & Zheng, J. (2013). Tanshinones inhibit amyloid aggregation by amyloid-β peptide, disaggregate amyloid fibrils, and protect cultured cells. *ACS Chemical Neuroscience*, *4*(6), 1004–1015. https://doi.org/10.1021/cn400051e

Wang, Yi, & Padua, G. W. (2010). Formation of zein microphases in ethanol-water. *Langmuir*, *26*(15), 12897–12901. https://doi.org/10.1021/la101688v

Wang, Yi, & Padua, G. W. (2012). Nanoscale characterization of zein self-assembly. *Langmuir*, *28*(5), 2429–2435. https://doi.org/10.1021/la204204j

Wang, Q., Crofts, A. R., Padua, G. W. (2003). Protein−lipid interactions in zein films investigated by surface plasmon resonance. *Journal of Agricultural and Food Chemistry, 51,* 7439–7444.

Wang, Ying, & Padua, G. W. (2006). Water barrier properties of zein-oleic acid films. *Cereal Chemistry, 83*(4), 331–334. https://doi.org/10.1094/CC-83-0331

Watanabe, T., Kawai, T., & Nonomura, Y. (2018). Effects of fatty acid addition to oil-in-water emulsions stabilized with sucrose fatty acid ester. *Journal of Oleo Science*, *67*(3), 307–313. https://doi.org/10.5650/jos.ess17097

Weissmueller, N. T., Lu, H. D., Hurley, A., & Prud'Homme, R. K. (2016). Nanocarriers from GRAS zein proteins to encapsulate hydrophobic actives. *Biomacromolecules*, *17*(11), 3828–3837. https://doi.org/10.1021/acs.biomac.6b01440

Xu, J., Yin, A., Zhao, J., Li, D., & Hou, W. (2013). Surfactant-free microemulsion composed of oleic acid, n-propanol, and H2O. *Journal of Physical Chemistry B*, *117*(1), 450–456. https://doi.org/10.1021/jp310282a

Xu, Q., Nakajima, M., Nabetani, H., Iwamoto, S., & Liu, X. (2001). The effects of ethanol content and emulsifying agent concentration on the stability of vegetable oil-ethanol emulsions. *JAOCS, Journal of the American Oil Chemists' Society*, *78*(12), 1185–1190. https://doi.org/10.1007/s11745-001-0411-z

Yang, Y., Chaisoontornyotin, W., & Hoepfner, M. P. (2018). Structure of ssphaltenes during precipitation investigated by ultra-small-angle X-ray scattering. *Langmuir*, *34*(35), 10371–10380. https://doi.org/10.1021/acs.langmuir.8b01873

Yuan, Y., Li, H., Liu, C., Zhang, S., Xu, Y., & Wang, D. (2019). Fabrication and characterization of lutein-loaded nanoparticles based on zein and sophorolipid : Enhancement of water solubility , stability , and bioaccessibility. *Journal of Agricultural and Food Chemistry*,

67(43), 11977–11985. https://doi.org/10.1021/acs.jafc.9b05175

Zhang, B., Luo, Y., & Wang, Q. (2011). Effect of acid and base treatments on structural, rheological, and antioxidant properties of α-zein. *Food Chemistry*, *124*(1), 210–220. https://doi.org/10.1016/j.foodchem.2010.06.019

Zhang, M., & Weiss, R. G. (2015). Self-assembled networks and molecular gels derived from long-chain, naturally-occurring fatty acids. *Journal of the Brazilian Chemical Society*, *27*(2), 1–17. https://doi.org/10.5935/0103-5053.20150247

Zhang, Y., Cui, L., Che, X., Zhang, H., Shi, N., Li, C., … Kong, W. (2015). Zein-based films and their usage for controlled delivery: Origin, classes and current landscape. *Journal of Controlled Release*, *206*(2699), 206–219. https://doi.org/10.1016/j.jconrel.2015.03.030

Zhang, Y., Cui, L., Li, F., Shi, N., Li, C., Yu, X., … Kong, W. (2016). Design, fabrication and biomedical applications of zein-based nano/micro-carrier systems. *International Journal of Pharmaceutics*, *513*(1–2), 191–210. https://doi.org/10.1016/j.ijpharm.2016.09.023

Zhong, Q., & Ikeda, S. (2012). Viscoelastic properties of concentrated aqueous ethanol suspensions of α-zein. *Food Hydrocolloids*, *28*(1), 46–52. https://doi.org/10.1016/j.foodhyd.2011.11.014

Zou, Y., Thijssen, P. P., Yang, X., & Scholten, E. (2019). The effect of oil type and solvent quality on the rheological behavior of zein stabilized oil-in-glycerol emulsion gels. *Food Hydrocolloids*, *91*, 57–65. https://doi.org/10.1016/j.foodhyd.2019.01.016

Zou, Y., Yang, X., & Scholten, E. (2018). Rheological behavior of emulsion gels stabilized by zein/tannic acid complex particles. *Food Hydrocolloids*, *77*, 363–371. https://doi.org/10.1016/j.foodhyd.2017.10.013

CHAPTER 5   MIRCROSTRUCTURAL CHARACTERISTICS OF ZEIN-BASED OLEOGELS DETERMINED BY USAXS

5.1 Abstract

Zein in diluted ethanol solutions has been studied for a long time. However, the physical nature of concentrated zein self-assembled in the wet state remains unclear. Also, the gelation process during the formation of complex oleogel system is still vague. The objective of this study was to utilize ultra-small-angle X-ray scattering (USAXS) to determine the microstructural changes and protein-solvent interactions in the 70% ethanol/zein/oleic acid emulsion systems. Two sets of Guinier's knees and power law scattering slopes were observed in most of the samples, indicating the existence of two levels of repeating or ordered structures. The sizes and the shapes of the periodic structures were fitted with the unified-fit-model at different scattering vector (q), which generated the radius of gyration (R_g) and shape index (P), respectively. At high q region ($q > 10^{-2}$ Å^{-1}), R_{g1} and P_1 were defined as the size and shape of the primary structures, while R_{g2} and P_2 located at intermediate to low q region ($q < 10^{-2}$ Å^{-1}) were interpreted as the second level structures. The primary unit size (R_{g1}) ranged from 3.5 nm to 12.6 nm which grew with the increasing amount of 70% ethanol (30 to 55%). The structural shape, P_1, at this level was assumed to be the disk-like structure referred as zein building blocks ($1.2 < P_1 < 1.8$). R_{g1} was mostly affected by the solvent composition but remained stable with storage time. The Kratky plots were useful to differentiate the arrangement of zein building block as elongated long rods or side-by-side zein molecule stacks. It was suggested that with the rearrangement of these unit blocks, the second level fractal structures (P_2) were developed with R_{g2} sizes between 251 nm to over a micron. R_{g2} values were higher for the high ethanol-low oleic acid containing samples suggesting the formation of larger dimension of oleogel network structures required higher zein molecule mobility and lower discontinuous phase volume fraction. Unlike building block size (R_{g1}), R_{g2} values increased with storage time. This was the evidence for the self-assembly mechanism of the zein molecules in oleogel system which the fractal structures grew in size while keeping the geometry unchanged.

5.2 Introduction

Proteins are crucial for living organisms, which they act as fundamental roles in physiological processes, and have functional and structural importance for cells and tissues. However, sometimes the proteins may be misfolded and aggregate into undesired structures which are insoluble and toxic, called as amyloid fibrils (Benson et al., 2018). These amyloidogenic peptides are discovered as the cause of many neurodegenerative disorders such as Parkinson (α-synuclein aggregates), Alzheimer (β-amyloid plaques), Huntington (polyglutamine aggregates) and Creutzfeldt-Jacob (amyloid deposits of the prion protein (PrP))(Schulz-Schaeffer, 2010; Guzhova et al., 2011; Renner & Melki, 2014; Lee, Suh, Chung, Yu, & Park, 2017; Wang et al., 2013). While the aggregation of disordered proteins accumulate, other benign diseases also occurred. For instance, the formation of collagen aggregates lead to the floaters in the eye and decrease the clarity of the vision (Milston, Madigan, & Sebag, 2016).

The mechanism of this fibrous aggregates formation from soluble monomers into long strands is investigated and found out similar to the self-assembly of surfactants. The fibrillation is time dependent and like common nucleation process of amphiphilic monomers, it dominantly affected by the concentration, pH, temperature and electrostatic interactions of monomer itself and the surrounding environment. In these decades, researchers have been focused on using model system to study the self-assembly process of proteins, surfactants or natural amphiphilic compounds. By doing so, the aggregation mechanism can be monitored, controlled, and tailored to fabricate ordered microstructures, moreover, it's possible that they can induce conformational changes of monomers thereby preventing the aggregation happens.

Zein, the highly hydrophobic protein of corn, is known as its natural amphiphilicity with edible, biodegradable and biocompatible characteristics. Out of 4 different fractions, α-zein studied here consisted of 9 to 10 anti-parallel adjacently packed α-helices linked by glutamine-rich turns (Argos, Pedersenfl, Marksl, & Larkinsflll, 1982.), which can be illustrated as a rectangular block with two hydrophilic patches on top and bottom and four hydrophobic surfaces surrounds the sides proposed by Matsushima, Danno, Takezawa, & Izumi, 1997. They used small-angle x-ray scattering (SAXS) technique to determine the elongated prism with a dimensions of $13 \times 1.2 \times 3$ nm^3. This distinct protein unit structure provides the driving force for zein to self-assemble into different structures including spheres, fibers, sponge or lamellar films which was promoted during

the solvent evaporation (Wang & Padua, 2010; Y. Wang & Padua, 2012).

Studied by rheological measurements and TEM techniques, zein formed gel in varied ethanol concentration and pH upon aging indicating the ability for zein to rearrange into more developed 3D network structures (Nonthanum et al., 2013). In Li et al., 2012, they also used static light scattering and SAXS to investigate the zein microstructure in different solvent medium and concluded that α-zein tended to form rodlike dimers in 70% ethanol solution. However, the submicron size of the large length scale of the zein structures has not been well defined. Not until Uzun, Ilavsky, & Padua, 2017 applied ultra-small-angle X-ray scattering (USAXS) to the fresh and four months aged zein samples in binary solvent systems of ethanol and water, three hierarchical structures were able to be identified as the rod-like primary units (R_g = 1.5-2.5 nm), 2D sheets (R_g = 80-200 nm) and 3D spherical aggregates (R_g > 1µm). Based on their findings, aging only affected the secondary level structural sizes but not primary units.

Owing to the amphiphilic properties of zein, recent studies of using zein as an oleogelator in designing oleogels were published (Scholten, 2014; Chen et al., 2016). They followed and modified the method of Osborne el al. (1897) by dissolving zein in 150 ºC glycerol then mixed with preheated oil to form thermos responsive oleogels. According to the proposed mechanism, zein molecules were hydrophobic oriented toward the oil droplets, which started by deposition onto the surface and self-assembled ribbon-like long strands then organized into 3D gel network (Zou, Thijssen, Yang, and Scholten., 2019). However, the time dependent molecular level of zien self-assembly aggregation process are still not clearly depicted.

Oleic acid has been widely used as a plasticizer in improving the brittleness of zein films (De Almeida, Corradini, Forato, Fujihara, & Filho, 2018). Early studies discovered the addition of oleic acid could facilitate the rearrangement of zein-oleic film with periodic d-spacing stacking of two layers of lamellar zein structure followed by bilayers of oleic acid. (Lai, Geil, & Padua, 1999). It was hypothesized that oleic acid interacted with soluble zein in ethanol water mixtures and promoted the organization of the structures.

Therefore, in this research we selected oleic acid as the hydrophobic discontinued phase in order to better monitor the interaction and self-assembly process of zein molecules which was pre-dissolved in 70% ethanol solution. Without temperature abuse, we used this 70% ethanol-zein-

oleic acid pseudo ternary system as a model system to investigate the effect of solvent composition (hydrophilic and lipophilic balance), zein concentration, time and extra shear force applied on the different levels of zein structure development by USAXS. The shape and size of the structural changes detected by USAXS provided valuable information for understanding the aggregation of proteins, and with this oil in water model system, wish to provide some insights related to cell aging.

5.3 Materials and Methods

5.3.1 Materials

Zein was purchased from Showa Sanyo Co. Ltd. (Tokyo, Japan). Oleic acid was from Fisher Scientific (Hanover Park, IL). Ethanol (200 proof) was supplied by Decon Laboratories Inc. (King of Prussia, PA). Mineral oil was purchased in the local market.

5.3.2 Ultra-small-angle X-ray scattering (USAXS)

USAX data were collected to observe the microstructural organization of sample gels. The USAXS combined with pinhole SAXS were conducted at beamline 9-ID-C at the Advanced Photon Source in Argonne National Laboratory (Lemont, IL). The instrument is equipped with a Bonse-Hart camera double-crystal configuration and operates at one-dimensional collimation, which enables the collection of slit-smeared data. The specimen was measured at scattering vectors range $q = 1 \times 10^{-4}$ Å^{-1} to 1.2 Å^{-1} with about 200 data points, where q is defined as $q = 4\pi \sin(\theta/2)/\lambda$ and θ, λ are the scattering angle and x-ray beam wavelength, respectively. Emulsion samples were loaded in NMR capillaries with 4 mm internal diameter (Wilmad-LabGlassTM Thin Walled High Throughput NMR Tubes, Fisher Scientific, MA) and capped with corresponding rubber caps. The monochromatic x-ray energy used was 18 keV. The slit-smeared data were fitted with the unified model by the Modeling II macro of the Irena 2 package in IGOR PRO v8.03 (Wavemetrics, Lake Oswego, OR). The radius of gyration of aggregates (R_g) and shape factor (P), calculated from the power law slope were evaluated. The experimental design consisted of 30 samples with 2 replicates, totaling 60 experimental units, average values were reported.

USAXS unified fit model describes scattering from complex systems containing multiple levels of related structural features. It is derived from the Beaucage model, which predicts radius of gyration (R_g), Porod exponent (P) and total intensity scattering (Beaucage, 1995, 1996). The

total intensity scattering is given by the formula:

$$I(q) \simeq G\exp\left(-\frac{-q^2 R_g{}^2}{3}\right) + B\left\{[\mathrm{erf}\left(qR_g/6^{\frac{1}{2}}\right)]^3/q\right\}^P$$

The first term corresponds to Guinier's law, where G is the Guinier prefactor, $G = n^2 N_p I_e$. N_p is the number of particles in the scattering volume, I_e is the scattering factor for a single electron and n is the number of electrons in a particle. R_g represents the size of the scatterers at the corresponding structural level. The second term corresponds to Porod's law, where P is the power low exponent for each level. B is the Porod's law prefactor, $B = 2\pi N_p \rho_e{}^2 S_p I_e$, where $\rho = n/V_p$. V_p and S_p are, respectively, the volume and surface area of the particle. The unified model (Beaucage, 1995) describes a complex morphology over a wide range of q in terms of structural levels. A structural level in scattering is described by Guinier's law and a structurally limited power law, which on a log-log plot is reflected by a knee (Guinier's knee) and a linear region (Porod region). Porod's law parameters are good descriptors of the local structure. Thin rods are one-dimensional objects, so a power law of -1 is expected ($P = 1$). Thin lamellar discs are two-dimensional objects, so that a power law of -2 is expected ($P = 2$) (Yi Wang & Padua, 2010b). For 3-dimensional scattering features, $P < 3$ can be associated with mass fractals, while $3 < P < 4$ can be associated with surface-fractals. A value of $P = 4$ is associated with sharp, smooth interfacial surfaces and $P > 4$ can be associated with a diffuse interface.

5.4 Results and Discussion

Zein-based oleogels were composed of different levels of microstructures, which could be determined and depicted by the powerful tool, the ultra-small x-ray scattering (USAXS) technique. Two sets of Guinier knee and Porod slope were shown in most of the samples and with unified fit model, we were able to calculate radius of gyration R_g and P value from the knees and slopes, respectively. Based on the q range where the knees and slopes appeared, we defined R_{g1} and P_1 located at high q region ($q > 10^{-2}$ Å^{-1}) and R_{g2} and P_2 were at intermediate to low q region ($q < 10^{-2}$ Å^{-1}).

5.4.1 Effect of solvent composition

The ultra-small-angle X-ray scattering (USAXS) profiles of 15% zein concentration samples were displayed in Figure 5.1. In general, all samples showed a Guinier knee and Porod slope at the

high q region ($q > 10^{-2}$ Å^{-1}), indicating there were repeating unit exists in zein containing samples. While increasing the amount of oleic acid from 0% to 55%, we can observe more signals revealed at lower q region ($q < 10^{-2}$ Å^{-1}) determined as another set of Guinier knee and Porod slope, suggesting as a higher level of structural arrangement. Table 5.1 summarized two levels of R_g and P values calculated with the unified fit model.

Based on the Guinier approximation, R_{g1} values were obtained at high q region ($q > 10^{-2}$ Å^{-1}) ranging from 3.5 to 12.6 nm, and P_1 index values were 1.0 to 1.8 (Table 5.1). For 33% zein dissolved in 70% ethanol, the average of R_{g1} was 13 nm and with a P index almost equaled to 1 (P_{rod} = 1). This size and shape of the zein molecule were mentioned in Lai, Geil, & Padua, (1998) and Argos., et al. (1982), described as a rod-like structure with dimension of 13 nm × 1.2 nm × 3 nm in ethanol-water with an axial ratio of 6 : 131. It was suggested that the high q USAX data were composed of the primary unit or the building block of the system, which here we assumed the signal was originated from zein molecules inside the oleogels.

While incorporating oleic acid into the system, R_{g1} gradually decreased from 13 nm to 3.5 nm and P index increased from 1 to 1.8. This change demonstrated the existence of long range 2D structures (P_{disk} = 2) with possible building block orientation illustrated in Table 1. According to the mechanism of zein self-assembly process proposed by Osborne et al. (1897), zein tri-blocks were tended to deposit onto the surface of oil droplets due to the hydrophobic interaction. In this arrangement, the opposite hydrophobic sides of the tri-blocks were available for further growth through associative interactions. And the orientation of how zein develop would result in ribbon-like strands, sheets or spheres (Wang & Padua, 2010b). When addition of oil into the system would facilitate the association of zein molecules, which also reported by Lai, Geil, & Padua, (1998). They used oleic acid as a plasticer for fabrication of zein-oleic acid and found out the periodic d-spacing generated in SAXS results. Tetramer model was therefore proposed with a dimensions of 13 nm × 4.2 nm × 3.2 nm, which depicted the four zein ribbons packed horizontally with the hydrophobic bonds in between the sides. Here, we assumed the R_{g1} of 3.5-3.9 nm with P_1 = 1.8 obtained from 30-15-55 could having this type of zein building block structure.

While slightly decreased the oleic acid amount from 55% to 45%, the size and shape of the primary units changed, indicating solvent composition was crucial to the orientation and self-

assemble behavior of zein molecules (Scholten, 2014). Based on Iwahashi et al. (1991), oleic acid was dimerized and forming simple bilayer packing with a thickness of 4.2 nm at low temperature. Presumed in 40-15-45 and 45-15-40 these two compositions, partial free fatty acid interacted with zein and packed into hydrophobic protein-oleic acid layered structure, which composed the size of R_{g1} as 10.7 nm. With relatively higher amount of 70% ethanol sample 55-15-30, we observed the similar size of R_{g1} around 11.5 to 12.6 nm as for zein only. It was possible that most of the zein molecules were randomly distributed in the continuous phase but still a part of zein attached to the surface of the oil droplets which affected the P_1 value departed from 1.

At low to intermediate q range, R_{g2} ranged relatively wide between 251 nm to over 1 μm with samples containing oleic acid higher than 40% at different storage time. It showed the variety of the three-dimensional continuous, percolating network that zein could form. And referred to researches of zein-glycerol oleogel system, it was confirmed that the secondary structures should be the extended gel network formed by the aggregation of the zein, not only the structures deposited on the surface of oil droplets (Zou et al., 2019).

When we focused on the effect of solvent composition, the highest oleic acid containing samples (55%) had the smallest fitted R_{g2} values, and R_{g2} size increased with decreasing of oil content. According to Nephomnyshy, et al. (2020), the hydrophobic phase in the system provided the anchor point for zein to attach. With same amount of zein dispersed in the system, more of the oil droplets meaning more of the surface area could allow zein molecules to stick on, but also caused less proteins available in the continuous phase for network formation. As a result, the scale of the developed structures were smaller.   Besides, in our system, less oleic acid corresponding to more ethanol, which zein had higher mobility to further organize and interact with the existed structures.

Although sample with high ethanol content (55-15-30) had no signal after intermediate to low q region, it might due to the slow self-assemble process at this composition which required long-term observation to see the differences. For P index, the values all fall between 3 to 4, indicating the oleogels contained 3D fractal structures, instead of spheres (P_{sphere} = 4). The shape did not have a clear relationship with the changing of solvent composition bases on the results showed in this study.
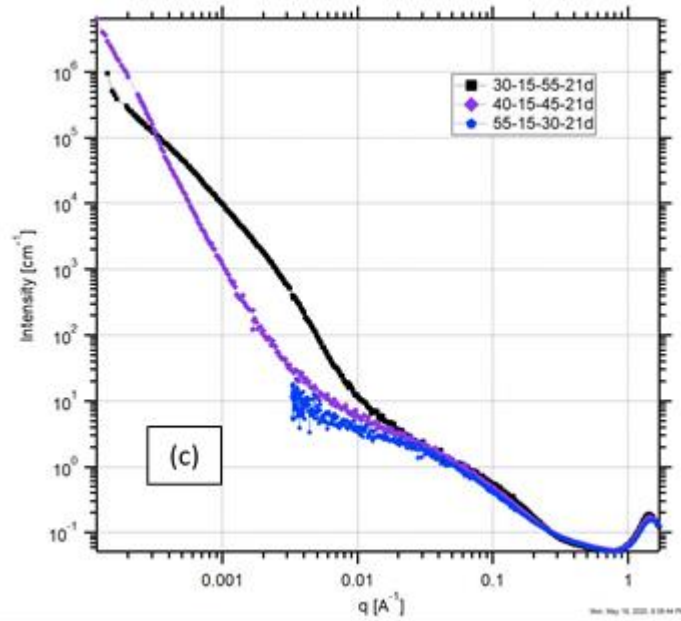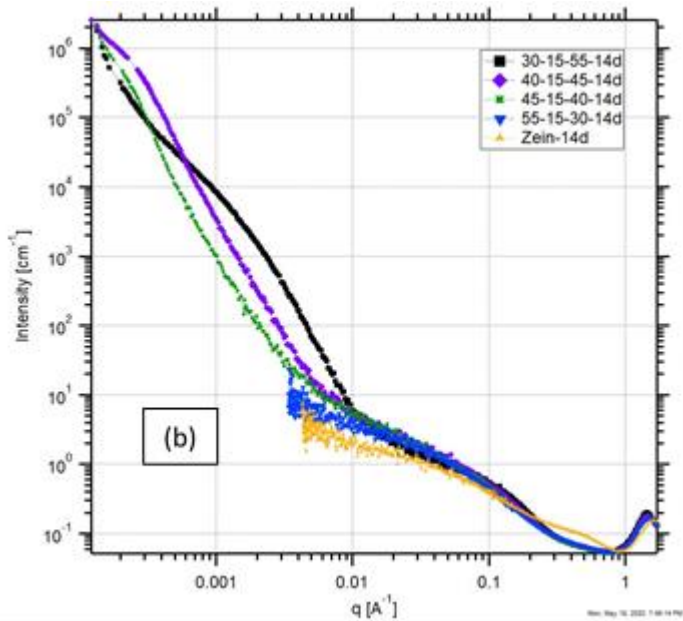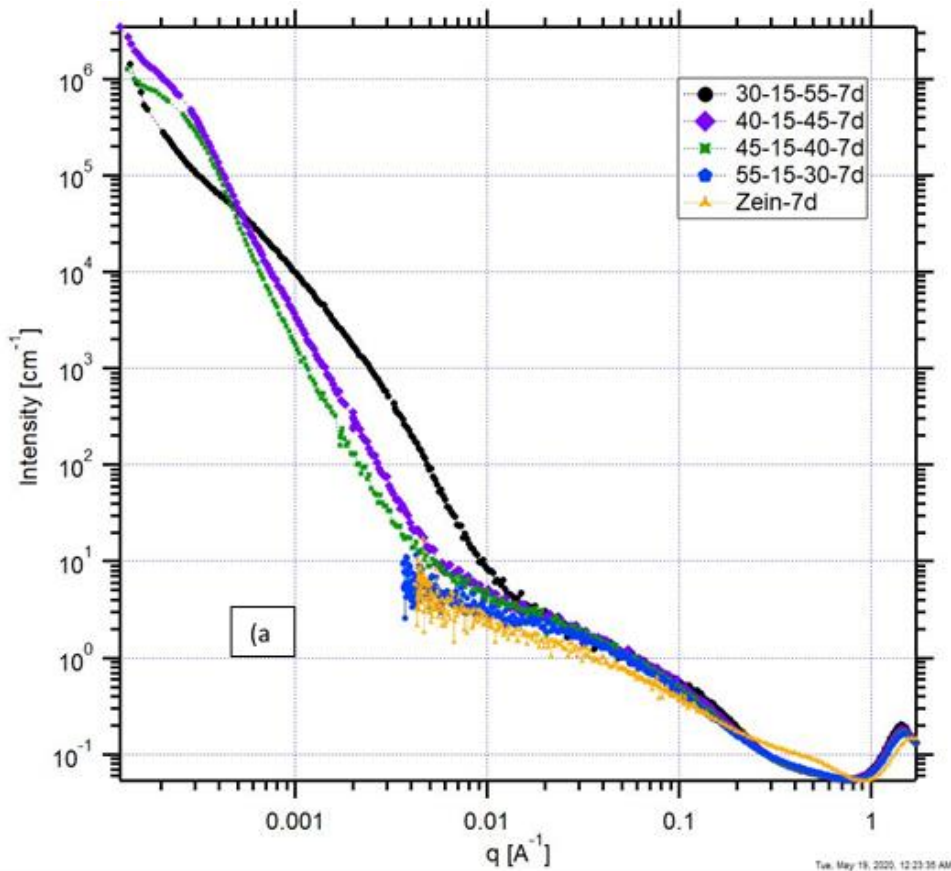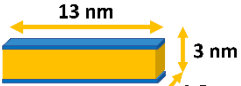
Figure 5.1 Desmeared and smoothened USAXS profiles of 15% zein-based oleogel with sample coding as 70% ethanol (wt%)-zein (wt%)-oleic acid (wt%) stored for 7 days (a), 14 days (b) and 21 days (c).

Table 5.1 R_g and P values for zein-based oleogels stored for 7, 14 and 21 days with corresponding schematic models proposed.

Sample code	R_{g1} (nm)	P_1 index	Schematic model	R_{g2} (nm)	P_2 index
			High q region	Low to intermediate q region	
30-15-55-7d	3.8	1.8		251	3.4
30-15-55-14d	3.5	1.8		276	3.5
30-15-55-21d	3.9	1.8		300	3.2
40-15-45-7d	5.7	1.6		772	3.6
40-15-45-14d	6.2	1.6		745	3.4
40-15-45-21d	10.7	1.5		>1200	3.2
45-15-40-7d	7.3	1.5		738	3.7
45-15-40-14d	8.5	1.5		1145	3.2
55-15-30-7d	11.5	1.2		---	---
55-15-30-14d	11.6	1.4		---	---
55-15-30-21d	12.6	1.4		---	---
67-33-0-7d (zein)	12.8	1.1		---	---
67-33-0-14d (zein)	13.1	1.0		---	---
40-20-40-7d	5.9	1.6		574	3.5
40-20-40-14d	6.2	1.6		560	3.6
40-20-40-21d	10.6	1.5		632	3.5
45-20-35-7d	6.1	1.6		642	3.4
45-20-35-14d	7.1	1.6		665	3.4
45-20-35-21d	10.4	1.6		744	3.5

For better interpretation of the multiple levels of structure observed in the USAXS data, the Kratky plots were constructed by two separated q ranges, one was high q region ($0.01 < q < 0.5$ Å^{-1}) (Figure 5.2, 5.4, 5.7, 5.9, 5.11, 5.14 and 5.17) and the other was located in low q range ($q < 10^{-3}$ Å^{-1}) (Figure 5.5, 5.12, 5.15 and 5.18). Obviously, pure zein in 70% ethanol solution showed as a rod-like structure and also behaved like a less compact protein (Figure 5.2). Samples with addition of oleic acid all had a peak grew in between q range 0.1-0.2 Å^{-1}, indicating the ribbon-like structure forming or a secondary level structural rearrangement of the molecules. The rod-like linear slope would decrease with the increasing of oleic acid amount could be result from the more aggregated protein unit structure. And this also confirmed by the strengthen sharpness of the peak shape with longer the plateau range. Suggesting the role of oleic acid is crucial for the organization of the protein packing and affecting the flexibility of the protein.

The shifting of the peak position to high q region was related to the increasing of oleic acid,

meaning the size of the radius of gyration was decreasing due to the addition of oleic acid amount, coincided with the R_{g1} calculated by the unified fit (Table 5.1). If we assumed zein unit structure behaved like Kuhn segment, approximately we can determine the kink position and this segment length was also decreased with the increasing of oil phase (Brosey & Tainer, 2019; Hammouda, 2010; Ochbaum & Bitton, 2018).
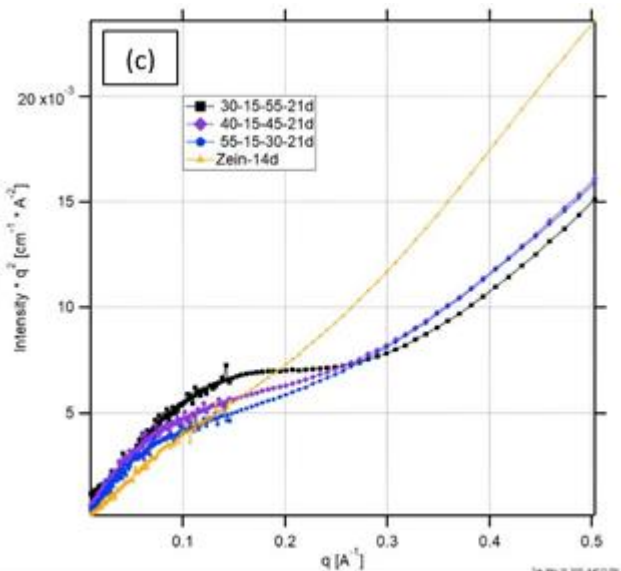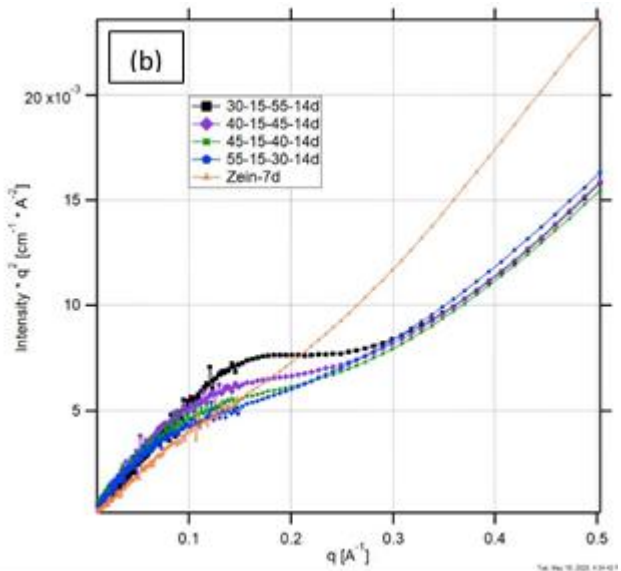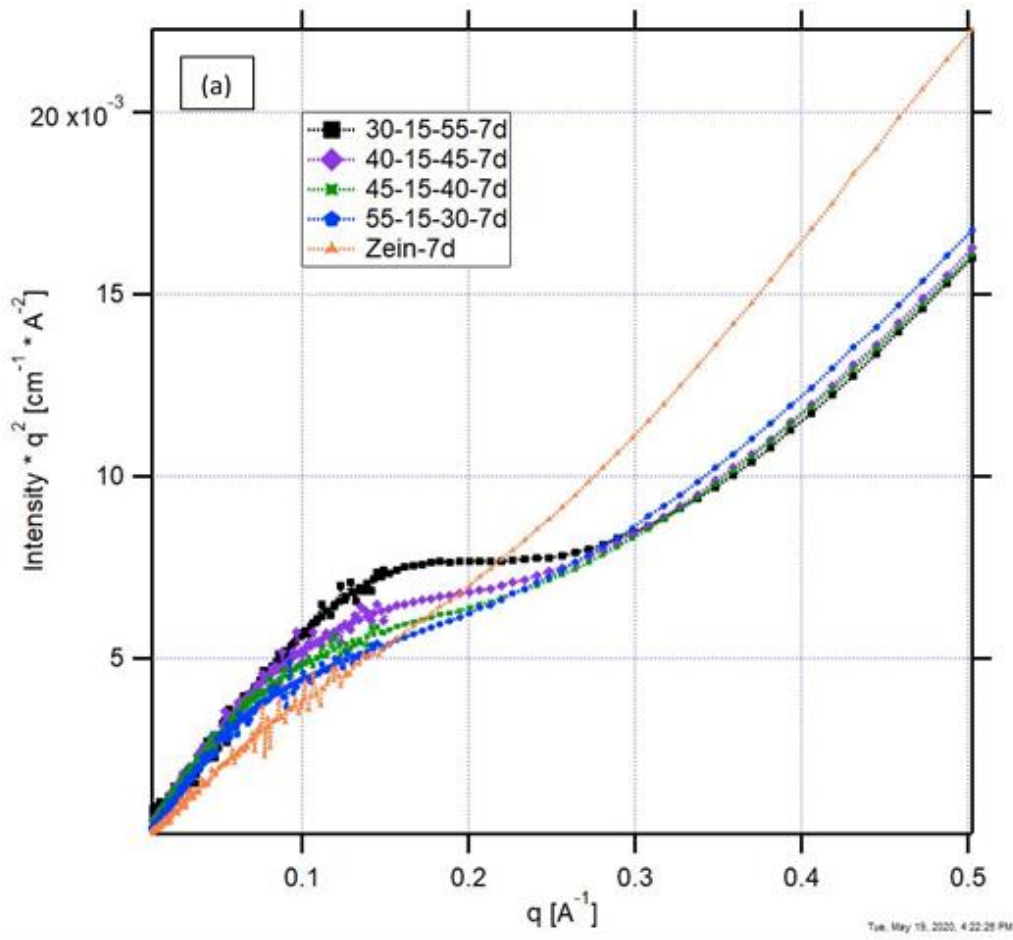
Figure 5.2 Kratky plots located at $0.01 < q < 0.5$ Å^{-1} derived from USAXS profile of 15% zein-based oleogel with sample coding as 70% ethanol (wt%)-zein (wt%)-oleic acid (wt%) stored for 7 days (a), 14 days (b) and 21 days (c).

5.4.2 Effect of zein concentration

In order to see the effect of zein concentration to the microstructure of the oleogel, four samples with similar solvent compositions of 15% and 20% zein concentration were selected and compared. Based on the slit desmeared USAXS results (Figure 5.3), all four samples were almost identical and merged together at high q region, but once plotting the data onto the Kratky plots, more information were revealed. In Figure 5.4, q range between 0.01 to 0.5 Å^{-1}, rod-like structures were displayed in two categories. 15% zein concentration samples had similar slopes, while 20% samples were also close to each other with higher scattering intensities. On the other hand when considered the peak shape and position, samples with same amount of 70% ethanol showed more alike behavior, indicating solvent composition had dominant effects. Both 40-15-45 and 40-20-40 had longer and flattened plateau region in comparison to 45-15-40 and 45-20-35. It may owe to the HLB of the solvents which caused the protein molecules tightened and became more compact with lesser amount of hydrophilic phase but more of the hydrophobic phase. And this could also account for the size differences of R_{g1} listed in Table 5.1. For 40-15-45 stored for 2 weeks, R_{g1} was between 5.7 to 6.2 nm similar to 5.9 to 6.6 for sample 40-20-40. Likewise, 45-15-40 had R_{g1} slightly larger at 7.3 to 8.5 nm while 45-20-35 was around 6.1-7.1 nm, indicating the unit structure size and shape were mainly dependent on the HLB of the solvents ($1.5 < P_1 < 1.8$) in comparison to the effect of zein concentration.
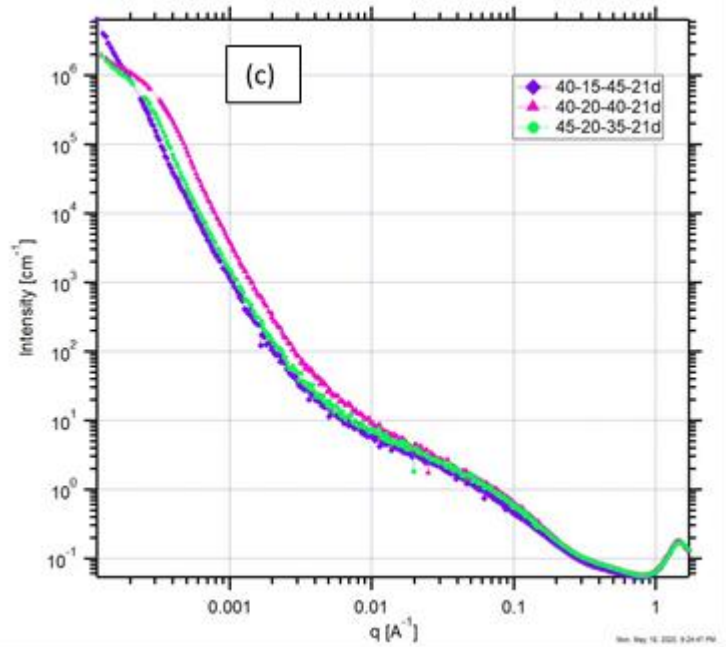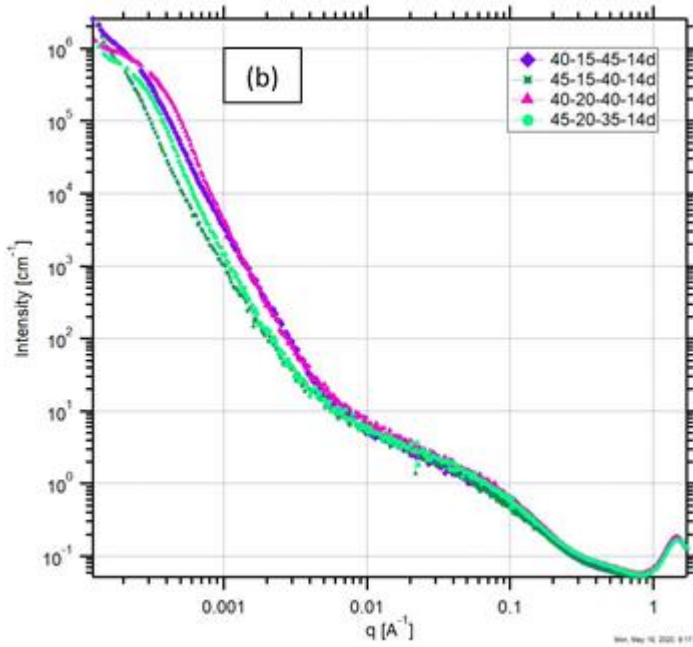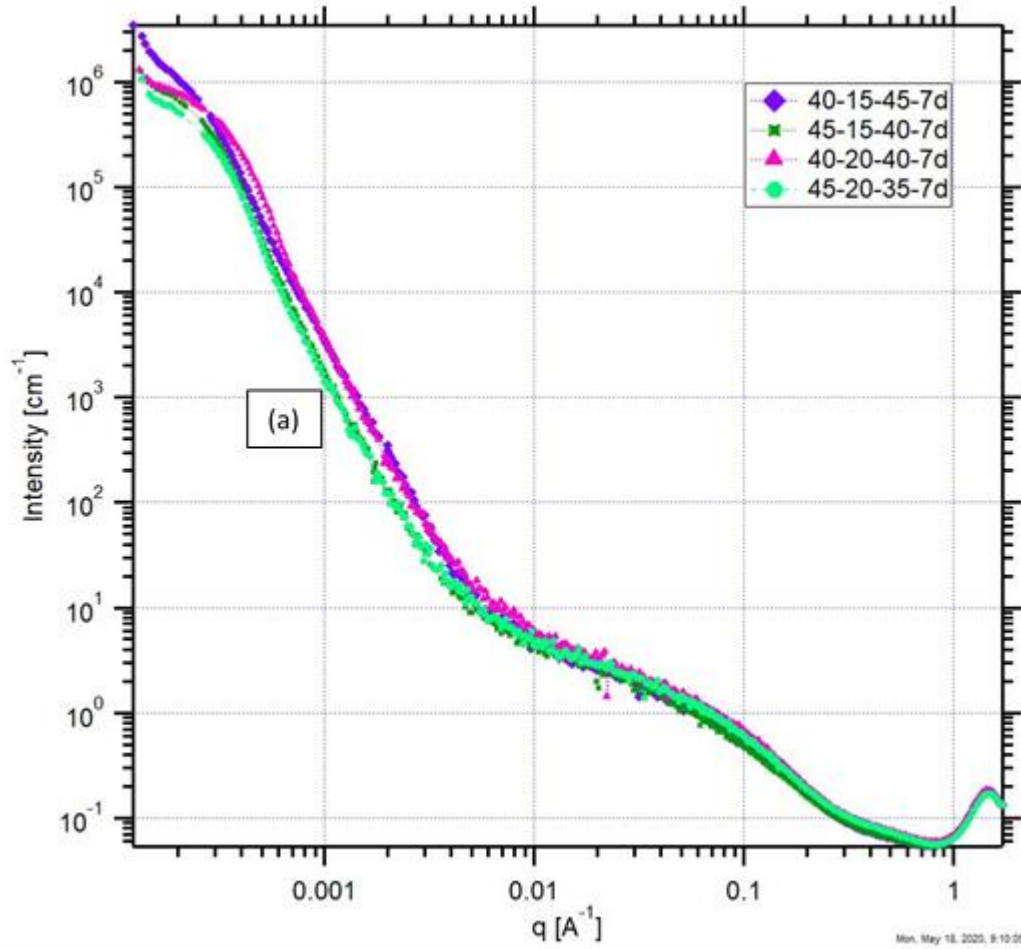
Figure 5.3 USAXS profiles of zein-based oleogels with 40 and 45% (w/w) of 70% ethanol and corresponding amount of oleic acid stored for 7 days (a), 14 days (b) and 21 days (c).
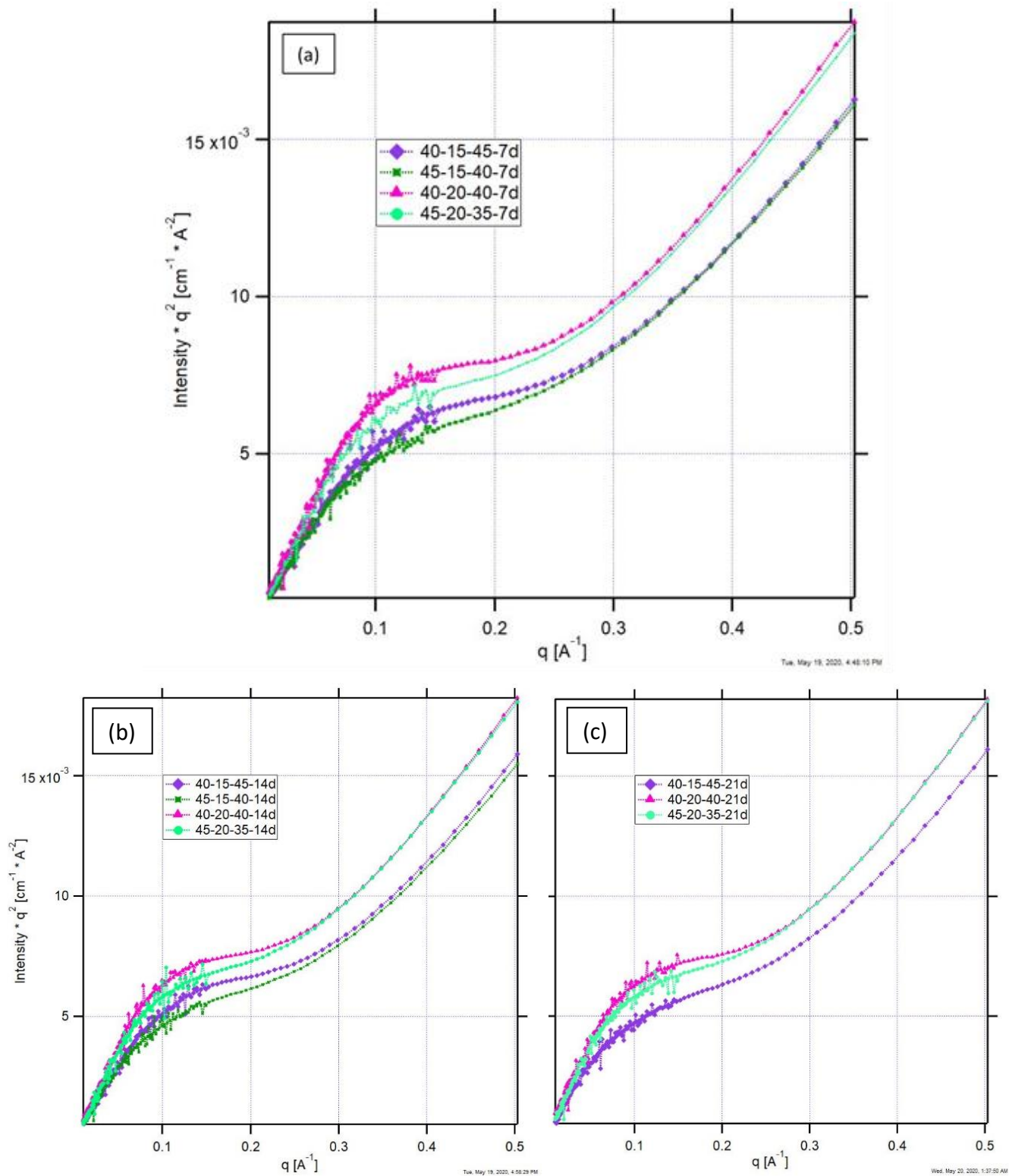
Figure 5.4 Kratky plots located at $0.01 < q < 0.5$ Å^{-1} derived from USAXS profile of zein-based oleogels contained 40 and 45% of 70% ethanol stored for 7 days (a), 14 days (b) and 21 days (c).

Noticeably, the scattering peaks at low q region varied within samples (Figure 5.3, $q < 10^{-3}$ Å^{-1}). According to the fitted results, R_{g2} for 15% zein concentration samples stored for 7 days were in the range of 738-772 nm, and for 20% ones, they were significantly smaller in between 574-632 nm. It may be explained as higher zein concentration meaning more of the protein molecules were competing for the ethanol, not only causing the mobility of protein itself decreased but also affecting the interaction with oleic acid and moreover to arrange into larger repetition structures. This R_{g2} size differences would follow the same trend in 14 and 21 days samples, whereas the 15% zein concentration samples were always larger than 20% samples. Kratky plot to enhance the signal to examine the peak shape and position at low q region (q < 10^{-3} Å^{-1}). We observed that all curves showed bell-shape, which could be interpreted as the oleogels contained compact fractal structures with specific sizes (Figure 5.5) and this statement was confirmed by Porod index $3 < P_2 < 4$ (Table 5.1). From the peak position, we knew 40-15-45-7d had the largest size at lowest q while 40-20-40-7d was the smallest.
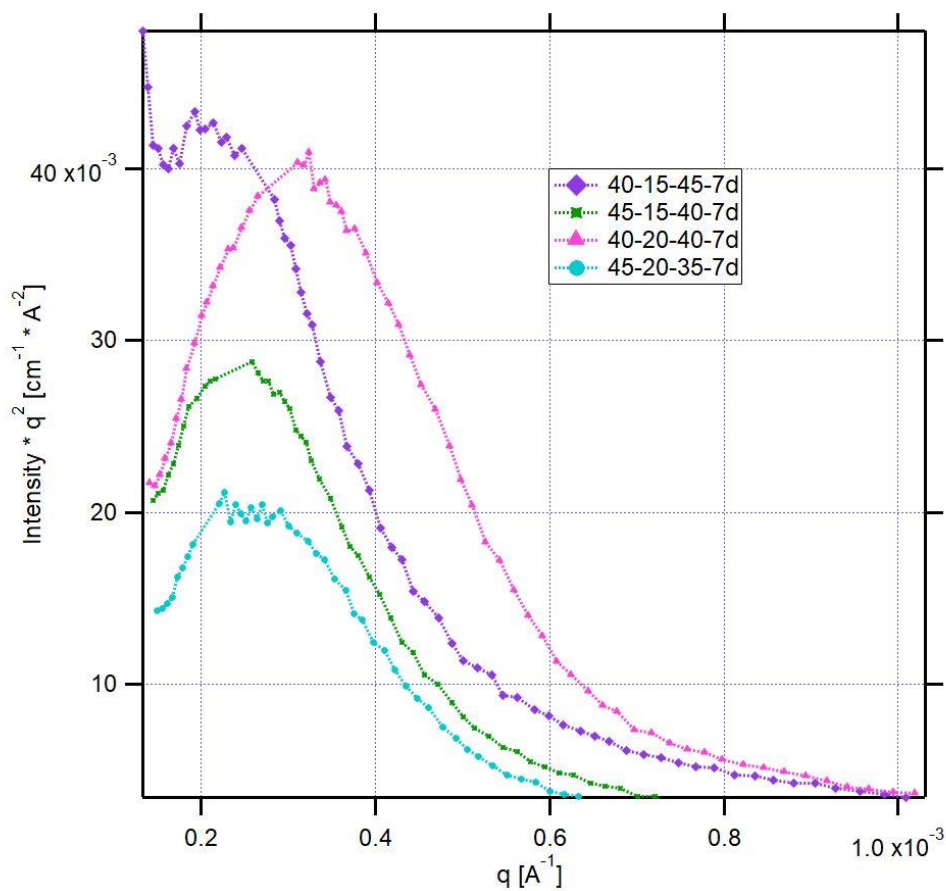

Figure 5.5 Kratky plots generated form USAXS profile low q region (q < 10^{-3} Å^{-1}) of 15% and 20% zein-based oleogels with 40 and 45% of 70% ethanol stored for 7 days.

5.4.3 Effect of storage time

For better clarity, samples with reversed 70% ethanol to oleic acid ratio were plotted in the same figure. First, in 30-15-55 three weeks storage samples (Figure 5.6), R_{g1} fall between 3.5-3.9 nm and P_1 maintained as 1.8, relatively consistent with size and shape during the storage. Confirmed by Figure 5.7, which the high q region linear slope did not change with time, meaning the zein protein rigidity behaved the same throughout the observation time. Before 14 days of storage, the intermediate q building block structures had almost no differences, but at 21 day, it had a pronounced change at the kick position of the segment length, which the position shifted to lower q and was suspected to be the elongation of zein ribbon-like structure by end-to-end connection between molecules. Interestingly, both R_{g1} and Kratky plot curves for 55-15-30 seemed having no observable changes under time effect. It might due to the high ethanol content which allowed the zein protein stayed as unfolded also distributed freely in the system.

The R_{g2} of 30-15-55 slightly increased with time, from 251 to 300 nm, it presented the self-assembled ability of zein molecules. And at this solvent composition the protein was believed to be more aggregated, making it harder to interact with oleic acid and rearrange into larger scale. Overall, both 40-15-45 and 45-15-40 sample profiles between 7 and 14th day at high q range had almost no differences, their P_1 kept as 1.5-1.6, and R_{g1} changed from 5.7/7.3 nm to 6.2/8.5 nm respectively. Not until 21st day, R_{g1} for 40-15-45 enlarged to 10.7 nm, and this primary unit change could also be observed by the hump in Figure 5.9, which it slightly shifted to lower q and merged into 45-15-40 curves. This indicated the slow self-assembly process of zein, moreover, with higher amount of oleic acid, the microstructures required more time to interact and array into more developed building blocks. (Unfortunately, we don't have sample 45-15-40-21d.)

As for second level wide range structure, the R_{g2} sizes significantly increased at 14th day for 45-15-40 and 21st day for 40-15-45, from hundreds nanometer to micrometer dimensions. In Figure 5.12 (purple and green curves), clear view of the low q region data plotted as $I(q)q^2$ versus q manifested the peak of 40-15-45-7d and 45-15-40-7d would disappear on the 21st day, supposed they shifted to further low q that beyond measurement limit. With zein 20% samples (40-20-40 and 45-20-35), the time would do very little effect on R_{g1} value before 14th day, and this phenomenon is similar to other zein 15% oleic acid containing samples especially alike 40-15-45 and 45-15-40.   And the position of humps at intermediate q interpreted as building block size

would have a bigger left shift on the 21st day profiles (Figure 5.11 light pick and light teal curves). And according to the fitting results, the R_{g1} size of both samples would come to around 10 nm at that time. We suggested the primary zein molecule packing unit with moderate amount of ethanol had the ability to further associate with other zein protein in an extended time frame.

In Figure 5.12, the time effect on the R_{g2} values can be easily monitored by the shifting of the structural peaks. For instance, 40-20-40-7d had a peak at $q = 0.32 \times 10^{-3}$ Å^{-1} with unified fit model result averaged as 574 nm for R_{g2}. After storage time elapsed, the peak moved to $q = 0.27 \times 10^{-3}$ Å^{-1}, R_{g2} fitted as 632 nm, indicating the growth of 3D fractal structures required time. In comparison, sample 45-20-35-7d had a peak already located at $q = 0.27 \times 10^{-3}$ Å^{-1}, and would further increased the R_{g2} size to 744 nm with the peak shifted to lower q $(0.20 \times 10^{-3}$ Å$^{-1})$. Summarizing the results, we knew time is a crucial factor for the size change of the R_{g2}. And with more of the ethanol in the sample, the effect is more prominent, assuming to be the higher mobility that zein molecules possessed which provides a more favored condition for the self-assembled process to take place.
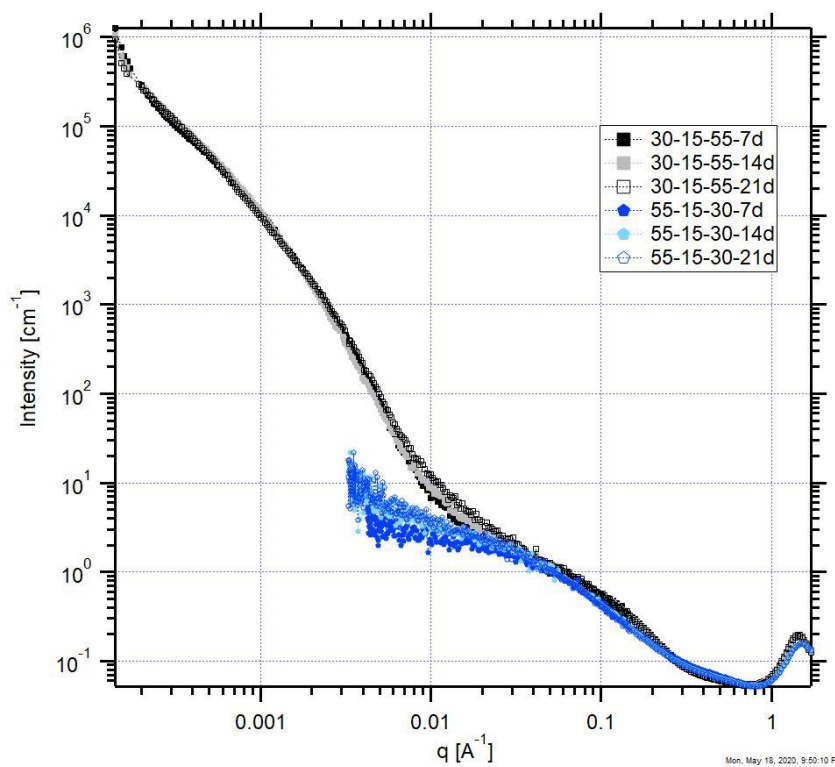

Figure 5.6 USAXS profile of oleogel compositions of 30-15-55 (black) and 55-15-30 (blue) stored for 7 days, 14 days and 21 days (log-log plot).
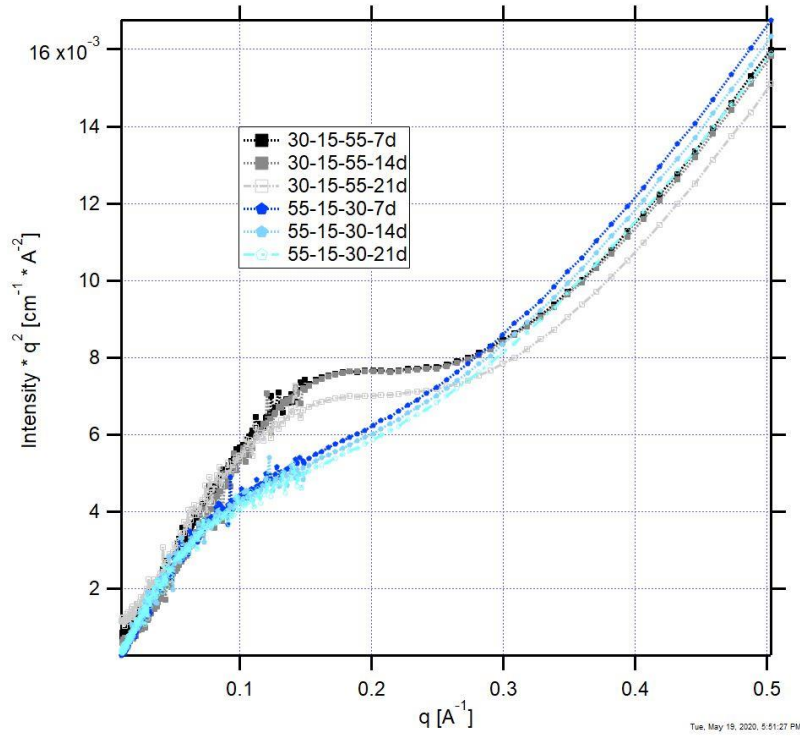
Figure 5.7 Kratky plots located at $0.01 < q < 0.5$ Å^{-1} derived from USAXS profile of oleogel compositions of 30-15-55 (black) and 55-15-30 (blue) stored for 7 days, 14 days and 21 days.
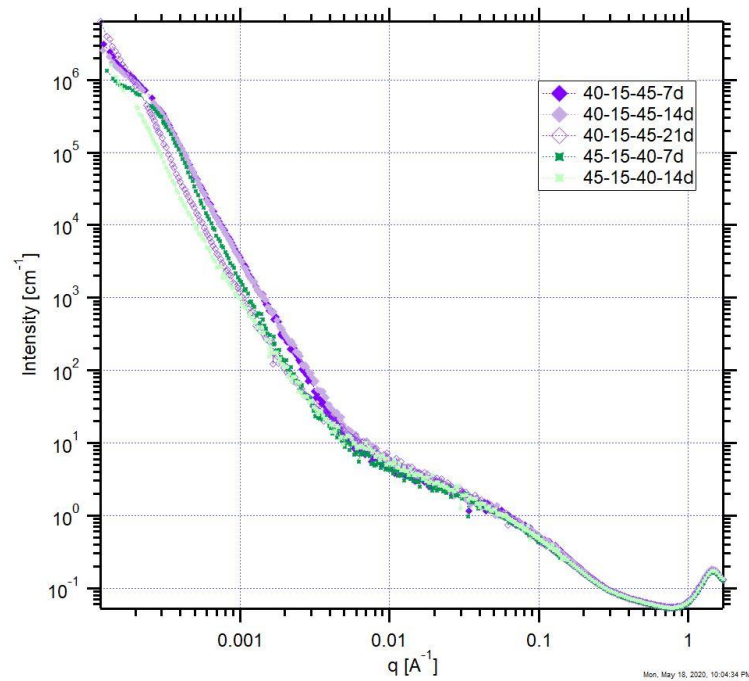

Figure 5.8 USAXS profile of oleogel compositions of 40-15-45 (purple) and 45-15-40 (green) stored for 7 days, 14 days and 21 days.
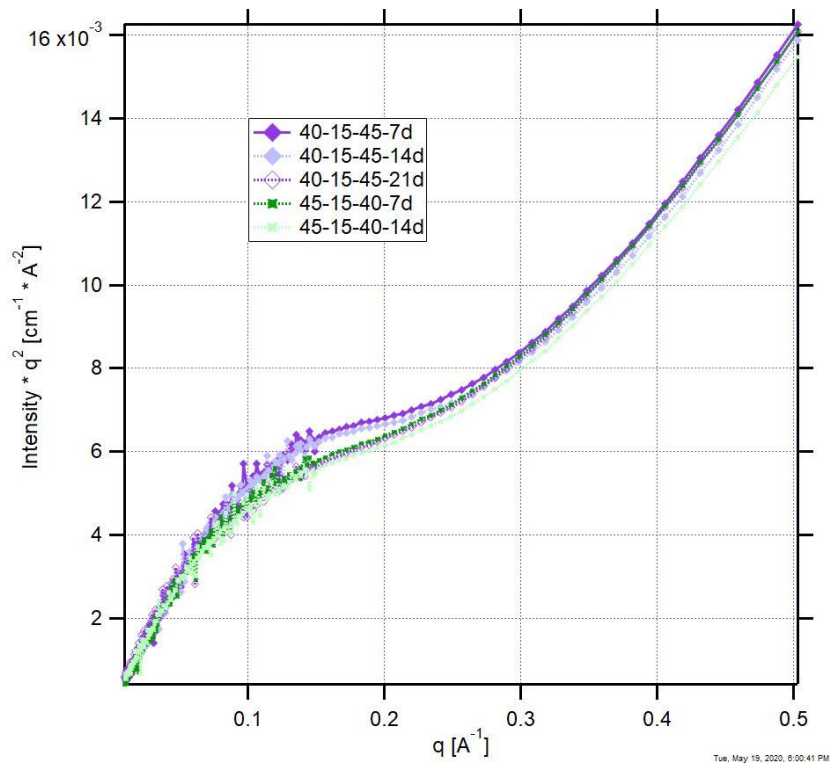
Figure 5.9 Kratky plots located at $0.01 < q < 0.5$ Å^{-1} derived from USAXS profile of oleogel compositions of 40-15-45 (purple) and 45-15-40 (green) stored for 7 days, 14 days and 21 days.

Figure 5.10 USAXS profile of oleogel compositions of 40-20-40 (pink) and 45-20-35 (teal) stored for 7 days, 14 days and 21 days.

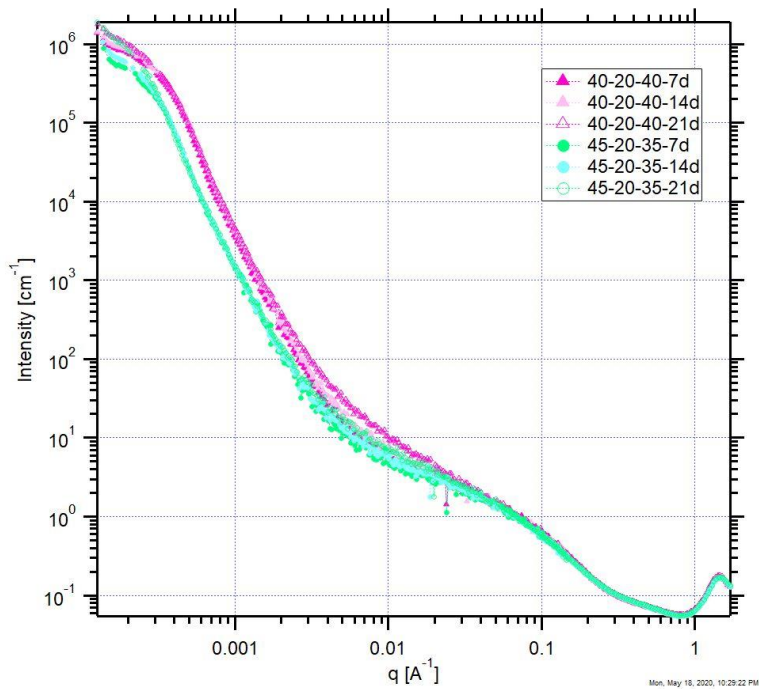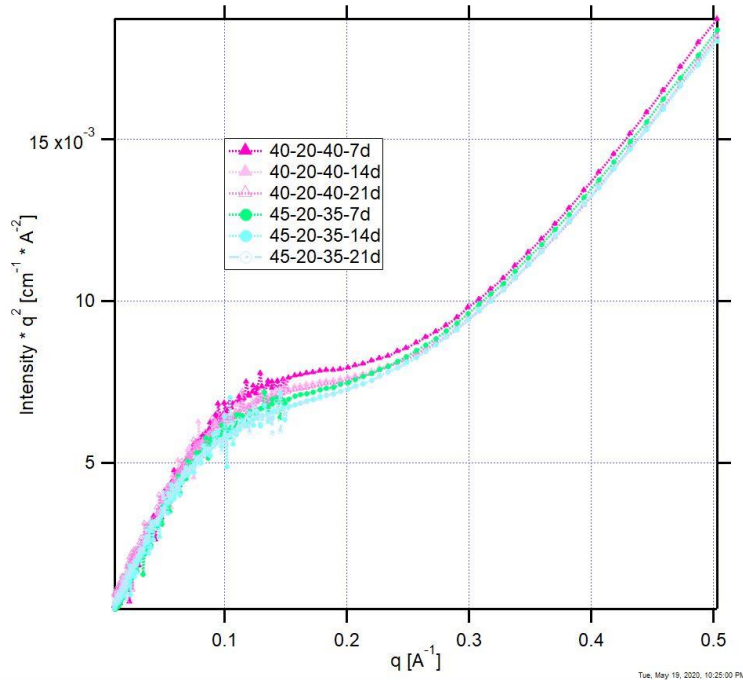Figure 5.11 Kratky plots located at 0.01 < q < 0.5 Å^{-1} derived from USAXS profile of oleogel compositions of 40-20-40 (pink) and 45-20-35 (teal) stored for 7 days, 14 days and 21 days. F
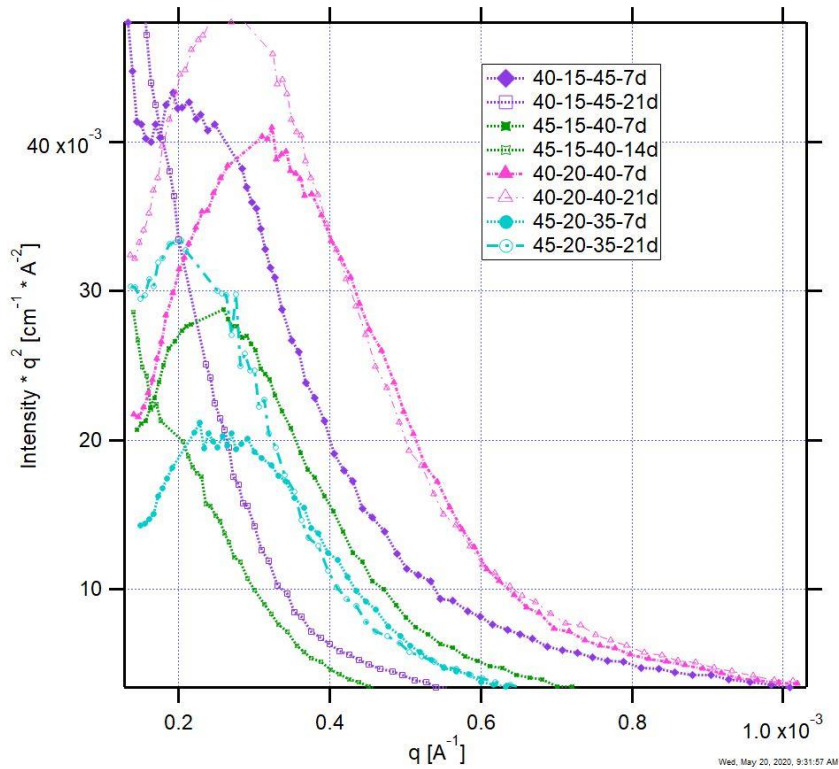

Figure 5.12 Kratky plots generated form USAXS profile low q region (q < 10^{-3} Å^{-1}) of 15% and 20% zein-based oleogels with 40 and 45% of 70% ethanol stored for 3 weeks.

5.4.4 Effect of sonication

As we found out in rheological results, sonication treatment could facilitate the gelation process and strengthen the oleogels rigidity. In order to better understand the microstructural changes of oleogels with high shear applied, four formula with 15% zein concentration were chosen and determined in this part of the research by USAXS. It was hypothesized that the sonication treatment would provide considerable high shear to decrease the size of solvent droplets and create a more homogenous emulsion before it self-assembled into a stable oleogel.

According to Figure 5.13, both with and without (as control group) sonication treatment samples of 30-15-55 and 55-15-30 were plotted and compared. Visually, sonicated samples stored for 7 days had little or no differences to the controls. However, for 21 days samples, we observed distinct changes such as three structural peaks in 30-15-55-21s (black crossed square curve) instead two for 30-15-55-21d, and 2nd peak appeared at intermediate q range for 50-15-30-21s (green cross curve) instead of 1 peak at high q range only. Looked deeper into the data, USXAS results of sonicated samples were fitted with unified model and gathered in Table 5.2. For sample 30-15-55-7s, R_{g1} and P_1 remained as 3.8 nm and 1.8, respectively, were identical to 30-15-55-7d. And for 55-15-30-7s, R_{g1} was 13.2 nm resembled to 55-15-30-7d 11.5 with same P_1 values of 1.4. Indicating the sonication treatment would not change the primary unit size of these two compositions at 7 days of storage time.

After storage for 21 days, in 30-15-55-21s USAXS profile two R_{g1} and P_1 ($0.01 < q < 0.5$ Å^{-1}) were observed and can be deduced from model fitting. The smaller one was 3.7 nm with a P_1 value of 1.8 and the other was 12.5 nm and $P = 3.1$, quiet different to 30-15-55-21d which only had single R_{g1} as 3.9 nm. It was believed that the sonication could significantly decrease the size of oil droplets but not zein molecules, so the sizes of R_{g1} detected by USAXS could be the result of completed distributed protein that took time and oriented into ordered building blocks then measured in varied directions (the emergence of the second peak close to low q in Figure 5.14).

55-15-20-21s had the smallest R_{g1} of 1.3 nm and a P value 1.6, instead of 55-15-30-21d seeing the unit block size of zein as 12.6 nm, it was assumed to be the diameter of α-helix structure of protein and could be explained later by the discussion of $R_{g2.}$

In Figure 5.15, using Kratky plot to amplify the data in low q region ($q < 0.01$ Å^{-1}), the peak

position of two sonicated samples (stored for 7 and 21 days) were observably right shifted, meaning the R_{g2} were smaller. Uniquely, the R_{g2} of 30-15-55-21s decreased significantly in comparison to the one without sonication. By checking the contour shape information provided by P_2 value, we knew it was 2.7, a 2D to 3D fractal structure, relatively different to the others that were bigger than 3. Furthermore, the P_3 not shown here equaled to 4, evidenced the existence of spherical shaped well organized structures this sample may form by the aid of sonication and time. So the R_{g2} could be a level of structure that built up the spheres.

While we focused on the 50-15-30-21s data, surprisingly, it grew out to have a second Guinier knee around $q = 0.01$ Å^{-1}. The fitted radius of gyration was around 74 nm, which was similar to 73.2 nm of 30% zein sample aged for 3 months measured by USAXS in Uzun, Ilavsky and Padua, 2017. This size was also closed to the hydrodynamic radius size of zein aggregates measured by dynamic light scattering technique mentioned in Kim & Xu, 2008 (60nm), and in Guardiola & Padua, 2019 (101 nm). Here, we believed this R_{g2} size presented the 2D plates which composed of well-organized rod-like zein molecules that attached on the oleic acid droplets ($P_2 = 1.7$), forming elongated sheets instead of aggregates. And this structural rearrangement process required the high mobility of protein which dedicated by the solvent composition and high shear applied. Also, this might explain the size seen at R_{g1} which 1.3 nm was the repeating unit (width of single zein block) that consisted of the 2D plates ; Yunqi Li et al., 2012).

We already discovered that the R_{g1} and P_1 (0.01 < q < 0.5 Å^{-1}) sizes were mainly affected by the composition of the solvents in the previous discussion. Time also acted as a factor for the growth of R_{g1}, however, due to the slow self-assembly process, the change of primary building block sizes required 21 days to observe differences with solvent ratio of 70% ethanol and oleic acid approached 1 : 1. With sonication, 40-15-45-7s had slightly larger R_{g1} size than sample without, showing high shear promoted the packing of zein molecules, and this effect was also observed in 45-15-40-7s. The identical R_{g1} size and P_1 value between 40-15-45-21s and 40-15-45-21d confirmed that the sonication facilitated the self-assembly behavior of zein protein into a favored building block size while not breaking down the zein original molecular structures (Table 5.2 and Figure 5.16 & 5.17).

Another important effect of sonication was to decrease the droplet size of dispersed phase and making the emulsion system more homogeneous. This assumption was validated indirectly by the

decreasing size of R_{g2} data after sonication showed in Figure 5.18. If the oleic acid droplets (dispersed phase) were sheared and downsized, meaning free zein molecules dissolved in 70% ethanol (continuous phase) would have higher possibility to interact with oleic acid instead of zein itself, which forming smaller clusters ($3 < P < 4$). But on the other hand, this smaller 3D structures provided more interconnected network in the gel system, resulted to faster gelation rate and stronger gel rigidity mentioned in Chapter 4 (Rheology). And this phenomenon was enhanced with composition contained higher amount of oleic acid. For example, R_{g2} of 40-15-45-7d decreased 36% from 772 to 493 nm, but for 45-15-40-7d was 19% (738 to 601 nm) after being sonicated. It was expected with larger oleic acid volume fraction, high shear would produce more droplets and evenly distributed zein molecules. And the densely packed oleic acid restrained the growth of zein from building blocks into wider ranged structures causing the decreased size of R_{g2}. If we imaging each oil droplet was an anchor point for zein molecules which acting as oleogelators to deposit on, it was predicted to see a more compact network developed in a high amount of oleic acid containing sample.
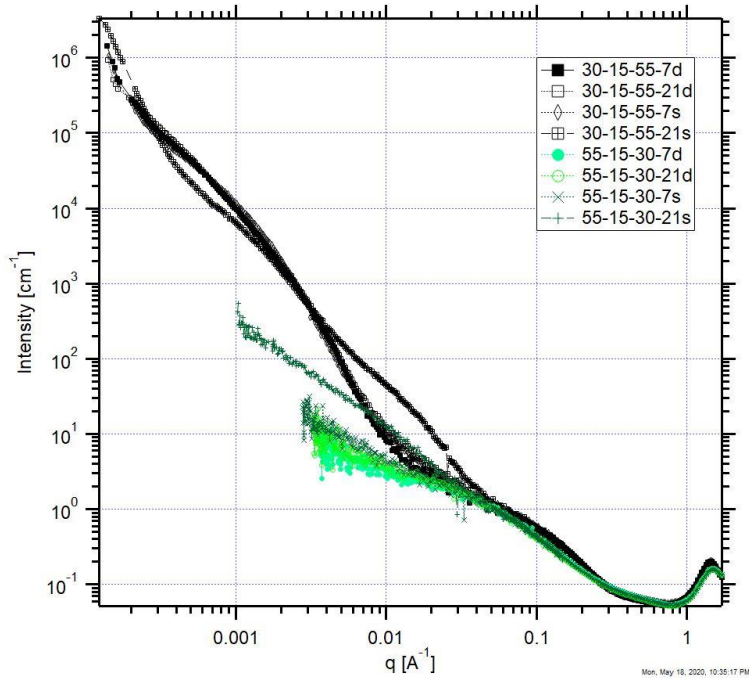
Figure 5.13 USAXS profile of oleogel compositions of 30-15-55 (black) and 55-15-30 (green) with or without sonication treatment stored for 7 days and 21 days (log-log plot).
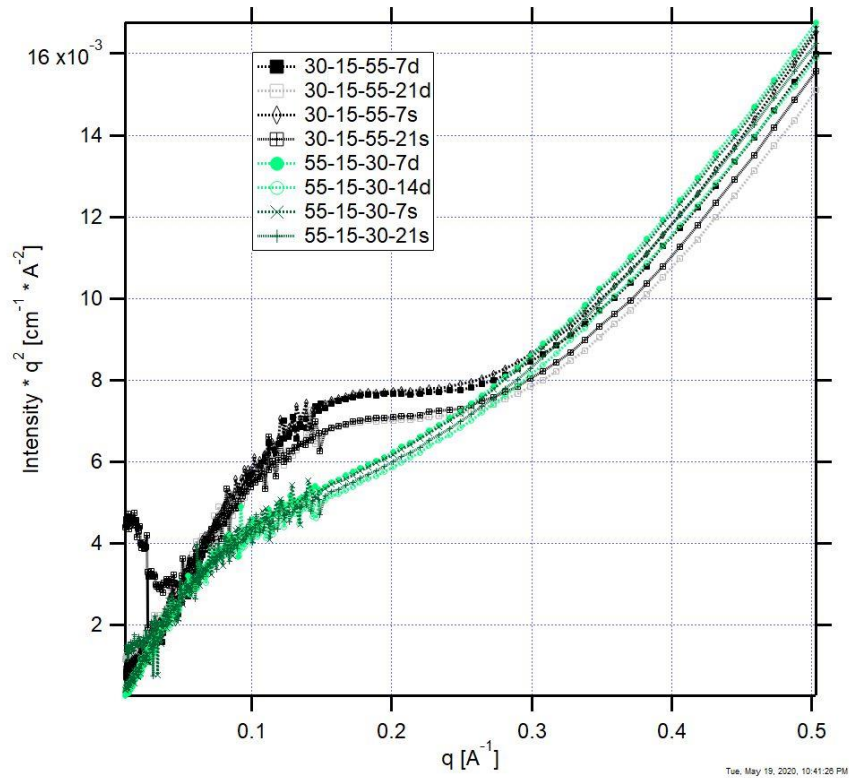

Figure 5.14 Kratky plot of oleogel compositions of 30-15-55 (black) and 55-15-30 (green) with or without sonication treatment stored for 7 days and 21 days located between $0.01 < q < 0.5$ Å^{-1}.

Figure 5.15 Kratky plot of oleogel compositions of 30-15-55 (black) with or without sonication treatment stored for 7 days and 21 days located at q < 0.01 Å^{-1}.

Table 5.2 R_g and P values for zein-based oleogels stored for 7 and 21 days with sonication treatment applied.

Sample code	R_{g1} (nm)	P_1 index	R_{g2} (nm)	P_2 index
	High q region		Low to intermediate q region	
30-15-55-7d	3.8	1.8	251	3.4
30-15-55-7s	3.8	1.8	245	3.5
30-15-55-21d	3.9	1.8	300	3.2
30-15-55-21s	1.3/11.3	1.5/2.6	168	2.6
40-15-45-7d	5.7	1.6	772	3.6
40-15-45-7s	8.3	1.5	493	3.4
40-15-45-21d	10.7	1.5	>1200	3.2
40-15-45-21s	10.7	1.5	500	3.3
45-15-40-7d	7.3	1.5	738	3.7
45-15-40-7s	8.5	1.5	601	3.4
45-15-40-21s	11.3	1.4	>1200	3.5
55-15-30-7d	11.5	1.2	---	---
55-15-30-7s	13.2	1.4	---	---
55-15-30-21d	12.6	1.4	---	---
55-15-30-21s	1.3	1.6	74.1	1.7

Figure 5.16 USAXS profile of oleogel compositions of 40-15-45 (purple) and 45-15-40 (green) with or without sonication treatment stored for 7 days and 21 days (log-log plot).

Figure 5.17 Kratky plot of oleogel compositions of 40-15-45 (purple) and 45-15-40 (green) with or without sonication treatment stored for 7 days and 21 days located between $0.01 < q < 0.5$ Å^{-1}.
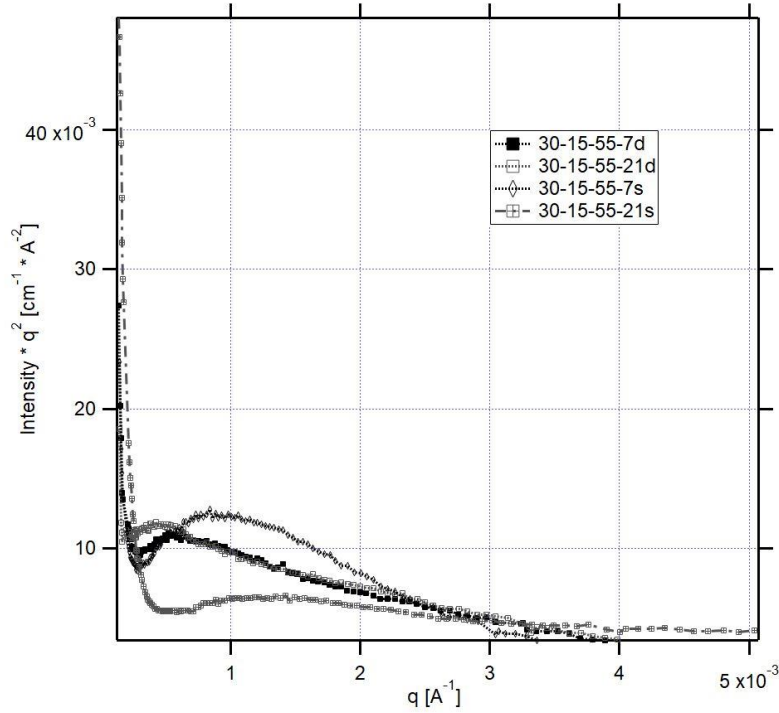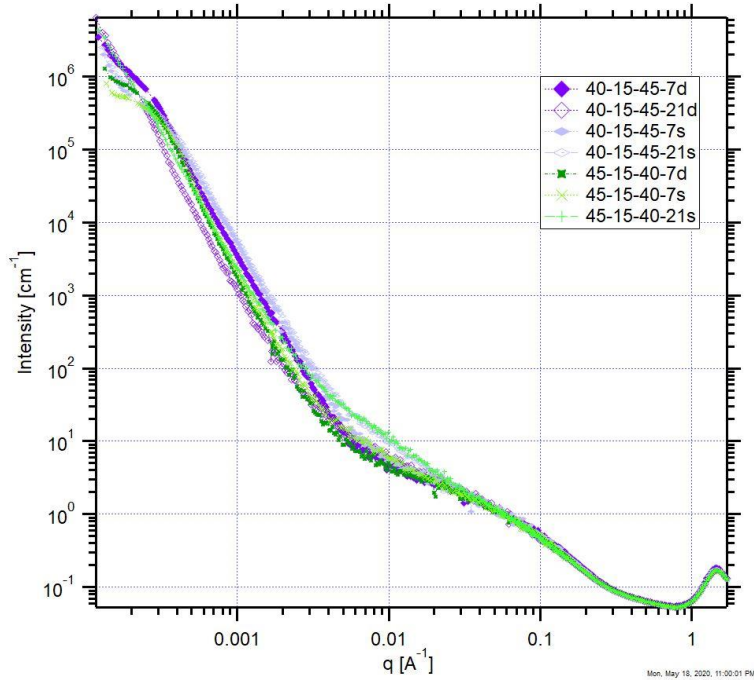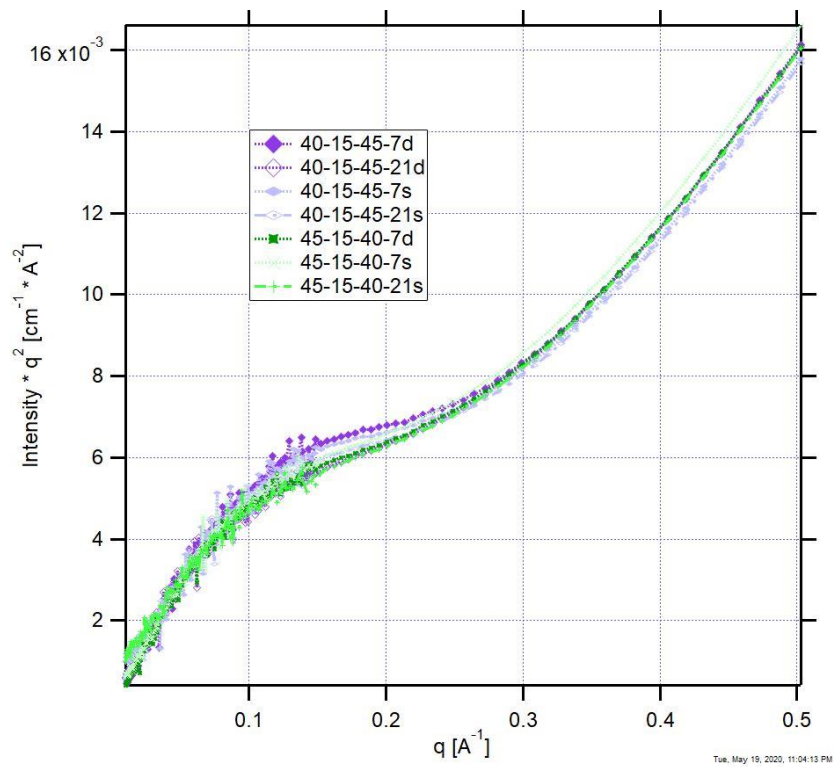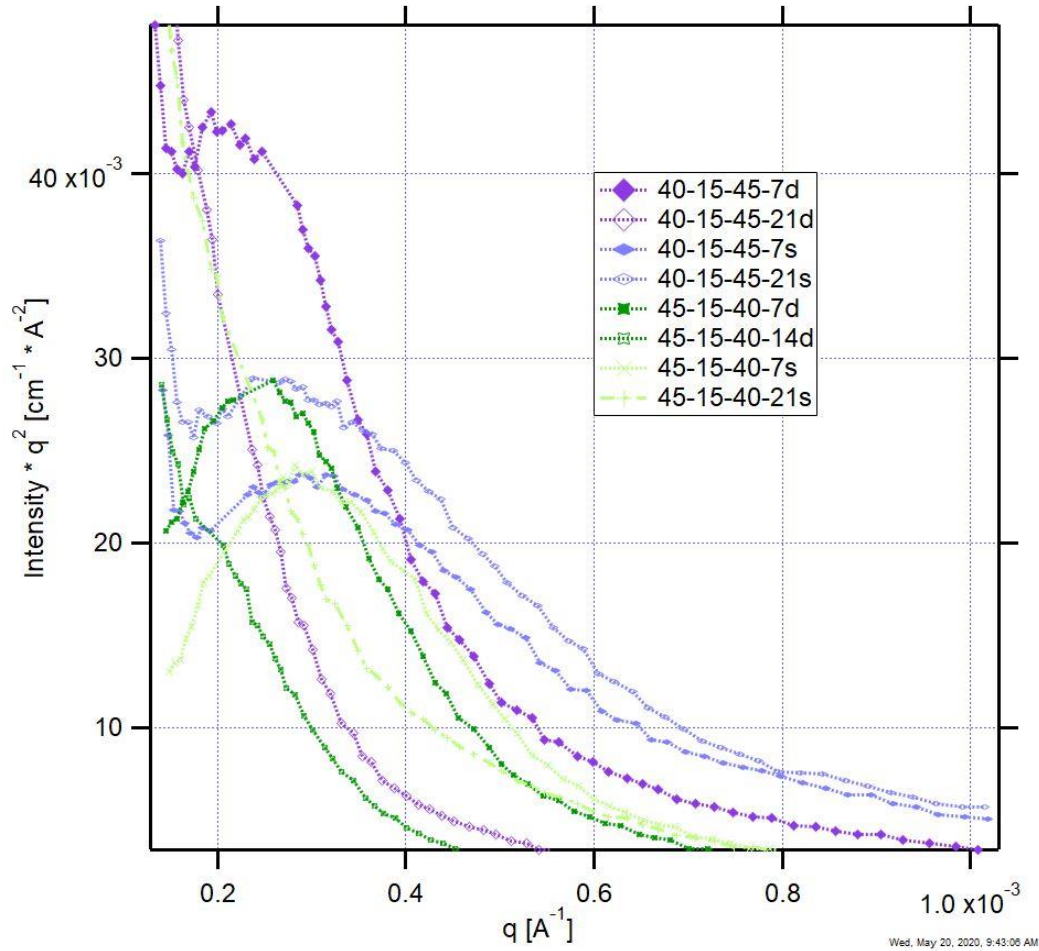
Figure 5.18 Kratky plot of oleogel compositions of 40-15-45 (purple) and 45-15-40 (green) with or without sonication treatment stored for 7 days and 21 days located at q < 0.01 Å^{-1}.

5.5 Conclusions

Ultra-small angle x-ray scattering (USAXS) was a powerful tool to help investigate soft biomaterial structural properties such as zein-based oleogels. Two levels of structure were determined by USAXS and calculated by unified fit model. At high q region ($q > 10^{-2}$ Å^{-1}), one set of Guinier knee and Porod slope represented the corresponding R_{g1} and P_1 values, interpreted as the size and shape of the primary building blocks that proposed in Table 1. And the other set located at intermediate to low q region ($0.01 < q < 0.5$ Å^{-1}) were defined as R_{g2} and P_2, providing information about the possible arrangement of hundreds nano sized network structure.

R_{g1} and P_1 values were mainly affected by the solvent composition. With the increasing amount of oleic acid (0 to 55%) and reversely decreasing amount of 70% ethanol (85 to 30%), R_{g1}

113

decreased from 13.1 to 3.5 nm, and P_1 increased from 1.0 to 1.8 (Table 5.1). Indicating the rod-like (P_{rod} = 1) or plate-like stacking structures (P_{disk} = 2) were generated from zein. In the Kratky plots, compactness of zein protein was studied and confirmed that with higher portion of ethanol in the system, the expansion of zein was favored, exhibited as ribbon-like chain with interconnected thin rods. And with the addition of oleic acid, the structures became more compact, shorter repeating unit sizes were monitored which schematic models were proposed in Table 1.

Solvent composition also affected the behavior and size of the secondary level structures (R_{g2}). The 3D branching like structures ($3 < P_1 < 4$) were more developed with the increasing amount of 70% ethanol and decreasing amount of oleic acid. The repeating size increased from 251 nm to more than 1 μm and even beyond the limit of measurement. This was assumed that zein had higher mobility in ethanol, and with the increasing of the oil volume fraction, the changing of solvent HLB not only induced the zein to aggregate but also occupied the space for zein ordered structure to grow.

While the amount of oleic acid decreased to 30% with the corresponding 70% ethanol as 55%, there was no signal detected by the USAXS in low q range ($q < 10^{-3}$ Å^{-1}), which this result was similar to 15% zein only sample (85-15-0). Meaning at this composition, zein molecules were loosely distributed in the system instead of attaching on the oil droplets and forming evaluable secondary level structure.

Zein concentrations between 15% and 20% had no significant difference between R_{g1} and P_1 at same levels of 70% ethanol. But we could observe slightly larger in R_{g1} for sample composition of 45-15-40 in comparison to 45-20-35. This might due to lesser protein in the emulsion, zein unit structure was less dense and had higher mobility to further interact with solvent molecules and arrange into equilibrium status. In other aspect, zein concentration did have impact on the size of R_{g2} but not P_2. Samples contained 15% zein had P_2 values between 3 to 4, indicating they were clusters with 3D surface fractal structures similar to 20% zein samples. However, 15% zein samples had one to two hundreds nanometer larger R_{g2} than 20% samples, this might due to the competition of ethanol for each zein molecules and decreased the mobility to organize into wider ranged packing.

For samples composed of more than 30% of 70% ethanol (less than 55% of oleic acid), overall,

114

time would increase the size of R_{g1}. However, the difference of the increment required 21 days of storage time to be significant. This showed the slow self-assembly process of this zein-based oleogel system. Additionally, it was assumed that with similar solvent ratio, the building block size (R_{g1}) would eventually reach to a constant size.

R_{g2} sizes were positively dependent to the time, indicating an increased level of organization of zein surrounded oleic acid and a continued structural development over time. Both P_1 and P_2 did not change with time, implying the shape of these two levels of structures were predictable.

In general, sonication treatment would not affect too much to the primary building block size and the attaching direction to the oleic acid droplets (R_{g1} and P_1). It provided kinetic energy by high shear to facilitate the rearrangement of zein into more stable and uniform primary unit. On the other side, R_{g2} values of all samples except 55-15-30 became smaller after being sonicated. It was presumed that the oleic acid droplets were downsized and well distributed in the continuous phase, which the distances between each droplet were shorter causing the zein elongated fractal structures had smaller spaces to grow into large scale. Sonication could also promoted the secondary structure to form, which was evidenced by the emergence of new Guinier peak in sample 55-15-30-21s.

5.6 References

Argos, P., Pedersen, K., Marksl, M. D., & Larkinsflll, B. A. (1982). Structural Model for Maize Zein Proteins. *Journal of Biological Chemistry, 257*(17), 9984–9990.

Beaucage, G. (1995). Approximations leading to a unified exponential/power-law approach to small-angle scattering. *Journal of Applied Crystallography*, *28*(6), 717–728. https://doi.org/10.1107/s0021889895005292

Beaucage, G. (1996). Small-angle scattering from polymeric mass fractals of arbitrary for mass-fractal dimension. *Journal of Applied Crystallography*, *29*(2), 134–146. https://doi.org/10.1107/S0021889895011605

Benson, M. D., Buxbaum, J. N., Eisenberg, D. S., Merlini, G., Saraiva, M. J. M., Sekijima, Y., Westermark, P. (2018). Amyloid nomenclature 2018: recommendations by the International Society of Amyloidosis (ISA) nomenclature committee. *Amyloid*, *25*(4), 215–219. https://doi.org/10.1080/13506129.2018.1549825

Brosey, C. A., & Tainer, J. A. (2019). Evolving SAXS versatility: solution X-ray scattering for macromolecular architecture, functional landscapes, and integrative structural biology. *Current Opinion in Structural Biology*, *58*, 197–213. https://doi.org/10.1016/j.sbi.2019.04.004

Burchard, W. (2014). Light scattering techniques. In Ross-Murphy, S. B. (Ed.). *Physical techniques for the Study of Food Biopolymers*, 1, 151–214. Springer-Science+Business Media, B.V.

Chen, X., Fu, S., Hou, J., Guo, J., Wang, J., & Yang, X. (2016). Zein based oil-in-glycerol emulgels enriched with b -carotene as margarine alternatives. *Food Chemistry*, *211*, 836–844. https://doi.org/10.1016/j.foodchem.2016.05.133

De Almeida, C. B., Corradini, E., Forato, L. A., Fujihara, R., & Filho, J. F. L. (2018). Microstructure and thermal and functional properties of biodegradable films produced using zein. *Polimeros*, *28*(1), 30–37. https://doi.org/10.1590/0104-1428.11516

Dill, D. B. (1926). Prolamins in 1 & fixed Solvents . II. *Journal of Biological Chemistry,* https://doi.org/0378-1119(94)90466-9

De Vries, A., Nikiforidis, C. V., D., & Scholten, E. (2014). Natural amphiphilic proteins as tri-block Janus particles : Self-sorting into thermo-responsive gels. *Europhysics Letters*, 107, 5, 100–109. https://doi.org/10.1209/0295-5075/107/58003

Guzhova, I. V., Lazarev, V. F., Kaznacheeva, A. V., Ippolitova, M. V., Muronetz, V. I., Kinev, A. V., & Margulis, B. A. (2011). Novel mechanism of Hsp70 chaperone-mediated prevention of polyglutamine aggregates in a cellular model of huntington disease. *Human Molecular Genetics*, *20*(20), 3953–3963. https://doi.org/10.1093/hmg/ddr314

Hammouda, B. (2010). *Probing Nanoscale Structures – The Sans Toolbox*. https://www.ncnr.nist.gov/staff/hammouda/the_SANS_toolbox.pdf

Iwahashi, M., Yamaguchi, Y., Kato, T., Horiuchi, T., Sakurai, I., & Suzuki, M. (1991). Temperature dependence of molecular conformation and liquid structure of cis-9-octadecenoic acid. *Journal of Physical Chemistry*, *95*(1), 445–451. https://doi.org/10.1021/j100154a078

Kim, S., & Xu, J. (2008). Aggregate formation of zein and its structural inversion in aqueous ethanol. *Journal of Cereal Science*, *47*(1), 1–5. https://doi.org/10.1016/j.jcs.2007.08.004

Lai, H. M., Geil, P. H., & Padua, G. W. (1999). X-ray diffraction characterization of the structure of zein-oleic acid films. *Journal of Applied Polymer Science*, *71*(8), 1267–1281. https://doi.org/10.1002/(SICI)1097-4628(19990222)71:8<1267::AID-APP7>3.0.CO;2-O

Lee, B. Il, Suh, Y. S., Chung, Y. J., Yu, K., & Park, C. B. (2017). Shedding light on Alzheimer's β-amyloidosis: Photosensitized methylene blue inhibits self-assembly of β-amyloid peptides and disintegrates their aggregates. *Scientific Reports*, *7*(1), 1–10. https://doi.org/10.1038/s41598-017-07581-2

Li, Y., Li, J., Xia, Q., Zhang, B., Wang, Q., & Huang, Q. (2012). Understanding the dissolution of α-zein in aqueous ethanol and acetic acid solutions. *Journal of Physical Chemistry B*, *116*(39), 12057–12064. https://doi.org/10.1021/jp305709y

Matsushima, N., Danno, G. I., Takezawa, H., & Izumi, Y. (1997). Three-dimensional structure of maize α-zein proteins studied by small-angle X-ray scattering. *Biochimica et Biophysica Acta - Protein Structure and Molecular Enzymology*. https://doi.org/10.1016/S0167-4838(96)00212-9

Milston, R., Madigan, M. C., & Sebag, J. (2016). Vitreous floaters: Etiology, diagnostics, and management. *Survey of Ophthalmology*, *61*(2), 211–227. https://doi.org/10.1016/j.survophthal.2015.11.008

Nephomnyshy, I., Rosen-Kligvasser, J., & Davidovich-Pinhas, M. (2020). The development of a direct approach to formulate high oil content zein-based emulsion gels using moderate temperatures. *Food Hydrocolloids*, *101*, 105528. https://doi.org/10.1016/j.foodhyd.2019.105528

Nonthanum, P., Lee, Y., & Padua, G. W. (2013). Effect of pH and ethanol content of solvent on rheology of zein solutions. *Journal of Cereal Science*, *58*(1), 76–81. https://doi.org/10.1016/j.jcs.2013.04.001

Ochbaum, G., & Bitton, R. (2018). Using small-angle X-ray scattering (SAXS) to study the structure of self-assembling biomaterials. In Azevedo, H. S., & De Silva, R. M. P. (Eds.). *Self-Assembling Biomaterials: Molecular Design, Characterization and Application in Biology and Medicine*, 291–304. Elsevier Ltd. https://doi.org/10.1016/B978-0-08-102015-9.00015-0

Renner, M., & Melki, R. (2014). Protein aggregation and prionopathies. *Pathologie Biologie*, *62*(3), 162–168. https://doi.org/10.1016/j.patbio.2014.01.003

Schulz-Schaeffer, W. J. (2010). The synaptic pathology of α-synuclein aggregation in dementia with Lewy bodies, Parkinson's disease and Parkinson's disease dementia. *Acta Neuropathologica*, *120*(2), 131–143. https://doi.org/10.1007/s00401-010-0711-0

Uzun, S., Ilavsky, J., & Padua, G. W. (2017). Characterization of zein assemblies by ultra-small-angle X-ray scattering. *Soft Matter*, *13*(16), 3053–3060. https://doi.org/10.1039/c6sm02717b

Wang, Q., Yu, X., Patal, K., Hu, R., Chuang, S., Zhang, G., & Zheng, J. (2013). Tanshinones inhibit amyloid aggregation by amyloid-β peptide, disaggregate amyloid fibrils, and protect cultured cells. *ACS Chemical Neuroscience*, *4*(6), 1004–1015. https://doi.org/10.1021/cn400051e

Wang, Yi, & Padua, G. W. (2010). Formation of zein microphases in ethanol-water. *Langmuir*, *26*(15), 12897–12901. https://doi.org/10.1021/la101688v

Wang, Yi, & Padua, G. W. (2012). Nanoscale characterization of zein self-assembly. *Langmuir*, *28*(5), 2429–2435. https://doi.org/10.1021/la204204j

CHAPTER 6   APPLICATIONS OF ZEIN-BASED OLEOGEL

6.1   Abstract

To create soft materials with novel functionalities, the formation of gels from hydrophobic media has gained attentions from food science, pharmaceutics, and tissue engineering areas. Often, this is accomplished through the assembly of oleogelators into multiple complex phases with intermolecular interactions. In this research, zein was pre-dissolved in 70% ethanol and used as an edible oleogelator to immobilize oleic acid to form self-assembled oleogels at room temperature. Rheological measurements and morphology observations indicated the ultra-sonication treatment would strength the gel rigidity and promote the gelation process, which may result from the breaking down of oil droplet size and facilitating the distribution of zein molecules for more interactions taking place. Both optical microscopy and confocal laser scanning images were helpful to characterize these oleogels as emulsion gels. And according to conductivity results, the oleogels were oil-in-water systems with conductivity linearly correlated to the ethanol weight fraction. Ultra-sonication did not affect the conductivity. It was assumed that zein molecules were attached to the surface of oil droplets or freely distributed throughout the continuous phase. USAXS determinations also revealed that the radius of gyration of the primary unit (R_{g1}) did not change much in comparison to the second level fractal structure size (R_{g2}) after ultra-sonication. Which was suggested that zein building blocks were stable under high shear force. The downsizing of the second level structures could be interpreted as the increasing amount of fractals developed in between the oil droplets. The higher density of the fractals in the systems led to faster gelation rate and stronger gel strength. Further, lutein was encapsulated by the zein-based oleogel, demonstrating the potential application as delivery carriers for hydrophobic bioactive compounds.

6.2 Introduction

Zein, a natural protein derived from corn with unique amphiphilic characteristic, film, fiber and foam forming abilities, also its biocompatibility and biodegradability make zein a promising biopolymer being utilized in food, eco-friendly packaging or coating, pharmaceutics, and tissue engineering realms (De Almeida et al., 2018; Kasaai, 2018b; Marín et al., 2018; Patel & Velikov, 2014; Raza, Hayat, Bilal, Iqbal, & Wang, 2020). Ever since Food and Drug Administration recognized zein as Generally Recognized as Safe (GRAS), the applications have been widely broadened in biomedical field such as oral drug delivery system (Weissmueller, Lu, Hurley, & Prud'Homme, 2016). With the self-assembly characteristics of zein, molecules can be easily transformed into microsphere, films, nanoparticles, nanofibers and micelles for developing safe, cost-effective encapsulation systems (Donsì, Voudouris, Veen, & Velikov, 2017; Wang et al., 2013). The positive charge and the wide range of isoelectric point possessed by zein provide advantages for delivery negatively charged drugs and nutrients into the body and able to be degraded also absorbed in the digestive system.

In the past decade, zein-based oral drug delivery systems are fabricated in the forms of tablets, capsules, micro and nano particles and electrospun fibers (Cheng, Ferruzzi, & Jones, 2019; Moradkhannejhad, Abdouss, Nikfarjam, Mazinani, & Heydari, 2018; Yuan et al., 2019). Due to the hydrophobicity of zein, delivery carriers all have moisture resistance and can withstand gastric environment by forming a layer of self-assembled polymer coating while in contact with fluid. Using zein as the shell material to encapsulate fatty acid, essential oils, fat soluble vitamins, food pigments and nutrient supplements has also been intensively studied and achieved by evaporation methods or spray drying (Khalil, Deraz, Elrahman, & El-Fawal, 2015; Masamba, Li, Hategekimana, Liu, & Ma, 2016; Santos et al., 2017; Y. Zhang et al., 2015)(Y. Zhang et al., 2016) In order to improve the bioavailability of the encapsulated hydrophobic compounds, other delivery systems composed of zein or zein composite have been discussed, including liposomes, emulsions and colloidal dispersions (Y. Chen et al., 2013; De Boer, Kok, Imhof, & Velikov, 2018; Maria B. Pérez-Gago & Krochta, 2001). In most of the emulsion cases, zein served as a stabilizer or Pickering agent to maintain the stability of the system (De Folter et al., 2012; Gao et al., 2014; Soltani & Madadlou, 2015). Not until recently, the ability for zein to act as a protein gelator in liquid oil has been discovered (Scholten, 2014).

Taking advantage of both self-assembly and amphiphilic natures of zein, De Vries et al. (2014) using heating homogenization method to prepare thermo-responsive zein based oil-in-glycerol emulsion gels. A 3D gel network structure which entrapped oil droplets inside glycerol continuous phase formed after cooling was composed of the ribbon-like long strands that originated from the rearrangement of zein building blocks. Followed by Chen et al. (2016), which they adapted this system and successfully incorporated β-carotenoid into the oleogel and found out the addition of active compound could retard oil oxidation. Elke Scholten and coworkers continued to investigate this heat induced gelation system by modulating the viscoelastic properties of the oleogel with different type of oil and tuning solvent polarity by addition of water. However, the biggest drawback for this encapsulation system is considerable heat involved. Which Nephomnyshy et al. (2020) also aware that, of the high processing temperature it would cause the deterioration of the oil medium, degradation of the bioactive additives and high costs for large-scale production. They tried to use ethanol dissolved zein before mixing with glycerol and the oil, however, 90 ℃ was still required to induce protein denaturation and sol-get transition to form gel upon cooling.

To avoid the heat, cold-set gelation such as acid-induced or by addition of salts has been reported for natural originated proteins (Kharlamova, Chassenieux, & Nicolai, 2018; Ying Li & Corredig, 2020)(Alavi, Momen, Emam-Djomeh, Salami, & Moosavi-Movahedi, 2018; Kharlamova, Nicolai, & Chassenieux, 2018). Nevertheless, cold-set gelation relies on the addition of gel inducing agents, salts, acids or enzymes, which may be rejected by consumer preferences in certain foods. Alternatively, the self-assembly gelation of zein in aqueous alcoholic solution environment could be employed (Uzun et al., 2017; Wang & Padua, 2010b, 2010a). Zein-ethanol solutions (55-90% ethanol concentration), formed into gels after storage was observed by Zhong and Ikeda. (2012). Kim and Xu (2008) reported that the hydrophilic-hydrophobic character of ethanol-water solvents affected zein aggregation thus, it may affect rheological behavior of zein solutions. Recently, Uzun et al. (2017) depicted the microstructures of zein self-assembly process in ethanol solution by ultra-small x-ray scattering. It was assumed that the molecule zein used the hydrophobic driving force underwent time-dependent rearrangement into nanoribbons and then developed into 2D lamellae. Further on, the layer-by-layer of lamellae would lead to form even more organized 3D spheres or elongated structures which dedicated to the solid-like viscoelastic behavior. In this research, we utilized the self-assembly gelation behavior of zein in ethanol solution, and incorporating oleic acid to form an emulsion based oleogel system. It was

hypothesized that with the aid of oleic acid as the hydrophobic phase, which has long been reported as a plasticizer that facilitate the ordered packing of zein molecules in zein film making (Pena-Serna & Lopes-Filho, 2013; Wang & Padua, 2006), a stable oleogel delivery vehicle could be obtained with desirable texture and encapsulation ability for heat labile nutrients or target drugs.

Lutein, a xanthophyll that is reported as a carotenoid with anti-inflammatory properties. It is synthesized by plants where can be largely found in leafy green vegetables and corn. Not only prevalent in plant for photosynthesis and photo-protection, lutein is also crucial for human which related to protection of the retina from damaging blue light, oxidative stress and aging caused macular degenerations (Buscemi et al., 2018; Roberts & Dennison, 2015). Associated with reduced cataract formation in the eye and decreased risk of coronary heart disease and stroke, lutein has also been reported affecting the brain function, which higher lutein status correlated to better cognitive performance (Johnson et al., 2013; Nolan et al., 2014). Although 3.8 mg lutein per day for a daily intake is recommended by USDA, the average daily intake of lutein in the United States is only 1.7 mg (Alves-Rodrigues & Shao, 2004). Not only because the bioaccessibility of lutein is moderately low (14-55%) in vegetables reported by Serrano et al. (2005), but also similar to other carotenoids, it is prone to degrade by heat, oxygen and light before digest (Gorusupudi & Baskaran, 2013; Serrano et al., 2005; Zaripheh & Erdman, 2002). The aim of this work was to study the potential of zein as a natural oleogelator in constructing the zein-based oleogel further serve as an encapsulating matrix with tunable texture for enhancing the bioavailability and also protect the degradation of hydrophobic compound, lutein.

6.3 Materials and Methods

6.3.1 Materials

Zein was purchased from Showa Sanyo Co. Ltd. (Tokyo, Japan). Oleic acid was from Fisher Scientific (Hanover Park, IL). Ethanol (200 proof) was supplied by Decon Laboratories Inc. (King of Prussia, PA). Mineral oil was purchased in the local market.

6.3.2 Rheology experiments

Sample preparation

Sonicated samples were firstly prepared following the preparation steps mentioned in

previous chapters, then sonicated in ultrasonic cleaning tank (CREST ULTRASONICS, model no. 4HT-1014-6, Trenton, NJ) with running cold water controlled at 27 $\pm$ 2 ℃ for 15 min (40 kHz for maximum frequency). A 30 g sonicated sample was allowed to equilibrium in the measuring cup for 12h before measuring. For formula 30-15-55, it was measured after storing for 1, 3, 4, 5 and 7 days, and the other three samples (25-15-60, 40-15-45 and 45-15-40) were monitored at the 4th days only.

Rheological behavior of zein-based emulsions was studied by ARES-G2 rheometer (TA Instruments, New Castle, DE) using DIN concentric cylinder (bob diameter of 27.7 mm and cup diameter of 30 mm). The 30 g of sample was placed in the measuring cup and 100% mineral oil (purchased from local market) was used to cover the top of the sample to prevent evaporation during the experiment.

The linear viscoelastic region was assessed by amplitude sweep experiments at a constant frequency of 1 Hz (strain = 0.01 to 100%) to obtain the suitable strain which 0.1% of strain was applied to the analysis. Oscillatory frequency sweep tests were performed over the frequency range of 1 to 100 Hz at 20 ℃ to measure the storage modulus (G') and loss modulus (G") of zein-based oleogels at 7, 14 and 21 days of standing at room temperature.

6.3.3 Optical microscopy

The microstructure of the distribution of zein protein was analyzed by optical microscopy on a Leitz Ortholux trinocular microscope (Leitz, Germany). All samples were investigated with Plan 10X and Plan 40X objectives to have a 400X magnification.

6.3.4 USAXS

USAXS data were collected to observe the microstructural organization of both and with or without sonicated sample gels. The USAXS combined with pinhole SAXS were conducted at beamline 9-ID-C at the Advanced Photon Source in Argonne National Laboratory (Lemont, IL). The instrument is equipped with a Bonse-Hart camera double-crystal configuration and operates at one-dimensional collimation, which enables the collection of slit-smeared data. The specimen was measured at scattering vectors range $q = 1 \times 10^{-4}$ Å^{-1} to 1.2 Å^{-1} with about 200 data points, where q is defined as $q = 4\pi \sin(\theta/2)/\lambda$ and θ, λ are the scattering angle and x-ray beam wavelength, respectively. Emulsion samples were loaded in NMR capillaries with 4 mm internal diameter

(Wilmad-LabGlassTM Thin Walled High Throughput NMR Tubes, Fisher Scientific, MA) and capped with corresponding rubber caps. The monochromatic x-ray energy used was 18 keV. The slit-smeared data were fitted with the unified model by the Modeling II macro of the Irena 2 package in IGOR PRO v8.03 (Wavemetrics, Lake Oswego, OR). The radius of gyration of aggregates (R_g) and shape factor (P), calculated from the power law slope were evaluated. The experimental design consisted of 30 samples with 2 replicates, totaling 60 experimental units. Average values were reported in Table 5.2 in Chapter 5 and 8 out of the 30 samples were selected and summarized in Table 6.3.

6.3.5 Confocal laser scanning microscopy (CLSM)

Confocal laser scanning fluorescence microscope images will be taken on a head mounted Leica TCS SP5 confocal laser scanning microscope (Leica Microsystems Inc., Heidelberg, Germany) equipped with an oil immersion objective lens. Prior to observation, the emulsion will be stained with mixed of Nile blue (0.1%) and Nile red (0.1%) and stationed on concave confocal microscope slides. Examined under an argon/krypton laser with excitation wavelength of 488 nm and a Helium Neon laser (He-Ne) with excitation at 633 nm for the mixed dyes respectively.

6.3.6 Conductivity

Conductivity of samples were measured by Orion^{TM} 2-Electrode conductivity cells with measurement ranges between 0.01 to 300 µS/cm on Thermo Scientific VSTAR10 Versa Star pH meter to obtain accurate results. Before starting of the measurement, cells were calibrated with 100 µS/cm standardizing solution and would wash with 70% ethanol between each test. 3 replicates were examined and averaged for each sample. The deionized water used for sample preparation of the 70% ethanol was recorded as 0.58 ± 0.04 µS/cm at 22.3 ± 1.2 ºC.

6.3.7 Atomic force microscopy (AFM)

Samples of lutein filled oleogels were prepared by dissolving lutein (0.5% or 1.0% w/w) in oleic acid before mixing with the corresponding amount of zein in 70% ethanol to reach the composition formula 30-15-55. The mixture was sonicated with the condition mentioned in session above, and 3 g of sample was poured into 60 mm × 15 mm polystyrene petri dish capped and sealed with parafilm. Sample was let stand at room temperature for 24h before cutting open.

AFM images were collected by Asylum Jupiter XR Atomic Force Microscope (Asylum

Research, Oxford Instruments, Santa Barbara, CA) with an ASYELEC.02-R2 cantilever (Oxford Instruments, Santa Barbara, CA) operating on tapping mode (AC mode) with 3.91 Hz scan rate in a scan size of 1.50 μm under ambient conditions. Images were analyzed using the software Ergo provided by Aylum Research (Oxford Instruments, Santa Barbara, CA).

6.4 Results and Discussion

6.4.1 Effect of sonication and solvent compositions on viscoelastic behavior

For an ideal oleogel, it should contain as much liquid oil and less of the oleogelators as it could be, so four compositions were selected out from the ternary phase diagram mentioned in chapter 3, where 15% zein were used and would form self-standing gel after stored for 14 days. Sample 25-15-60 had the highest oil content followed by 30-15-55, 40-15-45 and 45-15-40 were analyzed by ARES-G2 rheometer. The viscoelastic profiles were plotted on Figure 6.1 with storage modulus (G'), loss modulus (G") and tan delta values summarized in Table 6.1.

After applying sonication to the preparation steps, except 25-16-60, the other three emulsions self-assembled into gel-like structures at the 4th day (G' > G"), which dramatically elevated the gelation rate (Figure 6.1). Recalled from chapter 3, sample 30-15-55 required at least 21 days to be considered as a gel by tube inversion method, and 14 days for sample 40-15-45 also 45-15-40. The mechanism for the formation of zein-based oleogel was assumed that the dissolved zein tri-blocks would self-assemble on the interface of the oil nuclei, and gradually stacked into an ordered structure or spanning into an extended network (Scholten et al, 2014). The protein oleogel network structural characteristics were affected by the interactions between solvent, zein and the incorporated hydrophobic nuclei (de Vries, Jansen, van der Linden, & Scholten, 2018)(De Vries, Gomez, Van der Linden, & Scholten, 2017). By manipulating the balance between these interactions was believed to control the gelation rate and rheological properties in our oleogel system. The high shear force provided by sonication not only decreased the size of the oil droplets but also improved the distribution of the zein molecules (Sadeghpour, Pirolt, & Glatter, 2013)(De Vries, Lopez Gomez, Jansen, Van der Linden, & Scholten, 2017). While higher numbers of small oil droplets with larger surfaces areas acting as anchor points for zein to attach on, more of the interactions would take place between molecule-molecule (zein), molecule-nuclie (oleic acid droplets), and molecule-hydrophilic solvent (70% ethanol). Resulted from more of these

interactions, the speed of 3D networks formation was expedited. Storage modulus represented the solid like behavior the sample possessed, which after the sonication, G' > G" indicated the gel structures formed and had resistant to perturbation.

Considered the effect of solvent compositions on viscoelastic behavior, while oil content was below 60%, the gel strength and gel network structures stability determined by G' and yield point frequency values increased with increasing amount of oleic acid and decreasing amount of 70% ethanol. It was proposed that with higher volume fraction of oil droplets could form a denser emulsion gel (Pena-Serna & Lopes-Filho, 2013) (Masalova et al., 2006). Accompanied with the aid of high shear to avoid coalesce between oil droplets before zein molecules self-assembled into short range network structures also enhanced the gel strength. According to Y. Zou et al. (2018), storage modulus was contributed by the amount of protein-coated oil droplets which served as "active filler" in the emulsion gel system, which could strengthen the gel network (Figure 6.2). However, sample 25-15-60 showed lowest G' value among four formula, suspected was due to limited amount of 70% ethanol provided little mobility for zein to self-assembly into network structures, instead aggregated and may allowed the oil droplets to coalesce which become harder to entrap.

Tan δ was used to evaluate the elasticity of the emulsion gels, while tan δ > 1, viscous behavior is dominant, on the other hand, tan δ ≤ 1 elastic behavior is in place. Between 40-55% oleic acid content, tan δ decreased with increasing of oleic acid and decreasing of 70% ethanol. It was possible that more of the ethanol in the system would increase the polarity of the solvent, causing zein building block increased the hydrophobic interaction with oleic acid and decreased the zein-hydrophilic solvent interaction. Therefore, the amount of protein in the continuous phase were less available to form network which in return the structures were easier to deform (Zou et al., 2019). This phenomenon could be observed from the frequency value at (G' = G"), where higher oleic acid and lower ethanol contents had the stronger gel structure to resist higher frequency during the measurement before it turned into viscous liquid (Table 6.1).
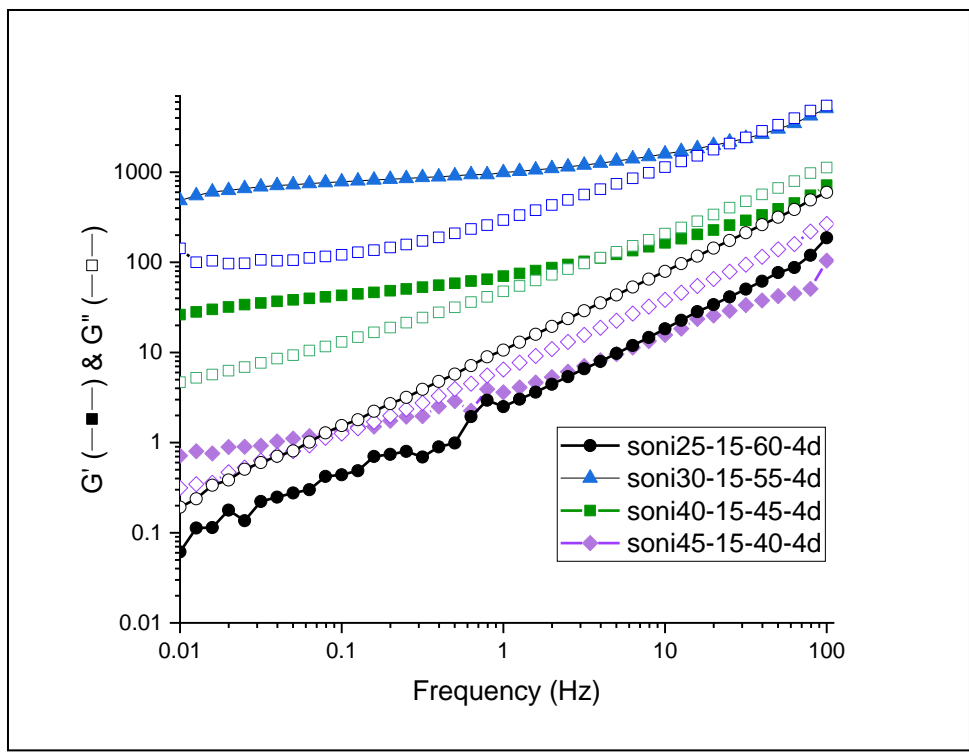
Figure 6.1 Frequency sweep results of 15% zein-based oleogel stored for 4 days after sonicated. Sample coding as 70% ethanol (wt%)-zein (wt%)-oleic acid (wt%)-4(days).

Table 6.1 Frequency sweep results of sonicated zein-based oleogels stored for 4 days.

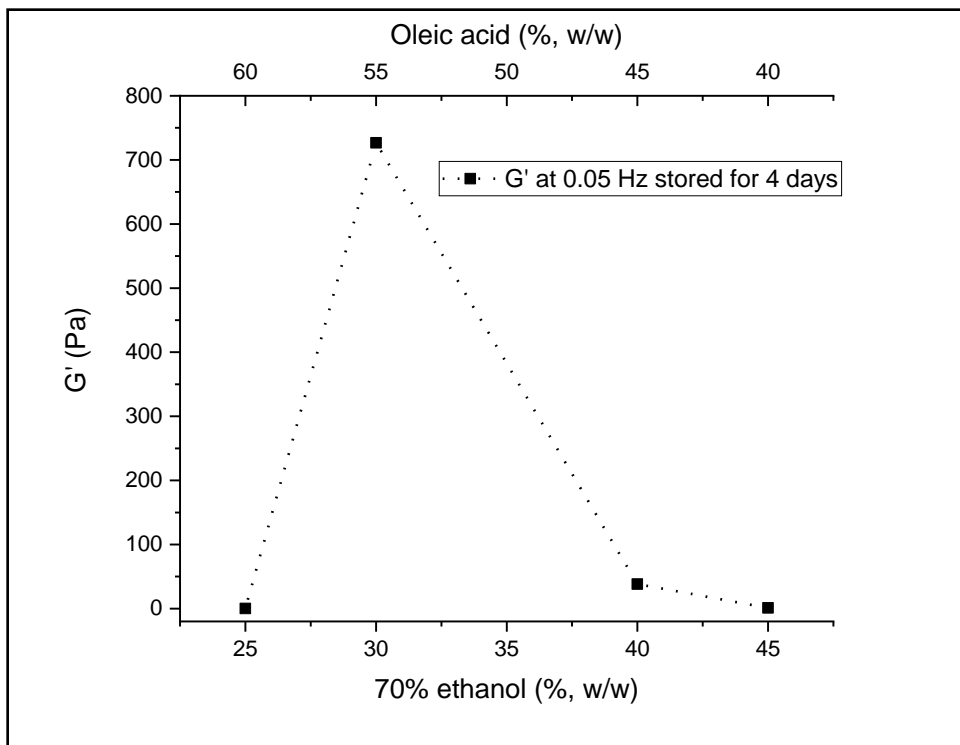| Sample code	Frequency sweep				
	At 0.05 Hz			At cross point (G′ = G″)	
	G′ (Pa)	G″ (Pa)	Tan δ	Frequency (Hz)	G′ (Pa)
soni25-15-60-4d	0.28	0.81	2.89	---	---
soni30-15-55-4d	726.6	105.5	0.15	31.62	2376.2
soni40-15-45-4d	38.30	9.34	0.24	3.98	111.85
soni45-15-40-4d	1.11	0.81	0.73	0.16	1.50

Figure 6.2 Storage modulus (G') values at fixed frequency of 0.05 Hz of sonicated 15% zein-based oleogels stored for 4 days.
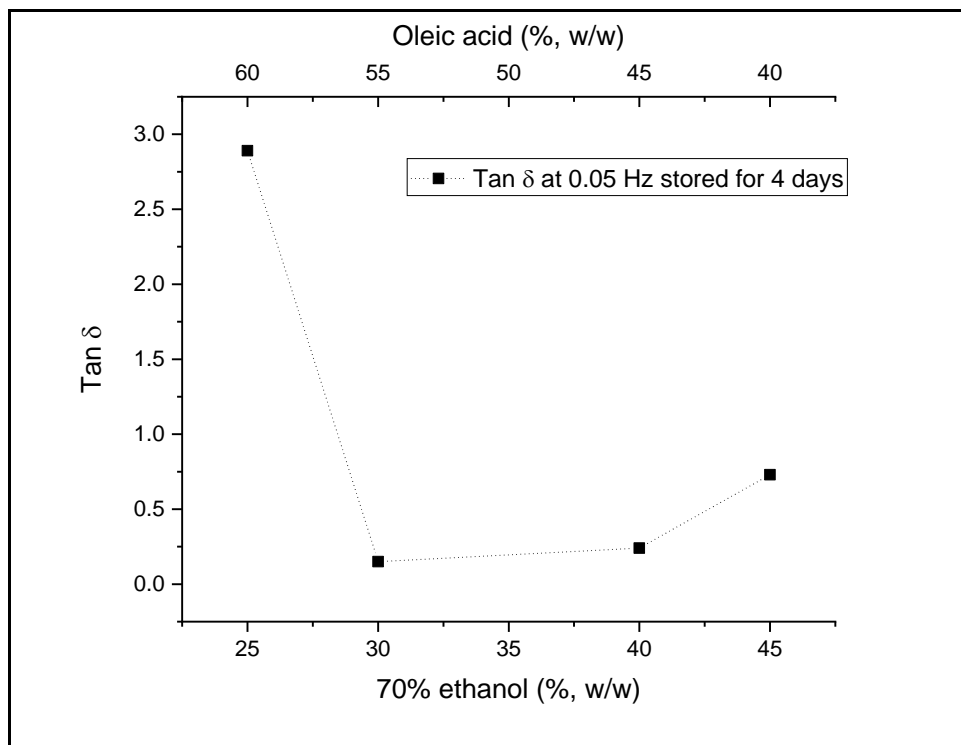

Figure 6.3 Tanδ results of sonicated 15% zein-based oleogel stored for 4 days.

6.4.2 Effect of storage time on viscoelastic behavior

Based on the Chapter 6.3.1 results, we knew sample 30-15-55 contained relatively high amount of oil and the original 21 days slow gelation process could be facilitated by applying sonication. So it was chosen to be a promising candidate for application such as nutrient-dense encapsulation matrix with controllable viscoelastic properties. First, we prepared the sonicated 30-15-55 in 2 mL Eppendorf and cut one open each day to monitor the visual appearance. Although we observed up-side-down oleogel inside Eppendorf after 1 day storage, when cutting open, it actually flowed like viscous liquid presented in figure 6.4. Not until the 4th day, the soni30-15-55 could maintain the cylinder shape and would have sharper cutting edge. And with extended storage time, cylinder shape and diameter was almost identical to the cutoff part of the Eppendorf (Figure 6.4 Day 6). The leaching of the oil phase was observed in every sample exposed to air for 24 h (bottom role in Figure 6.4). This phenomenon could be attributed to ethanol evaporation at the outer surface of the oleogel, which created an ethanol gradient from the surface to the center of the sample. The lower ethanol concentration at the surface would induce zein to rearrange into β-sheet conformation and expel the oleic acid out (Pena-Serna & Lopes-Filho, 2013; Yi Wang & Padua, 2012).

To qualify and quantify the zein-based oleogel gelation process, sonicated 30-15-55 was monitored by rehometry. Overall, the frequency sweep results showed both G' and G" were frequency dependent, which was commonly seen in emulsion systems and categorized as weak gel accompanied by a tan δ value > 0.1 (Ikeda & Nishinari, 2001). The storage modulus at 0.05 Hz and at the G' = G" cross point all increased with the time (Table 6.2). Clearly, this system gelled with time, self-assembly of zein was the primary driving force for the development of the network.

In Figure 6.6, the G' was plotted as a function of time and observably, between 3rd and 4th day of storage, there was a sudden spike of the value. And gel structure stability and resistance to perturbation which demonstrated by frequency values at cross points behaved the same (Figure 6.7). It was hypothesized that before 3 days, zein building blocks mostly were attached on the surface of the oil and only had short range fractal structures, it still needed time to rearrange the remaining zein in the continuous phase to form wide scaled network. At the 4th, possibly the ribbon-like structures grew large enough and met the other protein structures which extended from the nuclei causing the G' (gel rigidity) to jump a log. After that, the network kept grow larger and

more rigid, however, the differences of G' was not as pronounced as before, which might due to less proteins were available in the continuous phase and the mobility dramatically decreased.
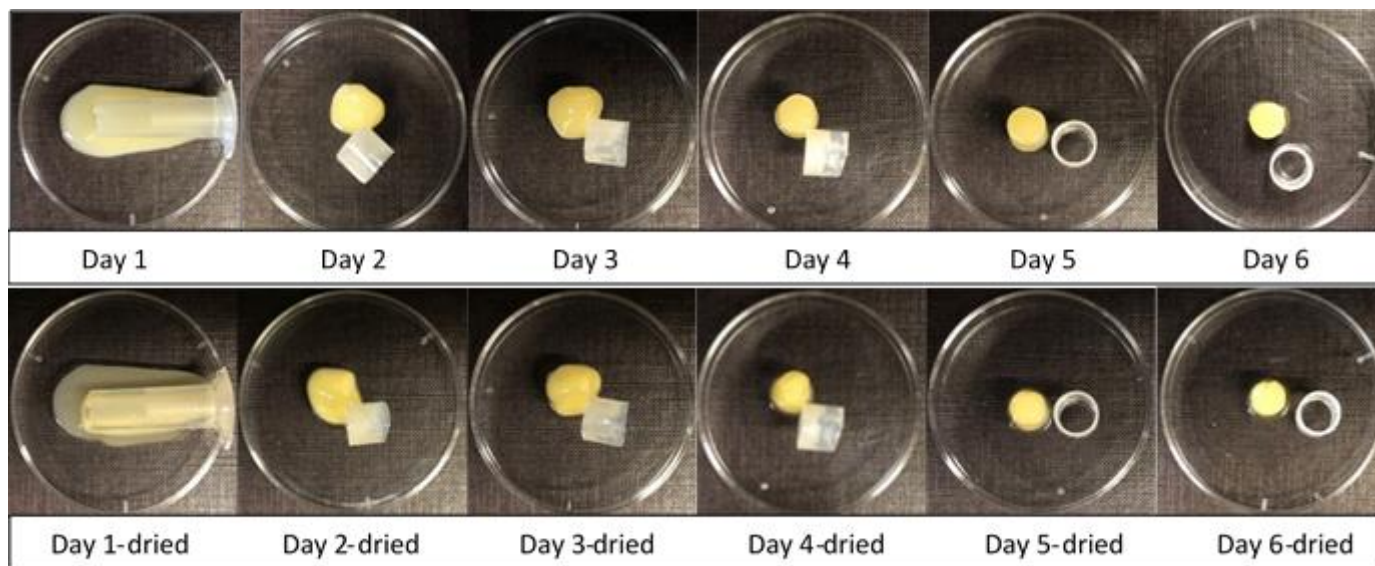
Figure 6.4 Digital images of 70% ethanol/zein/oleic acid oleogel under 1 h sonication and held for 7 days. Upper row images were taken right after cutting, bottom row were same samples as mentioned previously but dried at room temperature for another 24 h.
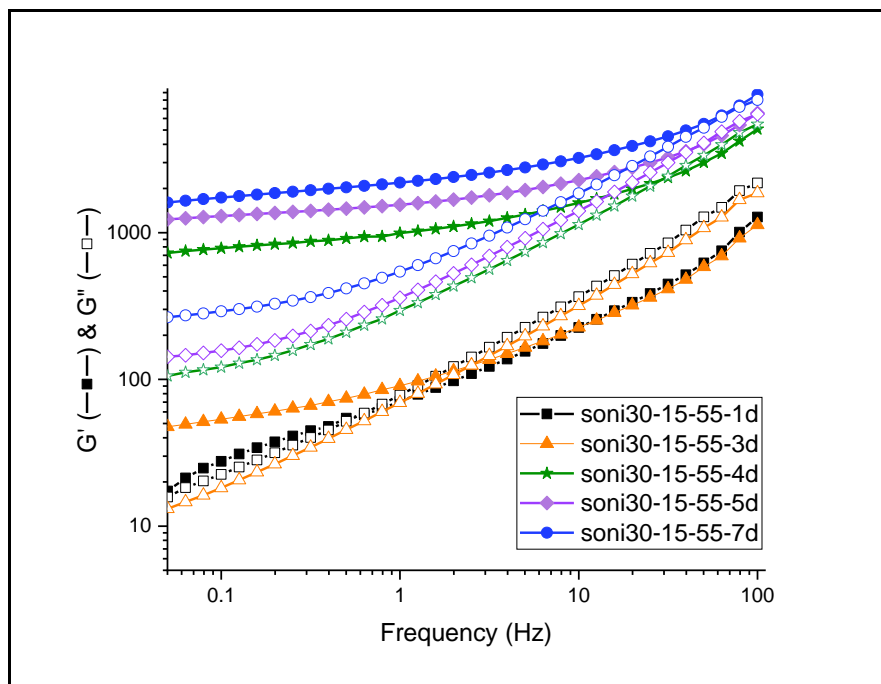
Figure 6.5 Frequency sweep results of 15% zein-based oleogel stored for 1, 3, 4, 5, and 7 days after sonicated. Sample coding as 70% ethanol (wt%)-zein (wt%)-oleic acid (wt%)-(days).

Table 6.2 Frequency sweep results of sonicated zein-based oleogels 30-15-55 measured at different storage time.

| Sample code | Frequency sweep | | | | |
| | At 0.05 1Hz | | | At cross point (G'=G") | |
	G' (Pa)	G" (Pa)	Tan δ	Frequency (Hz)	G' (Pa)
soni30-15-55-1d	17.35	15.78	0.91	0.63	57.34
soni30-15-55-3d	47.50	13.13	0.28	2.51	124.6
soni30-15-55-4d	726.6	105.5	0.15	31.62	2376.2
soni30-15-55-5d	1231.7	142.5	0.12	50.12	4008.2
soni30-15-55-7d	1605.4	264.9	0.17	> 100	> 8745.7

Figure 6.6 Storage modulus (G') values at fixed frequency of 0.05 Hz as a function of time for sonicated 30-15-55 zein-based oleogels.

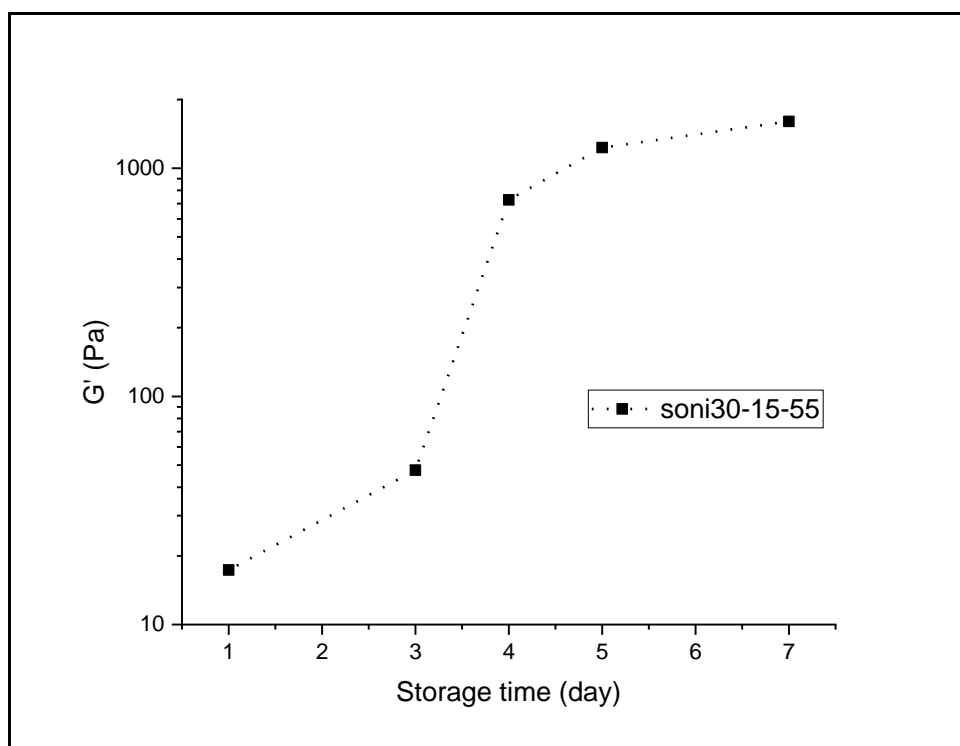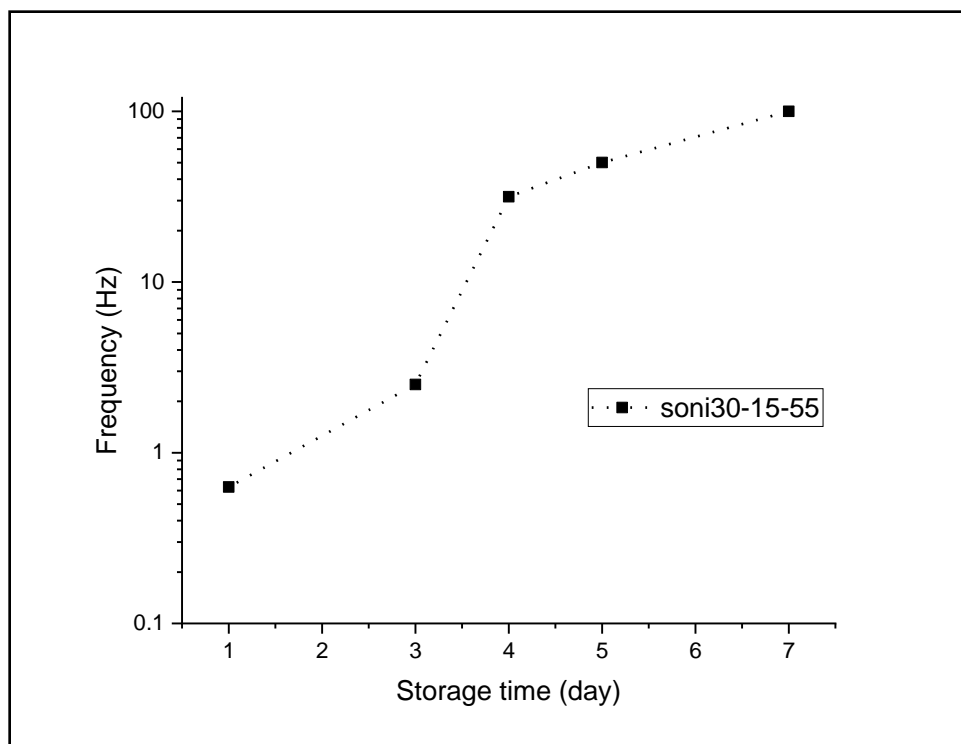Figure 6.7 Crossover frequency values at G'≤ G" as a function of time for sonicated 30-15-55 zein-based oleogels.

6.4.3 Effects of solvent composition and sonication on microstructures

In Figure 6.8, samples without sonication were observed by optical microscope instantly (left side) and after stored for 7 days (right side). All of them showed poly-dispersed emulsion characteristics, with spherical shaped droplets evenly distributed (Lv, Wang, Cai, Li, & Zhang, 2014)(J. Xu, Yin, Zhao, Li, & Hou, 2013). In a general view, the particles sizes varied between different solvent compositions with the order of 40-15-45 < 30-15-55 < 45-15-40 < 55-15-30 and 45-15-40 < 40-15-45 < 55-15-30 < 30-15-55 for 7 days storage ones. Started from 30-15-55 just prepared sample, it had second small sized droplets with few large ones embedded inside. And after 7 days, obviously, droplet size and size distribution both increased pronouncedly became the biggest among four samples. Which assumed to be the effect of high oil content that caused the coalescence of the oil droplets (Ochowiak & Rozanski, 2012). The coalescence phenomena was more significant on the 7th day might due to the self-assembly process of zein was not fast enough to form a network before it continued. For 40-15-45, the particle size for the just prepared one was the smallest, believed to be the suitable hydrophilic-lipophilic balance of the solvents that provided

131

enough surface tension to form stable emulsion. However, the relatively high volume fraction of the oleic acid still coalesced at 7th day causing the droplet size increased. Interestingly, the droplets for 45-15-40 did not change a lot for before and after storage, it was suspected the 45% ethanol increased the polarity of the solvent, which caused the interaction between zein-oleic acid decreased but zein-zein molecular interaction increased (Nephomnyshy et al., 2020)(Zou et al., 2019). As a result, the oleic acid droplet size was slightly larger, at the meantime, higher zein building blocks mobility was able to form ribbon-like structures also network in the continuous phase to immobilize the oil. Lastly, high ethanol but low oleic acid content sample 55-15-30 had the highest solvent polarity and protein mobility, showed as relative larger droplet size. And the loosely packed droplets in the 7th day photo should result from the minimum oil volume fraction.

According to CLSM result, the diameter of the oil droplets were ranging between 1 to 15 μm for sample 40-15-45-14d and some were closely packed forming flocs. The shapes were spherical and each droplet was apart from each other indicating the oil content hadn't reached the maximum solvent volume fraction. Unfortunately, in the image we could not distinguish zein protein from the hydrophilic continuous phase, it may due to the concentration of protein was too high and the formed structures were in the nanometer scale, not able to be see here.

In order to understand the emulsion type of each oleogel with different formulation, conductivity is an useful indicator to help determine whether the system is O/W or W/O (Bajpai, Sharma, & Mittal, 2009)(Komaiko & Mcclements, 2016)(Flores-Villaseñor, Peralta-Rodríguez, Ramirez-Contreras, Cortes-Mazatán, & Estrada-Ramírez, 2016). While the reading is < 1 μS/cm below value of pure water, then it can be considered as an O/W emulsion, or in contrary, conductivity is way above 1 μS/cm, determined as a W/O emulsion (Rutkevičius et al., 2018). Based on our results (Figure 6.10 and Table 6.3), all of the oleogel samples discussed in this research were O/W emulsion, even if the 70% ethanol to oleic acid weight ratio was 30 : 55 the conductivity measured as 7.17 ± 0.4 μS/cm which larger than deionized water 0.58 ± 0.04 μS/cm showing the continuous phase was conductive (Figura & A.Teixeira, 2007.). Interestingly, in Rutkevičius et al. (2018), the emulsions stablized by 5% zein (w/w) and soybean oil showed conductivity below 1 μS/cm while the water content (vol. %) was lower than 30% (defined and confirmed as oil continuous emulsion by microscopy image and drop-test method). However, in comparison to our result of sample 30-15-55, which contained the lowest water content 9% (w/w),

the conductivity measurement explained as a water continuous emulsion. This was discussed in Rutkevičius et al. (2018) and Kim & Xu, (2008) that the amphiphilic nature of zein molecule not only enhanced the stability of the emulsion, the hydrophilic surfaces would orient toward the continuous phase attribute to O/W emulsion. And with our 15% zein content, it was reasonable to have a more stable O/W emulsion system.

As reported by Ponton, Bose, & Delbos. (1991), percolation phenomenon was manifested when the water volume fraction reached a critical value at a constant temperature in an oil continuous microemulsion, and a rapid increase in the electrical conductivity was observed. Typically, in between the O/W and W/O microstructures, a bicontinuous structure formed spontaneously with the right amount of compositions (De Gennes & Taupin, 1982). The existence of bicontinuous structure would exhibit a surge of conductivity which attributed by the connected water paths in the system (J. Xu et al., 2013). In Table 6.3, the conductivity of sonicated samples had a nice linear correlation (R^2 = 0.99) with the increasing amount of 70% ethanol, no sharp increase of value was revealed. Indicating the microstructure of the system was O/W rather than W/O/W nor bicontinuous phase (Figure 6.10) (Lv et al., 2014). Time did not affect the conductivity as we expected, which from previous section 6.3.2, the gel formed at 4th day, however, there was no significant differences between 1st and 7th day (Table 6.3). Samples without sonication treatment were measured (data not shown), and the values of conductivity did not change as well. Based on these findings, we concluded the zein-based oleogel was an O/W emulsion system with zein molecules stabilized the hydrophobic dispersed phase. The addition of 70% ethanol (30% water) provided the volume fraction of hydrophilic continuous phase while not changing the microstructure of O/W, which in turn the conductivity increased linearly.

As discussed in Chapter 5, the microstructures of zein–based oleogel determined by USAXS were categorized into two levels, zein molecules building block size R_{g1} and secondary fractal structures size R_{g2}. Table 6.4 showed both R_{g1} and R_{g2} were mainly affected by the composition of the solvents, while sonication had more effects on the R_{g2}. The zein tri-block was sensitive to the ethanol content, pH and HLB of the solvents, which may form monomer or dimer and further developed into ribbon-like long strands, sheets or spheres (Kim & Xu, 2008; Li et al., 2012; Nonthanum, Lee, & Padua, 2013; Q. Wang, Yin, & Padua, 2008; Y. Wang & Padua, 2010). And the downsizing of secondary structures was believed to be the higher dispersing energy provided

by ultrasonication leads to finer dispersions and therefore greater interface area between the oil and water phases. The stabilizing particles could thus be adsorbed at the interface more easily, which normally leaded to smaller and more homogeneous droplets (Sadeghpour, Pirolt, & Glatter, 2013). More of the surface area meaning more interactions which might induce the increasing of gelation rate and gel rigidity mentioned in above section 6.3.1 and 6.3.2.
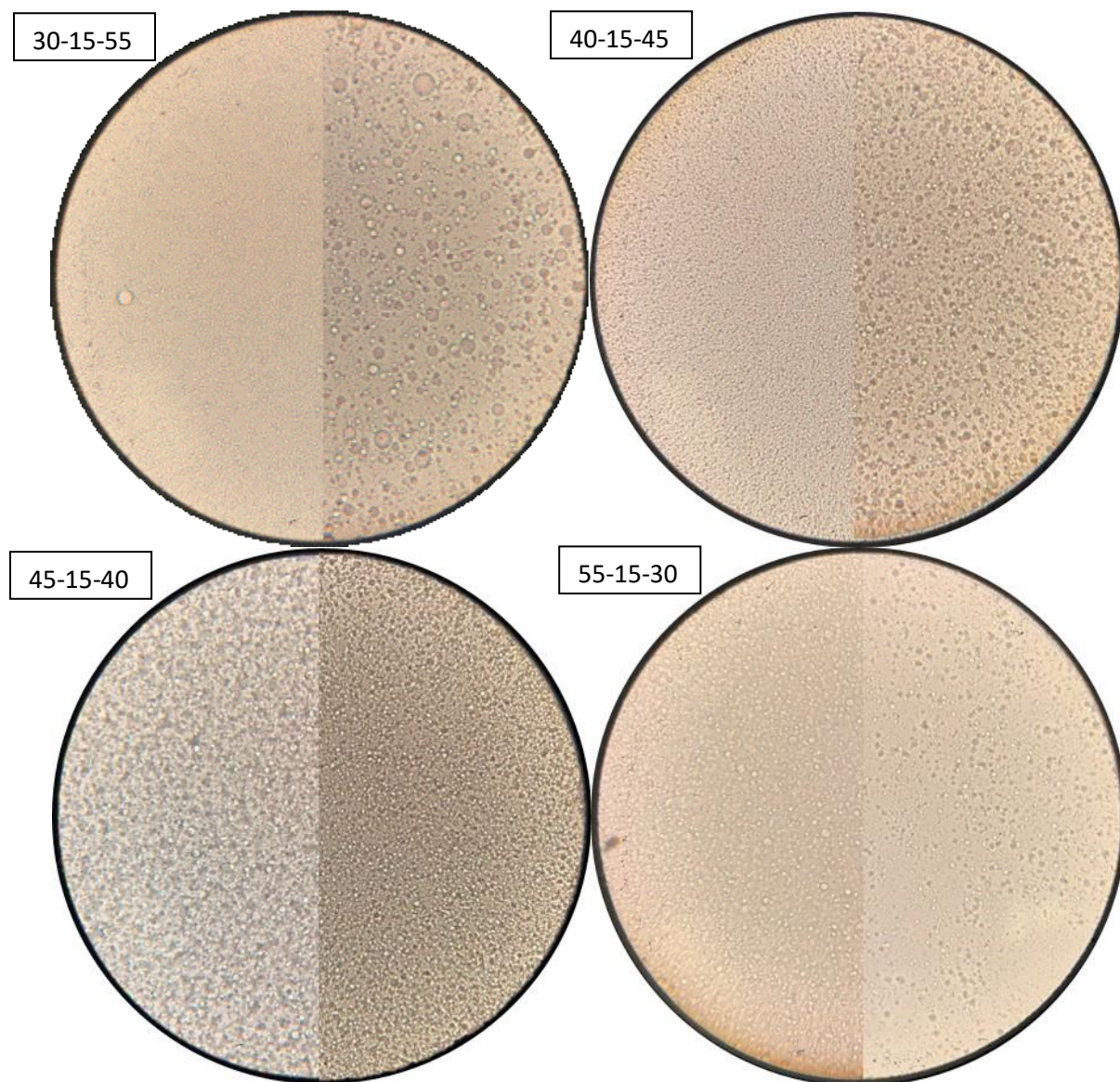
Figure 6.8 Optical microscopic images of four zein-based oleogel with sample code as 70% ethanol/ zein/oleic acid oleogel (%, w/w/w) photo took right after prepared (left half circle) and 7 days (right half circle) at room temperature.
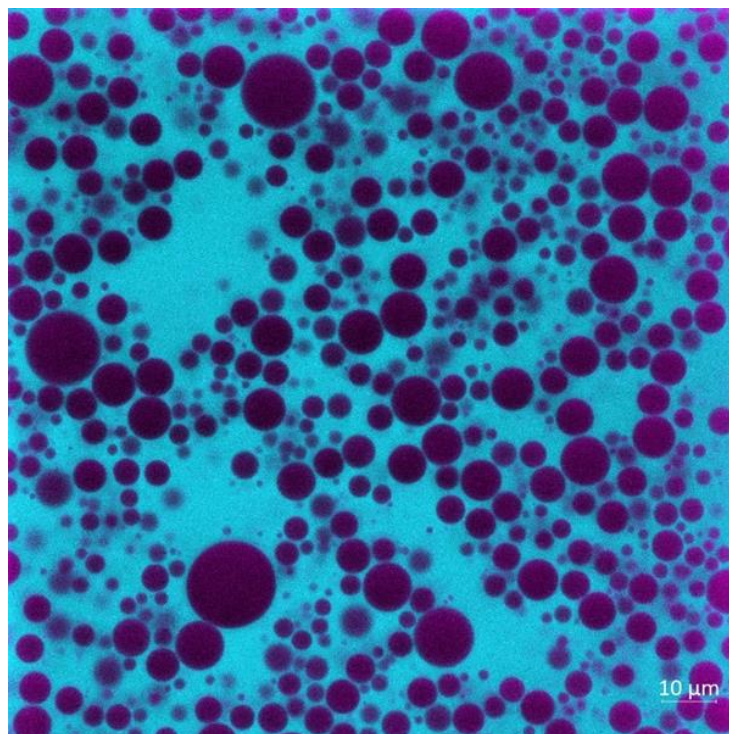
Figure 6.9 CLSM images of sonicated zein-based oleogel 40-15-45 corresponding to 70% ethnol/ zein/oleic acid (%, w/w/w/) stored for 14 days. The gel was stained with Nile Blue, for better contrast, the zein protein showed as light blue and pink for oleic acid droplet.

Figure 6.10 Conductivity of sonicated 15% zein-based oleogels measured after stored 1, 3, 5 and 7 days.

Table 6.3 Conductivity of 15% sonicated zein-based emulsions with sample coding as 70% ethanol (wt%)-zein (wt%)-oleic acid (wt%) stored for 1 and 7 days.

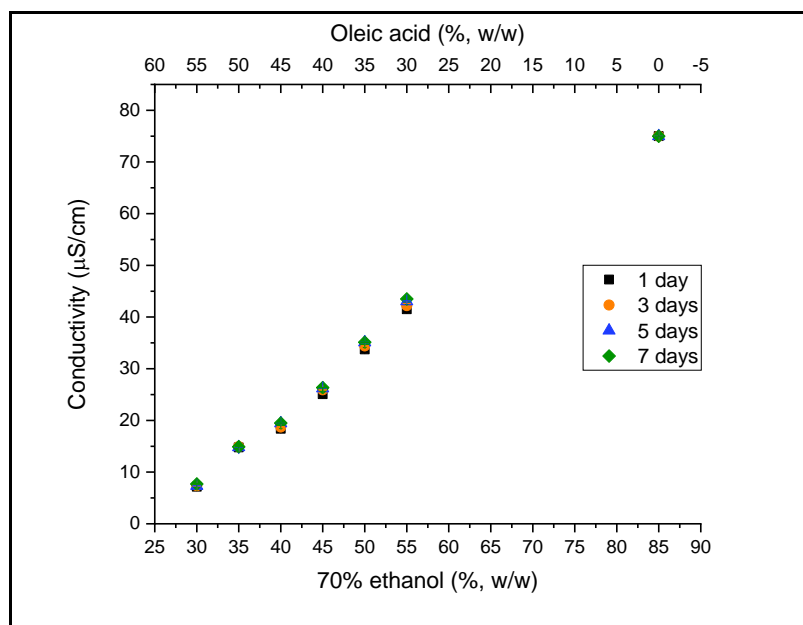| Sample	Conductivity (μS/cm)	
	Stored for 1 day	Stored for 7 days
soni30-15-55	7.17 ± 0.40	7.71 ± 0.02
soni35-15-50	14.78 ± 0.11	14.90 ± 0.01
soni40-15-45	18.38 ± 0.09	19.48 ± 0.02
soni45-15-40	25.08 ± 0.13	26.34 ± 0.01
soni50-15-35	33.73 ± 0.15	35.13 ± 0.06
soni55-15-30	41.50 ± 0.17	43.50 ± 0.01
soni85-15-0	75.10 ± 0.02	75.20 ± 0.02

Table 6.4 R_g and P values for zein-based oleogels stored for 7 days with and without sonication treatment. (Adapted and modified form Table 5.2)

Sample code	R_{g1} (nm)	P_1 index	R_{g2} (nm)	P_2 index
	High q region		Low to intermediate q region	
30-15-55-7d	3.8	1.8	251	3.4
soni30-15-55-7d	3.8	1.8	245	3.5
40-15-45-7d	5.7	1.6	772	3.6
soni40-15-45-7d	8.3	1.5	493	3.4
45-15-40-7d	7.3	1.5	738	3.7
soni45-15-40-7d	8.5	1.5	601	3.4
55-15-30-7d	11.5	1.2	---	---
soni55-15-30-7d	13.2	1.4	---	---

6.4.4 Lutein encapsulated in zein-based oleogel

Before incorporating lutein into the gel system, simple experiments were carried out to validate the solubility of lutein in ethanol or ethanol/oleic acid systems. From Figure 6.11, oleic acid was completely dissolved in pure ethanol (A) but showed phase separation in 70% ethanol (B). The bottom layer could be assumed as the water phase that initially existed inside the ethanol solution. After adding lutein into oleic acid and mixing with ethanol, we observed no phase separation or sedimentation of any of the three components (C). However, in 70% ethanol mixtures

(D) and (E), phase separation was obvious. Hydrophobic lutein only dispersed in ethanol/oleic acid solution but not in water.

Based on the results mentioned above, lipophilic lutein (highly hydrophobic) is a good target drug for the zein-based oleogel encapsulation. So 0.5% and 1% of lutein/oleic acid were prepared and successfully formed homogenized lutein containing emulsion. Simply by color, the higher the lutein concentration, more orange color the sample would have (Fig. 6.12 (left)). After 24 h standing at room temperature, 0.5% lutein containing sample could self-assemble into an up-side down gel structure while the 1% sample still behaved as flowing liquid (Fig. 6.12). This phenomenon had been observed in Chen et al., (2016) where they found out while increasing the incorporated β-carotenoid concentration would weaken the gel strength with decreasing of G'. They assumed the addition of hydrophobic carotenoids with zein in glycerol phase possibly interacted with zein ribbon-like chains, resulting into a more flexible structure.

In AFM images, numerous long strand-like structures entangled both on the surface and under. Some of the strand bundle had horizontal orientation, could be resulted from the lamellar packing of the zein proteins tri-blocks mentioned in zein-oleic acid films. Comparing the scale bar on AFM results, the strand size was smaller than 1 μm, few long strands were around 600 nm and the others were approximately 300 nm, which seemed related to USAXS data of fractal structure R_{g2} size 245 nm.

It is promising for zein-based oleogel to have various applications as a controlled release delivery carrier, not only for lutein but for encapsulating a wide range of hydrophobic nutrients or chemicals. And especially with the preparation method discussed in this research, the no heat self-assembly gelation mechanism is a great way for incorporating heat labile substances.
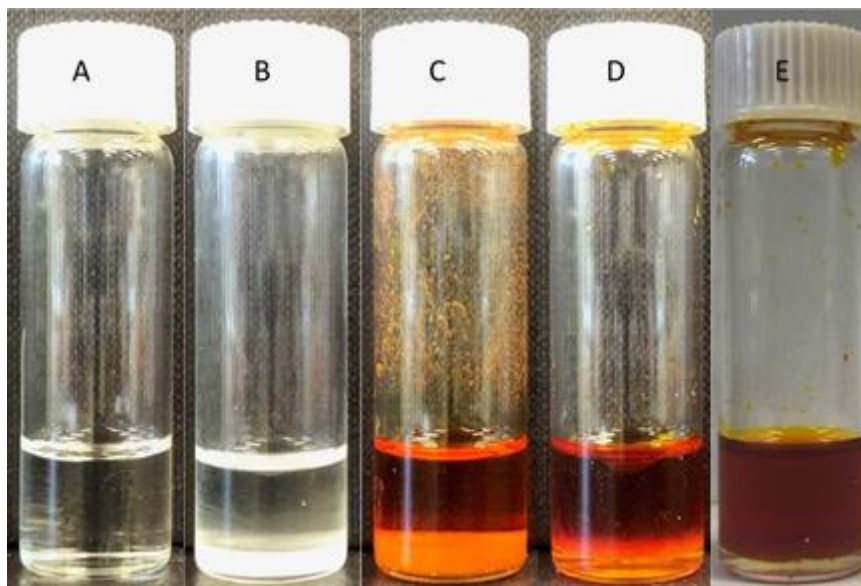
Figure 6.11(A) Digital photos of ethanol/oleic acid 50:50 (v/v), (B) 70% ethanol/oleic acid 50:50 (v/v), (C) ethanol/1% lutein in oleic acid, (D) 70% ethanol/1% lutein in oleic acid on black background, (E) same as D on white background.
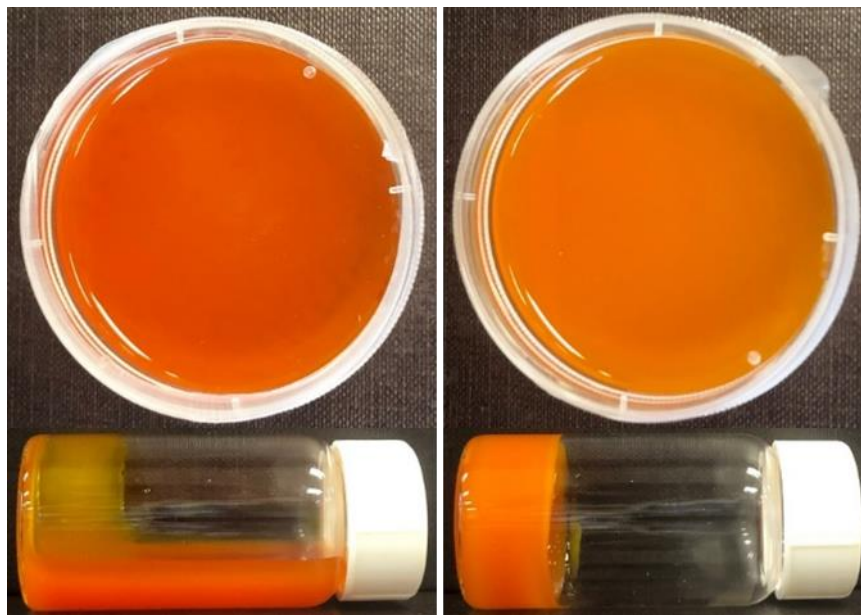
Figure 6.12 Digital photos of lutein encapsulated 70% ethanol/ zein/ oleic acid emulsions (30-15-55) after 24 h. 1 % lutein (left) and 0.5% lutein (right) in oleic acid respectively.
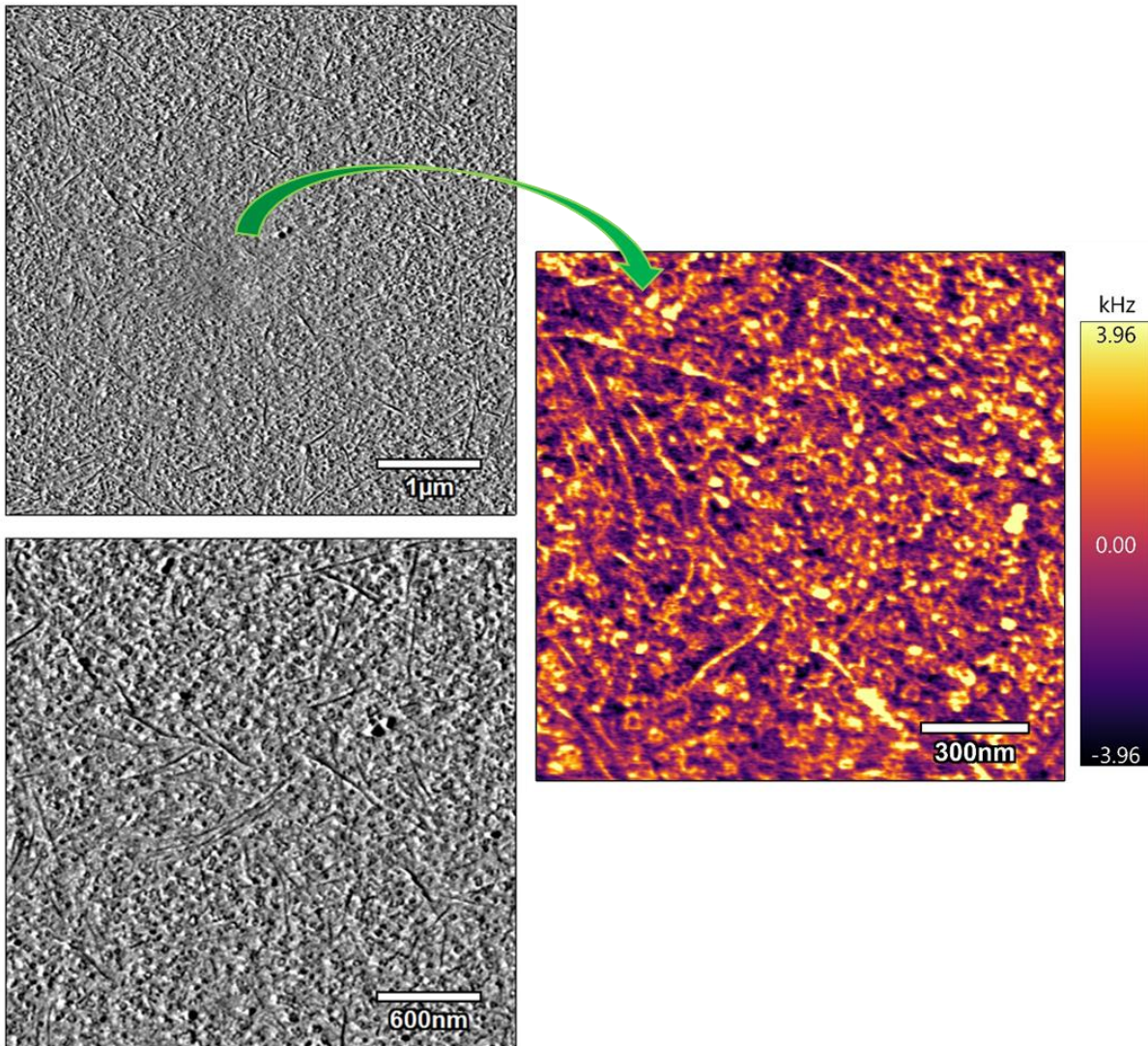
Figure 6.13 AFM images of 0.5% lutein encapsulated 70% ethanol/zein/oleic acid oleogel (%, w/w/w) 30-15-55. The arrow indicated the dent area was resulted from the scanning on the right side.

6.5 Conclusions

In the past decades, various routes for structuring edible oil without using *trans* and saturated fatty acid has been intensively studied. In this research, an effective no-heat evolved zein-based oleogel preparation method was proposed. The self-assembled gelation process was facilitated by ultra-sonication treatment that the high shear dramatically decreased the oil droplets size, resulted in more of the interactions between protein-protein, protien-70% ethanol and protein-oleic acid.

By controlling the solvent compositions of 70% ethanol and oleic acid weight ratios, varied viscoelastic properties of the oleogel could be obtained. Based on our rheological results, samples contained oleic acid between 40-55% (w/w), the G' value and the frequency happened at the cross point (where G' = G") increased with the increasing amount of oleic acid. These demonstrated the gel rigidity was strengthened and the residence to deformation was higher. Which believed to be the contribution of oil droplets homogeneously dispersed in the continuous phase and acting as anchor points for zein molecules to attach on, further arranged into fractal network structures in the system. And when the oleic acid was above 60%, instead of filling up the discontinuous phase, coalescence of oil droplets happened. Accompanied with limited mobility of zein to develop into an extended network that entrapped oil, the sample behaved like viscous liquid rather than gel.

Time was another crucial factor that affected the viscoelastic characteristic of our zein-based oleogel system. With increasing of the storage time, the G' value increased. And at the 4th day, the value jumped 10 times larger than the 3rd day's value. It might due to the gelation mechanism of this system was mainly attributed from the self-assembly properties of the zein protein. Firstly, the building blocks would deposit on the surface of oil droplets, then the building protein units gradually rearranged into 2D ribbon-like strands. With adequate amount of time, these long coils interconnected into 3D fractal structures and provided the rigid component of the gel structures. The hydrogen bonding between the particles and solvents were the driving forces for this spontaneous gelation process. Which we could not only observe the weak physical gel thixotropic property during the frequency sweep tests, but also shear-reversible behavior after force was removed.

The optical microscopic images showed the 15% zein-based oleogels were homogeneous emulsions, with coalescent effect happening when increasing of oleic acid volume fraction and extended storage time. The emulsions were further confirmed with conductivity measurement as oil in water (O/W) system. The amount of added 70% ethanol had positive correlation with the conductivity results, but no differences between storage time. Indicating the zein molecules were dissolved in continuous phase and distributed in between the 70% ethanol and oleic acid with charged side exposure to hydrophilic domain. Based on USAXS data, zein protein building unit size (R_{g1}) was only affected by the solvent compositions instead of sonication treatment, while secondary level R_{g2} assumed to be 3D fractal structure size was affected by both.

Lastly, we established an encapsulation system by incorporating lutein into the zein-based oleogel with direct self-assembly gelation method at room temperature. The lutein encapsulated oleogels stiffness and texture could be modulated by the lutein content and the shear applied. Overall, the increasing amount of lutein resulted in a weakened gel viscoelastic property, which required more time to develop into an up-side-down gel. This might associated with the hydrophobic interaction of zein and lutein. The ability of zein-based oleogel served as an encapsulation matrix for lutein demonstrated the potential of designing into a control-released carrier not only for hydrophobic target drug but also suitable for hydrophilic nutrients, even more, for heat sensitive active compounds. Besides, the tunable semi-solid characteristics should be desired and popular for various applications especially focused on people who have dysphagia or trouble in absorbing nutrients from foods.

6.6 References

Alves-Rodrigues, A., & Shao, A. (2004). The science behind lutein. *Toxicology Letters*, 150(1), 57–83.

Balerna, A., & Mobilio, S. (2015). Introduction to Synchrotron Radiation. In Mobilio, S., Boscherini, F., Meneghini, C. (Eds.) *Synchrotron Radiation: Basics, Methods and Applications:* 3–28. Springer. https://doi.org/10.1007/978-3-642-55315-8

Ahmed, E. M. (2015). Hydrogel: Preparation, characterization, and applications: A review. *Journal of Advanced Research*, *6*(2), 105–121. https://doi.org/10.1016/j.jare.2013.07.006

Alavi, F., Momen, S., Emam-Djomeh, Z., Salami, M., & Moosavi-Movahedi, A. A. (2018). Radical cross-linked whey protein aggregates as building blocks of non-heated cold-set gels. *Food Hydrocolloids*, *81*, 429–441. https://doi.org/10.1016/j.foodhyd.2018.03.016

Alger, M. (2017). *Polymer Science Dictionary.* Springer. https://doi.org/10.1007/978-94-024-0893-5

Angelova, A., Garamus, V. M., Angelov, B., Tian, Z., Li, Y., & Zou, A. (2017). Advances in structural design of lipid-based nanoparticle carriers for delivery of macromolecular drugs, phytochemicals and anti-tumor agents. *Advances in Colloid and Interface Science*, *249*(November), 331–345. https://doi.org/10.1016/j.cis.2017.04.006

Argos, P., Pedersen, K., Marksl, M. D., & Larkinsflll, B. A. (1982). Structural Model for Maize Zein Proteins. *Journal of Biological Chemistry, 257*(17), 9984–9990.

Bajpai, M., Sharma, P. K., & Mittal, A. (2009). A study of oleic acid oily base for the tropical delivery of dexamethasone microemulsion formulations. *Asian Journal of Pharmaceutics*, *3*(3), 208–214. https://doi.org/10.4103/0973-8398.56299

Beaucage, G. (1995). Approximations leading to a unified exponential/power-law approach to small-angle scattering. *Journal of Applied Crystallography*, *28*(6), 717–728.

https://doi.org/10.1107/s0021889895005292

Beaucage, G. (1996). Small-angle scattering from polymeric mass fractals of arbitrary mass-fractal dimension. *Journal of Applied Crystallography*, *29*(2), 134–146. https://doi.org/10.1107/S0021889895011605

Beaucage, G. (2012). Combined small-angle scattering for characterization of hierarchically structured polymer systems over nano-to-micron meter: Part II theory. In Matyjaszewski, K. & and Moeller, M. (Eds.). *Polymer Science: A Comprehensive Reference, 10 (*2), 399–409. Elsevier B.V. https://doi.org/10.1016/B978-0-444-53349-4.00032-7

Benson, M. D., Buxbaum, J. N., Eisenberg, D. S., Merlini, G., Saraiva, M. J. M., Sekijima, Y., Westermark, P. (2018). Amyloid nomenclature 2018: recommendations by the International Society of Amyloidosis (ISA) nomenclature committee. *Amyloid*, *25*(4), 215–219. https://doi.org/10.1080/13506129.2018.1549825

Berthaume, M. A. (2016). Food mechanical properties and dietary ecology. *American Journal of Physical Anthropology*, *159*, S79–S104. https://doi.org/10.1002/ajpa.22903

Blach, C., Gravelle, A. J., Peyronel, F., Weiss, J., Barbut, S., & Marangoni, A. G. (2016). Revisiting the crystallization behavior of stearyl alcohol : stearic acid (SO : SA) mixtures in edible oil. *RSC Advances*, *6*(84), 81151–81163. https://doi.org/10.1039/c6ra15142f

Brosey, C. A., & Tainer, J. A. (2019). Evolving SAXS versatility: solution X-ray scattering for macromolecular architecture, functional landscapes, and integrative structural biology. *Current Opinion in Structural Biology*, *58*, 197–213. https://doi.org/10.1016/j.sbi.2019.04.004

Buruiana, L. I., & Ioan, S. (2018). *Polymer Gel Composites for Bio-Applications. Polymer Gels: Perspectives and Applications*. https://doi.org/10.1007/978-981-10-6080-9_5

Buscemi, S., Corleo, D., Di Pace, F., Petroni, M. L., Satriano, A., & Marchesini, G. (2018). The effect of lutein on eye and extra-eye health. *Nutrients*, *10*(9), 1–24. https://doi.org/10.3390/nu10091321

Cerqueira, M. A., Fasolin, L. H., Picone, C. S. F., Pastrana, L. M., Cunha, R. L., & Vicente, A. A. (2017). Structural and mechanical properties of organogels: Role of oil and gelator molecular structure. *Food Research International*, *96*, 161–170. https://doi.org/10.1016/j.foodres.2017.03.021

Chakraborty, P., Das, S., & Nandi, A. K. (2018). Conducting gels: A chronicle of technological advances. *Progress in Polymer Science*, *88*, 189–219. https://doi.org/10.1016/j.progpolymsci.2018.08.004

Chavan, R. S., Khedkar, C. D., & Bhatt, S. (2016). Fat Replacer. *Encyclopedia of Food and Health*, 589–595. https://doi.org/10.1016/B978-0-12-384947-2.00271-3

Chaves, K. F., Barrera-Arellano, D., & Ribeiro, A. P. B. (2018). Potential application of lipid organogels for food industry. *Food Research International*, *105*, 863–872. https://doi.org/10.1016/j.foodres.2017.12.020

Chen, X., Fu, S., Hou, J., Guo, J., Wang, J., & Yang, X. (2016). Zein based oil-in-glycerol emulgels enriched with b -carotene as margarine alternatives. *Food Chemistry*, *211*, 836–844. https://doi.org/10.1016/j.foodchem.2016.05.133

Chen, Y., Ye, R., & Liu, J. (2013). Understanding of dispersion and aggregation of suspensions of zein nanoparticles in aqueous alcohol solutions after thermal treatment. *Industrial Crops and Products*, *50*, 764–770. https://doi.org/10.1016/j.indcrop.2013.08.023

Cheng, C. J., Ferruzzi, M., & Jones, O. G. (2019). Food Hydrocolloids Fate of lutein-containing zein nanoparticles following simulated gastric and intestinal digestion. *Food Hydrocolloids*, *87*, 229–236. https://doi.org/10.1016/j.foodhyd.2018.08.013

Choudhary, B., Paul, S. R., Nayak, S. K., Qureshi, D., & Pal, K. (2018). *Synthesis and biomedical applications of filled hydrogels*. *Polymeric Gels*. Elsevier. https://doi.org/10.1016/B978-0-08-102179-8.00011-9

Cornwell, D. J., & Smith, D. K. (2015). Expanding the scope of gels - Combining polymers with low-molecular-weight gelators to yield modified self-assembling smart materials with high-tech applications. *Materials Horizons*, *2*(3), 279–293. https://doi.org/10.1039/c4mh00245h

Dassanayake, L. S. K., Kodali, D. R., & Ueno, S. (2011). Formation of oleogels based on edible lipid materials. *Current Opinion in Colloid and Interface Science*. https://doi.org/10.1016/j.cocis.2011.05.005

De Almeida, C. B., Corradini, E., Forato, L. A., Fujihara, R., & Filho, J. F. L. (2018). Microstructure and thermal and functional properties of biodegradable films produced using zein. *Polimeros*, *28*(1), 30–37. https://doi.org/10.1590/0104-1428.11516

De Boer, F. Y., Kok, R. N. U., Imhof, A., & Velikov, K. P. (2018). White zein colloidal particles: Synthesis and characterization of their optical properties on the single particle level and in concentrated suspensions. *Soft Matter*, *14*(15), 2870–2878. https://doi.org/10.1039/c7sm02415k

De Folter, J. W. J., Van Ruijven, M. W. M., & Velikov, K. P. (2012). Oil-in-water Pickering emulsions stabilized by colloidal particles from the water-insoluble protein zein. *Soft Matter*, *8*(25), 6807–6815. https://doi.org/10.1039/c2sm07417f

De Gennes, P. G., & Taupin, C. (1982). Microemulsions and the flexibility of oil/water interfaces. *Journal of Physical Chemistry*, *86*(13), 2294–2304. https://doi.org/10.1021/j100210a011

De Vries, A., Gomez, Y. L., Van der Linden, E., & Scholten, E. (2017). The effect of oil type on network formation by protein aggregates into oleogels. *RSC Advances*, *7*(19), 11803–11812. https://doi.org/10.1039/c7ra00396j

De Vries, A., Jansen, D., van der Linden, E., & Scholten, E. (2018). Tuning the rheological properties of protein-based oleogels by water addition and heat treatment. *Food Hydrocolloids*, *79*, 100–109. https://doi.org/10.1016/j.foodhyd.2017.11.043

De Vries, A., Lopez Gomez, Y., Jansen, B., Van der Linden, E., & Scholten, E. (2017). Controlling agglomeration of protein aggregates for structure formation in liquid oil: A sticky business. *ACS Applied Materials and Interfaces*, *9*(11), 10136–10147. https://doi.org/10.1021/acsami.7b00443

Derkach, S. R. (2009). Rheology of emulsions. *Advances in Colloid and Interface Science*, *151*(1–2), 1–23. https://doi.org/10.1016/j.cis.2009.07.001

Dill, D. B. (1926). Prolamins in 1 & fixed Solvents . II. *Journal of Biological Chemistry,* https://doi.org/0378-1119(94)90466-9

Donsì, F., Voudouris, P., Veen, S. J., & Velikov, K. P. (2017). Zein-based colloidal particles for encapsulation and delivery of epigallocatechin gallate. *Food Hydrocolloids*, *63*, 508–517. https://doi.org/10.1016/j.foodhyd.2016.09.039

Dreher, J., Blach, C., Terjung, N., Gibis, M., & Weiss, J. (2020). Formation and characterization of plant-based emulsified and crosslinked fat crystal networks to mimic animal fat tissue. *Journal of Food Science*, *85*(2), 421–431. https://doi.org/10.1111/1750-3841.14993

Drozdov, A. D., & Christiansen, J. D. (2013). Stress-strain relations for hydrogels under multiaxial deformation. *International Journal of Solids and Structures*, *50*(22–23), 3570–3585. https://doi.org/10.1016/j.ijsolstr.2013.06.023

Erickson, D. P., Ozturk, O. K., Selling, G., Chen, F., Campanella, O. H., & Hamaker, B. R. (2020). Corn zein undergoes conformational changes to higher β-sheet content during its self-assembly in an increasingly hydrophilic solvent. *International Journal of Biological Macromolecules*, *157*, 232–239. https://doi.org/10.1016/j.ijbiomac.2020.04.169

Esposito, C. L., Kirilov, P., & Roullin, V. G. (2018). Organogels, promising drug delivery systems: an update of state-of-the-art and recent applications. *Journal of Controlled Release*, *271*(December 2017), 1–20. https://doi.org/10.1016/j.jconrel.2017.12.019

Figura, L. O., & A.Teixeira, A. (n.d.). *Food Physics*.

Flores-Villaseñor, S. E., Peralta-Rodríguez, R. D., Ramirez-Contreras, J. C., Cortes-Mazatán, G. Y., & Estrada-Ramírez, A. N. (2016). Biocompatible microemulsions for the nanoencapsulation of essential oils and nutraceuticals. In Grumezescu, A. M. (Ed.). *Encapsulations*. *Nanotechnology in the Agri-Food Industry*, 503–558 Elsevier Inc. https://doi.org/http://dx.doi.org/10.1016/B978-0-12-804307-3.00012-0

Flory, P. J. (1974). Introductory lecture. *Faraday Discussions of the Chemical Society*, *57*, 7–18. https://doi.org/10.1039/DC9745700007

Fu, D., & Weller, C. L. (1999). Rheology of zein solutions in aqueous ethanol. *Journal of Agricultural and Food Chemistry*, *47*(5), 2103–2108. https://doi.org/10.1021/jf9811121

Gao, Z. M., Yang, X. Q., Wu, N. N., Wang, L. J., Wang, J. M., Guo, J., & Yin, S. W. (2014). Protein-based pickering emulsion and oil gel prepared by complexes of zein colloidal particles and stearate. *Journal of Agricultural and Food Chemistry*, *62*(12), 2672–2678. https://doi.org/10.1021/jf500005y

Godoy, C. A., Valiente, M., Pons, R., & Montalvo, G. (2015). Effect of fatty acids on self-assembly of soybean lecithin systems. *Colloids and Surfaces B: Biointerfaces*, *131*, 21–28. https://doi.org/10.1016/j.colsurfb.2015.03.065

Gonzalez-Gutierrez, J., & Scanlon, M. G. (2018). Rheology and Mechanical Properties of Fats. In Marangoni, A. G. (Ed.). *Structure-Function Analysis of Edible Fats*, (2), 119–168. AOCS Press. https://doi.org/10.1016/B978-0-12-814041-3.00005-8

Gorusupudi, A., & Baskaran, V. (2013). Wheat germ oil: A potential facilitator to improve lutein bioavailability in mice. *Nutrition*, *29*(5), 790–795. https://doi.org/10.1016/j.nut.2012.11.003

Gupta, P., Vermani, K., & Garg, S. (2002). Hydrogels : from controlled release to pH-responsive

drug delivery. *Drug Discovery Today, 7*(10), 569–579.

Guzhova, I. V., Lazarev, V. F., Kaznacheeva, A. V., Ippolitova, M. V., Muronetz, V. I., Kinev, A. V., & Margulis, B. A. (2011). Novel mechanism of Hsp70 chaperone-mediated prevention of polyglutamine aggregates in a cellular model of huntington disease. *Human Molecular Genetics*, *20*(20), 3953–3963. https://doi.org/10.1093/hmg/ddr314

Hammouda, B. (2010). *Probing Nanoscale Structures – The Sans Toolbox*. https://www.ncnr.nist.gov/staff/hammouda/the_SANS_toolbox.pdf

Hashimoto, T., & Koizumi, S. (2012). Combined Small-Angle Scattering for Characterization of Hierarchically Structured Polymer Systems over Nano-to-Micron Meter: Part I Experiments. . In Matyjaszewski, K. & and Moeller, M. (Eds.). *Polymer Science: A Comprehensive Reference*, *10*(2), 381–398. Elsevier B.V. https://doi.org/10.1016/B978-0-444-53349-4.00297-1

Hughes, N. E., Marangoni, A. G., Wright, A. J., Rogers, M. A., & Rush, J. W. E. (2009). Potential food applications of edible oil organogels. *Trends in Food Science and Technology*, *20*(10), 470–480. https://doi.org/10.1016/j.tifs.2009.06.002

Ikeda, S., & Nishinari, K. (2001). "Weak gel"-type rheological properties of aqueous dispersions of nonaggregated κ-carrageenan helices. *Journal of Agricultural and Food Chemistry*, *49*(9), 4436–4441. https://doi.org/10.1021/jf0103065

Ilavsky, J., Zhang, F., Allen, A. J., Levine, L. E., Jemian, P. R., & Long, G. G. (2013). Ultra-small-angle X-ray scattering instrument at the advanced photon source: History, recent development, and current status. *Metallurgical and Materials Transactions A: Physical Metallurgy and Materials Science*, *44*(1), 68–76. https://doi.org/10.1007/s11661-012-1431-y

Ilavsky, Jan, & Jemian, P. R. (2009). Irena: Tool suite for modeling and analysis of small-angle scattering. *Journal of Applied Crystallography*, *42*(2), 347–353. https://doi.org/10.1107/S0021889809002222

Ilavsky, Jan, Jemian, P. R., Allen, A. J., Zhang, F., Levine, L. E., & Long, G. G. (2009). Ultra-small-angle X-ray scattering at the Advanced Photon Source. *Journal of Applied Crystallography*, *42*(3), 469–479. https://doi.org/10.1107/S0021889809008802

Iwahashi, M., Yamaguchi, Y., Kato, T., Horiuchi, T., Sakurai, I., & Suzuki, M. (1991). Temperature dependence of molecular conformation and liquid structure of cis-9-octadecenoic acid. *Journal of Physical Chemistry*, *95*(1), 445–451. https://doi.org/10.1021/j100154a078

Kasaai, M. R. (2018). Trends in food science & technology zein and zein-based nano-materials for food and nutrition applications : A review. *Trends in Food Science & Technology*, *79*, 184–197. https://doi.org/10.1016/j.tifs.2018.07.015

Khalil, A. A., Deraz, S. F., Elrahman, S. A., & El-Fawal, G. (2015). Enhancement of mechanical properties, microstructure, and antimicrobial activities of zein films cross-linked using succinic anhydride, eugenol, and citric acid. *Preparative Biochemistry and Biotechnology*, *45*(6), 551–567. https://doi.org/10.1080/10826068.2014.940967

Kharlamova, A., Chassenieux, C., & Nicolai, T. (2018). Acid-induced gelation of whey protein aggregates: Kinetics, gel structure and rheological properties. *Food Hydrocolloids*, *81*, 263–272. https://doi.org/10.1016/j.foodhyd.2018.02.043

Kharlamova, A., Nicolai, T., & Chassenieux, C. (2018). Mixtures of sodium caseinate and whey protein aggregates: Viscosity and acid- or salt-induced gelation. *International Dairy Journal*, *86*, 110–119. https://doi.org/10.1016/j.idairyj.2018.07.002

Kikhney, A. G., & Svergun, D. I. (2015). A practical guide to small angle X-ray scattering (SAXS) of flexible and intrinsically disordered proteins. *FEBS Letters*, *589*(19), 2570–2577. https://doi.org/10.1016/j.febslet.2015.08.027

Kim, S., & Xu, J. (2008). Aggregate formation of zein and its structural inversion in aqueous ethanol. *Journal of Cereal Science*, *47*(1), 1–5. https://doi.org/10.1016/j.jcs.2007.08.004

Komaiko, J. S., & Mcclements, D. J. (2016). Formation of food-grade nanoemulsions using low-energy preparation methods: A review of available methods. *Comprehensive Reviews in Food Science and Food Safety*, *15*(2), 331–352. https://doi.org/10.1111/1541-4337.12189

Kuo, W. Y., Ilavsky, J., & Lee, Y. (2016). Structural characterization of solid lipoproteic colloid gels by ultra-small-angle X-ray scattering and the relation with sodium release. *Food Hydrocolloids*, *56*, 325–333. https://doi.org/10.1016/j.foodhyd.2015.12.032

Lai, H. M., Geil, P. H., & Padua, G. W. (1999). X-ray diffraction characterization of the structure of zein-oleic acid films. *Journal of Applied Polymer Science*, *71*(8), 1267–1281. https://doi.org/10.1002/(SICI)1097-4628(19990222)71:8<1267::AID-APP7>3.0.CO;2-O

Laurati, M., Petekidis, G., Koumakis, N., Cardinaux, F., Schofield, A. B., Brader, J. M., Egelhaaf, S. U. (2009). Structure, dynamics, and rheology of colloid-polymer mixtures: From liquids to gels. *Journal of Chemical Physics*, *130*(13). https://doi.org/10.1063/1.3103889

Lee, B. Il, Suh, Y. S., Chung, Y. J., Yu, K., & Park, C. B. (2017). Shedding light on Alzheimer's β-amyloidosis: Photosensitized methylene blue inhibits self-assembly of β-amyloid peptides and disintegrates their aggregates. *Scientific Reports*, *7*(1), 1–10. https://doi.org/10.1038/s41598-017-07581-2

Li, Ying, & Corredig, M. (2020). Acid induced gelation behavior of skim milk concentrated by membrane filtration. *Journal of Texture Studies*, *51*(1), 101–110. https://doi.org/10.1111/jtxs.12492

Li, Yunqi, Li, J., Xia, Q., Zhang, B., Wang, Q., & Huang, Q. (2012). Understanding the dissolution of α-zein in aqueous ethanol and acetic acid solutions. *Journal of Physical Chemistry B*, *116*(39), 12057–12064. https://doi.org/10.1021/jp305709y

Lv, G., Wang, F., Cai, W., Li, H., & Zhang, X. (2014). Influences of addition of hydrophilic surfactants on the W/O emulsions stabilized by lipophilic surfactants. *Colloids and Surfaces A: Physicochemical and Engineering Aspects*, *457*(1), 441–448. https://doi.org/10.1016/j.colsurfa.2014.06.031

Marín, T., Montoya, P., Arnache, O., Pinal, R., & Calderón, J. (2018). Bioactive films of zein/magnetite magnetically stimuli-responsive for controlled drug release. *Journal of Magnetism and Magnetic Materials*, *458*, 355–364. https://doi.org/10.1016/j.jmmm.2018.03.046

Martins, A. J., Vicente, A. A., Cunha, R. L., & Cerqueira, M. A. (2018). Edible oleogels: An opportunity for fat replacement in foods. *Food and Function*, *9*(2), 758–773. https://doi.org/10.1039/c7fo01641g

Marze, S., Guillermic, R. M., & Saint-Jalmes, A. (2009). Oscillatory rheology of aqueous foams: Surfactant, liquid fraction, experimental protocol and aging effects. *Soft Matter*, *5*(9), 1937–1946. https://doi.org/10.1039/b817543h

Masalova, I., Malkin, A. Y., Ferg, E., Kharatiyan, E., Taylor, M., & Haldenwang, R. (2006). Evolution of rheological properties of highly concentrated emulsions with aging —Emulsion-to-suspension transition. *Journal of Rheology*, *50*(4), 435–451. https://doi.org/10.1122/1.2206712

Masamba, K., Li, Y., Hategekimana, J., Liu, F., & Ma, J. (2016). Effect of gallic acid on mechanical and water barrier properties of zein-oleic acid composite films. *Journal of Food Science and Technology*, *53*(May), 2227–2235. https://doi.org/10.1007/s13197-015-2167-7

Matsushima, N., Danno, G. I., Takezawa, H., & Izumi, Y. (1997). Three-dimensional structure of maize α-zein proteins studied by small-angle X-ray scattering. *Biochimica et Biophysica Acta - Protein Structure and Molecular Enzymology*. https://doi.org/10.1016/S0167-4838(96)00212-9

Mewis, J., & Wagner, N. J. (2011). *Colloidal Suspension Rheology*. Cambridge University Press. https://doi.org/10.1017/CBO9780511977978

Mezzenga, R. (2011). Protein-templated oil gels and powders. In Marangoni, A. G., & Garti, N. (Eds.). *Edible Oleogels: Structure and Health Implications*, 307–329. Elsevier Inc. https://doi.org/10.1016/B978-0-9830791-1-8.50015-2

Milston, R., Madigan, M. C., & Sebag, J. (2016). Vitreous floaters: Etiology, diagnostics, and management. *Survey of Ophthalmology*, *61*(2), 211–227. https://doi.org/10.1016/j.survophthal.2015.11.008

Moradkhannejhad, L., Abdouss, M., Nikfarjam, N., Mazinani, S., & Heydari, V. (2018). morphology investigation electrospinning of zein / propolis nano fibers; antimicrobial properties and morphology investigation. *Journal of Materials Science: Materials in Medicine*. https://doi.org/10.1007/s10856-018-6174-x

Nabetani, H., Ichikawa, S., Liu, X., Nakajima, M., & Xu, Q. (2007). Factors affecting the properties of ethanol-in-oil emulsions. *Food Science and Technology Research*, *8*(1), 36–41. https://doi.org/10.3136/fstr.8.36

Nephomnyshy, I., Rosen-Kligvasser, J., & Davidovich-Pinhas, M. (2020). The development of a direct approach to formulate high oil content zein-based emulsion gels using moderate temperatures. *Food Hydrocolloids*, *101*, 105528. https://doi.org/10.1016/j.foodhyd.2019.105528

Nikiforidis, C. V., Gilbert, E. P., & Scholten, E. (2015). Organogel formation via supramolecular assembly of oleic acid and sodium oleate. *RSC Advances*, *5*(59), 47466–47475. https://doi.org/10.1039/c5ra05336f

Nonthanum, P., Lee, Y., & Padua, G. W. (2012). Effect of γ-zein on the rheological behavior of concentrated zein solutions. *Journal of Agricultural and Food Chemistry*, *60*(7), 1742–1747. https://doi.org/10.1021/jf2035302

Nonthanum, P., Lee, Y., & Padua, G. W. (2013). Effect of pH and ethanol content of solvent on rheology of zein solutions. *Journal of Cereal Science*, *58*(1), 76–81.

https://doi.org/10.1016/j.jcs.2013.04.001

O'Sullivan, C. M., Barbut, S., & Marangoni, A. G. (2016). Edible oleogels for the oral delivery of lipid soluble molecules: Composition and structural design considerations. *Trends in Food Science and Technology*. https://doi.org/10.1016/j.tifs.2016.08.018

Ochbaum, G., & Bitton, R. (2018). Using small-angle X-ray scattering (SAXS) to study the structure of self-assembling biomaterials. In Azevedo, H. S., & De Silva, R. M. P. (Eds.). *Self-Assembling Biomaterials: Molecular Design, Characterization and Application in Biology and Medicine*, 291–304. Elsevier Ltd. https://doi.org/10.1016/B978-0-08-102015-9.00015-0

Ochowiak, M., & Rozanski, J. (2012). Rheology and structure of emulsions and suspensions. *Journal of Dispersion Science and Technology, 33*(2), 177–184. https://doi.org/10.1080/01932691.2010.548694

Pal, R. (2011). Influence of interfacial rheology on the viscosity of concentrated emulsions. *Journal of Colloid and Interface Science*, *356*(1), 118–122. https://doi.org/10.1016/j.jcis.2010.12.068

Patel, A. R. (2017). A colloidal gel perspective for understanding oleogelation. *Current Opinion in Food Science*, *15*, 1–7. https://doi.org/10.1016/j.cofs.2017.02.013

Patel, A. R., Cludts, N., Bin Sintang, M. D., Lewille, B., Lesaffer, A., & Dewettinck, K. (2014). Polysaccharide-based oleogels prepared with an emulsion-templated approach. *ChemPhysChem*, *15*(16), 3435–3439. https://doi.org/10.1002/cphc.201402473

Patel, A. R., & Dewettinck, K. (2016). Edible oil structuring: An overview and recent updates. *Food and Function*, *7*(1), 20–29. https://doi.org/10.1039/c5fo01006c

Patel, A. R., Dumlu, P., Vermeir, L., Lewille, B., Lesaffer, A., & Dewettinck, K. (2015). Rheological characterization of gel-in-oil-in-gel type structured emulsions. *Food Hydrocolloids*, *46*, 84–92. https://doi.org/10.1016/j.foodhyd.2014.12.029

Patel, A. R., & Velikov, K. P. (2014). Zein as a source of functional colloidal nano- and microstructures. *Current Opinion in Colloid and Interface Science*, *19*(5), 450–458. https://doi.org/10.1016/j.cocis.2014.08.001

Pehlivanoğlu, H., Demirci, M., Toker, O. S., Konar, N., Karasu, S., & Sagdic, O. (2018). Oleogels, a promising structured oil for decreasing saturated fatty acid concentrations: Production and food-based applications. *Critical Reviews in Food Science and Nutrition*, *58*(8), 1330–1341. https://doi.org/10.1080/10408398.2016.1256866

Pena-serna, C., & Lopes-filho, J. F. (2013). In fluence of ethanol and glycerol concentration over functional and structural properties of zein-oleic acid films. *Materials Chemistry and Physics*, *142*(2–3), 580–585. https://doi.org/10.1016/j.matchemphys.2013.07.056

Pérez-Gago, Maria B., & Krochta, J. M. (2001). Lipid particle size effect on water vapor permeability and mechanical properties of whey protein/beeswax emulsion films. *Journal of Agricultural and Food Chemistry*, *49*(2), 996–1002. https://doi.org/10.1021/jf000615f

Pérez-Gago, Maria Berna, & Rhim, J. W. (2013). Edible Coating and Film Materials: Lipid Bilayers and Lipid Emulsions. *Innovations in Food Packaging: Second Edition*, 325–350. https://doi.org/10.1016/B978-0-12-394601-0.00013-8

Peyronel, F., Ilavsky, J., Mazzanti, G., Marangoni, A. G., & Pink, D. A. (2013). Edible oil structures at low and intermediate concentrations. II. Ultra-small angle X-ray scattering of in situ tristearin solids in triolein. *Journal of Applied Physics*, *114*(23). https://doi.org/10.1063/1.4847997

Peyronel, F., Quinn, B., Marangoni, A. G., & Pink, D. A. (2014). Ultra small angle x-ray scattering in complex mixtures of triacylglycerols. *Journal of Physics Condensed Matter*, *26*(46). https://doi.org/10.1088/0953-8984/26/46/464110

Ponton, A., Bose, T. K., & Delbos, G. (1991). Dielectric study of percolation in an oil-continuous microemulsion. *The Journal of Chemical Physics*, *94*(10), 6879–6886. https://doi.org/10.1063/1.460268

Quemada, D., & Berli, C. (2002). Energy of interaction in colloids and its implications in rheological modeling. *Advances in Colloid and Interface Science, 98*. https://doi.org/10.1016/S0001-8686(01)00093-8

Raeburn, J., Cardoso, A. Z., & Adams, D. J. (2013). The importance of the self-assembly process to control mechanical properties of low molecular weight hydrogels. *Chemical Society Reviews*, *42*(12), 5143–5156. https://doi.org/10.1039/c3cs60030k

Raza, A., Hayat, U., Bilal, M., Iqbal, H. M. N., & Wang, J. Y. (2020). Zein-based micro- and nano-constructs and biologically therapeutic cues with multi-functionalities for oral drug delivery systems. *Journal of Drug Delivery Science and Technology*, *58*. https://doi.org/10.1016/j.jddst.2020.101818

Renner, M., & Melki, R. (2014). Protein aggregation and prionopathies. *Pathologie Biologie*, *62*(3), 162–168. https://doi.org/10.1016/j.patbio.2014.01.003

Roberts, J. E., & Dennison, J. (2015). The photobiology of lutein and zeaxanthin in the eye. *Journal of Ophthalmology*, *2015*. https://doi.org/10.1155/2015/687173

Ross-Murphy, S. B. (1995). Structure–property relationships in food biopolymer gels and solutions. *Journal of Rheology*, *39*(6), 1451–1463. https://doi.org/10.1122/1.550610

Rutkevi, M., Allred, S., Velev, O. D., & Velikov, K. P. (2018). Stabilization of oil continuous emulsions with colloidal particles from water-insoluble plant proteins. *Food hydrocolloids, 82*, 89–95. https://doi.org/10.1016/j.foodhyd.2018.04.004

Rutkevičius, M., Allred, S., Velev, O. D., & Velikov, K. P. (2018). Stabilization of oil continuous emulsions with colloidal particles from water-insoluble plant proteins. *Food Hydrocolloids*, *82*, 89–95. https://doi.org/10.1016/j.foodhyd.2018.04.004

Sadeghpour, A., Pirolt, F., & Glatter, O. (2013). Submicrometer-sized pickering emulsions stabilized by silica nanoparticles with adsorbed oleic acid. *Langmuir*, *29*(20), 6004–6012. https://doi.org/10.1021/la4008685

Samateh, M., Sagiri, S. S., & John, G. (2018). *Molecular Oleogels*. *Edible Oleogels*. AOCS Press. https://doi.org/10.1016/b978-0-12-814270-7.00018-6

Sangeetha, N. M., & Maitra, U. (2005). Supramolecular gels: Functions and uses. *Chemical Society Reviews*, *34*(10), 821–836. https://doi.org/10.1039/b417081b

Santos, T. M., Souza Filho, M. de S. M., Muniz, C. R., Morais, J. P. S., Kotzebue, L. R. V., Pereira,

A. L. S., & Azeredo, H. M. C. (2017). Zein films with unoxidized or oxidized tannic acid. *Journal of the Science of Food and Agriculture*, *97*(13), 4580–4587. https://doi.org/10.1002/jsfa.8327

Schulz-Schaeffer, W. J. (2010). The synaptic pathology of α-synuclein aggregation in dementia with Lewy bodies, Parkinson's disease and Parkinson's disease dementia. *Acta Neuropathologica*, *120*(2), 131–143. https://doi.org/10.1007/s00401-010-0711-0

Selling, G. W., Hamaker, S. A. H., & Sessa, D. J. (2007). Effect of solvent and temperature on secondary and tertiary structure of zein by circular dichroism. *Cereal Chemistry*, *84*(3), 265–270. https://doi.org/10.1094/CCHEM-84-3-0265

Sengupta, T., & Han, J. H. (2013). Surface Chemistry of Food, Packaging, and Biopolymer Materials. In Han, J. H. (Ed.). *Innovations in Food Packaging: Second Edition*. 51–86. Elsevier Ltd. https://doi.org/10.1016/B978-0-12-394601-0.00004-7

Serrano, J., Goñi, I., & Saura-Calixto, F. (2005). Determination of β-caroten and lutein available from green leafy vegetables by an in vitro digestion and colonic fermentation method. *Journal of Agricultural and Food Chemistry*, *53*(8), 2936–2940. https://doi.org/10.1021/jf0480142

Sharma, S. K. (2018). *Handbook of Materials Characterization*. Springer. https://doi.org/10.1007/978-3-319-92955-2

Shukla, R., Cheryan, M., & DeVor, R. E. (2000). Solvent extraction of zein from dry-milled corn. *Cereal Chemistry*, *77*(6), 724–730. https://doi.org/10.1094/CCHEM.2000.77.6.724

Siraj, N., Shabbir, M. A., Ahmad, T., Sajjad, A., Khan, M. R., Khan, M. I., & Butt, M. S. (2015). Organogelators as a saturated fat replacer for structuring edible oils. *International Journal of Food Properties*, *18*(9), 1973–1989. https://doi.org/10.1080/10942912.2014.951891

Soltani, S., & Madadlou, A. (2015). Two-step sequential cross-linking of sugar beet pectin for transforming zein nanoparticle-based Pickering emulsions to emulgels. *Carbohydrate Polymers*, *136*, 738–743. https://doi.org/10.1016/j.carbpol.2015.09.100

Tabilo-Munizaga, G., & Barbosa-Cánovas, G. V. (2005). Rheology for the food industry. *Journal of Food Engineering*, *67*(1–2), 147–156. https://doi.org/10.1016/j.jfoodeng.2004.05.062

Terech, P. (1997). Low-molecular weight organogelators. *Specialist Surfactants*, 208–268. https://doi.org/10.1007/978-94-009-1557-2_8

Terech, Pierre, & Weiss, R. G. (1997). Low molecular mass gelators of organic liquids and the properties of their gels. *Chemical Reviews*, *97*(8), 3133–3159. https://doi.org/10.1021/cr9700282

Thakur, V. K., & Thakur, M. K. (2018). *Polymer gels. Science and Fundamentals*. Springer. https://doi.org/10.1007/978-981-10-6086-1

Uzun, S., Ilavsky, J., & Padua, G. W. (2017). Characterization of zein assemblies by ultra-small-angle X-ray scattering. *Soft Matter*, *13*(16), 3053–3060. https://doi.org/10.1039/c6sm02717b

Wang, L. J., Yin, Y. C., Yin, S. W., Yang, X. Q., Shi, W. J., Tang, C. H., & Wang, J. M. (2013). Development of novel zein-sodium caseinate nanoparticle (ZP)-stabilized emulsion films for improved water barrier properties via emulsion/solvent evaporation. *Journal of Agricultural and Food Chemistry*, *61*(46), 11089–11097. https://doi.org/10.1021/jf4029943

Wang, Qin, Yin, L., & Padua, G. W. (2008). Effect of hydrophilic and lipophilic compounds on zein microstructures. *Food Biophysics*, *3*(2), 174–181. https://doi.org/10.1007/s11483-008-9080-9

Wang, Qiuming, Yu, X., Patal, K., Hu, R., Chuang, S., Zhang, G., & Zheng, J. (2013). Tanshinones inhibit amyloid aggregation by amyloid-β peptide, disaggregate amyloid fibrils, and protect cultured cells. *ACS Chemical Neuroscience*, *4*(6), 1004–1015. https://doi.org/10.1021/cn400051e

Wang, Yi, & Padua, G. W. (2010). Formation of zein microphases in ethanol-water. *Langmuir*, *26*(15), 12897–12901. https://doi.org/10.1021/la101688v

Wang, Yi, & Padua, G. W. (2012). Nanoscale characterization of zein self-assembly. *Langmuir*, *28*(5), 2429–2435. https://doi.org/10.1021/la204204j

Wang, Q., Crofts, A. R., Padua, G. W. (2003). Protein − lipid interactions in zein films investigated by surface plasmon resonance. *Journal of Agricultural and Food Chemistry, 51,* 7439–7444.

Wang, Ying, & Padua, G. W. (2006). Water barrier properties of zein-oleic acid films. *Cereal Chemistry, 83*(4), 331–334. https://doi.org/10.1094/CC-83-0331

Watanabe, T., Kawai, T., & Nonomura, Y. (2018). Effects of fatty acid addition to oil-in-water emulsions stabilized with sucrose fatty acid ester. *Journal of Oleo Science*, *67*(3), 307–313. https://doi.org/10.5650/jos.ess17097

Weissmueller, N. T., Lu, H. D., Hurley, A., & Prud'Homme, R. K. (2016). Nanocarriers from GRAS Zein Proteins to Encapsulate Hydrophobic Actives. *Biomacromolecules*, *17*(11), 3828–3837. https://doi.org/10.1021/acs.biomac.6b01440

Xu, J., Yin, A., Zhao, J., Li, D., & Hou, W. (2013). Surfactant-free microemulsion composed of oleic acid, n-propanol, and H2O. *Journal of Physical Chemistry B*, *117*(1), 450–456. https://doi.org/10.1021/jp310282a

Xu, Q., Nakajima, M., Nabetani, H., Iwamoto, S., & Liu, X. (2001). The effects of ethanol content and emulsifying agent concentration on the stability of vegetable oil-ethanol emulsions. *JAOCS, Journal of the American Oil Chemists' Society*, *78*(12), 1185–1190. https://doi.org/10.1007/s11745-001-0411-z

Yang, Y., Chaisoontornyotin, W., & Hoepfner, M. P. (2018). Structure of ssphaltenes during precipitation investigated by ultra-small-angle X-ray scattering. *Langmuir*, *34*(35), 10371–10380. https://doi.org/10.1021/acs.langmuir.8b01873

Yuan, Y., Li, H., Liu, C., Zhang, S., Xu, Y., & Wang, D. (2019). Fabrication and characterization of lutein-loaded nanoparticles based on zein and sophorolipid : Enhancement of water solubility , stability , and bioaccessibility. *Journal of Agricultural and Food Chemistry*, *67*(43), 11977–11985. https://doi.org/10.1021/acs.jafc.9b05175

Zhang, B., Luo, Y., & Wang, Q. (2011). Effect of acid and base treatments on structural, rheological, and antioxidant properties of α-zein. *Food Chemistry*, *124*(1), 210–220. https://doi.org/10.1016/j.foodchem.2010.06.019

Zhang, M., & Weiss, R. G. (2015). Self-assembled networks and molecular gels derived from long-chain, naturally-occurring fatty acids. *Journal of the Brazilian Chemical Society*, *27*(2), 1–17. https://doi.org/10.5935/0103-5053.20150247

Zhang, Y., Cui, L., Che, X., Zhang, H., Shi, N., Li, C., Kong, W. (2015). Zein-based films and their usage for controlled delivery: Origin, classes and current landscape. *Journal of Controlled Release*, *206*(2699), 206–219. https://doi.org/10.1016/j.jconrel.2015.03.030

Zhang, Y., Cui, L., Li, F., Shi, N., Li, C., Yu, X., Kong, W. (2016). Design, fabrication and biomedical applications of zein-based nano/micro-carrier systems. *International Journal of Pharmaceutics*, *513*(1–2), 191–210. https://doi.org/10.1016/j.ijpharm.2016.09.023

Zhong, Q., & Ikeda, S. (2012). Viscoelastic properties of concentrated aqueous ethanol suspensions of α-zein. *Food Hydrocolloids*, *28*(1), 46–52. https://doi.org/10.1016/j.foodhyd.2011.11.014

Zou, Y., Thijssen, P. P., Yang, X., & Scholten, E. (2019). The effect of oil type and solvent quality on the rheological behavior of zein stabilized oil-in-glycerol emulsion gels. *Food Hydrocolloids*, *91*(December 2018), 57–65. https://doi.org/10.1016/j.foodhyd.2019.01.016

Zou, Y., Yang, X., & Scholten, E. (2018). Rheological behavior of emulsion gels stabilized by zein/tannic acid complex particles. *Food Hydrocolloids*, *77*, 363–371. https://doi.org/10.1016/j.foodhyd.2017.10.013

CHAPTER 7   CONCLUSIONS AND FUTURE WORK

This dissertation established a self-assembly oleogel model system composed of 70% ethanol/zein/oleic acid. The construction of ternary phase diagrams helped to identify the extents and boundaries of zein-based oleogel in terms of composition. It concluded that the minimum amount of zein to form a gel was 10%, and the turbidity of the gel increased with oleic acid content. The viscoelastic properties of the oleogels were tunable by the solvent composition, protein concentration, storage time and sonication treatment, which made this system had great potential for further applications. With this non-thermal gelation process, the zein-based oleogels would require relatively longer time for gels to be prepared. However, this drawback could be successfully improved by applying sonication to facilitate the gelation rate, which opened a door for encapsulating heat-liable compounds. Based on the USAXS results, the gel network systems were developed by two levels of building structures. The primary building units were assumed to be the stacking of zein molecules and were affected by the solvent composition but not storage time nor high shear. But for the second level fractal structures, they were affect by all. These indicated that in the self-assembly gelation process of the zein-based oleogels, was adapting zein as the oleogelator. At the right hydrophilic-hydrophobic balance of the solvents, zein anchored on the surface of the oil droplets to form entangled networks that created a stable oil-in-water emulsion. According to these findings, it is believed that the zein-based oleogels in this study will be promising candidates for the applications of:

- Utilizing as a controlled-release carrier for bioactive compounds, especially for encapsulation of lipophilic nutrients which need to be protected and slow released in the later stages of the digestion process.
- Serving as a nutrient-dense food matrix with tunable texture and high lubricity for geriatric and hard-to-feed patients.
- Substituting of semi-soft and solid fat products that contain *trans* or saturated fatty acids, such as margarine, spreads or shortening.
- Applying in the diets for calorie control or for tailoring the fatty acid profile by incorporating polyunsaturated fatty acid in the system while not affecting the consumer's perception.
- Using as a type of biocompatible cultural media for cell growth in bioengineering field.

- Producing biodegradable microfibers with ordered nanostructure in electrospinning or 3D printing techniques.